UNIVERSITAT DE BARCELONA

Immunochemical diagnostic strategies based on Quorum Sensing

Enrique José Montagut Cañete

Immunochemical diagnostic strategies based on Quorum Sensing

Enrique José Montagut Cañete

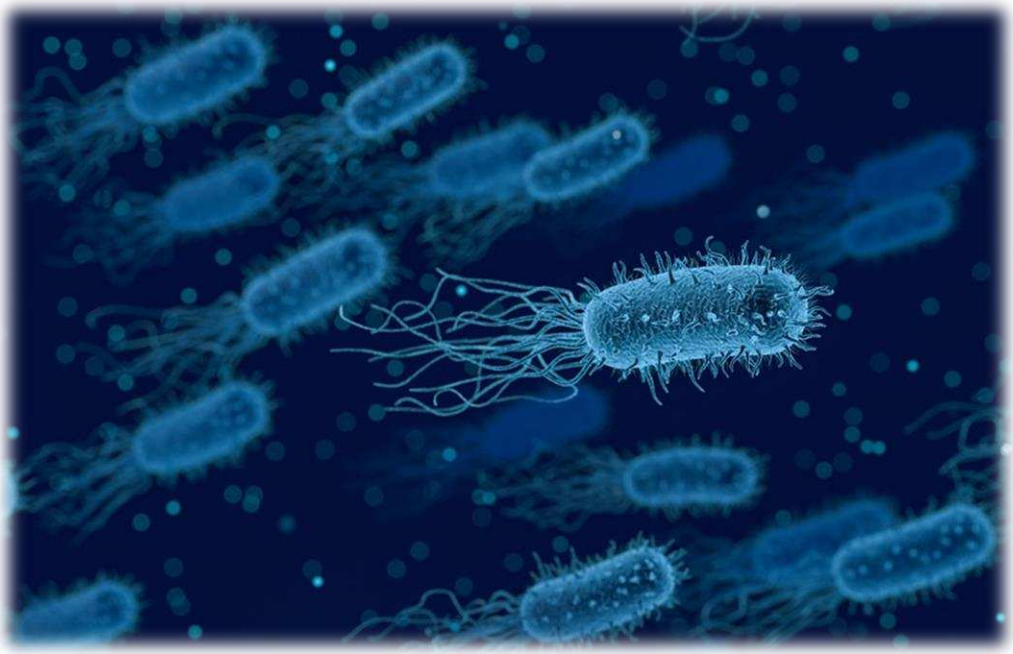

UNIVERSITAT DE BARCELONA

CSIC
CONSEJO SUPERIOR DE INVESTIGACIONES CIENTÍFICAS

Document signat digitalment per: ENRIQUE JOSE MONTAGUT CAnETE

Universitat de Barcelona, Facultad de Química, Departamento de Química Orgánica

Consejo Superior de Investigaciones Científicas

Instituto de Química Avanzada de Cataluña

Nanobiotechnology for Diagnostics group

Centro de Investigación Biomédica en Red en Bioingeniería, Biomateriales y Nanomedicina

Immunochemical diagnostic strategies based on Quorum Sensing

Memoria para optar al grado de Doctor por la Universitat de Barcelona presentada por:

Enrique José Montagut Cañete

Barcelona, diciembre de 2020

Document signat digitalment per: ENRIQUE JOSE MONTAGUT CAnETE

Universitat de Barcelona

Facultad de Química – Departamento de Química Orgánica
Programa de doctorado de Química Orgánica

Immunochemical diagnostic strategies based on Quorum Sensing

Memoria para optar al grado de Doctor por la Universitat de Barcelona
presentada por:

Enrique José Montagut Cañete

Directora:

Prof. Mª Pilar Marco Colás
Profesora de Investigación
Dept. de Surfactantes y
Nanobiotecnología
Nb4D group, IQAC-CSIC

Tutora:

Cat. Anna Grandas Sagarra
Catedrática de Química Orgánica
Departamento de Química Orgánica
Facultad de Química
Universitat de Barcelona

AGRADECIMIENTOS

Costaba creer que este momento iba a llegar o, al menos, siempre se veía desde una posición bastante lejana de la realidad que estaba viviendo. Pero al fin, todo el trabajo de estos años está (parcialmente) resumido en este documento. Lo que no se puede resumir son todas las vivencias, momentos, miedos, frustraciones, alegrías o sentimientos que he ido encontrando y compartiendo con la gente durante estos, ahora ya, casi 4 años. Tengo muchísimas cosas que agradecer a todas las personas que, no sólo me han ayudado o guiado durante la tesis, sino que también me han aportado, de una manera o de otra, su granito de arena para crecer como persona.

En primer lugar, me gustaría empezar por todos los que han formado parte del Nb4D. A pesar de ser un grupo de investigación (en el que inevitablemente y por desgracia mucha gente está por un tiempo definido), hemos llegado a formar una gran familia, con todo lo que ello conlleva. Por ello, quería dedicaros una gran parte de esta tesis:

- A Mª Pilar Marco, mi directora y la persona que abrió las puertas de su casa para darme una oportunidad para desarrollarme como científico. Pilar, sense tú totes les vivències i aquesta experiència inolvidable mai hauria sigut possible. Saps que estaré eternament agraït per tot el que has fet per mi, però sobretot per escoltar-me quan ho necessitava i per valorar les meves opinions, ha sigut una sort poder fer ciència amb tú.
- A todas las personas que me han brindado un poco de su tiempo para discutir cuestiones científicas o simplemente poder charlar y reírnos un rato: Roger, Pablo, Montse, Nuria... y sobre todo a Lluisa, sin ti la tesis no hubiera tenido el mismo contenido, gracias por tanto esfuerzo.
- A la gente que han compartido conmigo muchas vivencias durante un periodo de tiempo relativamente corto: Ana G., Pablico, Izaskun… y cómo no, ¡al equipo Collider! Ha sido un placer trabajar con vosotros.
- Y por supuesto, a las personas con las que más momentos he compartido tanto en el terreno personal como en el laboral. A David por todos esos pitins, chismorreos y risas. A Ana Sanchis, por la ayuda científica incalculable y las birras de los viernes. A Klaudia, por nuestras charlas de desahogo. A Julián, por el buen humor y tu energía contagiosa. Y finalmente a Ginevra, sai che per te non ho abastanza parole, grazie per esserci sempre. Gracias a todos por las risas, los

cafés, las cenas, los momentos de fiesta (alguno que otro ha caído, creo recordar) y por la ayuda que me habéis dado durante estos 4 años. Sois gente maravillosa que me encantaría conservar. (¡El próximo almuerzo lo pago yo!)

También quiero agradecer a toda la gente que no ha tenido una influencia directa en el terreno laboral pero que, sin embargo, ha tenido una gran repercusión en esta tesis y en todo lo vivido este tiempo:

- Indudablemente, a la gente del Forat. Solis, Abel, Oscar, Irina, Sara, Alfon, Laura, Manolo… Me cuesta todavía asimilar el hecho de haber conocido a un grupo de personas tan auténticas y tan afines a mí. La escalada nos unió en un primer momento, pero ahora os habéis convertido en amigos para toda la vida. Gracias por todas las risas y los momentos que hemos pasado juntos, con vosotros la vida es mucho mejor.
- A la gente que, por desgracia, tengo a cierta distancia, pero quiero un montón. Joan, en Estrasburgo se formó algo único y lo que aprendimos juntos me ha acompañado durante todo el doctorado. He echado mucho de menos nuestras charlas y nuestras bromas tontas. Y a la gente de Garrafone, que siempre que he vuelto a casa, es como si el tiempo no hubiese pasado entre nosotros.
- A mi abuelo Ramón, a mis hermanos Jose Ramón y Carla, a mis tíos Araceli y Alberto. A toda mi familia, gracias por estar ahí siempre que lo he necesitado. Y en especial a vosotros, Papá y Mamá, que me habéis ayudado a conseguir lo que me propusiese. Jamás podré devolveros todo el cariño y apoyo que me habéis dado durante toda mi vida. Gracias por haberlo hecho a pesar de la distancia, ya sea en Valencia, Estrasburgo o Barcelona. Sin ninguna duda, gracias a vosotros he llegado hasta aquí. Y no me olvido de ti, Yaya, aunque ya no estés, tu luz siempre me ha guiado. Ojalá tenerte todavía.
- Y por supuesto a Laura, sin ti nada de esto hubiera sido lo mismo. No te imaginas lo que has contribuido a que consiga este reto. Gracias por aguantarme en mis peores momentos, por escuchar mis reflexiones, por seguirme las bromas, por compartir el tiempo conmigo y hacerme un poco más feliz cada día, ya sea en la montaña, en Tailandia o en casa durante el confinamiento. Por todo ello, esta tesis también es tuya. Has hecho que mire estos años atrás y me salga una sonrisa. Y es que juntos somos un poquito más fuertes, podemos con todo.

TABLE OF CONTENTS

1 INTRODUCTION TO BACTERIAL QUORUM SENSING

1.1 QUORUM SENSING (QS)

Formerly, pathogenic processes carried out by bacteria were considered the result of independent bacterium performance and thus, bacteria were seen and studied as individual entities rather than collectives driven by group behaviours. However, nothing could be further from reality. Bacteria communicate, and indeed, their fitness depends on an intricate signalling network that determines the orchestrated and efficient deployment of pathogenic and survival mechanisms. The communication system of bacteria, named Quorum Sensing (QS), was discovered more than 40 years ago by Nealson and co-workers in the marine symbiotic bacterium *Vibrio fischeri* during the study of population density dependent activation of bioluminescence[1]. The study demonstrated that the transcription of bacterial luciferase was only activated when the population density reached a certain level. Therefore, the question was about how could bacteria activate these specific genes and similarly activate bioluminescence collectively. After a few years, it was discovered that the transcription of all the machinery required for this process was subjected to the local concentration of a small organic molecule, elucidated as a homoserine lactone (HSL) type structure[2]. The increase of HSL concentration up to a certain threshold allowed the individual bacteria to sense the population density and activate bioluminescence collectively. Subsequently, the process was carried out more efficiently than if bacteria were performing individually.

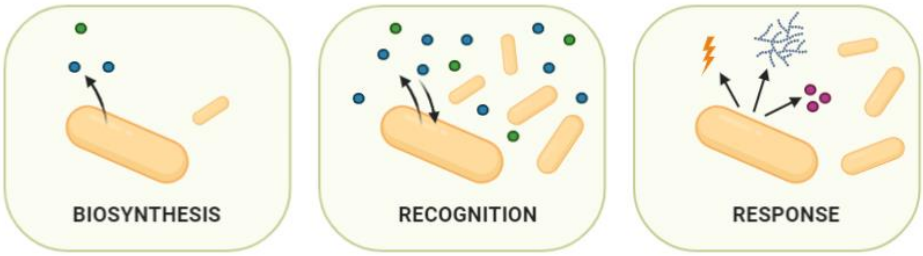

Figure 1.1 Quorum Sensing (QS) process summarized in its three main stages: biosynthesis of signalling molecules, recognition by the surrounding bacteria and response upon attainment of a threshold limit.

During the following years, this communication system was demonstrated to be responsible for the collective activation of the gene expression related to a huge number of bacterial mechanisms. The QS communication, present in every bacterial species, is based on the biosynthesis, liberation and detection of low molecular weight signals called autoinducers (AIs)[3] (see Figure 1.1). These AI are released to the extracellular space and sensed by the surrounding microbial community. Then, when a certain threshold is reached, the coordinated genetic expression is triggered. In a similar manner to *Vibrio fischeri*, pathogenic bacteria drive group behaviour and collectively respond to host environmental stress through QS, otherwise the individual performance of such processes would be ineffective.

Even though all types of bacteria are able to communicate through QS, there are fundamental differences in the communication systems between gram-positive and gram-negative bacteria[4]. For instance, the characteristic AIs used for signalling (e.g. homoserine lactone, quinolone or oligopeptides) and the mode of activation of the related genes triggered by these AI are substantially different in one type of bacteria or another. For that reason, the research about QS has diverged during the past years, concentrating the efforts mainly on the study of one example of each type of bacteria. *Pseudomonas aeruginosa* has been selected as a model in the case of gram-negative bacteria, being characterized by a complex hierarchical network between different sub-systems of communication, relying on different families of small organic molecules[5] (see Figure 1.2). On the other hand, *Staphylococcus aureus* is the most studied bacterium in gram-positive bacteria, relying its communication network on four types of cyclic autoinducer peptides (AIPs). Both pathogens are among the most commonly isolated microorganisms in healthcare-associated and community-acquired infections and it is no wonder that the research has evolved selecting them as a communication system models of each type of bacteria.

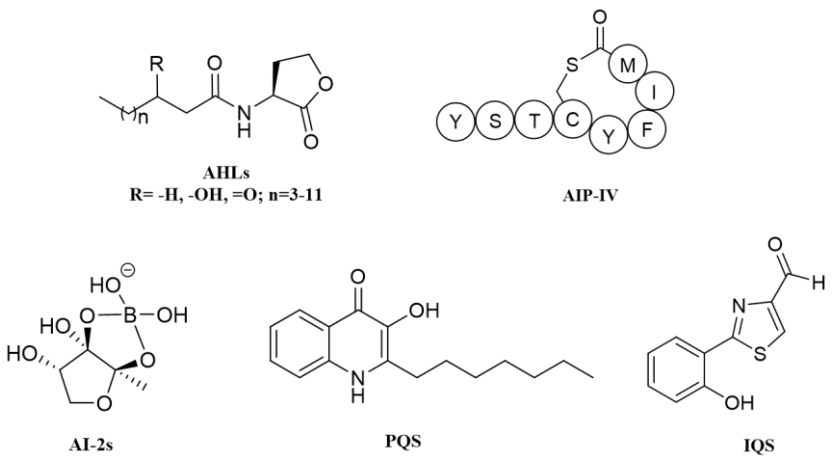

Figure 1.2. Examples of autoinducers (AIs) used by gram-negative bacteria (AHLs, PQS, IQS), by gram-positive bacteria (AIPs, e.g. AIP-IV) or for interspecies interaction (AI-2s) in the quorum sensing signalling process.

1.2 GRAM-NEGATIVE QS: THE *P. AERUGINOSA* MODEL

P. aeruginosa is a ubiquitous gram-negative bacterium able to thrive in a wide array of environments (soil, water, plants, animals and humans). Although it is a commensal bacterium normally kept in check by a healthy host immune system, it behaves as an opportunistic pathogen when there is a breach in the host tissue or the immune response[6]. Healthcare-associated and community-acquired infections (HAI and CAI, respectively) have become a major burden for public health worldwide[7] and *P. aeruginosa* is particularly found among the most commonly isolated microorganisms in clinical settings. According to the Centers for Disease Control and Prevention (CDC), an estimated 51,000 *P aeruginosa* HAIs cases occur each year in US hospitals. This pathogen has developed a vast adaptive response and significant resistance to innate immune effectors and to antibiotics, particularly during chronic infections. Such is the case in CF patients, a disease caused by a genetic disorder that predominantly affects the mucociliary clearance of the respiratory tract[8], creating an ideal scenario for opportunistic pathogens such as *P. aeruginosa*. This pathogen colonizes the lungs of these patients at the age of 2-3 years old and ends up persisting in 60 to 80% of CF cases as a chronic infection, compromising their life and frequently ending in

respiratory failure and premature death[9]. On the other hand, antibiotic therapy rarely leads to elimination of the pathogen from chronically infected CF respiratory airways.

P. aeruginosa is listed in the 2019 Antimicrobial Resistance Threats Report[10] of the US CDC as a serious threat because it shows anti-microbial resistance (AMR) to multiple drugs causing a critical healthcare and economic burden worldwide[11-13]. Hence, in 2017, multidrug-resistant *P. aeruginosa* caused an estimated 32,600 infections among hospitalized patients and 2,700 estimated deaths in the US[14]. According to the 2017 Annual report of the ECDC (European Center for Disease Control), *P. aeruginosa* was found to be resistant to ceftazidime and carbapenem in 26.5% and 25.9% of the cases, respectively. It should be noticed that prescription of these antibiotics was established to precisely treat bacteria that had already developed resistance to other drugs. In that respect, WHO has recently published a list declaring the urgent need of finding new antibiotics for treatment of infections caused by resistant bacteria, such as carbapenem-resistant *P. aeruginosa*[15]. However, as important as the treatment of infections is the fast identification of the causative agent, crucial for an early eradication of the pathogen, avoiding the shift between transient and persistent infections[16]. The lack of reliable tools for rapid diagnostic of infectious diseases has contributed to the overprescription and misuse of broad-spectra antibiotics, strengthening the generation of multi-drug resistant bacteria[17].

For instance, lung diseases caused by microbial infections affect hundreds of millions of children and adults throughout the world. Particularly, in Western countries, the treatment of lung infections is a primary driver of antibiotic resistance[18]. Moreover, molecular analyses of the lung microbiota are revealing profound adverse responses to widespread antibiotic use, urbanization and globalization. Therefore, there is an urgent need to improve diagnosis of these diseases. In most clinical laboratories bacteriological diagnosis depends on microbial culture followed by subsequent identification using biochemical, molecular o mass spectrometric technologies. However, such approach has many subjective elements, such as differentiation of pathogens from commensals by colony morphology. On the other hand, the use of specialized culture media or anaerobic culture can stretch the capacity of routine clinical laboratories, and protocols may be erratically guided by clinical suspicion. It has

been reported that failure to identify causal organisms occurs in 50% of patients who have been hospitalized with pneumonia in intensive care units[19]. As consequence, the administration of antibiotics before specimen collection and pathogen identification is an omnipresent problem.

For all these reasons, many diagnostic alternatives have emerged as potential complements of the standard techniques, providing more complete and accurate results. Subsequently, new strategies and biomarkers are also under study for the diagnostic of *P. aeruginosa* infections. With this aim, one of the targets that has attracted the attention of many researchers in both therapy and diagnostics of infectious diseases is the bacterial communication process known as QS[20,21].

The study of QS in gram-negative bacteria has been mainly focused in *Pseudomonas aeruginosa*, selected as a model by its particularly intricate QS circuit and the relevance and incidence of this pathogen in clinical settings. *P. aeruginosa* possesses a complex QS structure in which four interconnected systems (*las*, *rhl*, *pqs* and *iqs*) perform in a hierarchical manner, following a sophisticated regulatory network in order to maintain the population homeostasis during an infectious process[22]. Each QS circuit has a characteristic chemical signal that binds its cognate receptor protein, initiating the corresponding positive and/or negative regulation cascades. The signalling molecules of the *las* and *rhl* systems were discovered more than 20 years ago and they consist into two structurally different homoserine lactones, N-(3-oxododecanoyl)-L-homoserine lactone (3-oxo-C12-HSL) and N-butyryl-L-homoserine lactone (C4-HSL), respectively[23,24]. The main signalling molecule of the *pqs* system is 2-heptyl-3-hydroxy-4(1H)-quinolone or PQS (*Pseudomonas* quinolone signal), which accomplish multiple functions besides its signalling activity[25]. The biological precursor of PQS, 2-heptyl-4-quinolone or HHQ can also take over signalling and modulate bacterial functions[26] (see Chapter 3 for additional information on the pqs system and its biological and clinical significance). The characteristic AI of the forth and most recently discovered QS system corresponds to 2-(2-hydroxyphenyl)-thiazole-4-carbaldehyde, also named as the system in which participates, IQS (Integrated Quorum Sensing signal)[27].

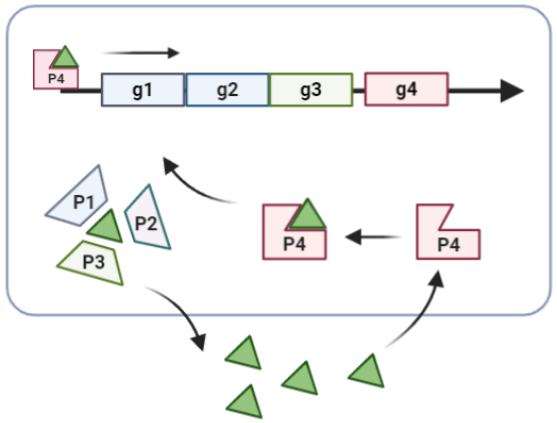

Figure 1.3. General representation of the QS systems auto-induction loop mode of action in gram-negative bacteria. This process involves the biosynthesis, release and detection of autoinducers (green) and eventually, the regulation of the corresponding implicated genes.

Once the aforementioned signalling molecules are biosynthesized and released, they can enter into the cytoplasm and bind to their cognate transcriptional activators (LasR, RhlR, PqsR and unknown receptor for *iqs* system). Afterwards, upon binding of the complexes to the gene promoters, the expression of the associated regulons is triggered (see Figure 1.3). In these particular activated genome regions are located the sequences of the synthase proteins associated to the AI production (LasI, RhlI, PqsABCDH and PchABCDEF, respectively). Therefore, each complex (e.g., PqsR/PQS) generates an autoinduction loop that increases dramatically the number of QS signals while also being responsible for the regulation of a wide variety of genes related with virulence, biofilm formation and secondary metabolism[5]. Nevertheless, not only the complexes activate their associated regulons but also are able to exert control over the regulons or genes related to other systems (Figure 1.4).

At the top of the signalling network is the *las* system, which LasR/3-oxo-C12HSL complex, after multimerization, positively regulates the expression of receptor and synthase genes of all other QS systems, thus establishing a regulation feed-forward loop[22,28,29]. The *rhl* system exerts negative control over the expression of *pqsABCDE* and *pqsR* genes. Hence, the activation of *pqs* signalling system seems to be dependent of the ratios between 3-oxo-C12-HSL and C4-HSL[30]. Interestingly, the PqsR/PQS complex activates the expression of RhlI, thus increasing the production of C4-HSL and the overall expression of the *rhl*

system[31]. Therefore, the *rhl* system, which controls a great number QS-dependent virulence factors, is boosted by both *las* and *pqs*. Similarly, IQS activates the expression of *pqs* genes and subsequently the *rhl* signalling system[27]. This convoluted communication structure is even more complex if we take into account the possible QS system mutations found in CF patients[32], the capability to overcome the mutations by other systems[33] and the effect of environmental stress on the signalling process[27].

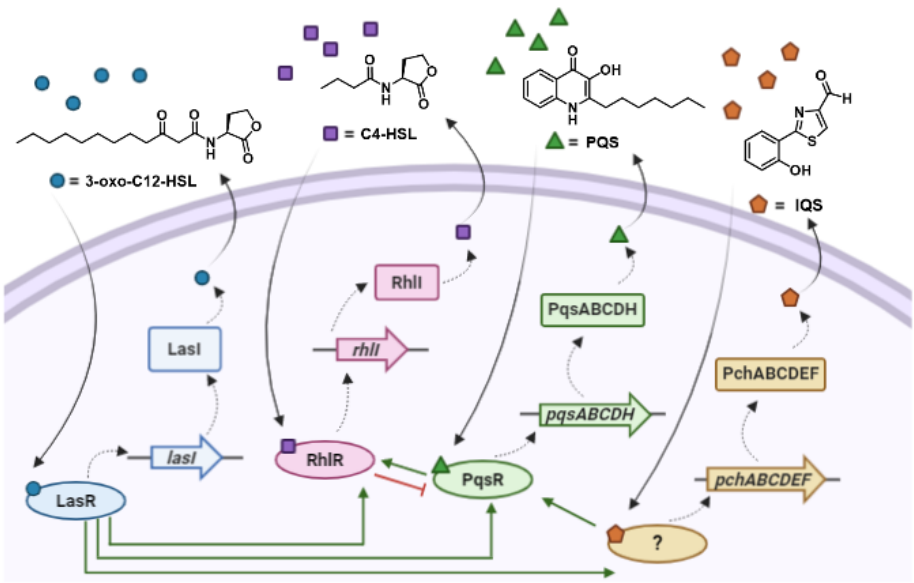

Figure 1.4. Pseudomonas aeruginosa Quorum Sensing signalling network. Each of the systems (las, rhl, pqs and iqs) are schematically represented including the transcriptional activators (LasR, RhlR, PqsR and unknown for iqs system), the genes related to biosynthesis of autoinducers and the synthase proteins (LasI, RhlI, PqsABCDH and PchABCDEF). The hierarchical character of the QS network is represented by green/red arrows).

1.3 GRAM-POSTIVE QS: THE *S. AUREUS* MODEL

Staphylococcus aureus is both, a commensal bacterium and a human pathogen able to cause a diverse array of infections[34]. Particularly, *S. aureus* is a major agent of healthcare-associated infections, being one of the most prevalent causes of nosocomial bacteraemia, hospital-acquired pneumonia, and surgical

site infections[35]. The situation gets even worse in immunocompromised patients or individuals presenting other underlying diseases such as Cystic Fibrosis (CF), the most common autosomal hereditary disease in Caucasians. CF is caused by a mutation in a transmembrane conductance regulator that leads to an abnormal production of mucus and blockages in the digestive and respiratory systems. This scenario favours the appearance of recurrent bacterial airways infections that eventually, prompt respiratory failure and death[36]. *S. aureus* is one of the earliest pathogens isolated from the airways of CF patients (more than 70% of neonates have positive culture and 45% become persistently colonized[37]) and the differentiation of simple carriers from infected individuals during their lifetime remains a great challenge. Therefore, the fast and proper identification of the causative agent is crucial providing an appropriate treatment. However, the identification of *S. aureus* infections, such as that of the respiratory tract, using the current standard techniques based on culture plate, leads to poor or inaccurate results that are aggravated by the presence small colony variants (SCVs). These auxotrophic variants are not particularly virulent but rather show higher persistence due to its reduced metabolism and become more relevance during chronic infections. SCVs have a slower growth rate and thus, are frequently overlooked or misidentified in culture plates[38,39]. In addition, culture diagnostic techniques may take up to 72 hours after pure growth to confirm a positive result, promoting the use of broad-spectrum antibiotics and generation of antimicrobial resistance[40].

On the other hand, the genomic plasticity of this pathogen has prompt the emergence of hyper virulent and drug-resistant strains. After its first report in 1961, methicillin-resistant *S. aureus* (MRSA) it is known to spread worldwide, causing major outbreaks in form of acute and chronic infections[41,42], the prevalence of which varies geographically. In 2017, the Centre for Disease prevention and Control (CDC) of the US, estimated 323,700 MRSA cases in hospitalized patients, which led to 10,600 estimated deaths and a healthcare cost of 1,7 billion dollars[43]. In 2014, the European centre for disease, prevention and control (ECDC) reported that in Europe the percentage of *S. aureus* strains identified as MRSA ranged from 0.9% in Netherlands to 56% in Romania, from which 7 out of 29 countries showed percentages over 25%[44]. However, the surveillance effectuated in North America and Europe, which has been extensively conducted in comparison to other areas, do not represent the global

S. aureus epidemiology, as the population of the corresponding countries do not account for one-third of the world's total population[45].

Therefore, there is an increasing need of finding novel approaches that allow fast and accurate pathogen identification to complement current bacterial diagnostic methods, allowing in turn a faster and more specific management of the patients. Subsequently, there is still a research demand on developing new diagnostic methods that meet, ideally, the technical requirements covered by the ASSURED acronym criteria: affordability, sensitivity, specificity, user-friendliness, rapidity and robustness, no equipment needed and deliverable to end users[46]. Devices and techniques that fulfil the aforementioned requirements are included in the point-of-care (PoC) testing and their implementation in infectious diseases diagnostic would substantially improve the management of the patients and facilitate a more complete epidemiologic evaluation of the *S. aureus* infections. PoC devices usually incorporate biorecognition elements that allow the specific detection of a selected target, and such is the case of antibodies. These bio-macromolecules allow to detect with a high degree of specificity a selected target in complex samples by means of their great affinity. In the case we sought to implement these type of testing for the diagnostic of *S. aureus* infections, the most important step would be the selection of a representative target that provide relevant information about the subject of study. This might be the case of bacterial Quorum Sensing, which close connection with the fitness and development of pathogenic bacteria makes it a suitable target for diagnostic and therapy purposes. In the case of gram-positive bacteria, the bacterium unanimously chosen as a model for the study of the QS has been *Staphylococcus aureus*.

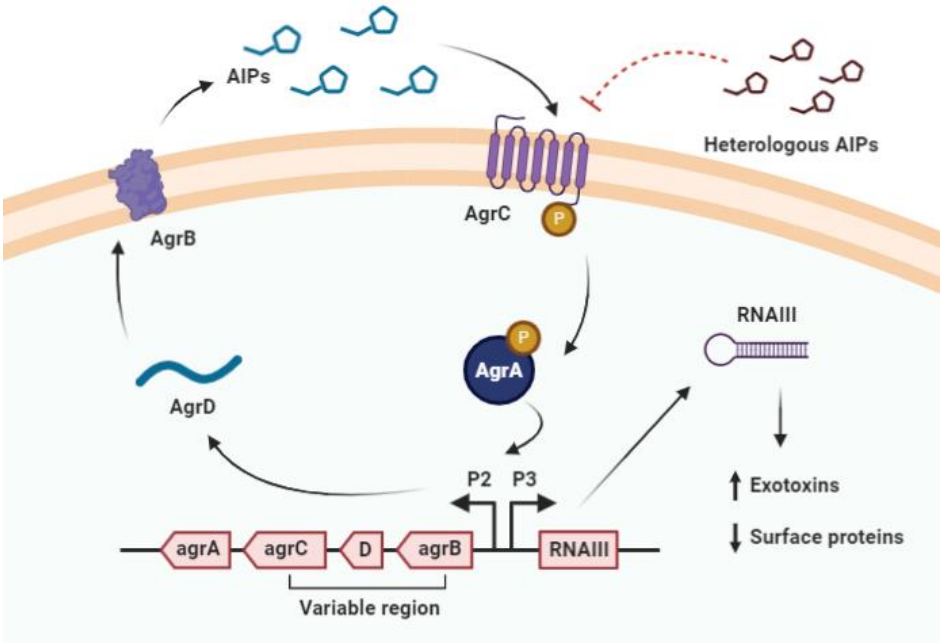

Figure 1.5. General representation of the Quorum Sensing signalling system of *S. aureus*. The representation includes all the proteins and factors involved in the signalling process, the *agr* locus and RNAIII.

QS in gram-positive bacteria is based on the release and detection of oligopeptides, which may differ in the length, sequence and three-dimensional structure between the different bacterial species[4]. In the case of *S. aureus*, these peptides and all the proteins and factors required for the communication system (AgrB, AgrD, AgrC, AgrA) are encoded by the *agr* locus (*agrBDCA*), which contains two divergent transcription units (effector and response regulator)[47]. The biosynthetic route (see Figure 1.5) of AIPs and signalling pathway starts with AgrD, corresponding with the pro-peptide sequence of the AIP. AgrD is first processed by the membrane peptidase AgrB, to generate a thiolactone intermediate[48]. This intermediate is immediately exported across the membrane and submitted to a second cleavage to release the mature AIP into the extracellular space. The AIP is the active signal of the sensing network, which is detected by a classic two-component signalling system (TCS) consisting of AgrC, the membrane receptor histidine kinase, and AgrA, the response regulator. The AIP interacts with AgrC to activate a phosphorylation cascade that leads to the

phosphorylation of AgrA[49]. Afterwards, AgrA binds to the P2 promoter and up-regulates the transcription of RNAII and thus, the biosynthesis of all *agr* proteins, conferring positive feedback loop to the AIP production. The activated AgrA is also able to bind to the P3 operon which encodes RNAIII, the mRNA for δ-toxin and a pleiotropic regulatory factor[47]. RNAIII primarily functions through base-pairing to the 5' ends of virulence-factor mRNAs, suppressing the synthesis of proteins required for the adhesion phase of the life cycle, while de-repressing those involved in the invasion phase (see Chapter 8 for additional information on the S. aureus QS system and the biological and clinical significance of the AIPs).

1.4 QS AS DIAGNOSTIC TARGET

Both aforementioned bacteria are included in the group of so-called ESKAPE pathogens (*Enterococcus faecium, Staphylococcus aureus, Klebsiella pneumoniae, Acinetobacter baumannii, Pseudomonas aeruginosa, and Enterobacter species*), a classification of multidrug resistant "superbugs'', and have been classified as critical pathogens in the World Health Organization (WHO) list of research and priorities for the development of new antibiotics[50]. Therefore, there is an increasing urgent need of finding novel strategies to deal with this new generation of resistant bacteria[51].

The fast detection and correct identification of a disease causative microorganism in the context of an infectious process is crucial for an adequate treatment (see Figure 1.6). However, the lack of approved rapid and efficient *in vitro* diagnostic (IVD) methods capable of providing reliable and fast results, has led to the prescription and misuse of broad-spectra antibiotics, contributing to the generation of resistance[17]. Current laboratory diagnostic methods for the detection of both microorganisms are mostly based on standard culture techniques, which can take up to 72h in order to obtain conclusive results, and that are hampered by suboptimal sensitivity[40]. Mass spectrometry, particularly MALDI-TOF-MS[52-54] and molecular detection tools, namely PCR[55-57], have emerged as interesting approaches to overcome culture handicaps[58]. However, these methods normally require specific equipment, highly qualified personnel, and tedious extractions and/or purification steps[59]. A rapid, low-cost, user-friendly option would be the use of Point of Care (PoC) devices based on the use

of biorecognition elements[60,61] to detect and identify bacterial agents, which could improve the performance of the existing gold standard techniques in terms of specificity and sensitivity. In this context, biosensor techniques provide great versatility allowing development of interesting and innovative optical and electrochemical biosensor approaches incorporating the latest knowledge in microelectronics and nanobiotechnology. However, a key issue is the availability of high quality bioreceptors addressing recognition of appropriate specific biomarker targets related to the microorganism causing the infection.

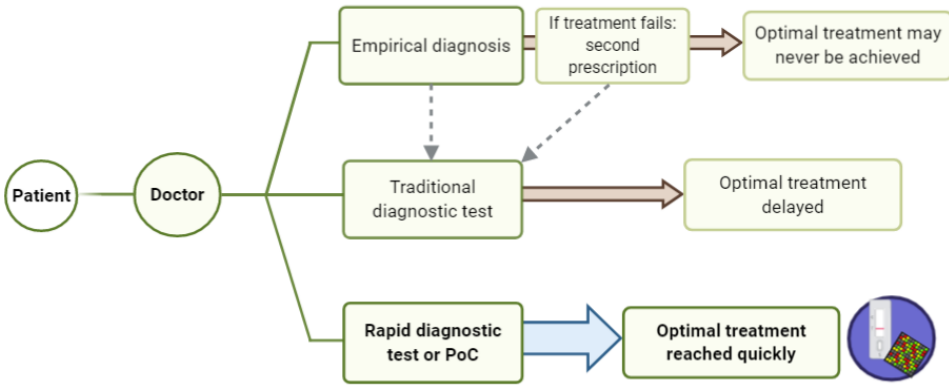

Figure 1.6. Schematic representation of the current methodology on the diagnostics of infectious diseases, including the hypothetical use of rapid diagnostics tests and the possible outcomes derived from the use of such methodology.

Recently, bacterial Quorum Sensing (QS) has attracted attention as an interesting goal to develop innovative therapeutic and diagnostic approaches[62-66]. This intercellular population-density based communication system might serve not only for pathogen identification strategy but also for providing important information about the stage of disease and/or and virulence of the causative strain due to its close relation with bacterial fitness and pathogenic transitions (see Figure 1.7).

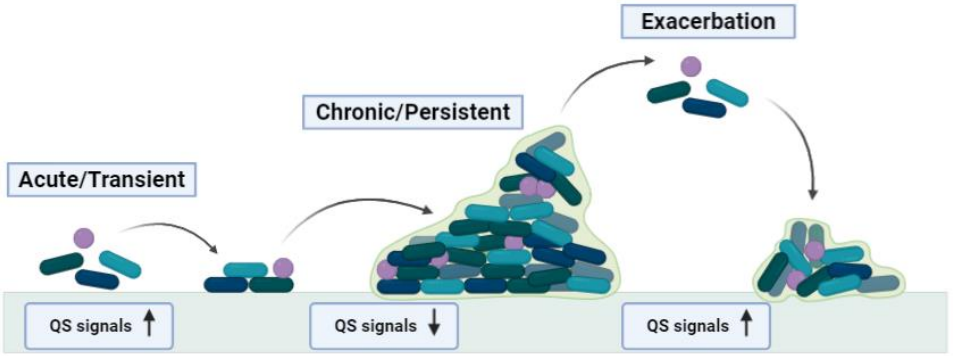

Figure 1.7. Lifestyle transitions adopted by pathogenic bacteria in the host, type of infection and relative concentration of QS signals during the transitions.

The QS signalling molecules are released to the extracellular space for communication and regulation purposes. Therefore, when the pathogen is inside the host and due to their chemical nature, these molecules can be found in the infected tissue and several body fluids[63,67-69]. As a result, AIs could potentially work as biomarkers of infection, providing relevant information and helping clinicians on the decision-making process for the management of infected patients. Several analytical approaches have been developed for the quantification of several QS molecules in clinical samples or bacterial cultures mainly based on the use of LC-MS[70-74]. Its effective detection points to the potential value of these molecules as biomarkers of infection. However, a major drawback of these techniques is the need of prior sample treatment or pre-concentration in order to detect and quantify these molecules, making the procedure complex and difficult for routine implementation in clinical settings. Moreover, there is the risk of degradation or neglecting the analytes of interest. As an alternative, immunochemical techniques offer the advantage to be able to quantify biomarkers at very low concentration levels directly in clinical samples or culture media without the need of previous extraction, pre-concentration or purification steps. This is due to the high affinity and specificity of the antibodies used as biorecognition elements. Antibodies are exceptional molecules for this purpose, but small molecules do not elicit an immune response, and therefore sometimes are difficult to obtain. This the case of the QS molecules from the bacteria discussed herein and the starting point of this thesis.

2 CONTEXT SCENARIO, OBJECTIVES AND STRUCTURE

2.1 RESEARCH PROJECT

The present thesis has been developed within the framework of two different research projects:

1. **ImmunoQS project. Immunochemical Diagnostic and Therapeutic Strategies based on the Quorum Sensing System.** (SAF2015-67476-R, MINECO, Dirección General de Investigación Científica y Técnica, Subdirección General de Proyectos de I+D.)
   The final goal of the **Immuno-QS** project was to advance in the knowledge of the mechanisms involved in the pathogenesis caused by two important microorganisms (*Pseudomonas aeruginosa* and *Staphylococcus aureus*) with a clear intention of improving the treatment and the diagnostics of infectious diseases caused by these pathogens, through immunochemical studies of their Quorum Sensing (QS) systems as therapeutic and biomarker targets. Within the objectives of the Immuno-QS project was to develop specific antibodies against relevant QS signalling molecules which regulate secretion of the most important virulence factors and the formation of biofilms in these bacteria. The project addressed the investigation of the possibility of quenching these QS signals by antibody capture as a therapeutic approach that could accomplish neutralizing both, the QS activity and the toxic and virulence mechanisms. Moreover, the potential value of the QS molecules as biomarkers of infection was investigated by developing immunochemical methods addressed to profile the expression of different QS signalling molecules. To ensure the translational character of the research proposed, the project counted with the implication of two clinical groups: 1. HGTiP, Microbiology Laboratory (Hospital Germans Trias i Pujol, Badalona, Spain) and 2. HUVH, Microbiology Laboratories and Respiratory Units of the Hospital Vall d'Hebrón (Hospital Vall d'Hebron, Barcelona, Spain).

2. **QS4CF Project. Targeting Quorum Sensing for the Management of Cystic Fibrosis**. (RTI2018-096278-B-C21, MINECO, Dirección General de Investigación Científica y Técnica, Subdirección General de Proyectos de I+D.)

The **QS4CF** project is a continuation of the **Immuno-QS** project. With the same final goal. The project will address three applied objectives: i) generating knowledge on the QS role driving *colonization towards infection* (in collaboration with HGTiP), ii) investigating the potential value of QS molecules as biomarkers of infection in patients suffering respiratory diseases and CF (in collaboration with HGTiP and HUVH) and iii) assessing the potential therapeutic value of the anti-QS antibodies on in *vitro* assays. The selection of the new QS targets was based on the knowledge obtained from the Immuno-QS project, which pointed several relevant targets for *P. aeruginosa* and *S. aureus*. Patients suffering CF were identified as a priority based on the prevalence of infection by these bacteria and the impact in their life expectancy. In this context, PoC devices have been considered in the project as an important need for appropriate CF routine microbiological controls. For this purpose, the project counted with the collaboration of the Bioanalysis and Biosensors group of the University of Alcalá de Henares. Moreover, the above mentioned clinical groups were also involved.

2.2 OBJECTIVES AND SCIENTIFIC STRATEGY

With this scenario, the final goal of this thesis was to improve the efficiency of the diagnostic of infections caused by *P. aeruginosa* and *S. aureus* through a better understanding of the bacterial communication process known as Quorum Sensing (QS) and its implication on the pathogenesis. Particularly, we were interesting on getting knowledge on the correlation of the appearance of these metabolites in the body fluids or selected clinical samples, and their concentration, with the status of the disease in order *to* assess the potential role of these molecules as biomarkers of infection.

The strategy proposed to accomplish this objective was the development of immunochemical methods to profile the expression of different QS signalling molecules, to obtain additional information of their implication in the progress the pathogenesis of *S. aureus* and *P. aeruginosa*. To accomplish this aim, the following specific objectives were addressed:

1. Design and synthesis of haptens for the non-immunogenic QS molecules produced by *P. aeruginosa* (2-heptyl-4-quinolone (**HHQ**), 2-heptyl-3-hydroxy-(1H)-4-quinolone (**PQS**) and 2-heptyl-4-hydroxyquinoline N-oxide (**HQNO**)) and *S. aureus* (**AIP-I to IV**).

2. Synthesis of bioconjugates for the generation of specific polyclonal antibodies against the QS molecules from both aforementioned pathogenic bacteria

3. Development of immunochemical analysis tools for the quantification of these bacterial QS molecules.

4. Investigating the potential of developing a multiplexed platform containing the different immunochemical reagents previously generated for QS profiling.

5. Performance of preliminary studies about the potential value of selected target QS molecules as biomarkers of infection using the developed immunochemical techniques.

2.3 THESIS STRUCTURE

The structure of the present thesis, including the content of each chapter is shown in Figure 2.1. The main chapters (3 to 9) are divided according to the different bacteria studied in this thesis. With this purpose, Chapters 3 and 8 are introductory chapters that summarize the most recent findings regarding the biological and clinical significance of *P. aeruginosa* and *S. aureus*, respectively, providing also an overview of the state of the art regarding quantification techniques of the QS molecules. Afterwards, Chapters 4 to 6 report the results from the research performed in this thesis in respect to the development and evaluation of immunochemical techniques for the quantification of three different *P. aeruginosa* QS molecules, which give name to the chapters. Chapter 7 is an overview of Chapters 4 to 6, including preliminary studies about the multiplexation of the techniques for *P. aeruginosa* QS molecules. Chapter 9

describes the immunochemical strategy accomplished for the quantification of AIP-IV, used as a model for future development of analytical tools for the quantification of the other AIPs from *S. aureus*. Chapter 10 contains the main conclusions of this thesis and summarizes the contributions of each chapter. Chapter 11 contains a summary written in one of the original languages of the PhD program and Chapter 12 includes all the bibliography on which all the work has been supported. Finally, in chapter 13 are gathered all the acronyms used in the present thesis and table of figures and tables.

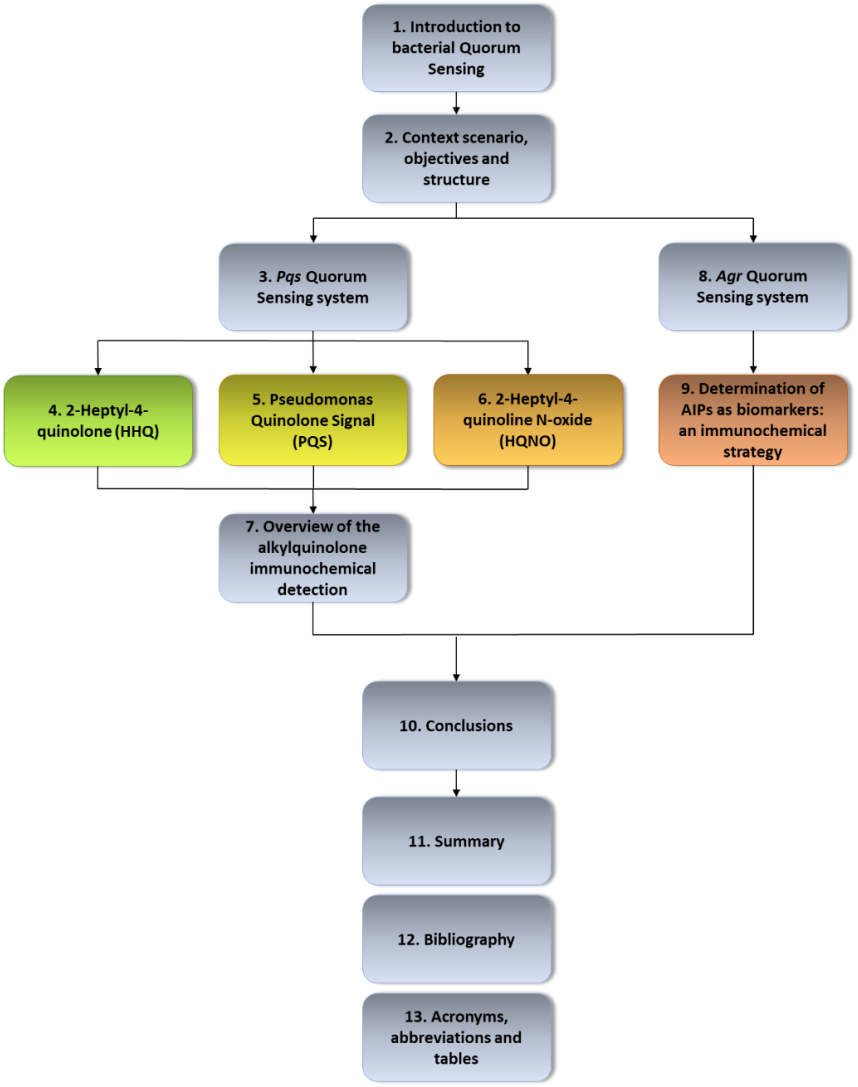

Figure 2.1. Structure of this thesis related to the different chapters.

3 *PQS* QUORUM SENSING SYSTEM

3.1 CHAPTER PRESENTATION

The main objective of this chapter is to provide an updated review about the biological and clinical significance of the quinolone-based QS communication system of *P. aeruginosa*. The *pqs* QS system has a wide implication in bacterial survival and pathogenicity and for this reason might serve as a promising diagnostic and therapeutic target. This chapter aims to be a common introduction of Chapters 4, 5 and 6 reporting the research performed in respect to the development of immunochemical techniques for the detection of different alkylquinolone QS metabolites from *P. aeruginosa*. The schematic representation of the chapter structure is shown in Figure 3.1.

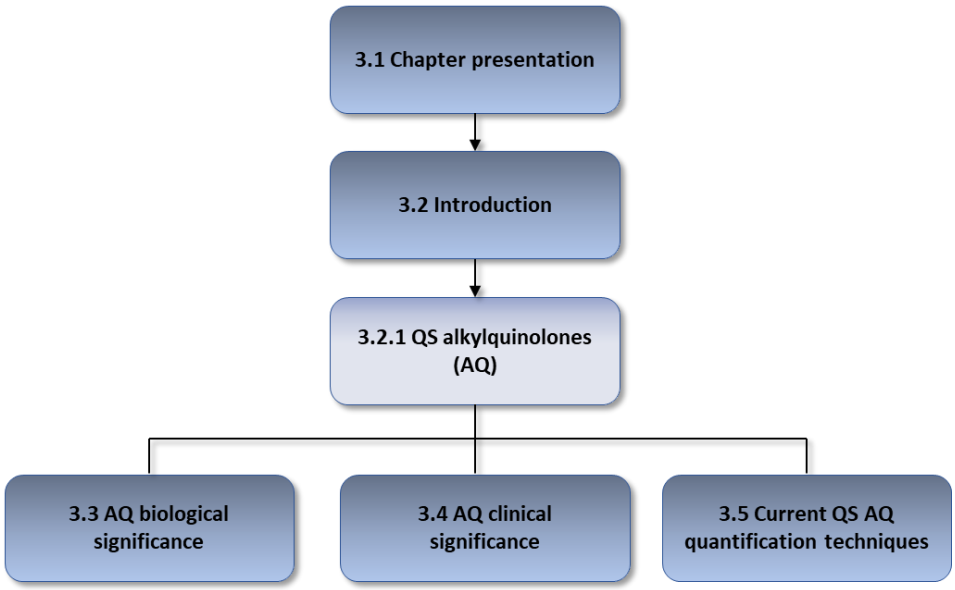

Figure 3.1. Structure of Chapter 3 related to the different sections.

3.2 INTRODUCTION

3.2.1 QS ALKYLQUINOLONES (AQ)

Host-pathogen interaction involves the release of a large amount of molecules, which potential as biomarkers for diagnosis, patient stratification, disease monitoring or for guiding antibiotic treatment is being the subject of investigation[75,76]. Because of their key role in the development of the pathogenesis, the signalling molecules of the Quorum Sensing (QS) system could be potential biomarker targets.

Particularly in *P. aeruginosa*, the quinolone-based *pqs* QS system, responsible for the regulation of virulence factors including pyocyanin (PYO), elastase, lectine and rhamnolipids[22], has specially attracted the attention of the scientific community due to their QS-dependent and independent functions. The main signalling molecule in the alkylquinolone (AQ) based *pqs* communication system is 2-heptyl-3-hydroxy-4(1H)-quinolone (PQS) and performs many bacterial functions besides its signalling activity[25]. Although PQS has focused the vast majority of studies, *P. aeruginosa* produces other AQ that also carry out crucial processes for bacterial survival, such as 2-heptyl-4-quinolone (HHQ) or 2-heptyl-4-hydroxyquinoline N-oxide (HQNO).

3.2.1.1 AQ biosynthesis

The *pqs* QS system is genetically composed by at least five transcriptional units. Namely, *pqsABCDE* together with *pqsR* and *phnAB* are gathered in the same locus and the units *pqsL* and *pqsH* are both in distal regions[77]. Altogether, the codified proteins and factors from these regions are responsible for the biosynthesis of more than 50 quinolone metabolites from which PQS, HHQ and their C-9 alkyl chain homologues activate the PqsR transcriptional activator and subsequent regulate the *pqs* signalling system[78,79].

The biosynthetic route starts with anthranilic acid (Figure 3.2) which is produced, at least in part, by the PqsR-dependent anthranilate synthase codified by *phnAB*[80,81]. Then, the carboxylic acid is activated by action of PqsA, an

anthranilate-Coenzyme A ligase[82]. Interestingly, it has been shown that PqsA is implicated in virulence by regulating pyoverdine production and biofilm formation in a PQS-independent manner under rich medium. However, PQS can also prompt and take over a biofilm-independent pyoverdine production[83]. Furthermore, the inactivation of *pqsA* leads to the elimination of AQ production and the accumulation of anthranilic acid[84].

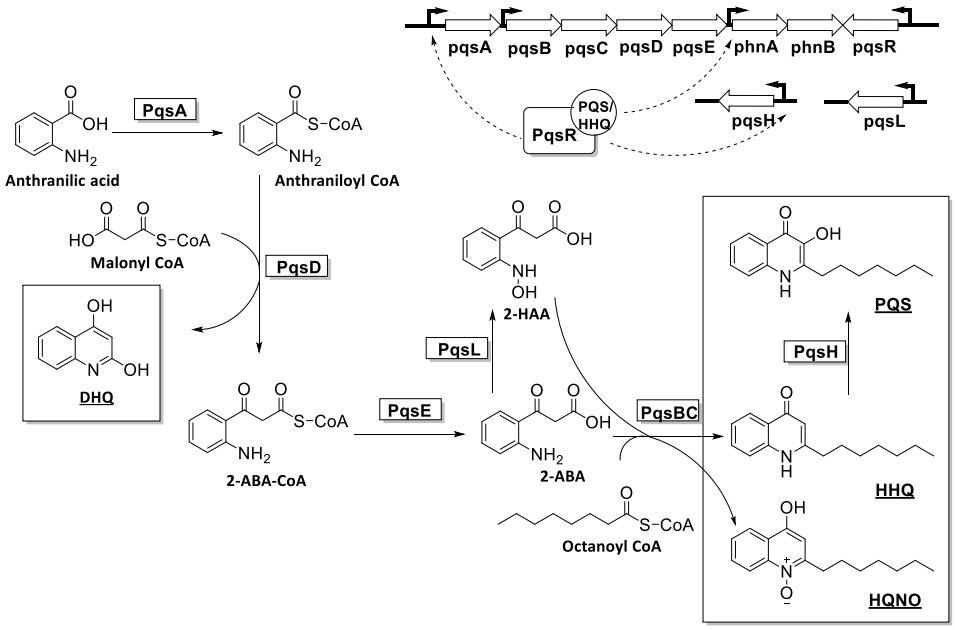

Figure 3.2. Schematic representation of regulated *pqs* system quorum sensing genes and the corresponding implicated enzymes, substrates, signalling molecules and secondary metabolites in *P. aeruginosa*. DHQ: 2,4-dihydroxyquinoline; 2-ABA-CoA: 2-aminobenzoylacetyl-Coenzyme A; 2-ABA: 2-aminobenzoylacetate; 2-HAA: 2-hydroxylaminoacetophenone; HHQ: 2-heptyl-4-quinolone; HQNO: 2-heptyl-4-hydroxyquinoline N-oxide; PQS: 2-heptyl-3-hydroxy-4(1H)-quinolone.

The biosynthetic pathway continues with condensation of anthraniloyl-CoA with malonyl CoA to form 2-aminobenzoylacetyl-CoA (2-ABA-CoA) by action of PqsD, a 3-oxoacyl-acyl carrier protein (ACP). In addition, PqsD is responsible for the formation of 2,4-dihydroxyquinoline (DHQ). This non-alkylated quinoline specie has gone unnoticed in many publications about the QS of *P. aeruginosa*, and yet this molecule could have an important role for the bacterium pathogenicity[85]. For instance, mutant strains just producing DHQ are able to maintain PYO production and antifungal activity. Unlike PQS, DHQ biosynthesis does not need

oxygen species and can be produced in anaerobic conditions, a situation normally found in the thick mucus of CF patient lungs. Eventually and even more strikingly, this molecule can interact with PqsR and influence the expression of the *pqs* operon[86].

Compared to the function of the rest of *pqs* operon encoded factors, the enzymatic role of PqsE in AQ biosynthesis has been recently found out, being responsible for converting 2-ABA-CoA into 2-aminobenzoylacetate (2-ABA) due to its thioesterase activity. It was formerly thought that this enzyme did not participate in AQ biosynthesis because *pqsE* mutants still produced HHQ and PQS[87]. However, this effect has been attributed to the presence of other enzymes in *P. aeruginosa*, such as the TesB and other un-identified broad-specificity thioesterases. Nevertheless, this enzyme is currently target of several and controversial hypotheses due to its yet unexplained multiple functions[88,89]. For instance, the activity of PqsE has also been proved to be tightly linked with the *rhl* QS system. Similar to the *rhl* mutants, *pqsE* mutants completely abolished the production of PYO, thus demonstrating the importance of PqsE in virulence and giving rise to the relation with *rhl* system. Mukherjee and co-workers revealed that *pqsE* and *rhlR* mutants show similar phenotype in contrast to *rhlI* mutants, thus suggesting that PqsE and RhlR might be a synthase-transcriptional activator pair that control several virulence genes and drives group behaviours in *P. aeruginosa*[90] (Figure 3.3). Moreover, the authors demonstrate that PqsE is required and RhlI is dispensable for RhlR directed virulence. They prove the existence of a yet un-identified autoinducer that would connect this two QS factors, showing the dual functionality of RhlR, performing into two separate regulation pathways. PqsE also regulates the expression of hydrogen cyanide, rhamnolipids and chitinase biosynthesis and thus, considering that PqsE does not have DNA-binding domain, it further supports the hypothesis of the existence of an alternative autoinducer[91].

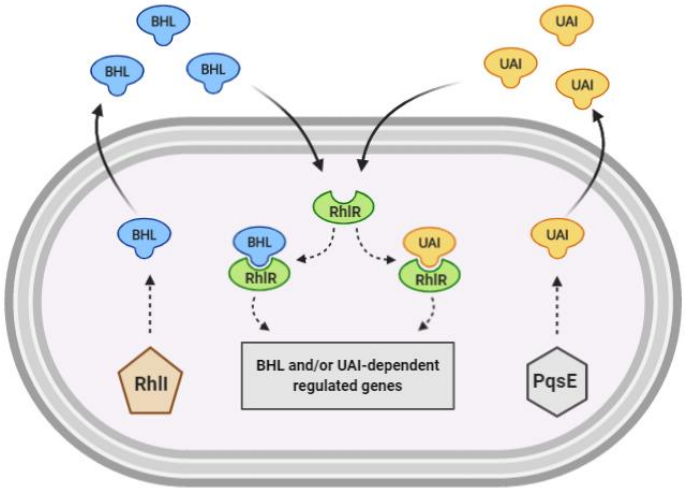

Figure 3.3. Schematic representation of the RhlR dual ligand binding and the role of PqsE as synthase protein of the unknown autoinducer (UAI) required for the regulation of the RhlI-independent virulence genes.

Following the biosynthesis of quinolones, the aforementioned 2-ABA substrate can follow different synthetic pathways in order to produce two different of quinolone related metabolites in *P. aeruginosa*. One of the routes is HHQ production, catalysed by the heterodimer ACP FabH like PqsBC. It carries out the condensation of 2-ABA and octanoyl-CoA, and not 3-ketodecanoic acid as it was previously thought[92,93]. On the other route, 2-ABA suffers oxidation of the amino group to form 2-hydroxylaminoacetophenone (2-HAA) by action of PqsL flavin dependent monooxygenase[94]. Afterwards, PqsBC is similarly responsible for the condensation of octanoyl-CoA with 2-HAA to form HQNO, a non-signalling molecule with great importance for *P. aeruginosa* virulence and interspecies interaction[95]. PqsBC not only uses octanoyl-CoA as the AQ alkylic chain provider but also employs other medium-chain length acyl-CoAs to produce AQ and AQ-N-oxides (AQNO) saturated and mono-unsaturated alkyl chain congeners[96]. Therefore, PqsBC remains a crucial factor for the production of signalling molecules and metabolites in *P. aeruginosa* and similarly to a *pqsA* mutant, the inactivation of *pqsBC* results into non-production of quinolone/quinoline derivatives[84,97].

Eventually, HHQ is converted to PQS by action of PqsH, another putative flavin dependent monooxygenase that hydroxylates HHQ at C-3 position[98]. PQS presents the highest affinity for the transcriptional activator PqsR in the *pqs*

system, although HHQ can also work as signalling molecule but around 100 times less potently[22]. It has been observed that PqsH shows higher affinity for quinolone substrates with C-7 and C-9 alkyl chain length, thus establishing a selection step for other quinolone metabolites. On the other hand, the production of PQS is also affected by the environmental conditions. For instance, PQS is not produced under anaerobic conditions due to PqsH oxygen requirement. However, the production of PQS is immediately restored upon exposure to molecular oxygen, a transition frequently found in the lungs and mucus of CF patients (planktonic/acute to biofilm/chronic or exacerbations periods)[9,99]. In summary, the biosynthesis of quinolones and *pqs* signalling molecules of *P. aeruginosa* depends on several interconnected factors with multiple roles in the pathogenicity and survival of *P. aeruginosa*.

3.3 AQ BIOLOGICAL SIGNIFICANCE

AQ or AQNO are a groups of metabolites with high influence in the pathogenicity and survival of *P. aeruginosa* by either QS-dependent or independent mechanisms. Regarding QS, the main signalling molecule of the *pqs* system is PQS. This AI increases dramatically the expression of the genes involved in the signalling process, virulence and secondary metabolism by binding to its cognate receptor and transcriptional activator PqsR[100]. However, it has been demonstrated that HHQ, the immediate precursor of PQS, is also able to bind PqsR. Upon binding, HHQ induce a conformational change in the receptor and, the generated complex, binds in turn to the *pqsABCDE* promoter region in similar manner to PQS, although around 100-fold less potently. Interestingly, a *pqsH* mutant unable to produce PQS overcome PqsR-dependent gene expression and virulence by action of HHQ[101]. It is noteworthy that a mutation in *pqsR* leads to lowered production of elastase, exoprotein, LecA, rhamnolipid and pyocyanin together with termination of *phnAB* and *pqsABCDE* expression[30,97,102]. Hence, the proper transcription of *pqsR*, controlled in turn by *las* and *rhl*, is crucial for AQ production and pathogenicity in plants and animals. On the other hand, overexpression of *pqsR* leads to repressed metabolic degradation of anthranilate to ensure AQ production[103].

Certainly, QS molecules are the key element of a sophisticated communication system in bacteria. Nonetheless, these molecules are also able to exert multiple functions besides their signalling activity and regulate a great number of biological processes (Figure 3.4).

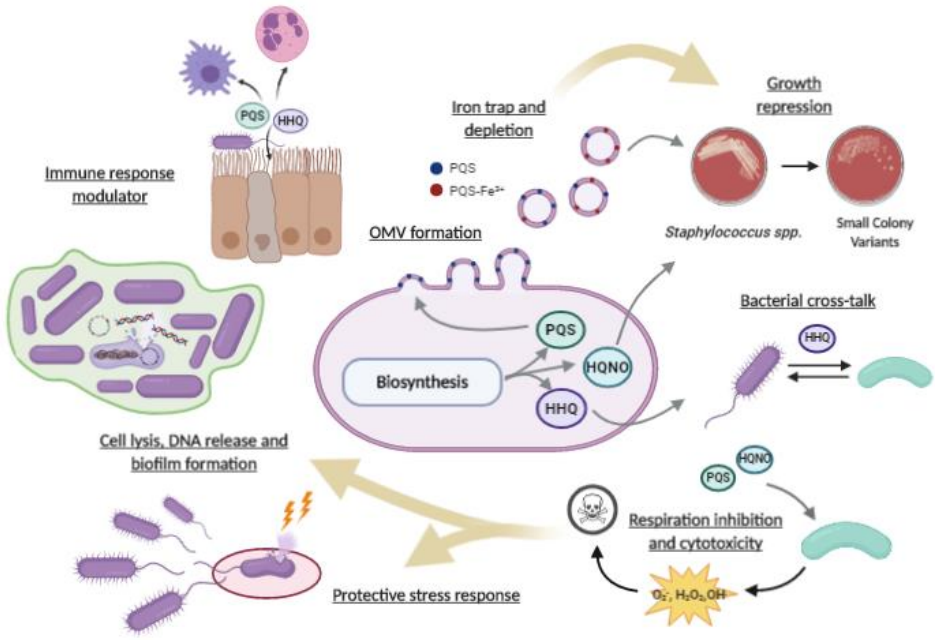

Figure 3.4. Quorum Sensing dependent and independent biological functions summary of the main alkylquinolone metabolites secreted by *P. aeruginosa*.

Among the AQ produced by *P. aeruginosa*, PQS can be highlighted due to its characteristic chemical nature. Its hydrophobic alkyl chain combined with a remarked chelating functionality confers it several particular functions[104]. As the main molecule from the *pqs* system, the implication of PQS in bacterial processes and its multiple roles have been widely studied[25]. Doubtlessly, PQS possesses an extraordinary affinity for ferric iron (Fe^{3+}) due to its chelating moiety, forming complexes PQS-Fe^{3+} in a mixture of ratios 2:1 and 3:1 at physiological pH[105]. PQS complexes iron in a non-available manner, thereby working as an iron trap rather than as a siderophore. Afterwards, the Fe^{3+} retained by PQS can be scavenged and delivered by the siderophores pyoverdine and pyochelin more efficiently[105]. The production of PQS may play a role as an iron depletion strategy for outcompeting other bacterial species under iron-deficient conditions (Figure 3.5). It has been demonstrated that *P. aeruginosa* is able to repress the growth

in gram-positive and gram-negative bacteria through PQS, and addition of exogenous PQS results into growth repression also to *P. aeruginosa* strains[106,107]. However, the addition of Fe^{3+} to the medium reduces PQS growth repression activity, thus demonstrating that iron-chelating activity is involved in this process[105,107]. On the other hand, this AQ is also able to prompt the expression of pyochelin biosynthetic gene cluster and pyoverdine synthetase in a concentration-dependent manner under iron-depletion condition[108,109]. Furthermore, PQS has been shown to modulate the response to iron in other organisms such as *Aspergillus fumigatus*, the commonest fungus isolated from CF compromised host airways[110]. In summary, the *P. aeruginosa* response to iron is partially mediated by PQS, either through activation of the siderophores gene expression or by trapping and storing Fe^{3+} for later use, allowing the competition with bacterial species and other pathogenic organisms.

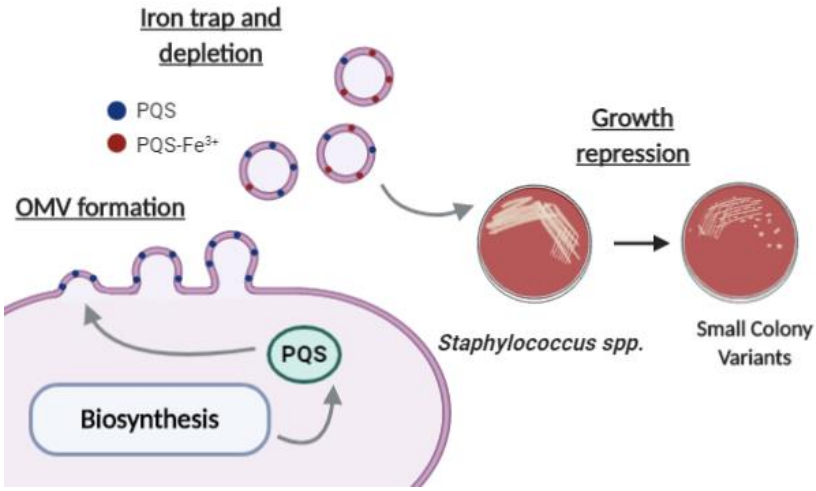

Figure 3.5. Schematic representation of the outer-membrane vesicles (OMV) formation and iron chelating activity of Pseudomonas Quinolone Signal (PQS) and their effect repressing the growth of other bacterial species.

PQS has also been shown to induce oxidative stress in lung epithelial cells and macrophages by production of reactive oxygen species (ROS) and reduction of antioxidant related factors gene expression[70]. Nevertheless, it has been observed a dual effect of PQS in *P. aeruginosa* communities. On the one hand, PQS acts as a pro-oxidant and sensitizes bacteria towards environmental stress and, on the other, induces a protective stress response effect that may be beneficial for

promoting survival of the fittest[111]. Therefore, by secreting PQS, *P. aeruginosa* would repel healthy unexposed bacterial cells from the source of stress, influencing spatial organization and population dynamics (Figure 3.6). This effect has been observed in bacterial populations that were exposed to bacteriophages or antibiotics, thus limiting the damage to a sub-population[112]. Similarly, PQS has been observed to act as a UVA radiation sensitizer for *P. aeruginosa* populations by the generation of ROS[113]. The release of PQS has been also shown to prompt cytotoxicity by showing a negative effect on the mitochondrial respiration. It inhibits of the cytochrome I of the respiratory chain and the prolonged exposure had an effect on the activity of complex III in HeLa and A549 alveolar epithelial cells[114]. PQS has also been related to the formation of biofilms by either LecA induced production[115], increased iron bioavailability[116] and/or sub-population cell lysis and subsequent release of DNA, which is one of the major matrix components in *P. aeruginosa* biofilms[117,118] (Figure 3.6).

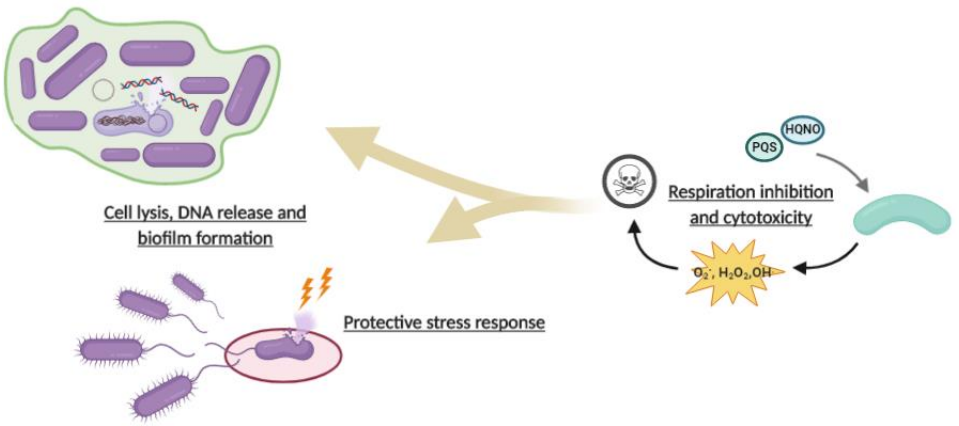

Figure 3.6. Graphical summary of the beneficial effects of the self-respiration inhibition and cytotoxicity caused by PQS and HQNO towards *P. aeruginosa* strains.

Due to the low aqueous solubility of PQS (1 mg/L), it cannot be transmitted in a freely diffusible manner as its precursor HHQ. Instead, *P. aeruginosa* solves the traffic problem by packaging PQS molecules as an integral component of outer membrane vesicles (OMVs) (Figure 3.5). About 80 % of the total PQS produced by a reference strain such as the PA14 is encased into OMVs[119,120]and interestingly, when the production of PQS is altered, it directly affects the production of these vesicles[108]. It has been demonstrated that OMVs production is not a QS-dependent but rather a spontaneous process caused by the chemical

nature of this molecule. PQS prompts the curvature of the membrane by interacting with the acyl chains, 4'-phosphates and divalent cations of the bacterial lipopolysaccharide molecules (LPS), incorporating this quinolone at the outer membrane[121,122]. Furthermore, some authors have recently discovered that the distribution of PQS in the membrane and the bacterial factors exporting this molecule to the outer membrane dictates the amount of OMVs produced[123].

The importance of PQS for *P. aeruginosa* in biological and pathogenic processes is beyond argument. Nonetheless, this bacterium secretes other characteristic AQ with remarkable functions. For instance, not only has HHQ an important role in *pqs* the signalling system and regulation of gene expression but also it exhibits potent bacteriostatic activity against several gram-negative bacteria[124]. HHQ and PQS are able to influence the interspecies behaviour by repressing surface-associated phenotypes in gram-positive and gram-negative bacteria as well as in pathogenic yeast[124]. This fact has a strong relevance in CF pulmonary infections where *P. aeruginosa* is the most prevalent pathogen and the other organisms can be often found forming mixed biofilms[125,126]. On the other hand, other bacteria such as *Burkholderia pseudomallei* or *Pseudomonas putida* produce HHQ, bringing more evidences about the AQ inter-species or inter-genus signalling[127]. The ability of HHQ to freely diffuse out of the cells may confer advantages in some cases in the cell-to-cell communication process respect to PQS[84]. Eventually, HHQ holds a more important role than PQS during chronic biofilm type infections due to the non-requirement of molecular oxygen for its biosynthesis[99,128].

HQNO is a secondary metabolite and virulence factor produced by *P. aeruginosa* without implication in the signalling network[84]. Nevertheless, this AQNO is characterized by its anti-staphylococcal properties and ability to inhibit the oxidative respiration by interfering with the electron transport chain, inducing also a significant depletion of cellular ATP[129]. The production of HQNO is one of the mechanisms that *P. aeruginosa* carry out to subjugate *S. aureus* to persist as small colony variants (SCVs). On the other hand, this behaviour benefits the prevalence of *Staphylococcus spp.* by decreasing the susceptibility to antibiotics targeting the cell wall or the protein synthesis such as vancomycin[130]. Moreover, Hazan et al. demonstrated that HQNO causes a beneficial auto-poisoning in *P. aeruginosa* by triggering cell lysis (Figure 3.6). HQNO disrupts the electron

transport chain and prompts the generation of ROS that compromises the membrane integrity, causing lysis and DNA release. As previously mentioned, DNA is a major component of the biofilm matrix and consequently promotes the resistance to beta-lactam antibiotics[131]. Auto-poisoning could be a problem for *P. aeruginosa* if it weren't for the developed fine-tuned mechanisms of resilience driven by specialized factors such as ubiquinone oxidoreductase, highly resistant to HQNO[132]. The biosynthesis of HQNO also needs molecular oxygen and therefore, the production of this metabolite under anaerobiosis in the mucus of chronic CF infected patients might be compromised[133].

The C-9 derivatives of the aforementioned alkylquinolones are expected to have identical biological roles due to the similarity of the chemical structure and electronic distribution. The two additional carbon atoms in the alkyl chain might provide them higher lipophilic character, although they have not been as deeply studied as their C-7 alkyl congeners.

3.4 AQ CLINICAL SIGNIFICANCE

P. aeruginosa specially affects immunocompromised or CF patients through recurrent and devastating airways infection. During an acute infectious process, this pathogen is known to secrete a wide array of exoenzymes and virulence factors that actively degrade and cause damage of the tissues[134]. By means of bacterial communication, AQ are responsible of the regulation of these tissue-degrading products. Afterwards, if the infection progresses and the bacterial population switches to a persistent or chronic infection, the release of tissue-degrading products is attenuated and the damage is mostly generated by the excessive host immune response[135]. However, AQ may also have an important role through the regulation and evasion of the host immune system in both infectious processes, and not just bacterial signalling purposes as previously thought. Bacteria usually have to face extreme hostile environment and AQ are one of the weapons that *P. aeruginosa* release for fighting and/or evading the host immune system. For instance, the expression of adhesion and inflammatory markers in endothelial cells was significantly modulated by the addition of QS molecules[136]. In this study, the pro-inflammatory cytokines and chemokines IL-1α, IL-1β, IL-6 and TNF-α was altered by PQS and/or HHQ (Figure 3.7).

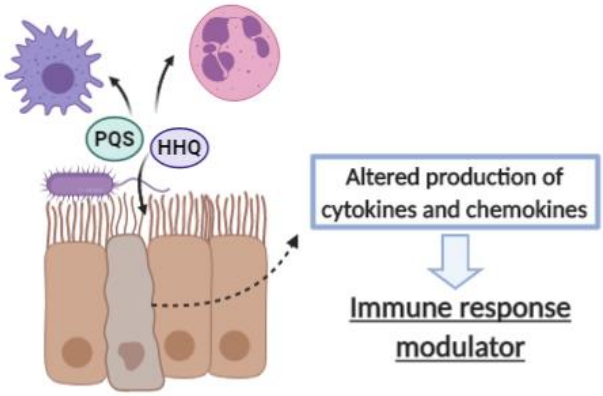

Figure 3.7. Schematic representation of the effects of PQS and HHQ on the modulation of the immune response.

Other studies also suggest the suppression of the host innate immune response by suppression of IL-6 and TNF-α either by action of PQS and HHQ in J774.A1 mouse monocyte/macrophages cell line[137] or by PQS in human bronchial epithelial cells[138]. In the first example, Kim and co-workers observe a reduction of nuclear factor-κB (NF-κB) by HHQ and/or PQS binding to its active sites and altering the overall gene expression of NF-κB pathway. This pathway is connected with the antioxidant protein expression regulator Nrf2, in turn dampened by PQS and the generation of ROS[70]. PQS can also prompt the inactivation of T-cells and thus the antibacterial activity of the adaptive immune response by hindering the generation of IL-12 from bone-marrow dendritic cells[139]. In a different scenario, the use of regenerative medicine including mesenchymal stem cells (MSCs) is of outmost importance for patients after a lung transplantation, and *P. aeruginosa* supposes a major threat. HHQ has been shown to induce apoptosis in MSCs and together with PQS influence the cytokine release profile[140]. On the other hand, the aforementioned AQ can be detected by the family 2 bitter taste receptors (T2Rs), able to activate the innate immune response and also expressed in the epithelial airways cells[141]. The activation of T2Rs triggers the release of nitric oxide which shows bactericidal activity and in turn promotes ciliary clearance. PQS has also been shown to activate the chemotaxis of polymorphonuclear neutrophils, which are the first defence line versus bacterial infection. However, the excess of neutrophil elastase produced in the lung could lead to tissue damage and excessive inflammation[142,143].

Regarding the AQNO metabolites, their clinical significance has not been deeply studied and its role influencing the immune system has to be further explored due to the properties of such molecules at inhibiting the respiratory chain and the potential damage of the endothelial and epithelial cells. Furthermore, as previously mentioned, its role in interspecies interaction with other pathogens, such as *S. aureus*, might be crucial to understand the ability of *P. aeruginosa* to outcompete other bacterial species and understand the outcome and incidence of this pathogen in patients such as CF.

Altogether, the relevance of AQ such as PQS, HHQ and homologous metabolites in the dysregulation of the immune response during an infection is becoming clearer. Nevertheless, more studies have to be carried out to elucidate all the mechanisms of action and pathogen-host interactions in which these molecules are implicated. With this regard, if we are able to quantify QS molecules produced in the host and compare the levels, for instance, with its cytokine footprint we might be able to understand which kind of consequences are triggered in the patient, to prognoses an infectious process or to profile the transition between an acute and a chronic infection state. The current developed techniques for the AQ quantification and evaluation of their role as biomarkers of infection will be discussed in the next section.

3.5 CURRENT QS AQ QUANTIFICATION TECHNIQUES

Currently, bacterial cultures are the gold standard technique for infectious diseases diagnostic; however, they require an excessive analysis time (up to 72 hours) and sensitivity limitations[40]. The fast detection and correct identification of a disease causative strain in the context of an infectious process is crucial for an adequate treatment and, without them, the prescription and misuse of broad-spectrum antibiotic and generation of antimicrobial resistance is inevitably promoted. In order to fulfil the lack of fast and reliable tools of diagnostic, the development of a diverse collection of new methods, strategies and techniques is taking place. For instance, Surface-Enhanced Raman Spectroscopy (SERS) has been successfully applied for the detection of infectious pathogens and PCR is well-recognized technique used in microbiology hospital departments[144-147]. MALDI-TOF-MS has also become an important tool for clinical microbiologists,

providing the characteristic protein footprint from bacteria[148]. Nonetheless, these techniques require expensive equipment, tedious extractions and purifications procedures and still need culture pre-enrichment steps to accomplish the necessary sensitivity[149,150].

One of the strategies under development for the diagnostic of bacterial infections is to use AI and QS molecules as biomarkers of infection, yet the potential of this strategy and the role of these molecules is far from being completely exploited and understood. With this regard, liquid chromatography-mass spectrometry (LC/MS), electrochemical and bioreporter methods have been developed for the detection and quantification of QS molecules in either bacterial cultures or clinical samples. Furthermore, due to the close connection of QS molecules production with bacterial fitness or mode of growth, these molecules are promising targets for a greater knowledge of bacterial infections. The results seem to indicate that these small molecules could serve for prognosis studies, studying the progression and state of the disease or as an indicator of the effectiveness of an antibacterial treatment. For that reason, in the present section it will be discussed and summarized the state of the art in the detection and quantification of QS AQs and their potential as biomarkers of *P. aeruginosa* infections. Similarly, it will be discussed the potential of the techniques as future complemental diagnostic methods and their applicability and implementation in clinical settings.

3.5.1 LC/MS TECHNIQUES

The first attempt to quantify AQs is found more than 20 years ago when Pesci and co-workers addressed the objective of profiling and studying the QS molecules production in *P. aeruginosa* in culture media using HPLC and TLC techniques. Despite the authors did not developed a characterized quantification method, they situated the production of PQS at the end of the log-phase of the bacterial growth, estimating a total concentration of 6 μM[151]. Few years later, a stable isotope dilution method assay, using deuterated PQS as internal standard, for the quantification of PQS and the N-oxide derivative (HQNO) with the same exact mass, was developed. The production of these quinolone metabolites in culture was also established at the end of the logarithmic growth and the maximum at the onset of the stationary phase[152]. According to them, PQS

reached a maximum concentration of 16 µM and HQNO of 22 µM. In 2010, Otori and colleagues developed a LC/MS-MS method for the simultaneous detection of HSL and AQ QS molecules and its application for determining the relative molar ratios of both molecule types in *P. aeruginosa* and the consequences of mutations in the QS synthase genes[72]. The method developed in this work presented a lower limit of quantification (LLOQ) for AQ of 0.6 nM in culture broth, nevertheless it presented recovery issues with the PQS type analogues, probably due to the required extraction process, and to the particular solubility features discussed above, obtaining poor chromatographic peaks that hampered the proper quantification.

The aforementioned research works aimed at studying and comprehending the fundamentals of QS and the biological relevance of these molecules in the *P. aeruginosa* communication systems. However, in the recent years, new technological developments have mostly evolved pretending to elucidate also the importance and significance of these molecules in the biomedical field, as targets for novel diagnostics and therapeutic approaches[153-155]. For instance, Barr and co-workers applied the LC/MS-MS protocol developed by Otori and co-workers to get knowledge on the clinical significance of AQ in CF patients in several independent studies. The analytical protocol required pre-concentrating the sample at least 20-times to attain a LLOQ (Lower Limit of Quantification) of 0.5 nM (Figure 3.8). In one of the examples, the authors analysed the sputum, plasma and urine of 60 patients with a chronic infection by *P. aeruginosa* who required intra-venous antibiotics for pulmonary exacerbations[67]. They found a positive correlation between the levels (nM range) of AQ in all three bio-fluids. The plasma levels of 2-nonyl-4-hydroxyquinoline N-oxide (NHQ), the C-9 alkyl chain derivative of HHQ, showed correlation with clinical status. Two years later, the same author studied the diagnostic and prognostic significance of six AQ in the same type of samples from 176 adults and 68 children with CF and followed up and compared patients without *P. aeruginosa* infection at baseline for one year to determine if AQ were early biomarkers of pulmonary infection[63]. The authors did not provide the concentrations of AQs in samples, yet indicated that a positive result for the samples that contained these metabolites above the corresponding LLOQs. The results indicated that HHQ and HQNO were the most promising biomarkers, having the greatest diagnostic accuracy (Area under Receiver Operating Characteristics Curve analysis of AQ compared to culture results). Eventually, the study concluded that HHQ in plasma could be an early

biomarker of infection in adults and children with CF and that the systemic levels of all AQs were higher in individuals with newly acquired *P. aeruginosa* infection. Recently, the same method has been applied for analysing sputum and plasma over 8-year period for 90 people with CF to study the relation with long-term adverse clinical outcomes in CF patients[69]. However, no statistical association was found for none of the six analysed AQ with all-cause mortality, lung transplantation or lung function decline. Nevertheless, C-9 PQS in sputum was associated with increased antibiotic usage for pulmonary exacerbations.

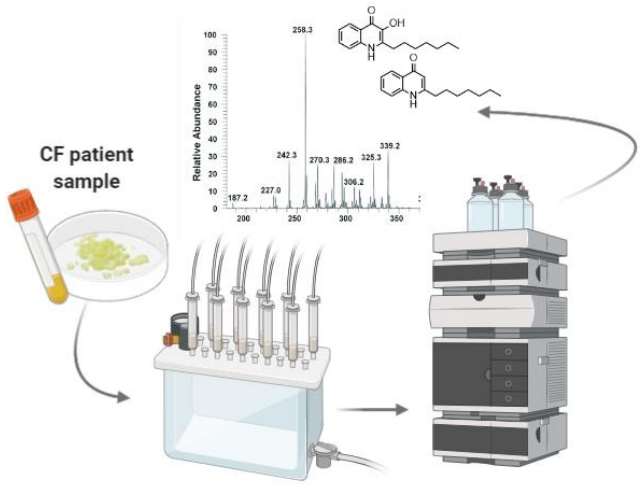

Figure 3.8. Schematic representation of the LC/MS protocol carried out by Barr and co-workers for the analysis of sputum or plasma samples from cystic fibrosis (CF) patients[63,67].

A study carried out by Abdalla and co-workers in 2017 regarding the oxidative stress caused by PQS in lung epithelial cells, involved the use of a LC-MRM-MS method to measure 22 sputa from patients with CF. The sputa samples were extracted and concentrated 10 times in order to quantify PQS and the results showed concentrations of PQS ranging from 0.34 to 36 nM from patients cultured positive with *P. aeruginosa*[70]. However, the number of samples included and patient status information (acute/chronic infection) in this work is insufficient to extract conclusions and, besides, the analytic features of the developed technique are neither included. Brewer and co-workers developed a method for the quantification of six AQ congeners in a selected reaction monitoring (SRM) LC-MS/MS method in bacterial culture and mice lung tissue[156]. The technique presented a dynamic range of 25 to 1000 nM and it was applied

for studying the effect of iron deprivation on *P. aeruginosa*. They also found NHQ to be present in all the 6 infected mice tissue in concentrations up to 6770 nM, although the method presented issues with the matrix and recovery for PQS and AQNO congeners. In a previous study about the pharmacodynamics inhibition of PqsR, the authors developed a highly sensitive technique for HHQ and PQS quantification in mice infected tissue, reaching LLOQs about 4 and 38 pM respectively[157].In this work the sample had to be treated similarly, and there exists doubts about interferences of the matrix and recovery values.

The assessment of the therapy efficacy of certain new antibiotics based on QS molecules production has also prompted to the development of quantification techniques such as the one of Kushwaha and co-workers[71], all of them based on LC-MS/MS. The authors performed a qualitative and quantitative analysis of QS molecules and virulence factors from different chemical nature in the reference strain PAO1 and evaluated the effect of different biofilm inhibitors. In another approach for the discovery of new QS inhibitors carried out by Maurer and colleagues, it was developed an UHPLC-MS/MS method for PQS quantification by microwave-assisted acetylation[158], which allowed to overcome the poor chromatographic properties described by other authors[72]. In this research the authors worked under the hypothesis that new anti-infective therapies interfered on the PQS biosynthesis or release. Nonetheless, the method presents a relatively high LOQ, might present cross reactivity with other AQ metabolites and requires an aggressive sample treatment and chemical derivatization.

In general, the techniques discussed herein are highly sensitive, provide structural information and present high mass accuracy, thus allowing the proper identification of the analytes and becoming appropriate techniques for studying QS at a fundamental level or for research purposes. Nevertheless, as it has been mentioned above, often these techniques require tedious, time-consuming extractions, clean-up, and/or pre-concentration steps, in some cases even chemical derivatization, which makes these technologies difficult to implement on routine clinical diagnostics. In addition, the often lacking expensive equipment and highly trained personnel required for implementing these techniques in clinical settings makes them not suitable for implementing them in routine clinical diagnostics of bacterial infections.

3.5.2 MSI AND RELATED TECHNIQUES

Mass spectrometry imaging (MSI) is an analytical tool used for visualizing the spatial distribution of a wide range of metabolites and proteins based on their molecular masses. The techniques are normally classified depending on the type and source of ionization, namely MALDI (Matrix-assisted laser desorption ionization), SIMS (Secondary ion mass spectrometry) or DESI (Desorption spray ionization). With the use of a proper internal standard, the quantification of small molecules such as AQ becomes possible. Although QS AQ have only been quantified in one example using this technique, we consider that the methods developed for AQ imaging in biofilms and other matrices deserve further discussion due to its potential in diagnostics of infectious diseases.

For instance, MALDI-TOF in combination with LC-MS/MS has been shown to be effective for visualizing the effect of the macrolide antibiotic azithromycin in cultured biofilms[159]. By using this imaging approach, the authors demonstrate that pathogenicity and related metabolites were not affected through the use of this antibiotic, as previously thought. SIMS has been also used for studying the distribution of AQ and AQNO metabolites in biofilms[160]. This example represents the first quantification of *pqs* QS system molecules by MSI. The developed techniques reached LOQ in the low $pM.cm^{-2}$ range, determining an average concentration of 30 and 17 µM for PQS and HQNO respectively. However, the experiments were carried out in agar-based biofilm model that required a dehydration step, potentially affecting the distribution of some diffusible metabolites and subsequently the mapping during the drying process. Therefore, if the proper internal standards are used, the technique could be extended for the quantification of every QS molecule in biofilms, biological samples or infected tissues. Lanni and co-workers successfully combined the techniques mentioned in both previous examples for establishing a more efficient and precise spatial distribution of several QS controlled metabolites. The authors used MALDI-TOF for obtaining low-resolution molecular maps of a sample. Then, the resulting maps were analysed with SIMS and tandem MS/MS to examine the selected regions of interest[65]. This MALDI-guided SIMS approach was validated using cultured biofilms of *P. aeruginosa*, visualizing metabolites such as rhamnolipids and AQ (Figure 3.9). A recent example using MALDI for imaging purposes is the one developed by Brockmann and co-workers, in which the authors detect 39 different AQ from bacterial cultures. The study evaluates the

secretion of these metabolites in co-cultures of *P. aeruginosa* and *S. aureus*, obtaining altered QS release profile due to microbial interactions[53]. Furthermore, the authors assess the intrusion of these molecules in the colonies and their up-regulation in the interaction zone. MALDI has been also used for quantification of pyocyanin (PYO), a relevant virulence factor from *P. aeruginosa*, and the detection of AQ from CF sputum cultures[161]. The method is related to imaging purposes, however it includes an interesting liquid-liquid micro-extraction of 10 µL volume samples and the use of a liquid ionic matrix, suppressing the background signals and achieving LOQ of 0.5 nM for PYO. Eventually, a different example application of MS to perform a metabolomics phenotyping of *P. aeruginosa* has been developed by Bardin and co-workers[162]. The authors carry out rapid evaporative mass spectrometry (REIMS) for detecting metabolites such as AQ from bacterial cultures of CF samples. In this approach, the culture broth sample is evaporated by application of an electrical current and then, after rapid heating and evaporation, the analyte containing vapour circulates to the mass spectrometer.

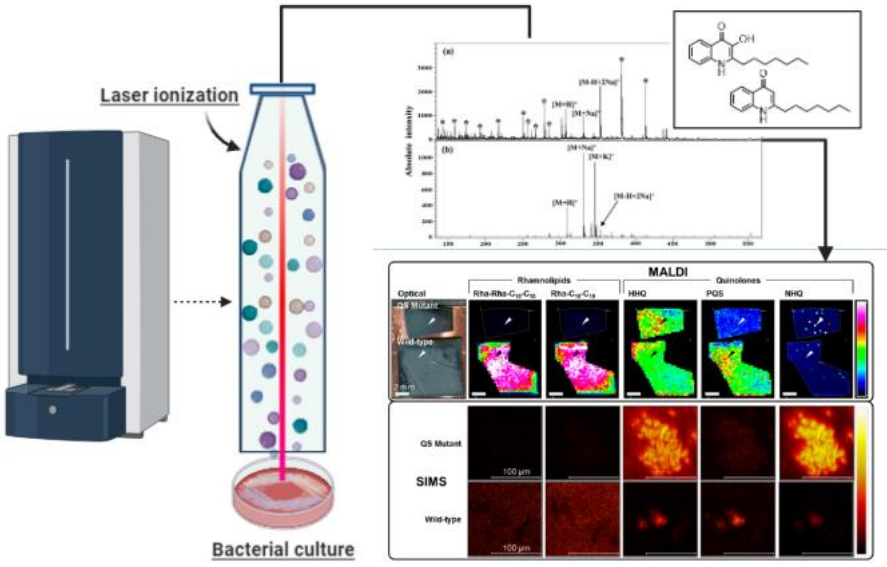

Figure 3.9. Schematic representation of the MALDI-guided SIMS approach carried out by Lanni and co-workers[65]. This figure uses content from **https://pubs.acs.org/doi/10.1021/ac5020222**, which further permissions related to this material should be directed to ACS.

In summary, the techniques presented here in present high potential for studying the QS population dynamics within bacterial cultures or biofilms models. Nevertheless, the applicability of the techniques for diagnostic purposes has to be further investigated, even though the translation to routine clinical analysis remains unlikely due to the same reasons explained for LC-MS techniques in the previous section.

3.5.3 BIOREPORTERS

Bioassays are analytical methods that allows to determine the concentration of a selected analyte and its effect on living cells or tissues. There are few examples of the quantification of QS molecules from *P. aeruginosa* and even less for AQ using these type of techniques. On year 2007 Fletcher and co-workers reported a bioassay for the quantification of HHQ and PQS[163] based on the development of a dual bioreporter based on the bioluminescence produced by luciferase by introducing either *lecA::luxCDABE* or *pqsA::luxCDABE* into a *P. aeruginosa pqsA* mutant unable to produce quinolones (Figure 3.10). The EC_{50} values of both bioreporters were in the μM range, being more sensitively activated the *pqsA::luxCDABE* by HHQ. Due to the different AQ metabolites produced by *P. aeruginosa* the biosensor was also activated by AQNO in addition to PQS and HHQ analogues. Furthermore, the PqsR transduction system in *P. aeruginosa* harnessed in the biosensor is influenced by the secretion of HSL and hence, the quantification of AQ might be altered depending on the conditions. Years later, other authors tried to disconnect the bioassay from the complex QS circuit of *P. aeruginosa* by choosing *P. putida* as host strain modified with a lacZ-based β-galactosidase bioreporter[164]. Nevertheless, this strain is also known to produce also HSL that could interfere with the *las*/*rhl* boxes of the *pqsR* promoter in the bioassay. The EC_{50} values of the bioreporter developed in this work were also in the μM range for HHQ and PQS. The authors used this technique for the assessment of AQ-converting enzymes aiming at using this assay for quorum quenching screening.

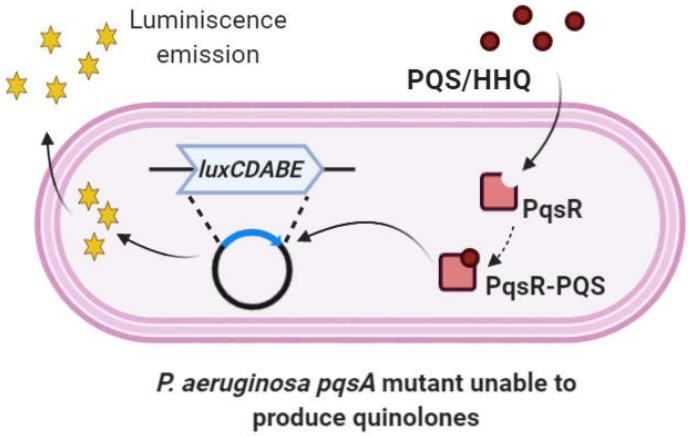

Figure 3.10. Schematic representation of the *P. aeruginosa* bioreporter method followed by Fletcher and co-workers for the detection of AQs[163].

No other examples on bioassays for *P. aeruginosa* AQ detection have been reported to our knowledge. On the other hand, their application of these assays may be limited due to the high complexity of the bacterial population communication system and its intrinsic variability. Otherwise, the dynamic ranges obtained by these techniques might be insufficient for measurement of clinical samples and diagnostic applications.

3.5.4 ELECTROCHEMICAL SENSORS

Electrochemical sensors offer an attractive opportunity due to their remarkable detectability, operating simplicity and low cost. Electrochemical detection of AQ QS molecules in biological samples has been reported in few cases. These technologies are based on the electrochemical behaviour of these molecules. This strategy has been reported in many occasions for the detection of PYO[165,166], one of the main virulence factors regulated by the QS, which shows well know redox properties. However, the electrochemical behaviour of AQs has been only partially known until very recently[167]. Thus, HHQ shows only one purely irreversible oxidation wave at high potential around +0.99 V over the first CV scan when using glassy carbon (GC) working electrodes (1mm diameter) and Ag/Ag^+ reference electrodes in organic media. The oxidation wave can be observed at higher potentials (+1.351 V, pH 5) if measured with boron doped

diamond electrodes. In contrast, PQS shows a redox system with an oxidation peak at +0.233 V coupled to a reduction wave at +0.178 V, with a quasi-reversible redox reaction in the cyclic voltammetry analyses.

Zhou and co-workers developed an electrochemical sensor for the quantification of HHQ, PQS and its methyl analogues from extracts of bacterial culture supernatant using capillaries coated with highly charged polyelectrolyte monolayers and boron-doped diamond electrode (BDDE)[168]. On the one hand, the coated capillary reverses the electroosmotic flow and allows the fast migration of the analytes and, on the other, the boron doped electrode features a wide potential range, high current density and low background, electrochemical stability and resistance to fouling. The authors implement the sensor to assess production of HHQ and PQS by *pqsA* and *pqsH* mutants together with PA14 wild type strain. The LOD of the technique was 65 and 94 nM for PQS and HHQ, respectively, and it was successfully validated by LC/MS. However, the author did not account for the specificity of the method caused by other different chain length AQ metabolites produced by *P. aeruginosa*. In another example, Buzid and co-workers produced an BDDE-based electrochemical technique based on differential pulse voltammetry (DPV) for the simultaneous quantification of HHQ, PQS and PYO in biological samples and spiked sputum samples of CF patients[169]. The technique presents a LOD in the nM scale for bacterial cultures and µM scale for sputa, although in that case they did not measure clinical samples from infected patients, but just spiked samples.

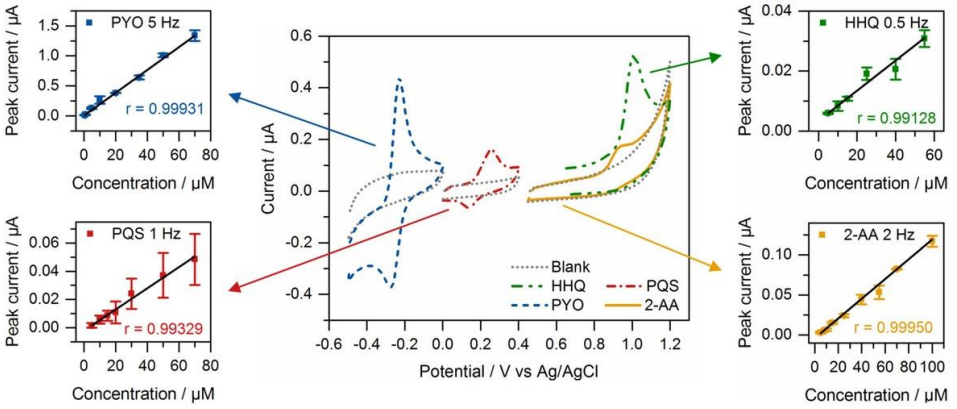

Figure 3.11. Cyclic voltammetry (central graph) of 100 µM of HHQ, PQS, PYO and 2-aminoacetophenone (2AA) in PBS using GC electrodes. The around graphs show the calibration

curves of the four *P. aeruginosa* metabolites recorded using Square Wave Voltammetry (SWV, (step 5mV, amplitude 10mV, frequency on the figure). Reproduced with permission from [167].

The same author developed a similar strategy using BDDE and DPV for the quantification of the same analytes, although studying the effect of a cationic surfactant in the assay[170]. This fact improved the measurement and allowed the direct quantification of AQs and PYO in PAO1 bacterial cultures after 10h growth without the need of extraction steps with organic solvents, yet obtaining worse limits of detection and dynamic ranges in bacterial culture broth. The last and most recent electrochemical detection of AQ quinolones was developed by Burgoyne and co-workers[171] (Figure 3.11). The technique is based on the detection of HHQ and PQS at the liquid-liquid interface between two immiscible electrolytic solutions. Interestingly, the method does not depend on the redox activity of the analytes and instead, it relies in the electrochemical monitoring of alkali metal ion and proton interfacial complexation with organic solubilized HHQ and PQS. All the techniques described here in, mostly require sample extractions due to the matrix effects normally found in electrochemical techniques when dealing with biological samples. The working ranges are distributed within the μM scale which is enough for bacterial culture AQs assessment but in turn could be insufficient for the determination of AQs in clinical samples. Therefore, more studies have to be undertaken to confirm the validity of these techniques as diagnostic approaches for infections caused by *P. aeruginosa*.

3.5.5 IMMUNOCHEMICAL BASED TECHNIQUES

Immunochemical analytical techniques comprise a broad variety of powerful set of technologies based on the high affinity and specific recognition of a wide diversity of target analytes (proteins, polysaccharides, peptides, small organic molecules) using antibodies. The specific interaction antibody/analyte usually allow to selectively quantify the selected molecule within complex matrices avoiding tedious pre-treatments of the sample, as in the case of LC/MS methods. There are few examples in the literature for the immunochemical quantification of QS signalling molecules and none of them related to AQ, except for the case of the recently reported antibodies and immunoassay for HHQ, PQS and HQNO by our group[172-174]. These analyte are the most representative *pqs* quorum sensing metabolites from *P. aeruginosa*. All three enzyme-linked immunosorbed

assays (ELISAs) allow the quantification of the aforementioned AQ in the low nM range, attaining LODs of 0.17, 0.36 and 0.15 nM for HHQ, PQS and HQNO, respectively. Despite the obvious structural similarities, these chemicals show considerably low cross reactivity in almost every combination. The three assays have been used for quantification of the corresponding quinolones in Mueller Hinton (MH) culture broth, where *P. aeruginosa* has been growth, without any sample pre-treatment thanks to the excellent antibody features, by just diluting the sample with the assay buffer. This fact allowed to evaluate the AQ release profile in MH culture broth of bacterial isolates coming patients diagnosed with *P. aeruginosa* airways infection indicating that the ELISAs could in all three cases be used to diagnose and stratify patients with acute or chronic infection. Notwithstanding the results have to be confirmed with a higher number of clinical isolates, the techniques shows great potential to be used as a complemental diagnostic tool to diagnose and follow-up infections caused by *P. aeruginosa*, providing to clinicians additional information useful in the decision-making process for the management of infected patients.

In a previous study, Pastells and co-workers also published an immunochemical method for the quantification of PYO and its precursor 1-hydroxyphenazine (1-OHphz) in bacterial cultures and sputum samples[175]. PYO quantification could be done in less than 2 hours after conversion to 1-OHphz under basic conditions, presenting a LOD of 0.6 nM. The developed ELISA allows the specific quantification of this relevant virulence factor secreted by *P. aeruginosa* and the assessment of its potential as biomarker of disease in clinical samples.

Immunochemical techniques appear as an interesting approach for quantification of AQ metabolites and their evaluation as biomarkers of disease. The high specificity and affinity of antibodies provide an opportunity for assessing the biological and clinical significance of AQ with minimal sample treatment, thus avoiding tedious extractions or enrichment steps. However, the greatest advantage of these immunochemical techniques is that the versatility of antibodies would allow their implementation into simple, rapid, low-cost, user-friendly and portable devices that fulfil the requirements of PoC testing, highly demanded in clinical diagnostics.

Table 3.1. Analytical methods for the quantification of AQ or AQNO summarized in the present section and the corresponding analyzed matrices. The table also includes the working range (DR) and limit of detection (LOD) if provided by the authors.

AQ	Method	Matrix	DR (nM)[a]	LOD (nM)[a]	Author/Ref./Year
PQS; HQNO	LC/MS	Culture broth	462-77118	-	Lepine et al.[152], 2003
C7 and C-9 AQs	LC-MS/MS	Culture broth	10-1000	-	Otori et al.[72], 2011
C7 and C-9 AQs	LC-MS/MS	Sputum, Plasma and Urine	0.5-10	-	Barr et al.[67], 2015
C7 and C-9 AQs	LC-MS/MS	Sputum, Plasma and Urine	0.5-10	-	Barr et al.[63] Webb et al.[69], 2017
PQS	LC-MS/MS	Sputum	0.3-36.3	-	Abdalla et al.[70], 2017
C7 and C-9 AQs	LC-MS/MS	Culture broth and infected mice tissue	25-1000	5	Brewer et al.[156], 2020
HHQ; PQS	LC-MS/MS	Infected mice tissue	0.004-20; 0.04-20	-	Turnpenny et al.[157], 2017
HHQ; PQS	Bioreporter	Culture broth	375-50000; 375-200000	375; 375	Fletcher et al.[163], 2007
HHQ; PQS	Bioreporter	Culture broth	100-10000; 10-5000	100; 10	Muller et al.[164], 2013
HHQ; PQS	Electrochem.	Culture broth	1000-100000	94; 65	Zhou et al.[168], 2012
HHQ; PQS	Electrochem.	Culture broth and spiked sputum	2000-75000; 2000-100000	250	Buzid et al.[169], 2016
HHQ; PQS	Electrochem.	Culture broth and spiked sputum	5000-50000	3610; 4850	Buzid et al.[170], 2017
HHQ	Immunoassay	Clinical isolates culture broth	0.5-20.6	0.17	Montagut et al.[172,174], 2020
PQS	Immunoassay	Clinical isolates culture broth	0.9-36.2	0.36	Montagut et al.[172,173], 2020
HQNO	Immunoassay	Clinical isolates culture broth	0.4-17.0	0.15	Montagut et al.[172], 2020

4 2-HEPTYL-4-QUINOLONE (HHQ)

4.1 CHAPTER PRESENTATION

This chapter aims to describe the research performed to develop and evaluate an immunochemical method to assess the potential value of 2-heptyl-4-quinolone (HHQ) as biomarker of *P. aeruginosa* infections. The chapter will describe the whole process to obtain an immunochemical assay for the quantification of the QS molecule HHQ in complex biological samples. Therefore, it describes efforts made starting from rational hapten design until the implementation of a microplate-based ELISA (enzyme-linked immunosorbent assay) to the measurement of this signalling molecule in culture broth samples of *P. aeruginosa* clinical isolates. The chapter structure can be found in Figure 4.1.

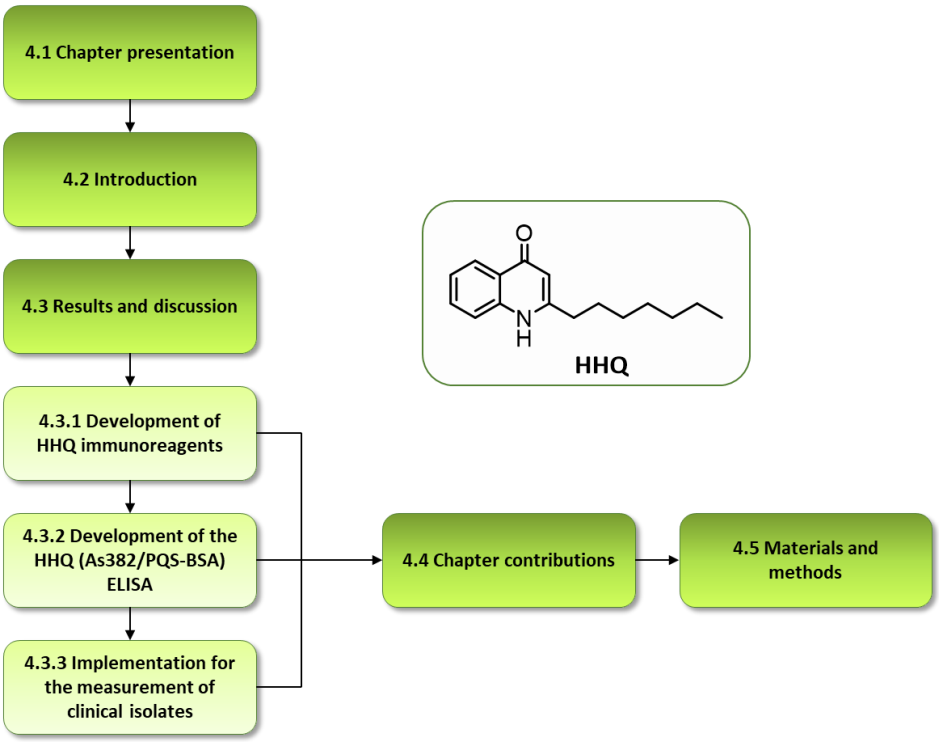

Figure 4.1. Structure of Chapter 4 related to the different sections.

4.2 INTRODUCTION

4.2.1 2-HEPTYL-4-QUINOLONE (HHQ)

In the *pqs* QS system of *P. aeruginosa*, 2-heptyl-4-quinolone or HHQ is the immediate precursor of the main signalling molecule, PQS. However, as discussed in the previous chapter, HHQ bears an important role in several biological processes and the communication of this pathogen, being able to activate the transcriptional activator PqsR and to take control of the signalling process under certain circumstances. It might have a strong relevance under anaerobic environments, such as the thick mucus of CF patients, where the production of PQS is lowered due to the requirement of molecular oxygen and thus, HHQ would be in charge of the quinolone-based communication system and the regulation of the corresponding genes.

The importance of HHQ in pathogenesis and its clinical significance may not be completely understood and thus, studies about the role of this molecule and its potential as biomarker of infection need to be conducted. The development of new techniques that facilitate the detection and quantification of HHQ may assists fundamental studies in this respect. Moreover, their use as diagnostic tools may provide information on the development and progress of the pathogenesis. However, in that respect, its potential value as biomarker during these infectious processes has to be demonstrated first. For this reason, in this chapter describes the research work performed to develop an immunochemical method for the quantification of HHQ and its implementation for the measurement of *P. aeruginosa* clinical isolates.

4.2.2 IMMUNOCHEMICAL ASSAYS

Immunochemical techniques are based on the high affinity of an antibody versus the corresponding antigen. This specific interaction allows to selectively detect or quantify the target molecule in complex samples or matrices. One of the most popular analytical methods that incorporates the use of antibodies is the enzyme-linked immunosorbent assay (ELISA). The ELISAs are immunochemical techniques that incorporate an enzyme, as label of one of the immunoreagents,

which catalyses a chemical reaction with a specific substrate which product has absorbance in the visible spectra. The colorimetric change in the solution is proportional to the amount of antibody bound to the target and this allows quantification of the target.

There are three main ELISA configurations (Figure 4.2) and, depending on the antigen/analyte to be detected, one type could be preferred over the others. For instance, high molecular weight analytes are usually detected using a sandwich-type ELISA, which employs two primary antibodies that will bind to different epitopes of the target molecule. For the case of low molecular weight analytes, these epitopes required for the recognition might be close enough to impede simultaneous detection by two different antibodies, and consequently, the proper detection of the analyte. Therefore, the preferred configuration would be a competitive ELISA, which is based on the competition between the analyte and a third specie (competitor antigen) for the binding to the antibody. The competitive ELISAs can be direct, when the competitor antigen is labelled with an enzyme that will catalyse the colorimetric reaction, or indirect, when the use of a secondary antibody labelled with this enzyme is required.

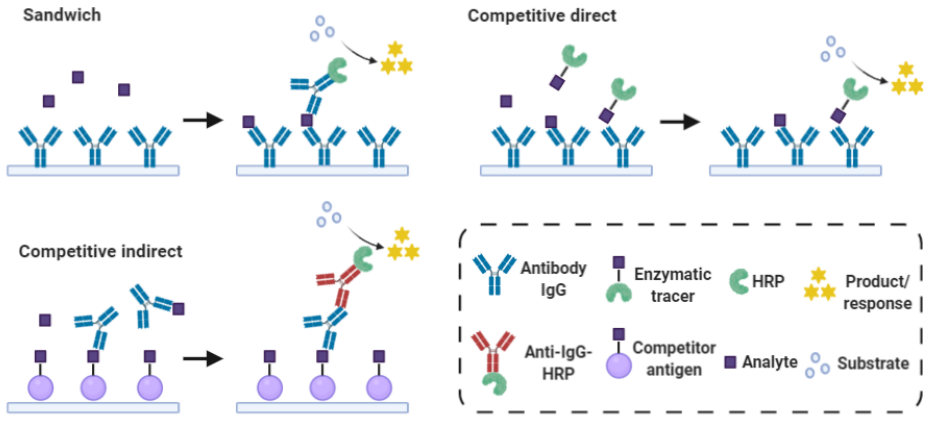

Figure 4.2. Scheme of the most representative ELISA formats, each of them represented by two steps: The competitive indirect ELISA, in which the coating or competitor antigen is immobilized in the plate, and the use of a secondary antibody is needed for obtaining the final signal. The competitive direct ELISA, in which an antibody is immobilized in the plate, and the final signal is obtained through an enzyme tracer. Finally, the sandwich ELISA configuration shows the detection of an analyte using a pair of antibodies (capture and detection).

In all ELISA types the experimental procedure is based on the chemical adsorption of a specie (antibody or competitor antigen) to a surface. In most of the cases, ELISAs are performed on 96-well microtiter plates made of polystyrene appropriately treated to favour protein adsorption. Afterwards, it is performed the sequential addition of the required reagents and washing steps to remove unbound materials, ending with the enzymatic reaction the produces the measurable colorimetric signal.

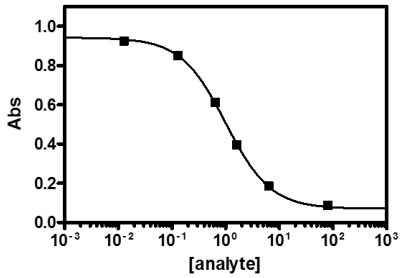

$$f(x) = A_{max}\frac{(A_{min} - A_{max})}{\left(1 - \left(\frac{x}{IC_{50}}\right)^{Hillslope}\right)}$$

Figure 4.3. Calibration curve of the competitive ELISA and its fitted equation. IC_{50}: half maximal inhibitory concentration, A_{max}: maximum absorbance, A_{min}: minimum absorbance, Hillslope: slope of the linear part of the curve.

In competitive assays, the concentration of the target analyte is indirectly proportional to colorimetric signal. The representation of the logarithm of the concentration of the analyte in respect to the measured signal (absorbance) gives the typical inhibition curve with a sigmoidal shape fitted to a 4 parameters equation, will give the features of the assay (Figure 4.3).

4.3 RESULTS AND DISCUSSION

4.3.1 DEVELOPMENT OF HHQ IMMUNOREAGENTS

4.3.1.1 Hapten design and synthesis

Antibodies are key molecules on immunochemical diagnostic technologies. Their features determine performance of the resulting bioanalytical technique. For the

case of non-immunogenic small molecules, such as the alkylquinolone quorum sensing molecules, antibody features are highly determined by the immunizing hapten used to raise antibodies (Figure 4.4). The hapten chemical structure has a great impact on the affinity and specificity of the antibodies produced and therefore, on the detectability and selectivity of the immunochemical technique. Hapten design involves identification of the molecule moieties more suitable for establishing strong non-covalent interactions (electrostatic, van der Waals forces, hydrogen bonds and hydrophobic) with the antibody molecule such as interactions[60,176,177].

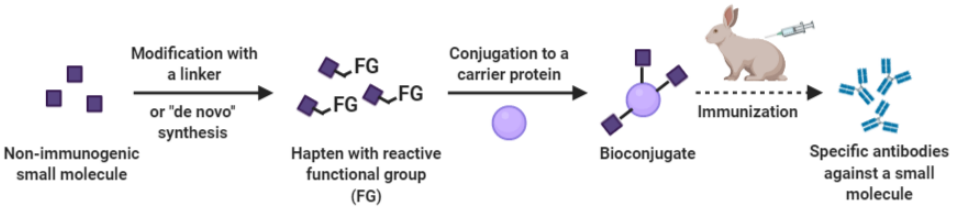

Figure 4.4. Schematic representation of the process for the obtention of antibodies against a non-immunogenic small molecule.

In the case of HHQ, preservation of the 4-pyridone ring with the C-7 alkyl chain at C-2 position was thought to provide the necessary epitopes for stablishing the aforementioned interactions (Figure 4.5). For this purpose, to maximize the exposure of these epitopes, an immunizing hapten was designed with a spacer arm at the C-6 position of the quinolone structure provided of a thiol group for its conjugation with an immunogenic bio-macromolecule. Thiol groups allow orthogonal conjugations trough a wide range of chemical reactions (thiol–halogen, thiol–maleimide, thiol–pyridyl disulphide, etc.)[178].

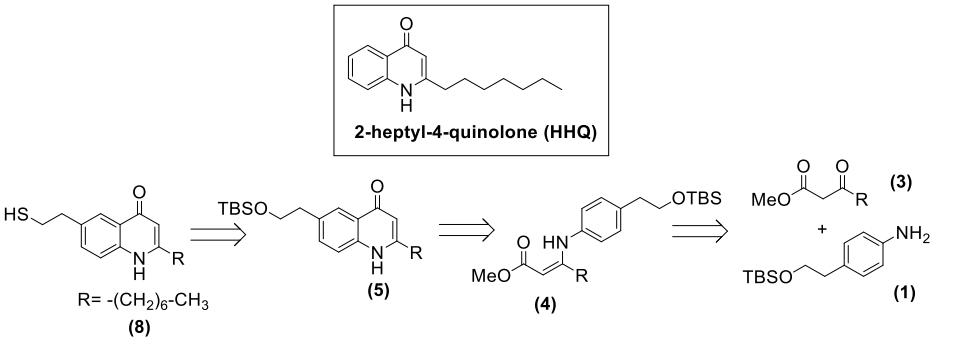

Figure 4.5. Retrosynthetic scheme for the synthesis of HHQ hapten (8), analogous to 2-heptyl-4-quinolone (HHQ) quorum sensing molecule of the pqs system from P. aeruginosa. The hapten was synthesized through a five steps synthetic pathway from 4-(2-((tert-butyldimethylsilyl)oxy)ethyl)aniline (1) and methyl 3-oxodecanoate (3) (see materials and methods section for additional information).

The synthetic approach to accomplish the HHQ hapten was inspired on the previously reported procedure of Reen et al[179]. The strategy involves the coupling of methyl-3-oxodecanoate (**3**) with aniline, followed by a Conrad-Umpach cyclization to obtain the quinolone core (Figure 4.6). In our case the final hapten had to incorporate a spacer arm, for which reason the aniline derivative 2-(4-aminophenyl)ethanol, that already offered an alcohol as functional group, was used as starting material for the coupling reaction. Previously, the alcohol was protected with tert-butyldimethylsilyl chloride (TBDMSCl) in the presence of a stoichiometric quantity of imidazole to obtain the protected aniline (**1**) (see figure 1). In parallel, Meldrum's acid was reacted with octanoyl chloride to obtain 5-hydroxyalkyldioxane intermediate (**2**) that after methanolysis, produced the necessary β-ketoester (**3**). The condensation reaction between (**1**) and (**3**) was carried out in the presence of a catalytic amount of p-toluene sulfonic acid to obtain the intermediate (**4**) in 97% yield. Then, the intermediate went under thermal cyclization at 270 ºC without further purification, due to the lack of stability of the product, to obtain the quinolone (**5**) with 51% yield, higher than that reported by Reen et al[179]. Subsequently, the TBDMS derivative was treated with BBr_3 in refluxing dicloromethane, to obtain the brominated intermediate (**6**) with an excellent yield. Afterwards, the bromine was substituted through a SN_2 reaction using potassium thioacetate, achieving the quantitative conversion to the acetylthio-derivative (**7**). Finally, the HHQ hapten (**8**) was obtained after removing the thiol protecting group with NaOH in anhydrous and degassed

methanol to avoid formation of dimers through the formation of disulphide bonds. Hence, the desired hapten could be obtained in eight synthetic steps, with an overall yield of 26%.

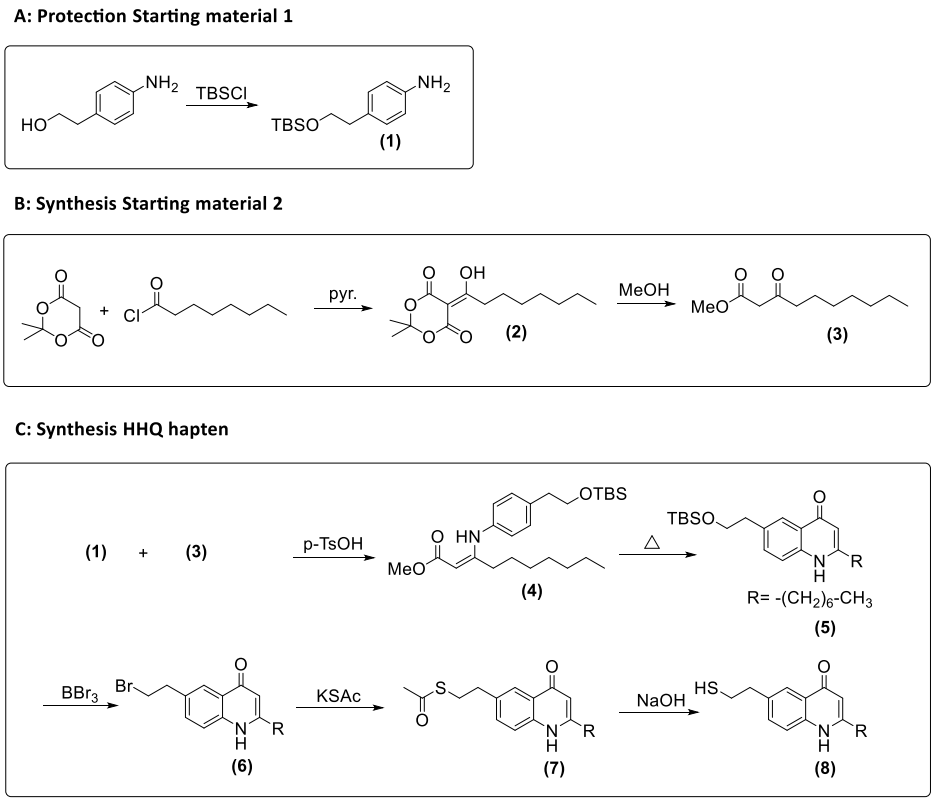

Figure 4.6. Schematic representation for the synthesis of HHQ hapten including: A. Protection of the aniline derivative starting material; B. Two step synthesis of the starting material β-ketoester; C. Five steps synthesis of the HHQ hapten. The main reagents or conditions used in each reaction are shown and the complete experimental procedure for obtaining each intermediate and final product is fully described in the materials and methods section.

4.3.1.2 Antibody production

The conjugation of the hapten (**8**) to BSA and HCH was carried out using succinimidyl iodoacetate as heterobifunctional linker through a two-step procedure. Firstly, the linker reacted with amino groups of the protein through the succinimide ester, and subsequently the available iodine was used to perform a SN_2 reaction with the thiol group of the hapten. The bioconjugation

yield and hapten densities can be found in Table 4.1. HHQ-HCH was used to raise polyclonal antibodies (As382, As383 and As384) in white New Zealand rabbits after application of well-established immunization procedures.

Table 4.1. Data on the bioconjugation yield and hapten densities of the HHQ bioconjugates.

	Quantity (mg)	Yield (%)	Hapten density
SIA-BSA	-	-	22
HHQ-BSA	18.73	75	13
HHQ-HCH	18.4	74	-

Hapten densities of BSA conjugates were calculated from MALDI-TOF-MS analysis. HCH conjugate could not be analyzed by MALDI-TOF-MS because of the large molecular weight. For this purpose, BSA ans HCH bioconjugates were prepared in paralell, under exactly the same conditions. The data obtained with the corresponding BSA bioconjugates was used as bioconjugation control.

4.3.2 DEVELOPMENT OF THE HHQ (AS382/PQS-BSA) ELISA

4.3.2.1 Antisera selection

The avidity of the obtained antisera for the BSA conjugates (HHQ-BSA and PQS-BSA[180]) was assessed through two-dimensional titration experiments and the ability of HHQ to compete and by combined experiments comparing the absorbance of the assay in the presence and absence of the analyte. PQS-BSA and HQNO-BSA (the obtention of which will be described in the following chapters) were incorporated in these studies with the expectation to improve detectability due to the hapten heterology. As it is shown in Table 4.2, all three antibodies gave usable assay, but the heterologous bioconjugate rendered always the best combinations. Finally, As382/PQS-BSA was selected for further evaluation of its performance under different physico-chemical conditions.

Table 4.2. Analytical parameters of the competitive indirect ELISA for the detection of HHQ that were selected after bi-dimensional titration experiments.

	As 382; 1/32000	**As 383; 1/128000**	**As 383; 1/4000**	**As 384; 1/32000**
[CA] (µg/ml)	PQS-BSA; 0.31	HHQ-BSA; 0.16	PQS-BSA; 0.31	PQS-BSA; 0.08
Bottom	0.04	0.02	0.12	0.02
Top	1.20	1.70	2.11	1.56
Hill Slope	-0.99	-0.73	-1.11	-0.59
IC_{50}	2.89	21.35	16.41	4.56
R^2	0.995	0.998	0.992	0.998

4.3.2.2 Physicochemical parameters optimization

No significant variation of the assay features was observed when the effect of time, pH, ionic strength or the concentration of the non-ionic surfactant was evaluated (see Figure 4.7), pointing to the robustness of the assay. Hence, the As382/PQS-BSA ELISA was able to work at pH values between 5 and 10, although the detectability was slightly better at pH>7.5. On the other hand, detectability was also better in media with higher ionic strength values (15-52 mS cm^{-1}), but the maximum absorbance (Amax) of the assay strongly decreased at values higher than 28 mS cm^{-1}. The percentage of Tween 20 did not affect the assay detectability, but the Amax decreased when the concentration increased. Regarding the duration of the competitive step, the detectability was not significantly affected at incubation periods between 10 and 30 min, but the Amax decreased with the reduction of the incubation time. Finally, the introduction of a pre-incubation step of the antibody with the analyte prior the competitive step, did not produce any improvement in the immunoassay features. At the light of this behaviour, optimal conditions were set which are described the experimental section (see also Table 4.3).

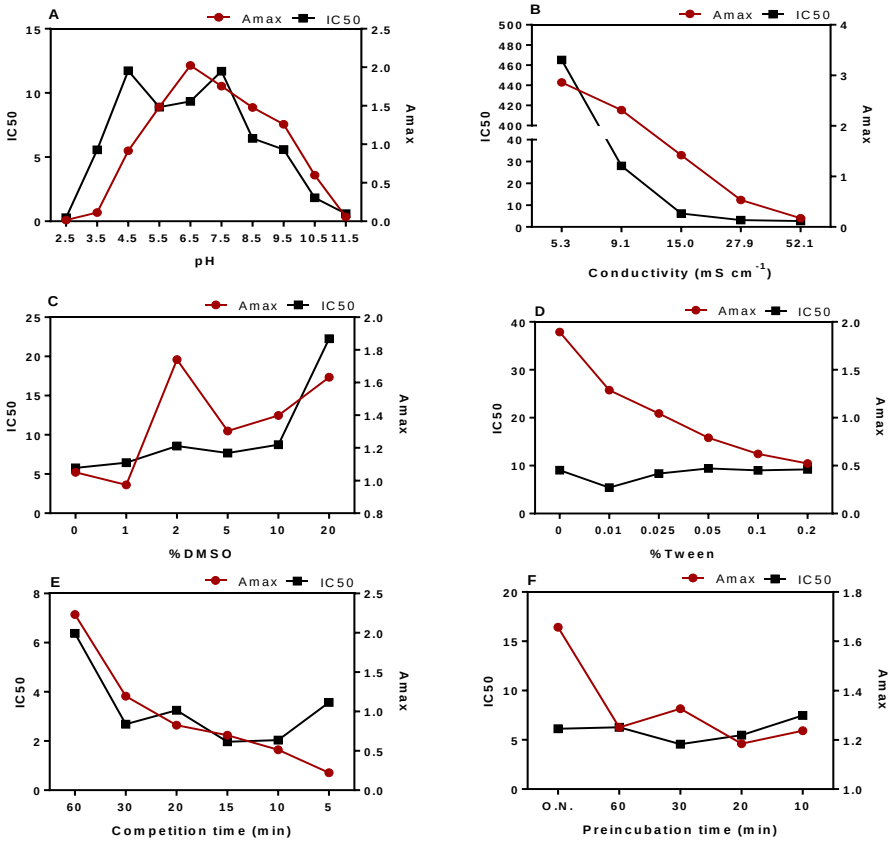

Figure 4.7. As382/ PQS-BSA ELISA performance in the physicochemical parameters optimization study. The selection of the most appropriate conditions (Table 4.3) was based on the variations in Amax, IC_{50} and slope values (not shown) of the generated calibration curves providing better signal/noise ratio, detectability and sensitivity. The studied parameters were A. pH B. Ionic Strength C. % organic solvent (DMSO) D. % Tween 20 E. competition time F. preincubation time. All the studies were performed by varying the composition of the buffer used in the competitive step or the antibody detection times. Eventually, the conditions providing better features were evaluated again separately and in conjunction.

Table 4.3. Physicochemical parameters selected for the As382/PQS-BSA ELISA.

	As382 PQS-BSA
As dilution	1/32000
[Competitor] (µg mL^{-1})	0.31
pH	7.5
Conductivity (mS cm^{-1})	15
Tween 20 (%)	0.05
Competition time (min)	30
Preincubation time (min)	0
Organic solvent (%)	0

4.3.2.3 Analytical characterization

Analytical characterization of the assay was performed by assessing performance on repetitive experiments performed on different days. Under the conditions established, the As382/PQS-BSA ELISA run in PBST was able to detect HHQ with a LOD of 0.34 ± 0.13 nM, an IC_{50} of 4.59 ±0.29 nM and a dynamic range placed between 0.89 ± 0.21 to 22.80 ± 3.69 nM (assay performed on three different days using three-well replicates, see calibration graph in Figure 4.8 and the analytical parameters on Table 4.4).

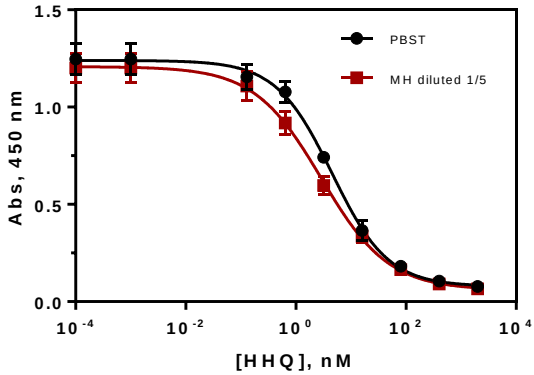

Figure 4.8. Calibration curves of the As382/ PQS-BSA ELISA for the detection of HHQ in buffer (PBST) and in 1/5 diluted MH broth, under the conditions established (Table 4.4). Each calibration point was measured in triplicates on the same ELISA plate and the results show the average and standard deviation of analysis made on three different days.

The detectability achieved is greater than that obtained by other techniques such as bioreporter assays[163,164] or electrochemical detection approaches[169,170]. In respect to the LC-MS/MS methods, the ELISA reported in this work allowed to obtain similar or higher detectability without including additional pre-concentration steps. These methods require the use organic solvents and/or solid phase extraction steps, having to concentrate 20 times the sample for obtaining the reported LOQ[63,72]. On the other hand, it has been reported that alkylquinolones are released to the culture growth media at concentration levels in the µM range [72,163,169]. Therefore, the detectability achieved by the HHQ ELISA here reported pointed to the high chances of this ELISA for quantification of HHQ in bacterial cultures and the assessment of QS activation at early stages of bacterial growth. Moreover, the LOD achieved is also below the concentration values reported in sputum samples by Abdalla and co-workers (up to 36 nM)[70], which points also to the possibility to use this ELISA to quantify HHQ also in clinical samples.

Table 4.4. Features of the As382/ PQS-BSA ELISA for the detection of HHQ.

	PBST[a]	**MH diluted 1/5**[b]
A_{min}	0.03 ± 0.01	0.01 ± 0.01
A_{max}	1.19 ± 0.08	1.17 ± 0.08
Slope	-0.87 ± 0.11	-0.70 ± 0.02
IC_{50}	4.59 ± 0.29	2.85 ± 0.30
Dynamic Range	0.89 ± 0.21 to 22.80 ± 3.69	0.45 ± 0.08 to 21.61 ± 4.74
LOD	0.34 ± 0.13	0.17 ± 0.05
R^2	0.995 ± 0.003	0.998 ± 0.002

[a] Assay conditions used PQS-BSA at 0.32 µg mL^{-1} and and the As382 diluted 32000 times in PBST. [b] Assay conditions used PQS-BSA at 0.15 µg mL^{-1} and the As382 diluted 64000 times in 1/5 PBST diluted MH. The analytical parameters correspond to assay performed in MH diluted 5 times in PBST. The concentrations are expressed in nM and the data shown correspond to the average of 3 different days using at least 3 well/replicates per concentration.

4.3.2.4 Specificity study

The specificity of the method was assessed taking into consideration the main effector molecules of the *P. aeruginosa pqs* quorum sensing system, which are HHQ, and two other alkylquinolones, PQS and HQNO that have very similar chemical structures, differing by the oxidized positions C3 and N1 respectively

(see Figure 4.9). Since these molecules will co-exist in the samples to be analyzed, their recognition by the As382/ PQS-BSA ELISA was evaluated. As it can be observed in Table 4.5, in spite of the structural similarities, PQS and HQNO cross reacted only 7% (IC_{50}=37 nM) and 3% (IC_{50}=86 nM), respectively, thus indicating much higher affinity of the antibodies versus HHQ than for the other alkylquinolones of the *pqs* system.

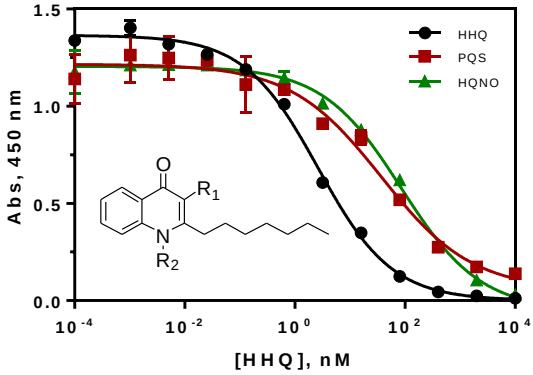

Figure 4.9. Calibration curves of the *pqs* quorum sensing metabolites HHQ, PQS and HQNO in buffer, where it can be observed the greater recognition of the HHQ in respect to the two other alkylquinolones. Calculated cross reactivity was 7% for PQS (IC_{50}=37 nM) and 3% for HQNO (IC_{50}=86 nM). HHQ: R1=-H, R2=-H; PQS: R1=-OH, R2=-H; HQNO: R1=-H, R2=OH. Each calibration point was measured in triplicates on the same ELISA plate and the results show the average and standard deviation of analysis made on three different days.

The recognition by the As382/ PQS-BSA ELISA of other structurally related (ciprofloxacin, norfloxacin) and non-related molecules (PYO and IQS) that might be present in a clinical sample from an infected patient was assessed. In all cases the CR was less than 0.01% and it was obtained a flat-type recognition profile (Figure 4.10).

Table 4.5. Half maximal inhibitory concentration (IC_{50}) of the As382/PQS-BSA ELISA using as analytes the *P. aeruginosa* metabolites HHQ, PQS, HQNO, pyocyanin and IQS and the quinolone type antibiotics ciprofloxacin and norfloxacin.

Quinolone	IC_{50}	C.R. (%)
HHQ	2,67	100
PQS	37,27	7
HQNO	85,97	3
Pyocyanin	-	<0.01%
IQS	-	<0.01%
Ciprofloxacin	-	<0.01%
Norfloxacin	-	<0.01%

The percentages of cross reactivity (C.R.) were calculated following the equation: CR (%) = IC_{50}(Cross reactant)/IC_{50}(Analyte) x 100

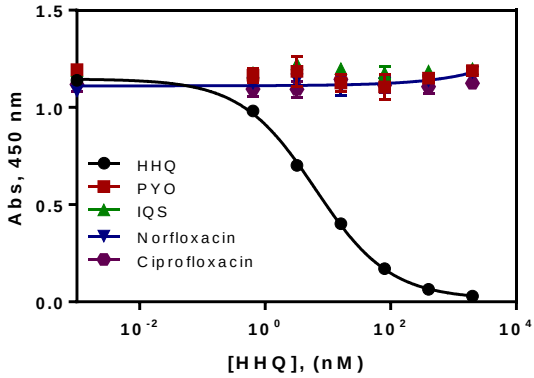

Figure 4.10. Calibration curves of the *P. aeruginosa* metabolites IQS and pyocyanin and the quinolone type antibiotics norfloxacin and ciprofloxacin, where it can be observed the non-recognition of all of them under the conditions of the As382/ PQS-BSA ELISA. Calculated cross reactivity was less than 0.01% in each case. Each calibration point was measured in duplicates on the same ELISA plate and the results show the average and standard deviation of analysis made on two different days.

4.3.3 IMPLEMENTATION OF AS382/PQS-BSA ELISA TO THE ANALYSIS OF CULTURE BROTH FROM *P. AERUGINOSA* CLINICAL ISOLATES

4.3.3.1 Matrix effect evaluation

As a pilot study, we evaluated the potential of the As382/PQS-BSA ELISA to follow-up HHQ production of *P. aeruginosa* clinical isolates grown in Müller-Hinton (MH) broth. However, on a first instance it was necessary to assess performance of the assay on culture broth samples. Bacterial cultures are confined systems where in addition to the culture components, virulence factors, proteins and other bacterial exoproducts are released. Therefore, these culture media could be quite complex samples. The calibration curves were built in MH broth at different concentrations and measured using the developed ELISA. The resulting calibration curves are shown in Figure 4.11. As it can be seen, at first sight, the MH media produced a substantial increase of the maximum signal and the IC_{50} value (PBST: 4.3 nM vs undiluted MH: 658 nM; 1/2 diluted MH: 23 nM or 1/5 diluted MH: 24 nM). Although the matrix effect diminished with the dilution with the assay buffer, this compromised the HHQ detectability in the MH media. Fortunately, two dimensional titration experiments performed in 1/5 diluted MH allowed to correct his effect by readjusting the concentration of the HHQ immunoreagents, allowing to reach an IC_{50} of 2.8 nM and a LOD of 0.17 nM in media (see Figure 4.8 and Table 4.4) which corresponds to 14.25 nM and 0.85 nM, respectively, on the original MH broth, much below the reported concentrations in these type of samples [72,163,164]. This dilution factor was selected taken into consideration reported concentration levels of HHQ, however a very good calibration curve was also obtained by just diluting the MH broth two times with PBST, as it can be observed in Figure 4.11. In respect to other reported techniques used to detect and quantify this type of QS molecules, the present ELISA allows direct quantification of HHQ on media culture broth without the need to perform any complex extraction and sample treatment procedures. Moreover, the ELISA is able to provide results in just about 1.5 h is simple to perform and has high-throughput screening capabilities due to the 96-well microplate configuration.

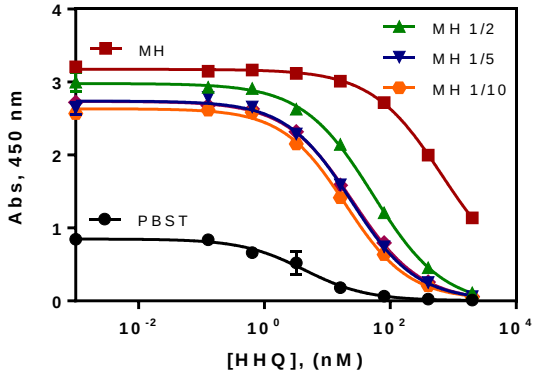

Figure 4.11. Matrix effect of the MH broth undiluted and diluted 2, 5 and 10 times with PBST on the As382/ PQS-BSA ELISA. The calibration curves were run using the conditions established for the assay in PBST. Modification of the assay conditions allowed achieving similar immunoassay features as when the assay was run in buffer (see Table 4.4 and Figure 4.8). The results shown are the average and standard deviations of analysis made on two different days measured by duplicates each day.

4.3.3.2 Accuracy studies

The accuracy of the As382/PQS-BSA ELISA in MH broth was assessed by measuring blind spiked samples prepared in MH and diluted 5 times with PBST. As it can be seen in Figure 4.12, the accuracy of the assay allowed to perform a precise quantification of HHQ. The coefficient of correlation between the spiked and measured concentrations is excellent (R^2 =0.999) and the slope of the linear regression is very close to 1 (slope: 1.07), indicating an almost perfect match of the measured values in respect to the spiked concentrations.

In order to properly characterize the immunochemical assay, it was calculated the coefficient of variation (CV) at three concentrations levels (low, medium and high) of the calibration curve on three different situations: intra-plate, inter-plate and inter-day variability (Table 4.6). The results were used to estimate the so-called "imprecision profile", which normally indicates higher coefficients of variation at lower concentrations. This behaviour falls within the standards because at low concentrations the precision of the immunochemical assays tends to be lower. Moreover, the CV was lower than 5% for the intra-plate variation, indicating excellent values of variability and demonstrating an adequate precision of the assay.

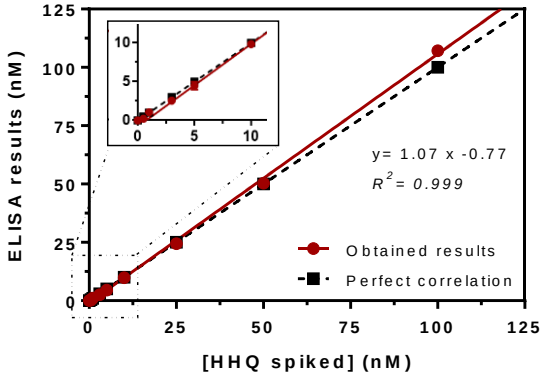

Figure 4.12. Results from the accuracy study. The graph shows the linear regression analysis of the MH broth HHQ spiked concentration and the concentration measured with the As382/ PQS-BSA ELISA. Assays were run in diluted MH culture media 1/5 using PBST. Each calibration point was measured in triplicates on the same ELISA plate and the results show the average and standard deviation of analysis made on three different days.

Table 4.6 Coefficients of Variation (CV) of the As382/PQS-BSA ELISA run in MH culture broth diluted 1/5 using representative concentrations at a low, medium and high concentration range (IC_{20}, IC_{50} and IC_{80}) .

	IC	R1	R2	R3	Mean	Desv. Est.	%CV
Inter-day	20	18,49	19,45	22,84	20,26	2,28	11,3
	50	2,93	2,67	3,65	3,08	0,51	16,4
	80	0,46	0,33	0,65	0,48	0,16	33,9
Inter-plate	20	17,68	20,27	22,01	19,99	2,18	10,9
	50	2,51	3,08	3,12	2,90	0,34	11,8
	80	0,36	0,47	0,46	0,43	0,06	14,7
Intra-plate	20	22,00	23,91	23,84	23,25	1,09	4,7
	50	3,23	3,47	3,39	3,36	0,12	3,6
	80	0,56	0,54	0,54	0,55	0,01	2,3

The coefficient of variation (CV) was calculated following the equation CV (%) = σ/μ x 100. The results were obtained by measurements performed in either triplicates on the same ELISA plate (intra-plate), made on three different days (inter-day) or by analysis on three different plates (inter-plate). The concentrations of the replicates, mean, standard deviation and ICs are expressed in nM. IC: Inhibitory Concentration; R: Replicate; σ: Standard Deviation; μ: Average.

4.3.3.3 HHQ measurement in bacterial culture broth

With these results, the kinetic of release of HHQ was investigated by culturing in MH media two bacterial clinical isolates named PAAI6 and PACI6, obtained from two different patients diagnosed of *P. aeruginosa* respiratory infections. On both cases, the HHQ production profiles measured with the As382/PQS-BSA ELISA matched very well the corresponding growth profiles, based on the measurement of the absorbance at λ 600 nm (OD_{600}), and the calculated CFUs (see Figure 4.13).

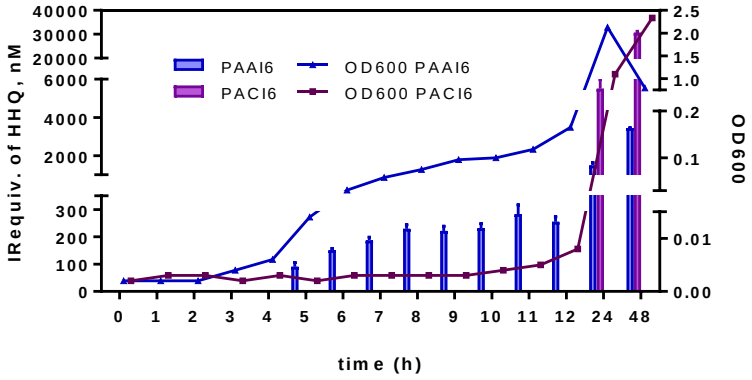

Figure 4.13. Bacterial growth, expressed as OD_{600} and HHQ immunoreactivity equivalents (IRequiv) measured in MH broth media where *P. aeruginosa* clinical isolates PAAI6 and PACI6 were cultured. Samples were taken at the selected times and measured using the As382/ PQS-BSA ELISA. Each calibration point was measured in triplicates on the same ELISA plate and the results show the average and standard deviation of analysis made on two different days.

However, significant differences in the behavior of both isolates were observed. Hence, for isolate PAAI6, HHQ could be detected in the culture media after 5 hours of culture. In contrast, measurable levels of HHQ for the bacterial isolate PACI6 could be quantified only after 12h of culture, although the concentration levels produced by this last isolate after 24 or 48h were higher than those of the first one. The decrease in the optical density of the PAAI6 isolate after 48 h was attributed to the bacterial exposure to high concentrations of self-exoproducts like PYO and PQS[118,181,182], causing autolysis. Interestingly, these bacterial isolates came from patients with distinct clinical infection histories. While bacterial isolate PAAI6 belonged to a patient with an acute infection, isolate PACI6 came from a patient with a chronic infection. These results pointed to the possibility

to use the here reported assay not only to diagnose *P. aeruginosa* infection, but also to stratify patients according to the nature of their infection (chronic or acute) as function of the HHQ concentration levels.

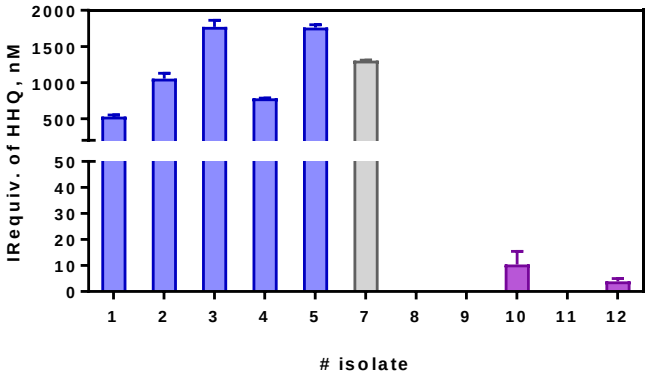

Figure 4.14. HHQ IRequiv recorded from a collection of clinical isolates from patients with different clinical profiles. Samples were growth in MH broth for 8 hours and the aliquots taken were diluted 5 times with PBST prior the ELISA analyses. Clinical isolates 1-5 were obtained from patients undergoing acute infection and isolates 8-12 were obtained from patients undergoing chronic infection. Isolate number 7 corresponds to the reference strain PAO1. The reference number of clinical isolates can be found in Table 5S. Each calibration point was measured in triplicates on the same ELISA plate and the results show the average and standard deviation of analysis made on two different days.

With the aim to probe this hypothesis, additional clinical bacterial isolates from patients with distinct respiratory infections and clinical histories were analyzed. To simplify and standardize the procedure, just end point measures were performed after 8 hours of growth in MH media at 37ºC. In parallel, a reference *P. aeruginosa* strain (PAO1) was also grown under the same conditions. As it can be seen in Figure 4.14, the HHQ levels recorded remarkably differed depending on whether the bacterial isolates were obtained from patients with chronic or acute infections. *P. aeruginosa* isolates from patients clinically diagnosed of an acute infection produced HHQ at concentrations between 0.5 and 2 µM under the above mentioned conditions. In contrast, those coming from patients with chronic infection showed HHQ levels in the low nM range or were below the limit of detection (see Figure 4.14 and Table 4.7).

Table 4.7. Clinical isolates reference number and concentration of HHQ measured with the developed As382/ PQS-BSA ELISA.

#Number	#Ref	Infection type	[HHQ](nM)	Desv. Est. (nM)
1	**PAAI1**	**Acute**	527.9	23.4
2	**PAAI2**	**Acute**	1054	74
3	**PAAI3**	**Acute**	1771	91
4	**PAAI4**	**Acute**	780.7	5.9
5	**PAAI5**	**Acute**	1762	37
6	**PAAI6**	**Acute**	229.3	14.3
7	**PAO**	**Reference**	1304	6
8	**PACI1**	**Chronic**	LLOQ	-
9	**PACI2**	**Chronic**	LLOQ	-
10	**PACI3**	**Chronic**	10.41	5.12
11	**PACI4**	**Chronic**	LLOQ	-
12	**PACI5**	**Chronic**	3.88	1.14
13	**PACI6**	**Chronic**	LLOQ	-

The clinical isolates were grown 8 hours in MH culture media at 37ºC following the protocol described material and methods section.

Recently, Barr and co-workers assessed the diagnostic and prognostic significance of several QS alkylquinolones using LC-MS/MS in a cross-sectional and longitudinal study of 176 adults and 68 children with CF and the analysis of several body fluids (plasma, urine and sputum), concluding that HHQ was the most promising biomarker and with higher diagnostic accuracy among all the studied quinolones[63]. In another study, on a longitudinal test performed with 10 adults and six children, it was found that HHQ detection in plasma was associated with a new positive culture of *P. aeruginosa,* pointing at the value of HHQ in plasma as early stage biomarker of pulmonary *P. aeruginosa* infection. Moreover, HHQ is the direct precursor of PQS and does not need molecular oxygen for its biosynthesis and thus, this fact raises its possibilities to be detected in clinical samples such as sputum, where the bacteria present in the sticky mucus of some patients do not have aerobic environment[99,128].

The ELISA could be an excellent tool to consolidate these preliminary clinical results own its excellent detectability, specificity, robustness and its high-throughput capabilities. Moreover, although it would be desirable to expand this study with more bacterial isolates from a high number of patients, the results of the small pilot study reported here already indicate the potential of this ELISA to provide interesting clinical information related to the stage of the disease. The data shown that it is possible to distinguish between isolates obtained from

chronic or acute infection, thus adding valuable clinical information that has been never reported based on the production of QS alkylquinolones. As an example, clear knowledge on the *P. aeruginosa* microbiological status is essential in order to take decisions[183]on whether a patient could be included on a clinical trial. Early diagnostic of pulmonary *P. aeruginosa* is a key issue, since infection by this bacterium is associated with poor outcomes in diseases such as CF. Definitions of either initial infection, eradication or chronic infection should be supported by objective clinical data. Up to know, the studies are mainly based on culture-based definitions and eventually serological analysis of antibodies against *P. aeruginosa* antigenic determinants. However, data recorded shows great variability leading to a lack of reliability with significant differences in responsiveness to treatments. Incorporation of such kind of test, could provide additional insights on the comprehension of the state of the disease and support clinicians on decision-making for the most appropriate treatment strategy.

4.4 CHAPTER CONTRIBUTIONS

- For the first time, antibodies against the *P. aeruginosa* QS signalling molecule HHQ have been developed. Rational hapten design, organic synthesis and bioconjugation techniques were key steps on the development of such antibodies.

- The polyclonal antibodies against HHQ were used to develop an ELISA able to detect and quantify this signalling molecule in low nM range, lower than reported concentrations in biological and clinical samples. The assay worked under a wide range of physico-chemical conditions, showed a very good specificity and an excellent accuracy, providing the necessary solid bases for further clinical implementation.

- The assay was successfully implemented for the measurement of HHQ in culture broth samples from *P. aeruginosa* clinical isolates by using a simple dilution of the sample. It allowed to stratify the clinical isolates, and subsequently the patients, relying on the production of this QS molecule, pointing to its potential use as biomarker of infection and

valuable source of information about the stage of disease and type of infection.

4.5 MATERIALS AND METHODS

4.5.1 SYNTHESIS

General methods and instruments. The chemicals used in the synthesis of the haptens were obtained from Aldrich Chemical Co. (Milwaukee, WI, USA), Sigma Chemical Co. (St. Louis, MO, USA) or Acros Organics B.V.B.A. (Morris Plains, NJ, USA). Thin-layer chromatography (TLC) was performed on 0.25 mm, pre-coated silica gel 60 F254 aluminium sheets (Merck, Darmstadt, Germany). 1H and 13C NMR spectra were obtained with a Varian Mercury-400 spectrometer (400 MHz ^{1}H and 101 MHz for ^{13}C). Liquid chromatography/electrospray ionization/mass spectrometry (LC/ESI/MS) was performed in a Waters (Milford, MA, USA) model composed by an Acquity UPLC system directly interfaced to a Micromass LCT Premier XE MS system equipped with an ESI LockSpray source for monitoring positive and negative ions. Data were processed with MassLynx (V 4.1) software (Waters).

4-(2-((tert-Butyldimethylsilyl)oxy)ethyl)aniline (1): A solution of imidazole (4.7 g, 0.07 mol) in DMF (10 mL) was added to a mixture of 2-(4-aminophenyl)ethanol (8.0 g, 0.05 mol) and TBSCl (10.5 g, 0.07 mol) in DMF (105 mL). The reaction was stirred at room temperature for 4h. Afterwards, water and ethyl acetate were added to the reaction and the mixture was extracted with ethyl acetate (3 X 40 mL). The combined organic layers were washed with water (40 mL), brine (40 mL), dried over $MgSO_4$ and evaporated under reduced pressure. The reaction crude product was purified by silica flash chromatography using as eluent AcOEt/Hexane 9:1 to obtain the pure aniline **1** (11.3 g, 0.045 mol, 90% yield) as an orange oil. ^{1}H NMR (400 MHz, $CDCl_3$) δ 6.99 (d, *J* = 8.5 Hz, 2H, H4 and H6), 6.62 (d, *J* = 8.5 Hz, 2H, H3 and H7), 3.74 (t, *J* = 7.3 Hz, 2H, H9), 2.72 (t, *J* = 7.3 Hz, 2H, H8), 0.88 (s, 9H, H15-16 and H17), 0.00 (s, 6H, H12 and H13). ^{13}C NMR (101 MHz, $CDCl_3$) δ 144.64, 130.05, 129.25, 115.28, 65.12, 38.95, 26.11, 18.52, -5.20. HRMS:

m/z (ES+) for $C_{14}H_{26}NOSi$ [$(M+H)^+$] calculated 252.1784 found 252.1788 (+1.6 ppm).

***5-(1-Hydroxyoctylidene)-2,2-dimethyl-1,3-dioxane-4,6-dione (2)**:* Meldrum's acid (10 g, 0.069 mol) was dissolved in anhydrous DCM (127.6 mL) and cooled to 0ºC under N_2 atmosphere. After cooling, pyridine (11.18 mL, 0.14 mol) was added followed by dropwise addition of octanoyl chloride (12.414 g, 0.076 mol). The reaction mixture was stirred 1h at 0ºC and monitored by TLC until completion at room temperature. The reaction mixture was washed with 5% HCl solution (40 mL) and distilled water (40 mL) and the organic layer was dried over anhydrous $MgSO_4$, filtered and concentrated under reduced pressure to yield the desired product **(2)** as an orange oil (18.59 g, 0.069 mol, quantitative yield) which was used in the next step without further purification. ^{1}H NMR (400 MHz, $CDCl_3$) δ 3.06 (t, *J* = 7.8 Hz, 2H, H7), 1.73 (s, 6H, H17 and H18), 1.69 (m, 2H, H6), 1.45 – 1.20 (m, 8H, H5-H4-H3 and H2), 0.87 (t, *J* = 6.8 Hz, 3H, H1).^{13}C NMR (101 MHz, $CDCl_3$) δ 198.47, 170.72, 160.33, 104.89, 91.37, 35.89, 31.75, 29.46, 29.03, 26.94, 26.29, 22.72, 14.19. HRMS: *m/z* (ES-) for $C_{14}H_{21}O_5$ [$(M-H)^-$] calculated 269.1389 found 269.1388 (-0.4 ppm).

methyl 3-oxodecanoate (3): 5-(1-hydroxyoctylidene)-2,2-dimethyl-1,3-dioxane-4,6-dione **(2)** (18.5 g, 0.068 mol) was dissolved in MeOH (84 mL) and heated at reflux for 5 h. The reaction was allowed to cool and the solvent was removed under reduced pressure yielding the crude product as an orange oil. Purification was performed using silica flash chromatography Hex/Et_2O 8:2 to obtain the desired product **(3)** as a yellow oil (8.85 g, 0.044 mol, 76% yield). ^{1}H NMR (400 MHz, $CDCl_3$) δ 3.72 (s, 3H, H11), 3.43 (s, 2H, H2), 2.51 (t, *J* = 7.4 Hz, 2H, H4), 1.57 (quin., 2H, H5), 1.34 – 1.17 (m, 8H, H6-H7-H8 and H9), 0.86 (t, *J* = 6.7 Hz, 3H, H10). ^{13}C NMR (101 MHz, $CDCl_3$) δ 202.94, 167.80, 52.41, 49.12, 43.19, 31.75, 29.12, 29.07, 23.58, 22.70, 14.16. HRMS: *m/z* (ES-) for $C_{11}H_{20}O_3$ [$(M-H)^-$] calculated 199.1334 found 119.1331 (-2.5 ppm).

Methyl 3-((4-(3-(tert-butyldimethylsilyl)propyl)phenyl)amino)dec-2-enoate (4): A solution of 4-(2-((tert-butyldimethylsilyl)oxy)ethyl)aniline **(1)** (9.7 g, 38 mmol) and *p*-toluene sulfonic acid (0.12 g, 0.7 mmol) in hexane (20 mL) was added to a solution of methyl 3-oxodecanoate **(3)** (7.0 g, 35 mmol) in dry hexane (80 mL). The reaction mixture was heated at reflux under a N_2 atmosphere for 16 h. Afterwards, it was allowed to cool down and the reaction mixture was

evaporated under reduced pressure, obtaining the crude product **(4)** (14.5 g, 34 mmol, 97% yield) as a pale orange oil which was used without further purification for the next step. ^{1}H NMR (400 MHz, $CDCl_3$) δ 10.22 (s, 1H, H9), 7.16 (d, *J* = 8.3 Hz, 2H, H17 and H19), 7.00 (d, *J* = 8.3 Hz, 2H, H16 and 20), 4.70 (s, 1H, H10), 3.80 (t, *J* = 6.8 Hz, 2H, H22), 3.68 (s, 3H, H14), 2.79 (t, *J* = 6.8 Hz, 2H, H21), 2.25 (t, *J* = 7.7 Hz, 2H, H7), 1.48 – 1.35 (m, 2H, H6), 1.38 – 1.09 (m, 8H, H5-4-3 and H2), 0.85-0.91 (m, 12H, H28-29-30 and H1), -0.05 (s, 6H, H25 and H26). ^{13}C NMR (101 MHz, $CDCl_3$) δ 171.19, 164.30, 137.34, 136.82, 129.99, 125.31, 84.09, 64.46, 50.37, 39.11, 32.33, 31.74, 29.21, 28.98, 28.16, 26.05, 22.72, 18.47, 14.19, -5.28. HRMS: *m/z* (ES+) for $C_{25}H_{44}NO_3Si$ [$(M+H)^+$] calculated 434.3090 found 434.3087 (-0.7ppm).

6-(2-((tert-Butyldimethylsilyl)oxy)ethyl)-2-heptylquinolin-4(1H)-one (5)*: 3-((4-(2((tertbutyldimethylsilyl)oxy) ethyl)phenyl) amino)dec-2-enoate* **(4)** (13.2 g, 30.4 mmol) was added dropwise to refluxing diphenyl ether (250 ml) at 270 ºC and maintained for 2h. Once the reaction cooled to room temperature, the reaction crude was filtered through a silica preparative column using hexane as eluent to eliminate the diphenyl ether. The crude product was then re-absorbed in the same silica using DCM and evaporated under reduced pressure. Afterwards, the product was purified by flash column chromatography using a concentration gradient of eluent from Hexane/AcOEt 4:6 to 3:7 to obtain the cyclized compound **(5)** as an off-white solid (6.23 g, 15.5 mmol, 51% yield). ^{1}H NMR (400 MHz, $CDCl_3$) δ 11.99 (s, 1H, H1), 8.18 (d, *J* = 1.9 Hz, 1H, H6), 7.65 (d, *J* = 8.5 Hz, 1H, H9), 7.47 (dd, *J* = 8.5, 1.9 Hz, 1H, H8), 6.20 (s, 1H, H3), 3.82 (t, *J* = 7.0 Hz, 2H, H13), 2.91 (t, *J* = 7.0 Hz, 2H, H12), 2.67 (t, *J* = 7.8 Hz, 2H, H23), 1.76 – 1.64 (m, 2H, H24), 1.38 – 1.09 (m, 8H, H25-26-27 and H28), 0.90 – 0.74 (m, 12H, H20-21-22 and H29), -0.04 (s, 6H, H17 and H18). ^{13}C NMR (101 MHz, $CDCl_3$) δ 178.89, 154.88, 139.34, 134.92, 133.57, 125.05, 124.93, 118.40, 108.04, 64.56, 39.43, 34.50, 31.80, 29.33, 29.22, 29.13, 26.05, 22.71, 18.43, 14.16, -5.24. HRMS: *m/z* (ES-) for $C_{24}H_{38}NO_2Si$ [$(M-H)^-$] calculated 400.2672 found 400.2678 (+1.5 ppm).

6-(2-Bromoethyl)-2-heptylquinolin-4(1H)-one (6): A 1M solution of BBr3 (1.1 mL, 3 eq.) in DCM was slowly added to a solution of *6-(2-((tert-butyldimethylsilyl)oxy)ethyl)-2-heptylquinolin-4(1H)-one* **5** (0.15 g, 0.37 mmol) in anhydrous DCM (5 mL), under inert atmosphere. The mixture was left at reflux overnight at 45-50ºC. The reaction mixture was evaporated under reduced

pressure. Subsequently, the crude product was re-suspended in water (20 mL) and extracted with AcOEt (3 x 5 mL). The combined organic layers were washed with $NaHCO_3$ satd., brine, dried over MgSO4 and evaporated under vacuum. The crude product was purified by silica column chromatography using DCM with 2 % MeOH as eluent to obtain the bromo derivative **(6)** (0.13 g, 0.36 mmol, 96% yield). ^{1}H NMR (400 MHz, CD_3OD) δ 8.07 (d, *J* = 2.0 Hz, 1H, H6), 7.59 (dd, *J* = 8.6, 2.0 Hz, 1H, H8), 7.54 (d, *J* = 8.5 Hz, 1H, H9), 6.21 (s, 1H, H3), 3.67 (t, *J* = 7.2 Hz, 2H, H13), 3.27 (t, *J* = 7.2 Hz, 2H, H12), 2.69 (t, *J* = 7.8 Hz, 2H, H15), 1.74 (p, *J* = 7.4 Hz, 2H, H16), 1.45 – 1.25 (m, 8H, H17-18-19 and H20), 0.89 (t, *J* = 6.7 Hz, 3H, H21). ^{13}C NMR (101 MHz, CD_3OD) δ 180.40, 156.96, 140.49, 136.57, 134.32, 125.52, 125.45, 119.31, 108.83, 39.78, 34.97, 33.68, 32.85, 30.18, 30.17, 30.08, 23.65, 14.38. HRMS: *m/z* (ES-) for $C_{18}H_{23}BrNO$ [$(M-H)^-$] calculated 348.0963 found 348.0963 (+0.0 ppm).

S-(2-(2-Heptyl-4-oxo-1,4-dihydroquinolin-6-yl)ethyl) ethanethioate (7)*:* A solution of 6-(2-bromoethyl)-2-heptylquinolin-4(1H)-one **(6)** (70 mg, 0.20 mmol) and potassium thioacetate (22.8 mg, 0.20 mmol) in of anhydrous DMF (2.0 mL) was stirred for 1h at room temperature. The reaction was diluted with AcOEt and washed 3 times with H_2O, brine, dried over Na_2SO4 and evaporated under reduced pressure to obtain pure desired compound **(7)** (69 mg, 0.20 mmol, quantitative yield) which was used in the next step without further purification. ^{1}H NMR (400 MHz, CD_3OD) δ 8.05 (d, *J* = 2.0 Hz, 1H, H6), 7.59 (dd, *J* = 8.6, 2.0 Hz, 1H, H8), 7.53 (d, *J* = 8.5 Hz, 1H, H9), 6.21 (s, 1H, H3), 3.16 (t, *J* = 7.1 Hz, 2H, H13), 2.98 (t, *J* = 7.1 Hz, 2H, H12), 2.70 (t, *J* = 7.6 Hz, 2H, H18), 2.30 (s, 3H, H17), 1.75 (p, *J* = 7.5 Hz, 2H, H19), 1.45 – 1.26 (m, 8H, H20-21-22 and H23), 0.89 (t, *J* = 6.9 Hz, 3H, H24). ^{13}C NMR (101 MHz, cd_3od) δ 197.12, 180.40, 156.87, 140.34, 137.50, 134.32, 125.41, 125.24, 119.31, 108.79, 36.49, 34.97, 32.85, 31.25, 30.51, 30.18, 30.08, 23.65, 14.38. HRMS: *m/z* (ES-) for $C_{20}H_{26}NO_2S$ [$(M-H)^-$] calculated 344.1684 found 344.1682 (-0.6 ppm).

2-Heptyl-6-(2-mercaptoethyl)quinolin-4(1H)-one (8)*:* The thioacetylated compound **(7)** (69 mg, 0.2 mmol) and KOH (11.2mg, 0.2 mmol) were dissolved under inert atmosphere in of anhydrous and degassed MeOH (1 mL). The reaction was stirred for 1h at room temperature. Subsequently, the mixture was acidified to pH 6-7 with degassed 1M HCl, diluted with water (5 mL) and extracted with AcOEt (3 x 2mL), washed with brine, dried over Na_2SO4 and

evaporated under reduced pressure to obtain the crude product **(8)** as a pale yellow solid. Eventually, the crude product was purified by crystallization using hexane/AcOEt to the pure HHQ hapten **(8)** (49 mg, 0.16 mmol, 81% yield). ^{1}H NMR (400 MHz, $CDCl_3$) δ 12.17 (s, 1H), 8.17 (d, *J* = 2.0 Hz, 1H, H6), 7.74 (d, *J* = 8.5 Hz, 1H, H9), 7.44 (dd, *J* = 8.5, 2.0 Hz, 1H, H8), 6.26 (s, 1H, H3), 3.00 (t, *J* = 7.3 Hz, 2H, H12), 2.79 (q, *J* = 7.5 Hz, 2H, H13), 2.71 (t, *J* = 7.8 Hz, 2H, H15), 1.72 (p, *J* = 7.6 Hz, 2H, H16), 1.37 – 1.12 (m, 8H, H17-18-19 and H20), 0.80 (t, *J* = 6.8 Hz, 3H, H21). ^{13}C NMR (101 MHz, $CDCl_3$) δ 178.54, 155.37, 139.44, 135.62, 133.00, 124.87, 124.70, 118.89, 108.08, 39.94, 34.49, 31.79, 29.30, 29.23, 29.12, 26.09, 22.71, 14.18. HRMS: *m/z* (ES-) for $C_{18}H_{24}NOS$ [$(M-H)^-$] calculated 302.1579 found 302.1575 (-1.0 ppm).

4.5.2 IMMUNOCHEMISTRY

General methods and instruments. Chemicals and biochemicals were obtained from Aldrich Chemical Co. (Milwaukee, WI, USA) and from Sigma Chemical Co. (St. Louis, MO, USA). The PQS hapten used in this study was prepared following a similar synthetic procedure as that described by Reen et al[179] and conjugated to BSA (PQS-BSA, hapten density 17). The stock solutions of the alkylquinolones (HHQ, PQS, HQNO) used as standards were prepared in DMSO at 10 mM and stored at -20ºC, then transferred to 4ºC prior to their use. Purification of conjugates was carried out in ÄKTA Prime Plus using 2 HiTrap desalting columns both from GE Healthcare (Chicago, IL, USA) or either by dialysis using Spectra/Por membranes from Spectrumlabs (Piraeus, Greece, EU) with molecular weight cut-off of 12-14 kDa. The matrix-assisted laser desorption ionization time-of-flight mass spectrometer (MALDI-TOF-MS) was a Bruker autoflex III Smartbeam spectrometer (Billerica, Massachusetts). Hapten densities of the conjugates were calculated by MALDI-TOF-MS by comparing the molecular weight recorded on the MALDI spectra of the native proteins to that of the BSA-SIA and HHQ-BSA bioconjugates. For this purpose, the bioconjugates were mixed with the freshly prepared matrix ((trans-3,5-dimethoxy-4-hydroxycinnamic acid, 10 mg mL^{-1} in 70:30 ACN/H2O, 0.1% HCOOH) following the ''sandwich'' sample preparation method. The bioconjugate aliquot is diluted ½ using ACN with HCOOH 0.2%. According to it, the matrix (2 µL) is deposited on the MALDI plate and dried, followed by the bioconjugate solution (2 µL, 2 to 5 mg mL^{-1} in 1:1 ACN/H2O, 0.1%

HCOOH), allowed to dry again and finally, the matrix solution (2 µL) was added over again. The resulting dried spot was then analyzed by MALDI-TOF-MS. Hapten densities were calculated through the equation: [MW(conjugate) − MW(native protein)]/[MW(hapten)-MW(lost atoms)]. The pH and the conductivity of all buffers and solutions were measured with a pH-meter pH 540 GLP and a conductimeter LF 340, respectively (WTW, Weilheim, Germany). Polystyrene microtiter plates used for the ELISAs were purchased from Nunc (Maxisorp, Roskilde, Denmark). Dilution plates were purchased from Nirco (Barberà del Vallés, Spain). Washing steps were performed on a Biotek ELx465 (Biotek Inc.). Absorbances were read on a Thermo Scientific MultiSkan GO (Thermo Fisher Scientific, Waltham, MA, USA) at a single wavelength mode (450 nm). The competitive curves were analyzed with a four-parameter logistic equation using the software GraphPad Prism 7.0 (GraphPad Software Inc., San Diego, CA, USA) according to the following formula: $y = B(A-B)/[1 - (x/C)^D]$, where A is the maximum absorbance, B is the minimum absorbance, C is the concentration producing 50% of the maximal absorbance, and D is the slope at the inflection point of the sigmoid curve. Unless otherwise indicated, the data presented correspond to the average of at least two well replicates.

Buffers. Unless otherwise indicated, phosphate buffer saline (PBS) corresponds to 10mM phosphate buffer and 0.8% saline solution (pH 7,5). Coating buffer is a 50 mM bicarbonate-carbonate buffer (pH 9,6). PBST is PBS with 0,05% Tween 20 (pH 7,5). Citrate buffer corresponds to a 40 mM sodium citrate solution (pH 5,5). The substrate solution contains 0,01% of 3,3',5,5'- tetramethylbenzidine (TMB) and 0,004% H_2O_2 prepared in citrate buffer. Borate buffer is 0,2 M sodium borate/boric acid (pH 8,7). All buffers were prepared using ultra-pure Milli-Q® water with a resistivity between 16-18 MΩ cm.

4.5.2.1 Antibody production

Synthesis of the bioconjugates HHQ-HCH and HHQ-BSA. A solution of succimidyl iodoacetate (SIA, 22 µmol) in in DMF (0.5 mL) was added dropwise to a solution of the protein (BSA or HCH, 5.5 mg mL^{-1}, 4.5 mL in Borax/Borate buffer) and the mixture was stirred 3.5 h at room temperature (RT) and overnight at 4ºC without agitation. The solution was purified by using a HiTrap size exclusion desalting column and Borax/Borate as eluting buffer, to isolate the protein-SIA

intermediates. A fraction (20 µL) of the BSA-SIA bioconjugate was kept for MALDI-TOF-MS analysis. Subsequently, the HHQ hapten **(8)** (8,0 mg, 26 µmol), dissolved in of anhydrous DMF (1.7 mL), was added dropwise (850 µL) to each of the protein-SIA intermediates (BSA-SIA and HCH-SIA, 9 mL). The mixtures were stirred 4h at RT and left overnight at 4ºC without agitation. The bioconjugates were purified by dialysis against 0.5 mM PBS (5 x 5 L) and Milli-Q water (1 x 5L), and stored freeze-dried at -80 ºC. A small fraction (20 µL) of the HHQ-BSA was kept for MALDI-TOF-MS analysis, rendering a hapten density of 13 haptens per molecule of BSA.

Polyclonal Antisera (PAb). Antibody production has been performed with the support of the ICTS "NANBIOSIS", more specifically by the Custom Antibody Service (CAbS, CIBER-BBN, IQAC-CSIC)**.** Three female New Zealand white rabbits weighing 1–2 kg were immunized with HHQ-HCH following established protocols in the research group. Immunizations were carried out in the animal facility of the Research and Development Center (CID) of the Spanish Research Council (CSIC) Registration Number: B9900083, employing approved procedures that avoid unnecessary treatments and minimize suffering of the animals. The protocol used in accordance with the institutional guidelines under a license from the local government (DAAM 7463) and approved by the Institutional Animal Care and Use Committee at the CID-CSIC. The antisera (As) obtained were named As382, As383 and As384. The animals were exsanguinated after 6 immunizations, and the final blood was collected in vacutainer tubes provided with a serum separation gel. Antisera were obtained by centrifugation at 4 °C for 10 min at 10 000 rpm, then stored at −80 °C in the presence of preservative 0,02% sodium azide. The antibody titer was assessed during the immunization process through non-competitive indirect ELISA. Microtiter plates were coated with a fixed concentration of HHQ-BSA conjugate (1 mg mL^{-1}) and the avidity of the produced antibodies was measured by preparing serial dilutions of the corresponding As.

4.5.2.2 ELISA

Non-competitive indirect two-dimensional titration experiments. Non-competitive indirect ELISA were carried out to select the concentrations of coating antigen (CA) and the As dilutions more suitable for the competitive

assays. For this purpose, the binding serial dilutions of the antisera (1/1000 to 1/1024000, and zero in PBST, 100 µL/well) to microplates coated with the BSA bioconjugates (5 µg mL-1 to 5 ng mL-1, and zero in coating buffer, 100 µL/well) was measured. From these experiments, optimum concentrations for coating antigens and antisera dilutions were chosen to produce around 0.7-1.2 units of absorbance after 30 min of competitive step.

As382/PQS-BSA ELISA. Microtiter plates were coated with PQS-BSA in coating buffer (0.25 µg mL–1, 100 µL/well) overnight at 4ºC covered with adhesive plate sealers. The day after, the plates were washed with PBST (4 x 300 µL/well) and solutions of HHQ standards (2 µM to 0.13 nM in PBST, 50 µL/well) were added followed by a solution of the As382 (1/32000 or 1/64000 in PBST, 50 µL/well) and the microplates left without agitation 30 min at RT. The plates were washed as before and a solution of goat anti-rabbit IgG-HRP (1/6000 in PBST) was added (100 µL/well) and incubated for 30 min more at RT. The plates were washed again and the substrate solution was added (100 µL) and left 30 min at RT in the dark. The enzymatic reaction was stopped by adding of 4N H2SO4 solution (50 µL/well) and the absorbance read at 450 nm.

Immunoassay performance evaluation. Performance of the assays was evaluated through the modification of different physicochemical parameters (competence time, incubation time, pH, ionic strength, presence of a surfactant (% Tween 20), solubility with addition of organic solvents or cation complexation by EDTA) in the competition step.

Cross Reactivity studies. Standard solutions of the main alkylquinolones from Pseudomonas aeruginosa (HHQ, PQS and HQNO) were prepared (1 pM–10 µM in PBST) and measured with the ELISA following the procedure described above. The standard curves obtained were fitted to the four-parameter equation mentioned above and the IC_{50} value used to calculate the cross-reactivity according to the following equation: CR (%) = IC_{50}(Cross reactant)/IC_{50}(Analyte) x 100.

4.5.2.3 Implementation of the ELISA to the analysis of clinical isolates

Samples. Clinical isolates were obtained by the group of M.-Teresa Martin (Microbiology Department, Vall d'Hebron University Hospital (VHUH), Barcelona, Spain) from lower respiratory tract samples, mainly sputum specimens, of patients diagnosed of acute or chronic respiratory infections[184]. Clinical samples were cultured in MacConkey agar, Blood agar and Chocolate agar, and incubated for up to 5 days at 37°C. *P. aeruginosa* isolates were selected and stored frozen at -20 ºC. Prior the analyses, *P. aeruginosa* isolates were cultured overnight at 37ºC in blood agar plates. The day after, a portion of the grown bacteria was diluted in MH culture broth (3 mL) and shaken at 37ºC. When the optical density at 600 nm (OD_{600}) reached a value of 0.2-0.3, a dilution (1/1000 in 20 mL of MH) was performed and the resulting solution shaken at 37ºC. Aliquots were taken at the selected times for measurement of OD_{600}, for Colony Forming Units (CFUs) calculation and measurement of HHQ by ELISA. The rest of isolates were grown using the same experimental procedure, yet the aliquots were extracted just at a selected time of 8 hours. HHQ concentrations measured by ELISA are expressed as HHQ immunoreactivity equivalents (IRequiv), due to the specific interferences caused by other alkylquinolones potentially present in the culture media.

Matrix effect study. MH culture media was diluted (1:2, 1:5, 1:10, 1:20), used to prepare HHQ standard calibration curves and to compare them with the standard curves prepared in PBST. Subsequently, the dilution providing the best ELISA parameters was selected and the conditions of CA and As dilution adjusted.

Accuracy studies. Blind spiked samples using diluted MH culture broth were prepared and measured using the above described ELISA. The samples were measured in triplicates and the experiment repeated on three different days.

5 PSEUDOMONAS QUINOLONE SIGNAL (PQS)

5.1 CHAPTER PRESENTATION

This chapter describes de development of an immunochemical method to evaluate 2-heptyl-3-hydroxy-4-quinolone or Pseudomonas Quinolone Signal (PQS), which is the main signalling molecule of the *pqs* QS system, as potential biomarker of *P. aeruginosa* infections. In this chapter it will be described the whole process to obtain an ELISA for the quantification of PQS, from "de novo" synthesis of the immunizing hapten till the application to the measurement of this signalling molecule in culture broth samples of *P. aeruginosa* clinical isolates. The chapter structure can be found in Figure 5.1.

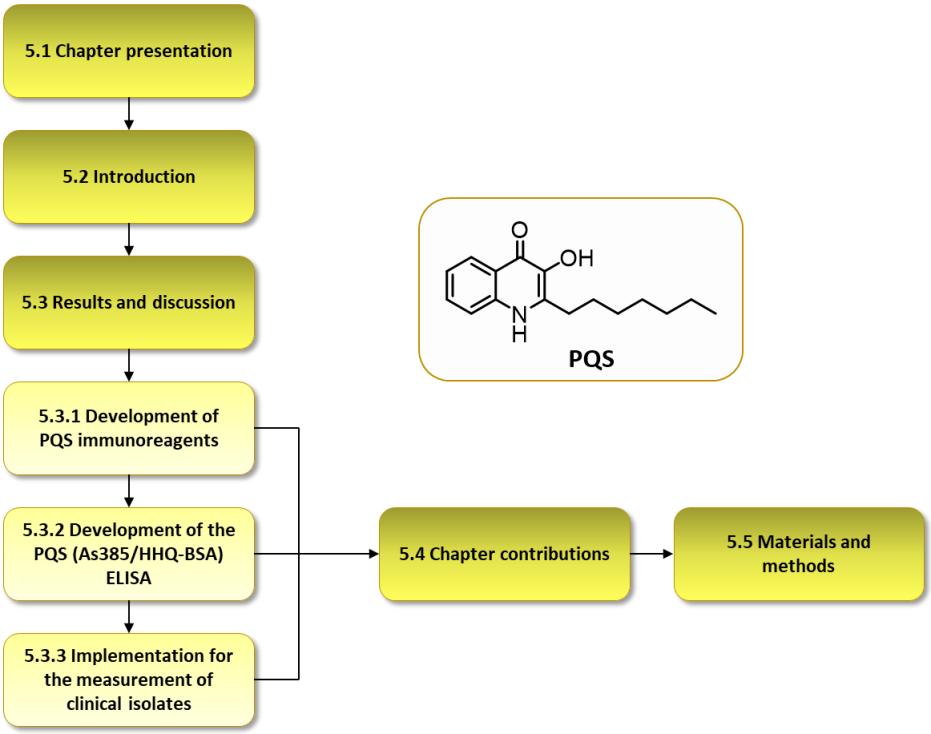

Figure 5.1. Structure of Chapter 5 related to the different sections

5.2 INTRODUCTION

5.2.1 PSEUDOMONAS QUINOLONE SIGNAL (PQS)

Understanding Quorum Sensing (QS) is key to apprehend about pathogenesis. The main signalling molecule from the *pqs* QS system of *P. aeruginosa*, 2-heptyl-3-hydroxy-4-quinolone or Pseudomonas Quinolone Signal (PQS), has been widely studied, as discussed in Chapter 3. The multiple bacterial functions besides its signalling and regulatory activity makes it an interesting subject of study. Furthermore, PQS has been shown to be specific from *P. aeruginosa* and therefore, its potential as biomarker of infection should be highlighted. The development of a diagnostic tool capable of confirm the presence of this bacterium through the measurement of PQS might be an interesting approach that should be further investigated. Moreover, if we are able to quantify and compare the levels of signalling molecules with different biological functions (e.g. HHQ and PQS) we might obtain valuable information about, for instance, the virulence of a specific pathogenic strain, the type of infection or the state of disease. Eventually, this information might help clinicians in the decision-making process for a better management of infected patients.

As it has been mentioned in Chapter 3, conventional detection methods used to quantify and identify autoinducers include mass spectrometry (MS) and/or high-performance liquid chromatography (HPLC) are not suitable for routine analysis. However, over the last few years, biosensors and PoC devices have emerged as a promising alternative for more rapid and efficient detection of biomarkers of disease. Between them, antibody-based technologies have demonstrated their capability to provide accurate and reliable diagnostic results, thanks to their great affinity and specificity. However, accomplishing high quality antibodies with the necessary affinity and specificity is crucial factor determined by the immunogen and the strategy used to produce antibodies. In this chapter it is reported, for the first time, an immunochemical strategy that implies the generation of highly specific antibodies against PQS and their implementation in an ELISA that might serve as an initial step towards the construction of such alternative and more efficient diagnostic tool for a proper evaluation of its potential as biomarker of infection.

5.3 RESULTS AND DISCUSSION

5.3.1 DEVELOPMENT OF PQS IMMUNOREAGENTS

5.3.1.1 Hapten design and synthesis

The Pseudomonas Quinolone Signal (PQS) is an autoinducer used specifically by *Pseudomonas aeruginosa* to regulate virulence (see Figure 5.2), and for this reason constitutes and excellent target to develop new diagnostic and therapeutic strategies. Due to its small size, is not immunogenic by itself, for which reason appropriate immunizing hapten design was performed to ensure the production of high affinity antibodies that will establish the strong non-covalent interactions, such as electrostatic, hydrogen bonds, hydrophobic and van der Waals forces, with our target[185,186].

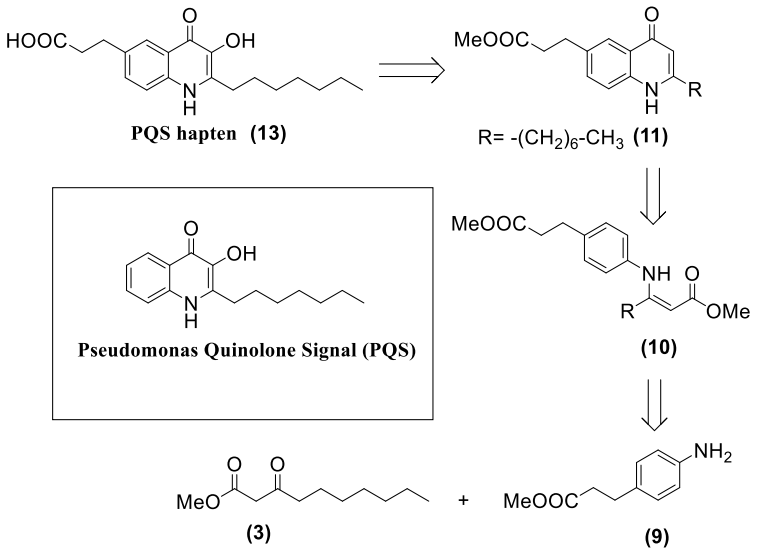

Figure 5.2. Retrosynthetic scheme for the synthesis of PQS hapten (8), analogous to 2-heptyl-3-hydroxy-4(1H)-quinolone (PQS) quorum sensing molecule of the *pqs* system from *P. aeruginosa*. The hapten was synthesized through a five steps synthetic pathway from 3-(4-aminophenyl)propanoic acid and methyl 3-oxodecanoate.

The quinolone ring and the characteristic catechol moiety of the native PQS structure were considered the most important epitopes, with capability to establish such kind of noncovalent interactions. Therefore, an immunizing hapten designed incorporating a spacer arm at C-6 position, promoting the exposure of the molecule moiety containing these functional groups. The end of the spacer arm was provided with a carboxylic acid, which eventually allowed the conjugation of the hapten to the lysine residues of an immunogenic protein through the use of orthogonal chemistry (active ester, anhydride mixed, etc.)[187].

The synthesis of the PQS hapten was inspired in a strategy previously described by Pesci and co-workers[151], based on two sequential modifications at the C-3 position of the PQS biological precursor, HHQ. The hapten synthesis (see Figure 5.3) started with esterification of 3-(4-aminophenyl)propanoic acid to obtain the protected aniline derivative **(9)**. The aniline derivative was subsequently reacted by amination reaction with the β-ketoester **(3)** in the presence of a catalytic amount of p-toluene sulfonic acid to obtain the intermediate **(10)**. Afterwards, the quinolone derivative **(11)** was obtained through Conrad-Umpach thermic cyclization in diphenyl ether at 270ºC. Formylation of the C-3 position through the Duff reaction [188] allowed to obtain the quinolone derivative **(12)** as precursor of the desired hapten. Concomitant hydrolysis of the methyl ester group occurred, however, this fact no longer affected the synthetic procedure. Finally, oxidation of the C-3 position through Dakin reaction allowed obtaining the PQS hapten **(13)**. This reaction relies on a characteristic hydrogen peroxide nucleophilic addition which promotes the [1,2]-aryl migration and elimination, subsequently obtaining an hydroxyl group directly bonded to the previously formylated position[189]. Overall, the pure proposed PQS hapten **(13)** was obtained in five synthetic steps with an overall yield of 16%.

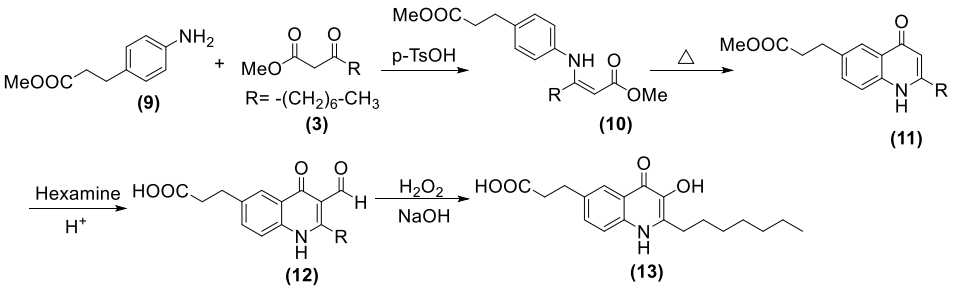

Figure 5.3. Schematic representation for the synthesis of PQS hapten. The main reagents or conditions used in each reaction are shown. The complete experimental procedure for obtaining each intermediate and final product can be found in materials and methods section.

5.3.1.2 Antibody production

The PQS hapten was used to prepare KLH and BSA protein bioconjugates following the anhydride mixed method. This method relies on the carboxylic acid activation using a chloroformate and a sterically hindered base, forming an anhydride that afterwards reacts with the lysine residues present in the protein[190]. Hapten bioconjugates were obtained with a high density ratio as demonstrated by MALDI-TOF-MS and fluorescence analysis, the last performed thanks to the emission band of PQS and the corresponding hapten **(13)** at 445 nm when using an excitation wavelength of 340 nm.

Table 5.1. Data on the bioconjugation yield and hapten densities of the PQS bioconjugates.

	Quantity (mg)	Yield (%)	Hapten density
PQS-BSA	5.95	119	17
PQS-KLH	5.29	105	116-130

Hapten densities of BSA conjugates were calculated from MALDI-TOF-MS analysis and fluorescence assay. KLH conjugate could not be analyzed by MALDI-TOF-MS because of the large molecular weight.

The conjugation degree on the fluorescence assays was established by interpolation of the fluorescence signal intensity of PQS-KLH, which cannot be analyzed by MALDI-TOF-MS due to its high molecular weight, or PQS-BSA bioconjugates solutions in a linear regression of fluorescence signal intensity versus PQS hapten concentration (see Figure 5.4). The number of conjugated

residues was calculated by iteration using initially the KLH molecular weight (350-400kDa), rendering a hapten density of 116-130 haptens per molecule of KLH (see Table 5.1). The PQS-BSA bioconjugate rendered an hapten density of 17 through both analytical methods, validating the results obtained by fluorescence assays. Eventually, antisera (As385, As386 and As387) were raised against PQS-KLH in female New Zealand white rabbits.

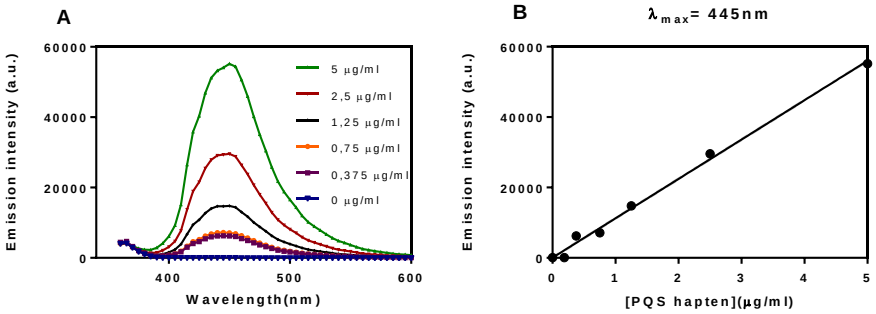

Figure 5.4. Graph A. Emission spectra at different concentrations of PQS hapten (13) in PBS 10 mM buffer using a λ_{exc} of 340 nm. Graph B. Linear regression of the emission intensity at 445 nm versus the concentration of PQS hapten (13) using a λ_{exc} of 340 nm.

5.3.2 DEVELOPMENT OF THE PQS (AS385/HHQ-BSA) ELISA

5.3.2.1 Antisera selection

The avidity of the obtained As for the BSA conjugates (HHQ-BSA, PQS-BSA and HQNO-BSA) and the competition of PQS for the binding to the antibodies was assessed by combined experiments comparing the absorbance of the assay in the presence and absence of the analyte and, after a preliminary selection, the most promising combinations were analyzed through two-dimensional titration experiments. The first set of experiments allowed to select the best As/bioconjugate combinations for competitive assays based on largest reduction of the signal when PQS was present in different combinations, while the second allowed to select the appropriate concentrations of the immunoreagents. As result 4 different As/bioconjugate combinations were assessed in competitive format (Table 5.2), from which the combination As385/HHQ-BSA was selected

for assessing the performance of the assay under different physico-chemical conditions with the aim of improving the detectability and the analytical features.

Table 5.2. Analytical parameters of the competitive indirect ELISA for the detection of PQS that were selected after bi-dimensional titration experiments.

	As 386; 1/8000	**As 385; 1/16000**	**As 385; 1/32000**	**As 387; 1/16000**
[CA] (µg/ml)	HHQ-BSA; 0.16	HHQ-BSA; 0.04	PQS-BSA; 0.08	PQS-BSA; 0.31
Bottom	0.12	0.06	0.03	-
Top	1.25	2.03	1.73	-
Hill Slope	-0.72	-0.77	-0.73	-
IC_{50}	24.1	18.5	19.1	-
R^2	0.991	0.999	0.995	-

5.3.2.2 Physicochemical parameters optimization

The performance of the assay under different physicochemical conditions such as the effect of time, pH, concentration of a non-ionic surfactant, ionic strength or presence of an organic solvent was evaluated (Figure 5.5). It was not observed a significant variation of the assay features by introducing a preincubation step and the optimum competition time was found to be 30 minutes. The assay was able to work at pH values between 4.5 and 9.5, although showing slightly better detectability/maximum absorbance ratio at pH 7.5. The addition of an organic solvent such as DMSO did not produce a significant enhancement, although the Amax increased, at concentrations greater that 2-5%, the detectability decreased. On the other hand, the sensitivity was dramatically affected by Tween 20.

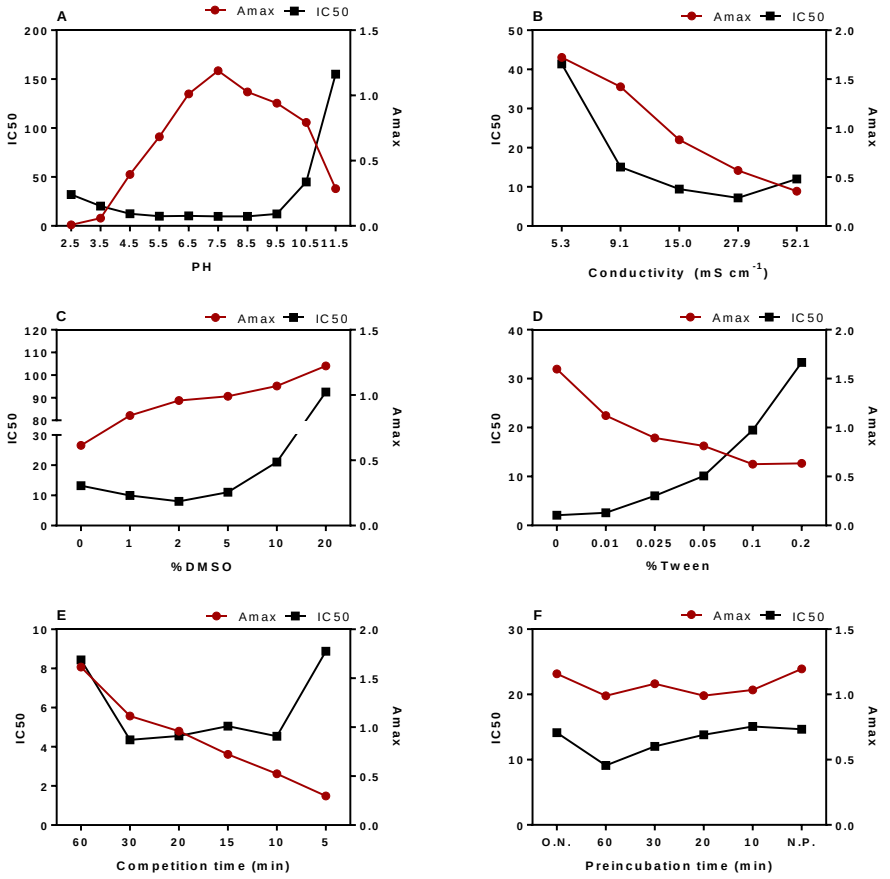

Figure 5.5. As385/HHQ-BSA ELISA performance in the physicochemical parameters optimization study. The selection of the most appropriate conditions (Table 5.2) was based on the variations in Amax, IC_{50} and slope values (not shown) of the generated calibration curves providing better signal/noise ratio, detectability and sensitivity. The studied parameters were A. pH B. Ionic Strength C. % organic solvent (DMSO) D. % Tween20 E. competition time F. preincubation time. All the studies were performed by varying the composition of the buffer used in the competitive step or the antibody detection times. Eventually, the conditions providing better features were evaluated again separately and in conjunction.

A substantial signal enhancement was observed when Tween 20 was not added to the assay buffer (see Figure 5.5D) while the IC_{50} value was significantly lower (better detectability) than under the standard conditions using a buffer with a 0.05% of this detergent. However, since it is known that the presence of a small amount of Tween 20 helps minimizing nonspecific interactions and solubilizing the analyte, it was decided to keep a concentration of just 0.01%. The

detectability was slightly better at conductivity values greater than 15mS cm^{-1}, however, the Amax decreased substantially, for this reason it was decided to keep the conductivity at 15 mS cm^{-1} for further experiments. Furthermore, it was added to the assay buffer 0.1 mM of EDTA as a result of the accuracy experiments (explained in the 4.3.3.2 section).

Table 5.3. Physicochemical parameters selected for the As385/HHQ-BSA ELISA run in the selected buffer (PBST-EDTA).

	As385 HHQ-BSA
As dilution	1/32000
[Competitor] (µg mL^{-1})	0.04
pH	7.5
Conductivity (mS cm^{-1})	15
Tween 20 (%)	0.01
Competition time (min)	30
Preincubation time (min)	0
Organic solvent (%)	0
EDTA (mM)	0.1

5.3.2.3 Analytical characterization

Analytical characterization of the assay was performed by assessing performance on repetitive experiments performed on different days. Under the selected conditions, the assay in buffer (PBST-EDTA) showed a LOD of 0.17 ± 0.01 nM and a dynamic range compressed between 0.53 ± 0.04 to 24.37 ± 3.18 nM (see Figure 5.6 and Table 5.4), which is below the average concentrations found in *P. aeruginosa* bacterial cultures (µM) and in the same range of concentrations (low-nM range) that the ones found in sputum samples by Abdalla and co-workers[70-72].

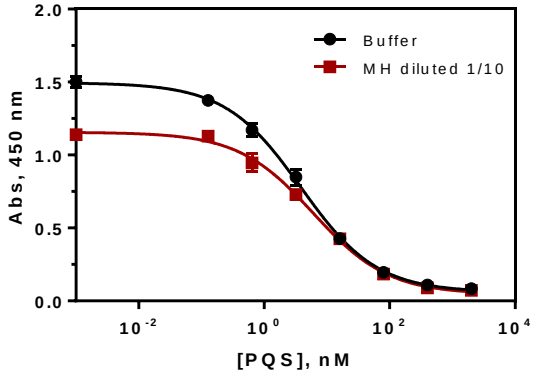

Figure 5.6. Calibration curves of the As385/ HHQ-BSA ELISA for the detection of PQS in buffer (PBST-EDTA) and in 1/10 diluted MH broth, under the conditions established (see Table 5.4). Each calibration point was measured in triplicates on the same ELISA plate and the results show the average and standard deviation of analysis made on three different days.

Furthermore, the detectability achieved with the As385/HHQ-BSA ELISA is greater than those obtained with other techniques such as those based on bioreporters[163,164] or electrochemical methods[169]. Regarding LC-MS/MS methods, the ELISA developed during this work allowed to obtain higher or similar detectability without including additional pre-concentration steps. These methods require the use of solid phase extraction and/or organic solvent extraction steps, ending up in a 20 times concentration factor of the sample for obtaining the reported LOQs[63,72].

Table 5.4. Features of the As385/ HHQ-BSA ELISA for the detection of PQS.

	PBST[a]	**MH diluted 1/10**[b]
A_{min}	0.03 ± 0.01	0.02 ± 0.01
A_{max}	1.45 ± 0.04	1.11 ± 0.03
Slope	-0.72 ± 0.01	-0.73 ± 0.11
IC_{50}	3.87 ± 0.53	6.05 ± 0.16
Dynamic Range	0.53 ± 0.04 to 24.37 ± 3.18	0.97 ± 0.25 to 36.16 ± 6.20
LOD	0.17 ± 0.01	0.36 ± 0.14
R^2	0.997 ± 0.002	0,995 ± 0,003

[a] Assay conditions used PQS-BSA at 0.04 µg mL^{-1} and the As385 diluted 48000 times in PBST. [b] Assay conditions used PQS-BSA at 0.04 µg mL^{-1} and the As385 diluted 64000 times in 1/10 PBST-EDTA diluted MH. The analytical parameters correspond to assay performed in MH diluted 10 times in

PBST-EDTA. The concentrations are expressed in nM and the data shown correspond to the average of 3 different days using at least 3 well/replicates per concentration.

5.3.2.4 Specificity study

PQS is the most important and active signalling molecule in the *P. aeruginosa pqs* QS system. However, other quinolones produced by this pathogen have also an important role in communication or interspecies interaction. The other two molecules are HHQ, precursor of PQS in the biosynthetic pathway and involved in the signaling process, and HQNO, a N-oxide quinolone able to inhibit the electron transport chain in other bacteria showing remarkable antistaphylococcal properties[191]. The only structural difference between HHQ, HQNO and PQS is one oxidized position (C-3 or N-1), reason why the recognition pattern by the As385/HHQ-BSA ELISA had to be assessed. Despite similarity between the different molecules, the percentage of cross-reactivity was less than 2% for HQNO (IC_{50}=236.2 nM) and about 13% in the case of HHQ (IC_{50}=27.2 nM) (see Figure 5.7). Hence, the ELISA developed recognized PQS much better even the great structural similarities of the other two autoinducer molecules from the *pqs* system, which pointed to the possibility to quantify specifically PQS from samples where all three quinolones might be present.

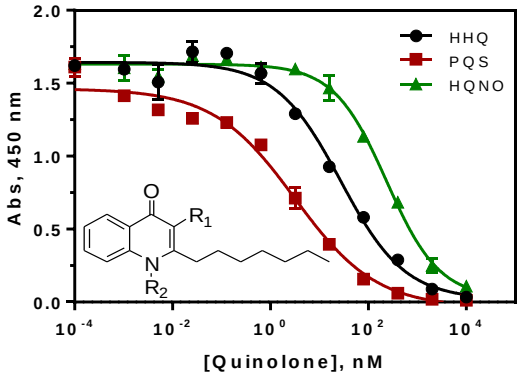

Figure 5.7. Cross reactivity study using the *pqs* quorum sensing metabolites HHQ, PQS and HQNO in buffer under the aforementioned conditions for As385/ HHQ-BSA ELISA. Calculated cross reactivity was 13% for HHQ (IC_{50}=27,2 nM) and 2% for HQNO (IC_{50}=236,2 nM). HHQ: R1=-H, R2=-H; PQS: R1=-OH, R2=-H; HQNO: R1=-H, R2=OH. Each calibration point was measured in triplicates on the same ELISA plate and the results show the average and standard deviation of analysis made on three different days.

Specificity studies using other molecules structurally related and non-related potentially present in clinical or bacterial culture samples was also assessed (Table 5.5). The molecules selected were PYO, IQS and the quinolone-type antibiotics ciprofloxacin and norfloxacin. In all cases the As385/HHQ-BSA ELISA did not respond to concentration up to 10 µM of all mentioned molecules and thus, the CR was assumed as less than 0.01% for all of them.

Table 5.5. Analytic parameters of the As385/HHQ-BSA ELISA using the *P. aeruginosa* metabolites PQS, HHQ, HQNO, PYO or IQS and the quinolone type antibiotics Ciprofloxacin and Norfloxacin.

	HHQ	PQS	HQNO	PYO	IQS	Ciprof.	Norf.
A_{min}	0.07	0.05	0.08	1.58	1.61	1.51	1.55
A_{max}	1.64	1.46	1.63	1.53	1.64	1.55	1.49
Slope	-0.66	-0.52	-0.80	-	-	-	-
IC_{50} **(nM)**	27.2	3.6	236.2	-	-	-	-
R^2	0.987	0.987	0.993	-	-	-	-
CR (%)	13	100	2	<0.01	<0.01	<0.01	<0.01

The percentages of cross reactivity (C.R.) were calculated following the equation: CR (%) = IC_{50}(Cross reactant)/IC_{50}(Analyte) x 100. PYO: pyocyanin; IQS: (2-(2-hydroxylphenyl)-thiazole-4-carbaldehyde); Ciprof.: Ciprofloxacin; Norf: Norfloxacin.

5.3.3 IMPLEMENTATION OF AS385/HHQ-BSA ELISA TO THE ANALYSIS OF CULTURE BROTH FROM *P. AERUGINOSA* CLINICAL ISOLATES

5.3.3.1 Matrix effect evaluation

As in the case as the HHQ assay, the ELISA was used to evaluate the profile of release of PQS on culture samples where *P. aeruginosa* was grown, as a pilot study. However, such type of samples may contain a variety of components from the media which may interfere with the assay. For this reason, on a first instance, the matrix effect caused by the Mueller-Hinton (MH) culture broth, frequently used to grow *P. aeruginosa* strains, was evaluated. This media contains nitrogenous compounds, vitamins, starch and amino acids which, added to the

products released by the bacteria itself such as virulence factors, proteins and other exo-products, which could make the sample quite complex. To estimate the extension of this effect, calibration curves were built in MH culture media at different dilution factors under the previously developed As385/HHQ-BSA ELISA. The resulting calibration curves and the effect caused by MH in the assay performance can be seen in Figure 5.8. The measurement in MH produced a substantial increase of the maximum signal and a decrease in the detectability of the assay. This effect could be diminished by increasing the dilutions of the MH media with the assay buffer, however the same features as the assay run in buffer could not be reach unless the MH broth was diluted at least 20 times, which compromised too much the detectability for our purposes. At the light of this behavior two-dimensional titration experiments were carried out using MH media diluted 10 times with the assay buffer to set up new assay conditions in respect to the concentration of immunoreagents.

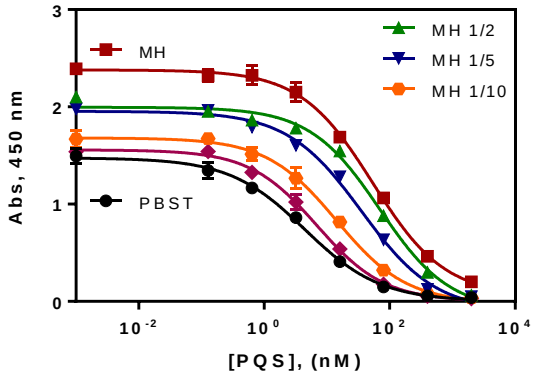

Figure 5.8. Matrix effect of the MH broth undiluted and diluted 2, 5, 10 and 20 times with PBST on the As385/ HHQ-BSA ELISA. The calibration curves were run using the conditions established for the assay in PBST. Modification of the assay conditions allowed achieving similar immunoassay features as when the assay was run in buffer (see Table 5.4 and Figure 5.6). The results shown are the average and standard deviations of analysis made on two different days measured by duplicates each day.

As it can be seen in Table 5.4 and Figure 5.6, the assay run in MH diluted 1/10 provided very good features in a similar range to the ones obtained in buffer. The IC_{50} value was 6.05 ± 0.16 nM while the obtained LOD was 0.36 ± 0.14 nM (Table 1), which taking into account the dilution factor would turn into 60.5 ± 1.6 nM and 3.6 ± 1.4 nM, respectively. PQS is normally found in the µM range[72] in *P.*

aeruginosa cultures and thus, the decrease in detectability caused by the MH dilution factor did not have to mean a negative impact on the PQS production kinetics assessment, allowing the quantification from a considerably low concentration.

5.3.3.2 Accuracy studies

Accuracy of the assay was evaluated by preparing blind spiked samples in MH culture broth and measuring them with the developed ELISA. Surprisingly, the results showed a critical underestimation of the spiked PQS concentrations (Figure 5.10). We hypothesized that this effect might be caused by the described chelating properties of PQS[192]. Thus, it is known the role of PQS chelating ferric iron (Fe^{3+}) in a non-deliverable manner [109] causing an iron starvation response and stimulating a concentration-dependent increase production of iron scavenging siderophores such as pyoverdine and pyochelin. PQS-Fe^{3+} has been found to accumulate in the membrane of the cell, acting as a storage molecule. Considering such behavior, it could be that PQS could be forming complexes with the cations present in MH culture broth. To probe this hypothesis, the calibration curve was run in the presence of different concentrations of ethylenediaminetetraacetic acid (EDTA), a powerful ion chelator able to displace the divalent cation complexation by PQS (Figure 5.9).

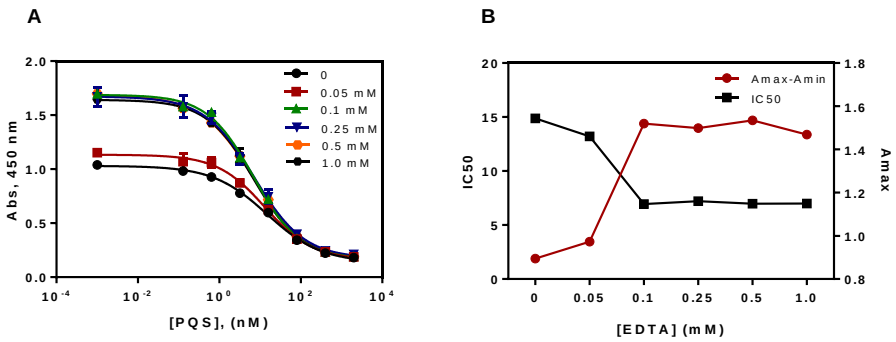

Figure 5.9. Graph A. Calibration curves of As385/ HHQ-BSA ELISA competitive indirect assay run in PBST buffer under the presence of different EDTA concentrations Graph B. Representation of the IC_{50} and maximum absorbance for the As385/ HHQ-BSA ELISA versus the assessed concentrations of EDTA.

The addition of EDTA caused a substantial increase of the maximum absorbance, nevertheless it produced an increase in detectability. At the light of these results, the addition of EDTA to the assay buffer (PBST-EDTA) was assessed during the accuracy studies. The experiments performed in the presence of EDTA produced a significant improvement of the quantification, as it is shown in Figure 5.10, where it can be observed the correlation between spiked concentrations and value measured with the ELISA. These results demonstrate that the PQS complexes are not recognized by the antibodies in the same manner as in the free form. Thus, subsequent experiments were performed in the presence of EDTA in the assay buffer.

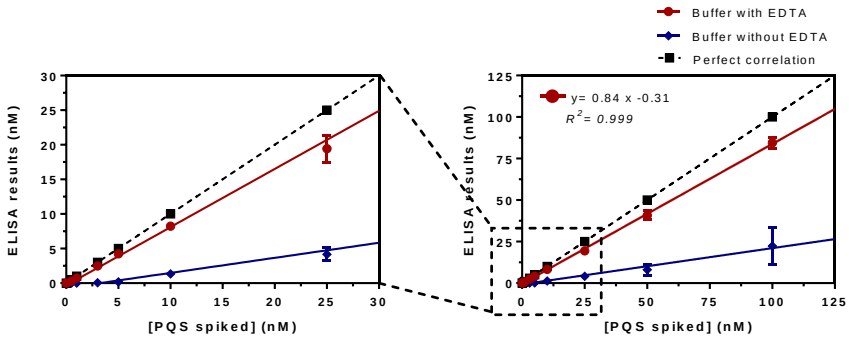

Figure 5.10. Results from the accuracy study. The graph shows the linear regression analysis of the MH broth PQS spiked concentration and the concentration measured with the As385/HHQ-BSA ELISA. Assays were run in diluted MH culture media 1/10 using PBST (blue line) and PBST-EDTA (red line). Each calibration point was measured in triplicates on the same ELISA plate and the results show the average and standard deviation of analysis made on three different days.

For a complete analytical characterization of the As385/HHQ-BSA ELISA intra-plate, inter-plate and inter-day precision was assessed, as it can be observed in Table 5.6, were the percentage of the coefficient of variation (%CV) at three different concentrations is shown (IC_{20}, IC_{50} and IC_{80}). The reproducibility is only slightly lower when measuring concentrations close to the limit of quantification during different days, but even at those very low concentration values the %CV is below of near 10% on intra-plate and inter-plate studies.

Table 5.6. Coefficients of Variation (CV) of the As385/HHQ-BSA ELISA run in MH culture broth diluted 1/10 using representative concentrations at a low, medium and high concentration range (IC_{20}, IC_{50} and IC_{80})

	IC	R1	R2	R3	μ	σ	%CV
Inter-day	**20**	31,45	35,30	40,59	35,78	4,59	12,8
	50	6,29	5,27	6,17	5,91	0,56	9,4
	80	1,30	0,80	0,93	1,01	0,26	25,4
Inter-plate	**20**	38,33	44,91	38,36	40,53	3,79	9,4
	50	5,51	5,95	6,04	5,84	0,28	4,8
	80	0,79	0,74	0,92	0,82	0,09	11,6
Intra-plate	**20**	29,93	30,21	31,68	30,61	0,94	3,1
	50	5,88	6,37	6,51	6,25	0,33	5,3
	80	1,09	1,20	1,28	1,19	0,09	7,9

The coefficient of variation (CV) was calculated following the equation CV (%) = σ/μ x 100. The results were obtained by measurements performed in either triplicates on the same ELISA plate (intra-plate), made on three different days (inter-day) or by analysis on three different plates (inter-plate). The concentrations of the replicates, mean, standard deviation and ICs are expressed in nM. IC: Inhibitory Concentration; R: Replicate; σ: Standard Deviation; μ: Average.

5.3.3.3 PQS measurement in bacterial culture broth

The implementation of the assay was carried through a first set of experiments addressed to find out the PQS production profile of clinical isolates growth on MH broth media. Previous experiments with HHQ (Chapter 3) already pointed at a different production profile between the clinical isolates that came from patients with chronic or acute infection[174]. For this reason, experiments with isolates PAAI6 and PACI6, obtained from patients with acute and chronic *P. aeruginosa* airways infection, respectively, were addressed to find out if the same profile was maintained for the main molecule of the *pqs* QS system, PQS. Interestingly, similarly to HHQ, PQS quantifiable levels were obtained after 5 h of growth for the clinical isolate PAAI6, while PQS could only be quantified after 12h for the PACI6 clinical isolate, even though the concentrations found at 48h were higher than in PAAI6 (see Figure 5.11). Moreover, the PQS release correlated to the growth as evidenced by the OD_{600} and the calculated CFUs. The decrease in the OD_{600} at 48h of growth observed in PAAI6 might be explained by the

prolonged exposure to high concentrations of self exo-products with lytic activity, such as pyocyanin and PQS[118,181,182].

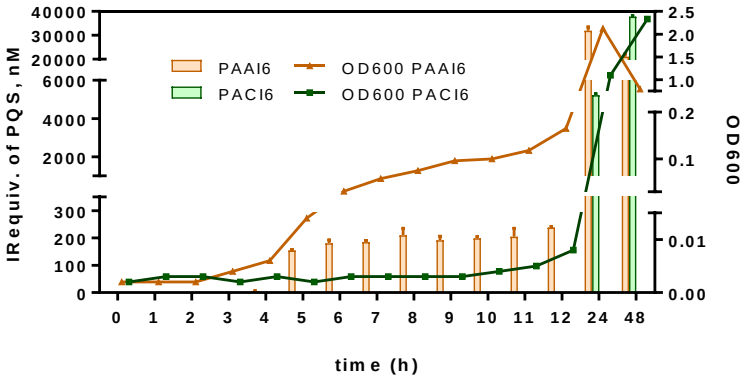

Figure 5.11. Bacterial growth, expressed as OD_{600} and PQS immunoreactivity equivalents (IRequiv) measured in MH broth media where P. aeruginosa clinical isolates PAAI6 and PACI6 were cultured. Samples were taken at the selected times and measured using the As385/HHQ-BSA ELISA. Each calibration point was measured in triplicates on the same ELISA plate and the results show the average and standard deviation of analysis made on two different days.

Next set of experiments were seeking to demonstrate that this was a general behavior for clinical isolates coming from patients with distinct degrees of severity of *P. aeruginosa* infection. For this purpose, clinical isolates from 12 different patients were grown in MH at 37ºC. After 8 h (time chosen as a compromise based on the above described behavior) sample aliquots were taken and measured with the PQS ELISA developed. As it can be observed in Figure 5.12 and Table 5.7, significant PQS concentration levels were found on the culture media from isolates belonging to acute or chronically infected patients. In the first group (patients 1-5), the PQS concentration values were in the range between 0.5 and 3 µM while for the second group (8-12) the PQS values were in the low nM range or below the LOD under these conditions.

In the light of this outcome, it seems clear that the concentration of QS molecules, such as HHQ or PQS, released to the media can be correlated with the type of infection or the disease status of the patient. Up to know applicability of this ELISA test has only been demonstrated analyzing culture media in which distinct *P. aeruginosa* clinical isolates have been growth. Further studies will be addressed to detect this QS molecule directly on clinical samples such as sputa in order to demonstrate the potential of this immunochemical technique to

provide diagnostic data in a rapid and reliable manner in order to support, assess and guide clinicians on the most appropriate management of *P. aeruginosa* infections.

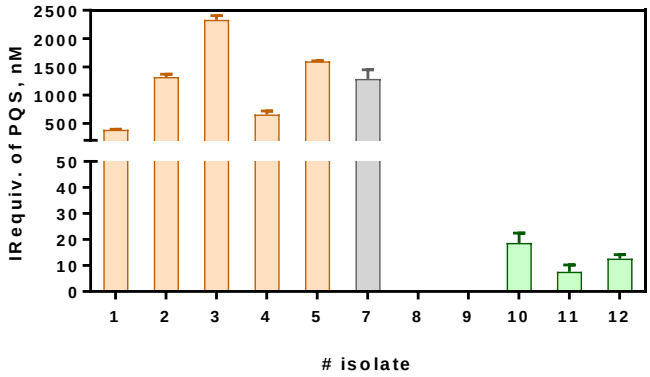

Figure 5.12. PQS IRequiv recorded from a collection of clinical isolates from patients with different clinical profiles. Samples were growth in MH broth for 8 hours and the aliquots taken were diluted 10 times with PBST-EDTA prior the ELISA analyses. Clinical isolates 1-5 were obtained from patients undergoing acute infection and isolates 8-12 were obtained from patients undergoing chronic infection. Isolate number 7 corresponds to the reference strain PAO1. The reference number of clinical isolates can be found in Table 6S. Each calibration point was measured in triplicates on the same ELISA plate and the results show the average and standard deviation of analysis made on two different days.

Table 5.7. Clinical isolates reference number and concentration of PQS measured with the developed As385/ HHQ-BSA ELISA.

#Number	#Ref	Infection type	[PQS](nM)	Desv. Est. (nM)
1	**PAAI1**	Acute	387.6	10.4
2	**PAAI2**	Acute	1320	51
3	**PAAI3**	Acute	2333	75
4	**PAAI4**	Acute	658.9	62
5	**PAAI5**	Acute	1599	6
6	**PAAI6**	Acute	210.0	25.1
7	**PAO**	Reference	1286	161
8	**PACI1**	Chronic	LLOQ	-
9	**PACI2**	Chronic	LLOQ	-
10	**PACI3**	Chronic	18.70	3.81
11	**PACI4**	Chronic	7.63	2.59
12	**PACI5**	Chronic	12.63	1.58
13	**PACI6**	Chronic	LLOQ	-

The clinical isolates were grown 8 hours in MH culture media at 37ºC following the protocol described in the main article.

5.4 CHAPTER CONTRIBUTIONS

- For the first time, antibodies against the main QS signalling molecule from the *pqs* system, Pseudomonas Quinolone Signal or PQS, have been developed. The synthesis of the hapten was performed following rational hapten design, keeping the most relevant epitopes and obtaining high specificity polyclonal antibodies

- The polyclonal antibodies against PQS were used to develop a competitive indirect ELISA able to quantify this signalling molecule with a LOD of 0.17 ± 0.01 nM and a dynamic range compressed between 0.53 ± 0.04 to 24.37 ± 3.18 nM. The assay works robustly in a wide range of physicochemical conditions, can be done in less than 2 hours and allows the measurement of the desired samples in a high-throughput manner.

- The assay was used for the measurement of PQS in culture broth samples from *P. aeruginosa* clinical isolates. It allowed to analyse and compare the production of PQS to the one of its precursor, HHQ (Chapter 3). Similarly, it allowed to stratify the clinical isolates between chronic and acute, relying on the production of PQS at low growth times, demonstrating the potential of QS molecules as potential biomarkers of infection and the usefulness of the developed ELISA.

5.5 MATERIALS AND METHODS

5.5.1 SYNTHESIS

General methods and instruments. The general methods and instruments can be found in section 4.5.1.

Methyl 3-(4-aminophenyl)propanoate (9): Thionyl Chloride (0.75 mL, 10 mmol) was added to stirred ice cooled MeOH (3mL). The mixture was left stirring 10 min and an ice cooled solution of 3-(4-aminophenyl) propanoic acid (0.5g, 3 mmol) in MeOH (0.5 mL) was slowly added. The mixture was stirred 16h under inert

atmosphere at room temperature. Afterwards, the mixture was evaporated under reduced pressure and aqueous $NaHCO_3$ satd. solution (10 mL) was added. The aqueous phase was extracted using ethyl acetate (3x5mL) and layers were combined, washed with brine (5mL), dried over Na_2SO_4 and evaporated under reduced pressure. The crude product was washed with hexane and dried to obtain **(9)** (0.53g, 3 mmol, 97% yield) as a single product. ^{1}H NMR (400 MHz, CD_3OD) δ 6.94 (d, *J* = 8.3 Hz, 2H, H8 and H12), 6.66 (d, *J* = 8.3 Hz, 2H, H9 and H11), 3.62 (s, 3H, H1), 2.78 (t, *J* = 7.6 Hz, 2H, H6), 2.55 (t, *J* = 7.6 Hz, 2H, H5).^{13}C NMR (101 MHz, CD_3OD) δ 175.37, 146.69, 131.64, 129.88, 116.93, 51.96, 37.12, 31.26. HRMS: *m/z* (ES+) for $C_{10}H_{13}NO_2$ [$(M+H)^+$] calculated 180.1025 found 180.1028 (+1.7 ppm).

Methyl 3-((4-(3-methoxy-3-oxopropyl)phenyl)amino)dec-2-enoate (10): A solution of methyl 3-(4-aminophenyl)propanoate (0.984 g, 5.5 mmol) and *p*-toluene sulfonic acid (0.017 g, 0.1 mmol) in dry toluene (3 mL) was slowly added to a stirring solution of methyl 3-oxodecanoate (1.0 g, 5 mmol) in dry toluene (15 mL). The reaction mixture was heated at 85ºC under a N_2 atmosphere for 16 h. The reaction mixture was allowed to cool down and was evaporated under reduced pressure. It was obtained the crude product **(10)** as a pale orange oil (1.26 g, 3.5 mmol, 70% yield) which was used without further purification for the next step. ^{1}H NMR (400 MHz, $CDCl_3$) δ 10.22 (s, 1H, H11), δ 7.15 (d, *J* = 8.3 Hz, 2H, H15 and H17), 7.00 (d, *J* = 8.3 Hz, 2H, H14 and H18), 4.70 (s, 1H, H9), 3.68 (s, 3H, H26), 3.67 (s, 3H, H23), 2.94 (t, *J* = 7.8 Hz, 2H, H19), 2.63 (t, *J* = 7.8 Hz, 2H, H20), 2.25 (t, *J* = 8.0 Hz, 2H, H7), 1.40 (quin., 2H, H2), 1.33 – 1.13 (m, 8H, H6-5-4 and H3), 0.84 (t, *J* = 6.9 Hz, 3H, H1). ^{13}C NMR (101 MHz, $CDCl_3$) δ 173.38, 171.16, 164.09, 129.07, 128.94, 125.43, 120.49, 84.38, 51.79, 50.39, 35.74, 32.32, 31.70, 30.48, 29.17, 29.14, 28.94, 22.69, 14.17. HRMS: *m/z* (ES+) for $C_{21}H_{31}NO_4$ [$(M+H)^+$] calcd 362.2331 found 362.2346 (+4.1 ppm).

Methyl 3-(2-heptyl-4-oxo-1,4-dihydroquinolin-6-yl)propanoate (11): Methyl 3-((4-(3-methoxy-3-oxopropyl)phenyl)amino)dec-2-enoate (1.26 g, 3.5 mmol) was added dropwise to refluxing diphenyl ether (40 mL) at 270 ºC and maintained for 2h. Once the reaction cooled to room temperature, the crude product was filtered through a silica preparative column using hexane as eluent to eliminate the diphenyl ether. The crude product was then re-absorbed in the same silica using DCM and evaporated under reduced pressure. Afterwards, the product was purified by flash column chromatography using DCM with 2% MeOH to

obtain the cyclized compound **(11)** as a pale-brown solid (0.93g, 2.6 mmol, 75% yield). ^{1}H NMR (400 MHz, $CDCl_3$) δ 11.64 (s, 1H, H1), δ 8.18 (d, *J* = 2.0 Hz, 1H, H6), 7.62 (d, *J* = 8.5 Hz, 1H, H9), 7.45 (dd, *J* = 8.5, 2.0 Hz, 1H, H8), 6.20 (s, 1H, H3), 3.64 (s, 3H, H17), 3.04 (t, *J* = 7.8 Hz, 2H, H12), 2.71 – 2.62 (m, 4H, H13 and H18), 1.76 – 1.61 (m, 2H, H19), 1.34 – 1.13 (m, 8H, H20-21-22 and H23), 0.81 (t, *J* = 6.8 Hz, 3H, H24). ^{13}C NMR (101 MHz, $CDCl_3$) δ 178.78, 173.28, 154.74, 139.23, 136.16, 132.70, 125.13, 124.26, 118.65, 108.27, 51.79, 35.73, 34.50, 31.79, 30.73, 29.28, 29.13, 29.11, 22.70, 14.15. HRMS: *m/z* (ES-) for $C_{20}H_{26}NO_3$ [$(M-H)^-$] calculated 328.1913 found 328.1904 (-2.8 ppm).

3-(3-Formyl-2-heptyl-4-oxo-1,4-dihydroquinolin-6-yl)propanoic acid (12): The cyclized compound **(11)** (700 mg, 2.1 mmol), hexamine (601 mg, 4.3 mmol) and *p*-TsOH·H2O (454 mg, 2.4 mmol) were dissolved in glacial acetic acid (54 mL). The mixture was heated at reflux for 3 h under a nitrogen atmosphere. After cooling, 6 M HCl (13 mL) was added and heating was continued at 115 °C for 1 h. The mixture was allowed to cool, diluted with water (20 mL), and extracted with ethyl acetate (3x20mL). The combined organic fractions were washed with brine (20mL), dried over $MgSO_4$, and concentrated under reduced pressure. The crude was purified by column chromatography on silica flash chromatography using DCM with 6% MeOH and 0.5% glacial acetic acid to obtain formylated compound **(12)** as an off-white solid (480 mg, 1.4 mmol, 66% yield). ^{1}H NMR (400 MHz, DMSO-d_6) δ 12.13 (s, 1H, H1), 10.38 (s, 1H, H25), 7.97 (d, *J* = 2.0 Hz, 1H, H6), 7.62 (dd, *J* = 8.4, 2.0 Hz, 1H, H8), 7.51 (d, *J* = 8.4 Hz, 1H, H9), 3.03 (t, *J* = 7.6 Hz, 2H, H17), 2.94 (t, *J* = 7.4 Hz, 2H, H12), 2.58 (t, *J* = 7.4 Hz, 2H, H13), 1.60 (quin., 2H, H18), 1.41 – 1.21 (m, 8H, H19-20-21 and H22), 0.86 (t, *J* = 6.7 Hz, 3H, H23). ^{13}C NMR (101 MHz, DMSO-d_6) δ 190.81, 177.98, 173.58, 159.61, 137.98, 137.59, 133.64, 126.12, 123.84, 118.74, 113.23, 48.59, 35.12, 31.54, 31.12, 29.98, 28.98, 28.85, 28.34, 22.04, 13.92. HRMS: *m/z* (ES-) for $C_{20}H_{24}NO_4$ [$(M-H)^-$] calculated 344.1705 found 344.1708 (+0.9 ppm).

3-(2-Heptyl-3-hydroxy-4-oxo-1,4-dihydroquinolin-6-yl)propanoic acid (13): Aqueous hydrogen peroxide (1.05 M, 1.0 ml, 1.0 mmol) and aqueous sodium hydroxide (1.08 M, 1.78ml, 1.9 mmol) were added to a solution of 3-(3-formyl-2-heptyl-4-oxo-1,4-dihydroquinolin-6-yl)propanoic acid (300 mg, 0.9 mmol) in ethanol (4.3 mL) under nitrogen atmosphere. The mixture was stirred overnight at room temperature. After completion, the reaction mixture was evaporated

under reduced pressure. The crude was purified by flash column chromatography using DCM with 4% MeOH and 0.5% glacial acetic acid. Eventually, it was obtained the hapten **(13)** as a pale brown solid (135 mg, 0.4 mmol, 47% yield). ^{1}H NMR (400 MHz, DMSO-d_6) δ 11.38 (s, 1H, H1), δ 7.90 (d, *J* = 1.6 Hz, 1H, H6), 7.45 (d, *J* = 8.6 Hz, 1H, H9), 7.43 (dd, *J* = 8.6, 1.6 Hz, 1H, H8), 2.91 (t, *J* = 7.5 Hz, 2H, H12), 2.71 (t, *J* = 7.5 Hz, 2H, H17), 2.57 (t, *J* = 7.5 Hz, 2H, H13), 1.64 (quin., 2H, H18), 1.37 – 1.18 (m, 8 H, H19-20-21 and H22), 0.84 (t, *J* = 6.6 Hz, 3H, H23). ^{13}C NMR (101 MHz, DMSO-d_6) δ 173.69, 168.59, 137.76, 135.95, 135.25, 134.14, 130.86, 122.96, 122.07, 117.86, 35.33, 31.19, 30.04, 28.77, 28.47, 28.12, 27.82, 22.06, 13.93. HRMS: *m/z* (ES-) for $C_{19}H_{25}NO_4$ [(M-H)$^-$] calculated 330.1705 found 330.1699 (-1.8 ppm).

5.5.1 IMMUNOCHEMISTRY

General methods and instruments. General methods and instruments can be found in section 4.5.2.

Buffers. The detailed composition of the general buffers can be found also in section 4.5.2. PBST-EDTA is PBS with 0.01% Tween 20 (pH 7.5) and 0.01mM EDTA.

5.5.1.1 Antibody production

Synthesis of the Bioconjugates PQS-KLH and PQS-BSA. A solution of the PQS hapten **(13)** (3.32 mg, 10 µmol) in anhydrous DMF (400 µL) was cooled to 4ºC. Afterwards, tri-n-butylamine (2.62 µL,11 µmol) and isobutyl cloroformiate (1.56 µL, 12 µmol) were added to the hapten solution and the mixture was left stirring 15 min at 4ºC and 30 min at room temperature. Then, 200 µL of the reaction mixture were slowly added over the protein solution (BSA or KLH, 2.5 mg mL^{-1}, 2 mL in PBS 10 mM) and the mixture was left stirring 2h at RT and overnight at 4ºC without agitation. The bioconjugates were purified by dialysis against 0.5 mM PBS (5 x 5 L) and Milli-Q water (1 x 5L), and stored freeze dried at -80 ºC. A small fraction (20 µL) of the PQS-BSA was kept for MALDI-TOF-MS analysis, rendering a hapten density of 17 haptens per molecule of BSA. Hapten densities of the PQS-BSA and the PQS-KLH were also assessed by fluorescence, measuring the

intensity of the emission at 445 nm, of the native protein and the bioconjugates, and interpolating the value on a regression line, rendering 116-130 hapten in the case of PQS-KLH and 17 hapten for PQS-BSA.

Polyclonal antisera (PAb). Antibody production has been performed with the support of the ICTS "NANBIOSIS", more specifically by the Custom Antibody Service (CAbS, CIBER-BBN, IQAC-CSIC)**.** Three female New Zealand white rabbits weighing 1–2 kg were immunized with PQS-KLH following established protocols in the research group. Immunizations were carried out in the animal facility of the Research and Development Center (CID) of the Spanish Research Council (CSIC) Registration Number: B9900083, employing approved procedures that avoid unnecessary treatments and minimize suffering of the animals. The protocol used in accordance with the institutional guidelines under a license from the local government (DAAM 7463) and approved by the Institutional Animal Care and Use Committee at the CID-CSIC. The antisera (As) obtained were named As385, As386 and As387. The animals were exsanguinated after 6 immunizations, and the final blood was collected in vacutainer tubes provided with a serum separation gel. Antisera were obtained by centrifugation at 4 °C for 10 min at 10 000 rpm, then stored at −80 °C in the presence of preservative 0,02% sodium azide. The antibody titer was assessed during the immunization process through non-competitive indirect ELISA. Microtiter plates were coated with a fixed concentration of PQS-BSA conjugate (1 mg mL^{-1}) and the avidity of the produced antibodies was measured by preparing serial dilutions of the corresponding As.

5.5.1.2 ELISA

Non-competitive indirect two-dimensional titration experiments. Non-competitive indirect ELISA were carried out to select the As dilutions and the concentrations of coating antigen (CA) more suitable for developing the competitive assays. With this regard, the binding serial dilutions of the antisera (As385-387, 1/1000 to 1/64000, and zero in PBST, 100 µL/well) to microplates coated with the BSA bioconjugates, 5 µg mL^{-1} to 5 ng mL^{-1}, and zero in coating buffer, 100 µL/well) were measured. From these experiments, optimum concentrations for coating antigens and antisera dilutions were chosen to produce around 1.0-1.5 units of absorbance after 30 min of competitive step.

As385/HHQ-BSA ELISA (in PBST-EDTA). Microtiter plates were coated with HHQ-BSA conjugate in coating buffer (0.04 µg mL^{-1}, 100 µL/well) overnight at 4ºC and covered with adhesive plate sealer. The day after, plates were washed with PBST (4 x 300 µL/well) and solutions of PQS standards (2µM to 0.13 nM in PBST-EDTA, 50 µL/well) followed by the As385 (dil. 1/48000 in PBST-EDTA, 50 µL/well) addition and the microplates left without agitation 30 min at room temperature. After another washing step, a solution of diluted goat anti-rabbit IgG-HRP (1/6000 in PBST) was added (100 µL/well) and incubated for 30 min at room temperature. The plates were washed again and the substrate solution (100 µL) was added and left 30 min at room temperature in the dark. The enzymatic reaction was stopped by adding 4N H_2SO_4 solution (50 µL/well) and the absorbance read at 450 nm.

Immunoassay performance evaluation. Performance of the assays was evaluated through the modification of different physicochemical parameters (competence time, incubation time, pH, ionic strength, presence of a surfactant (% Tween 20), solubility with addition of organic solvents or cation complexation (EDTA) in the competition step.

Cross Reactivity studies. This experimental procedure can be found in section 4.5.2.2.

5.5.1.3 Implementation of the ELISA to the analysis of clinical isolates

Samples. The obtention and experimental procedure used for growing the clinical isolates can be found in section 4.5.2.3. Aliquots were taken at the selected times for measurement of OD_{600}, for Colony Forming Units (CFUs) calculation and measurement of PQS by ELISA. The rest of isolates were grown using the same experimental procedure, yet the aliquots were extracted just at a selected time of 8 hours. PQS concentrations measured by ELISA are expressed as PQS immunoreactivity equivalents (IRequiv), due to the potential specific interferences caused by other alkylquinolones of different chain length potentially present in the culture media.

Matrix effect and accuracy studies. Both procedures are fully described in section 4.5.2.3.

6 2-HEPTYL-4-QUINOLINE N-OXIDE (HQNO)

6.1 CHAPTER PRESENTATION

In this chapter is described the development of an immunochemical method for the main quinolone-type virulence factor produced by *P. aeruginosa*, 2-heptyl-4 quinoline N-oxide or HQNO and the studies performed to assess its potential as biomarker of infection. This chapter also seeks to compare the production of HQNO by *P. aeruginosa* clinical isolates to the signalling molecules HHQ and PQS and evaluate their complementarity for the diagnostic of infections through their immunochemical measurement. The structure of the present chapter can be found in Figure 6.1.

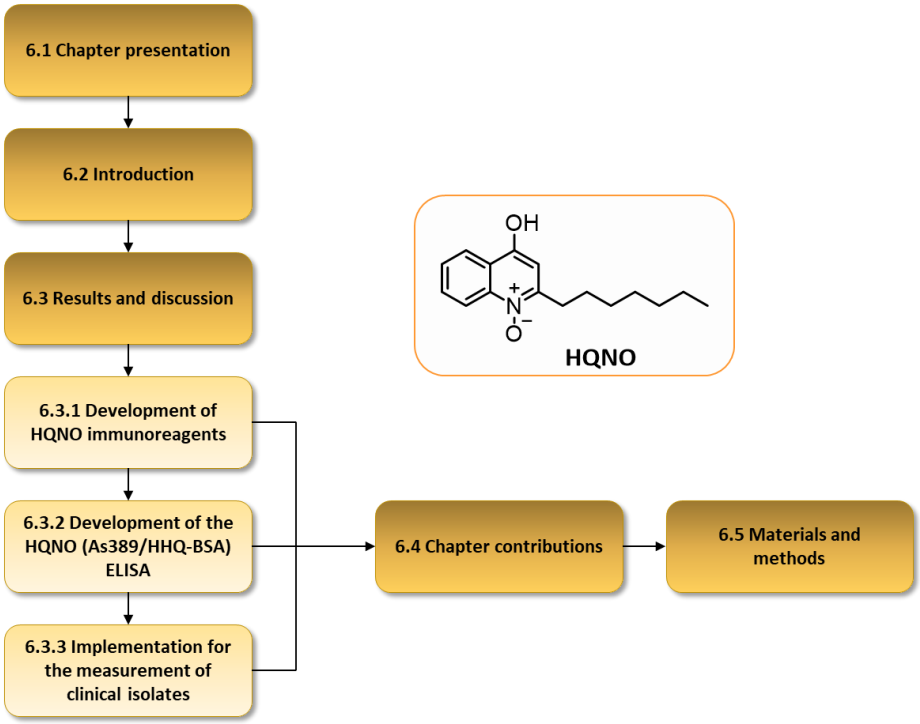

Figure 6.1. Structure of Chapter 6 related to the different sections.

6.2 INTRODUCTION

6.2.1 2-HEPTYL-4-QUINOLINE N-OXIDE (HQNO)

P. aeruginosa produces a great number of virulence factors that are key weapons during pathogenic processes. The importance of these factors is beyond argument and nevertheless, the entire biological and clinical significance of all of them is far from being known. Among all the relevant virulence factors produced by this pathogen it is possible to find HQNO, a QS-controlled secondary metabolite produced by the *pqs* system of *P. aeruginosa* without implication in the signalling network[84] Even though, HQNO has been demonstrated to have a wide implication on the anti-staphylococcal skills of *P. aeruginosa.* This molecule inhibits the oxidative respiration by interfering with the electron transport chain and the production of HQNO is one of the main mechanisms that *P. aeruginosa* carry out to subjugate *S. aureus* to persist as SCVs. It also causes cell lysis and DNA release, promoting the formation of biofilms. Altogether, the functions of HQNO, its role during pathogenesis and the clinical significance could be further studied if appropriate methods and techniques for its quantification are developed. With this aim, in this chapter is described the first immunochemical analysis of HQNO, including the synthesis of a rational designed immunizing hapten and the production of highly specific polyclonal antibodies.

6.3 RESULTS AND DISCUSSION

6.3.1 DEVELOPMENT OF HQNO IMMUNOREAGENTS

6.3.1.1 Hapten design and synthesis

Quorum Sensing (QS) has emerged as an attractive target for new therapeutic and diagnostic strategies and for the management and surveillance of bacterial infections. The key elements of this complex and sophisticated communication system are the autoinducers (AI), which provide bacteria a mechanism to sense

the population density and regulate intricate processes for survival and proliferation and that serve for many biological functions besides its signalling activity. Similarly, QS-directed metabolites without contribution in signalling such as pyocyanin and HQNO, also have an extreme importance for the interspecies competition and bacterial fitness. The detection of these molecules for evaluating their potential as biomarkers of infection might help and shed light over infectious processes, providing important information to clinicians about the pathogenesis, such as the state and progression of disease. For that reason, the strategy developed in this chapter was similar to the one used in chapters 3 and 4. However, the development of high-affinity antibodies against HQNO, a *P. aeruginosa* quinolone-type virulence factor, was essential for constructing an immunochemical method for its evaluation also as biomarker of infection, allowing a better comprehension of bacterial pathogenicity and the comparison with the signalling molecules HHQ and PQS.

As explained in previous chapters, small organic molecules such as alkylquinolones (< 500 Da) are not able to elicit an immune response by themselves and thus, preclude the direct production of antibodies. For that reason, these molecules have to be conjugated to a bio-macromolecule able to strongly activate the immune system in the selected animal of experimentation. In such case, an hapten that mimics the original structure has to be rationally designed incorporating a linker or spacer arm susceptible of bioconjugation to an immunizing protein. In the present work, HQNO hapten was designed for conserving functional groups and positions N-1 and C-2 to C-4 unaltered regarding the original HQNO metabolite (Figure 6.2). These positions were considered to contain the most reactive and characteristic epitopes that will establish the required strong and specific non-covalent interactions with the produced antibodies[185,186]. The spacer arm of the hapten was placed at C-6, thus maximizing the recognition of the most reactive epitopes and minimally altering the electronic structure of the original molecule. The spacer arm ended in a carboxylic acid that allowed the bioconjugation to the lysine residues of the protein through the use of orthogonal chemistry.

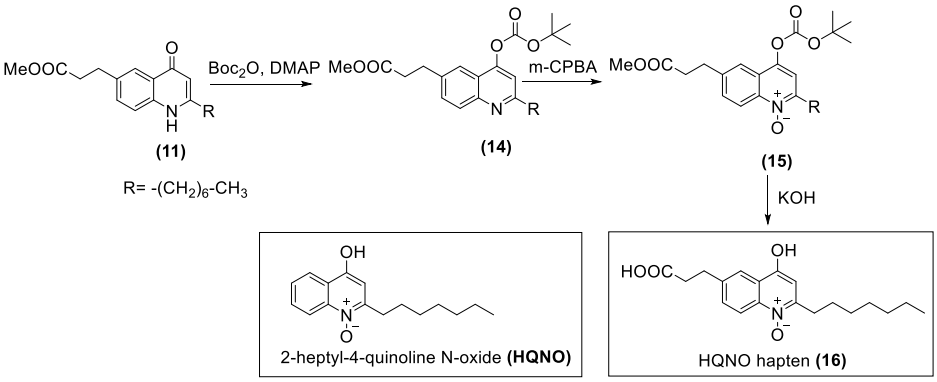

Figure 6.2. Synthetic scheme for the synthesis of HQNO hapten (16), analogous to 2-heptyl-4-quinoline N-oxide of the pqs system from *P. aeruginosa*. The hapten was synthesized through a three steps synthetic pathway from methyl 3-(2-heptyl-4-oxo-1,4-dihydroquinolin-6-yl) propanoate.

The synthesis of the hapten followed the same strategy as that the described by Woschek et al[193], but using methyl 3-(2-heptyl-4-oxo-1,4-dihydroquinolin-6-yl) propanoate **(11)**[180] (Figure 6.2). as starting material. To prevent undesired reactions of this ester due to the high nucleophilicity of the position C-3 and the electrophilic character of C-4 due to the carbonyl, blocking of the corresponding tautomer was addressed by protecting this carbonyl group with di-tert-butyl dicarbonate and a catalytic amount of DMAP, obtaining the intermediate **(14)** with 88% yield. Afterwards, the oxidation of the nitrogen to obtain the characteristic N-oxide functional group was achieved by reaction with m-CPBA, obtaining the intermediate **(15)** with 92% yield. Finally, the desired HQNO hapten **(16)** was obtained by simultaneous deprotection of the carbonyl and the carboxylic acid using a degassed solution of KOH. The overall yield of the three synthetic steps was 62%.

6.3.1.2 Antibody production

Bioconjugation of the hapten **(16)** was carried out using the anhydride mixed method, based on the generation of a reactive anhydride from the carboxylic acid of the hapten using chloroformiate and a hindered base, which reacted rapidly with the amino groups of the lysine residues of the proteins. The hapten density obtained for the HQNO-BSA bioconjugate was relatively high (21 conjugated lysine residues/ 35 available lysine residues) (Table 6.1),

notwithstanding the bioconjugate presented good solubility in PBS 10 mM and was kept for further experiments. The HQNO-KLH bioconjugate was used to raise polyclonal antibodies in female New Zealand white rabbits obtaining the antisera named As388, As389 and As390.

Table 6.1. Data on the bioconjugation yield and hapten densities of the HQNO bioconjugates.

	Quantity (mg)	Yield (%)	Hapten density
HQNO-BSA	3.38	67	21
HQNO-KLH	3.34	67	-

Hapten densities of BSA conjugates were calculated from MALDI-TOF-MS analysis. KLH conjugate could not be analyzed by MALDI-TOF-MS because of the large molecular weight. For this purpose, BSA ans KLH bioconjugates were prepared in paralell, under exactly the same conditions. The data obtained with the corresponding BSA bioconjugates was used as bioconjugation control.

6.3.2 DEVELOPMENT OF THE HQNO (AS389/HHQ-BSA) ELISA

6.3.2.1 Antisera selection

The avidity of these antisera for the BSA conjugates (HQNO-BSA, HHQ-BSA and PQS-BSA[194]) was assessed through two-dimensional non-competitive indirect ELISA experiments, which allowed determination of the suitable concentrations of these immunoreagents for developing competitive assays. The best antisera/bioconjugate combinations were selected based on the IC_{50} parameter and slope of the calibration curves (Table 6.2). As a result of those experiments, the selected combination for the development of competitive assay was As389/HHQ-BSA.

Table 6.2. Analytical parameters of the competitive indirect ELISA for the detection of HQNO that were selected after bi-dimensional titration experiments.

	As 388; 1/8000	**As 389; 1/4000**	**As 388; 1/16000**	**As 389; 1/8000**
[CA] (µg/ml)	HHQ-BSA; 0.25	HHQ-BSA; 0.25	HQNO-BSA; 0.31	HQNO-BSA; 0.16
Bottom	0.15	0.23	-	-
Top	2.62	1.80	-	-
Hill Slope	-0.67	-0.55	-	-
IC_{50}	4824	46.9	-	-
R^2	0.994	0.999	-	-

6.3.2.2 Physicochemical parameters optimization

As389/HHQ-BSA was finally selected for further studies about the performance under different physicochemical conditions such as pH, ionic strength, concentration of a non-ionic surfactant, presence of organic solvent and the effect of the incubation time. As it can be observed in Figure 6.3, the pH of the assay buffer and the concentration of the surfactant Tween 20 were the factors that most affected the assay. The best detectability was accomplished at pH values between 5.5 and 6.5, performing better under acidic than under basic conditions. Thus at pH 4.5 the assay still can be used with IC_{50} values slightly higher (38nM vs 23 nM at pH 6.5) while at pH 7.5 the IC_{50} value was 52 nM and pH 8.5 raised to 93 nM. The maximum absorbance of the assay reached the higher value at pH 6.5, while below this pH decreased significantly. In respect to the concentration of Tween 20 in the buffer, the best features were obtained in the absence of surfactant (IC_{50}, 19 nM), observing a decrease in the detectability already at 0.01% (IC_{50}, 43 nM) with raised dramatically when increasing the concentrations of the non-ionic surfactant. On the other hand, higher conductivities favoured the detectability, although the maximum absorbance and the slope proportionally worsened compromising the performance of the assay. A conductivity of 15 mS cm^{-1} was selected as a compromise between maximum signal of the assay and detectability for which the slope of the calibration curve was also acceptable (-0.75 ± 0.04) for a proper quantification of the target. The competition time was found to be optimal at 30 min and there was not a significant improvement of the assay features if adding a preincubation step. The parameters showing an enhancement were evaluated again separately and in conjunction to evaluate whether the effect was significant enough and the

resulting calibration curve and working features in the selected buffer (PBS-6.5) are shown in Table 6.3.

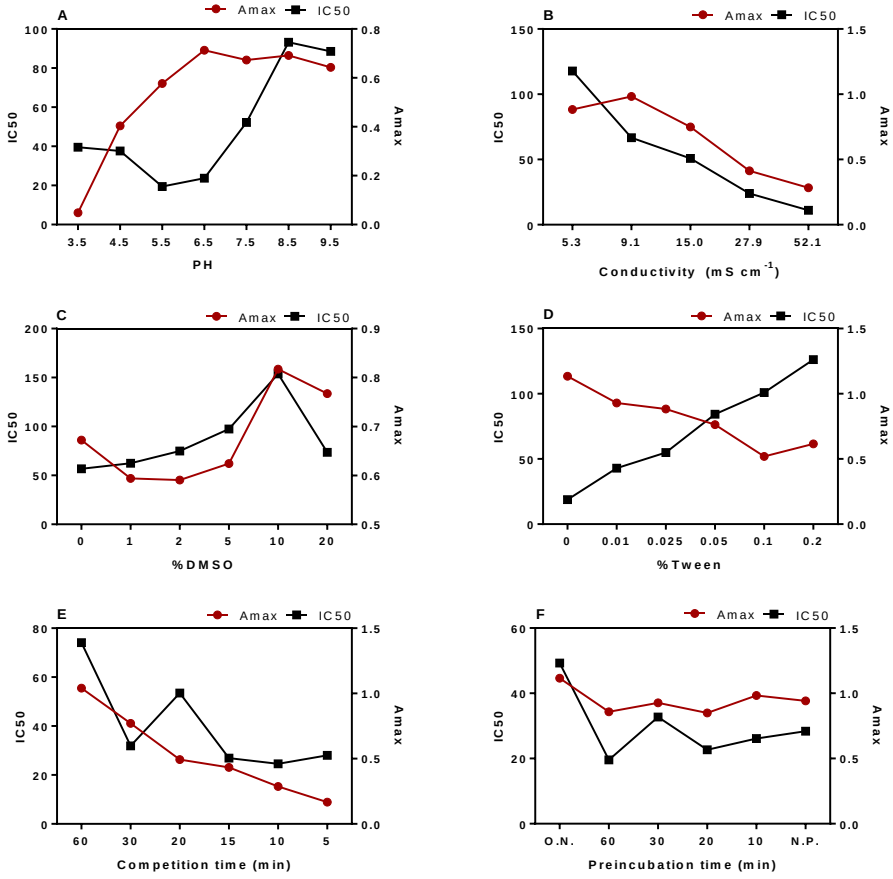

Figure 6.3. As389/ HHQ-BSA ELISA performance in the physicochemical parameters optimization study. The selection of the most appropriate conditions (Table 6.3) was based on the variations in Amax, IC_{50} and slope values (not shown) of the generated calibration curves providing better signal/noise ratio, detectability and sensitivity. The studied parameters were A. pH B. Ionic Strength C. % organic solvent (DMSO) D. % Tween20 E. competition time F. preincubation time. All the studies were performed by varying the composition of the buffer used in the competitive step or the antibody detection times. Eventually, the conditions providing better features were evaluated again separately and in conjunction.

Table 6.3. Physicochemical parameters selected for the As389/HHQ-BSA.

	As389 HHQ-BSA
As dilution	1/8000
[Competitor] (μg mL^{-1})	0.250
pH	6.5
Conductivity (mS cm^{-1})	15
Tween 20 (%)	0
Competition time (min)	30
Preincubation time (min)	0
Organic solvent (%)	0

The parameters improving the features of the assay were assessed separately and in conjunction.

6.3.2.3 Analytical characterization

After these studies, optimum conditions were established for the As389/HHQ-BSA ELISA that involved the use of PBS-6.5 as the assay buffer. The calibration recorded under these conditions is shown in Figure 6.4. HQNO could be detected with a LOD of 0.27 ± 0.09 nM, an IC_{50} of 4.20 ± 0.86 nM and a dynamic range compressed between 0.72 ± 0.18 to 26.71 ± 0.96 nM (Table 6.4). The detectability achieved was far below the values reported in bacterial cultures (μM range)[129,130,152,195] and in the same range as those found in clinical samples (nM range)[63,67]. Usually, HQNO quantification is made by LC-MS that despite their robustness require tedious extractions and intermediate pre-concentration steps to achieve the required detectability[63,67,72], while the ELISA here reported may achieve comparable performance on a direct manner.

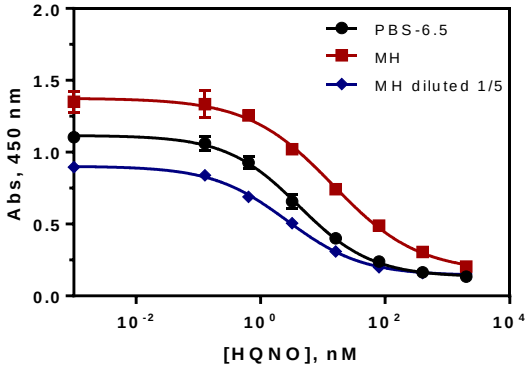

Figure 6.4. Calibration curves of the As389/HHQ-BSA ELISA for the detection of HQNO in buffer (PBS-6.5) and in 1/5 diluted MH broth, under the conditions established (). Each calibration point was measured in triplicates on the same ELISA plate and the results show the average and standard deviation of analysis made on three different days.

Table 6.4. Features of the As389/HHQ-BSA ELISA for the detection of HQNO.

	PBST	MH	MH diluted 1/5
A_{min}	0.09 ± 0.04	0.12 ± 0.01	0.09 ± 0.02
A_{max}	1.08 ± 0.06	1.32 ± 0.08	0.85 ± 0.01
Slope	-0.75 ± 0.04	-0.64 ± 0.03	-0.72 ± 0.06
IC_{50}	4.20 ± 0.86	14.65 ± 2.21	2.71 ± 0.04 (13.55 ± 0.20)
Dynamic Range	0.72 ± 0.18 to 26.71 ± 0.96	1.84 ± 0.38 to 105.37 ± 5.98	0.41 ± 0.10 to 17.04 ± 1.08
LOD	0.27 ± 0.09	0.60 ± 0.13	0.15 ± 0.05 (0.75 ± 0.25)
R^2	0.987 ± 0.013	0.998 ± 0.001	0.990 ± 0.004

The concentration of BSA conjugate and As dilution used in the assay run in buffer (PBS, pH=6.5) were 0.25 µg mL-1 and 1/8000, respectively. In the case of the assay run in MH diluted 1/5 the concentration of BSA conjugate and As dilution were 0.25 µg mL-1 and 1/8000, respectively. The parameters and features of the MH 1/5 curve correspond and refer to the values in the diluted sample. The concentrations are expressed in nM and the data shown correspond to the average of 3 different days using at least 2 well/replicates per concentration.

6.3.2.4 Specificity study

P. aeruginosa produces a wide variety of quorum sensing molecules among which quinolones are the main signals and metabolites from the pqs communication system. Despite the similarities of their chemical structures,

PQS, HHQ and HQNO have different roles and functions. Since there are high chances to find these quinolones secreted simultaneously during the course of an infection or in culture, there was necessary to assess the assay specificity towards these other QSMs. The results of these studies showed that the As389/HQNO-BSA ELISA recognized HQNO on a greater extent with low interferences from the PQS (7% cross reactivity (CR)) and HHQ (19% CR) (Figure 6.5). Presumably, HHQ was better recognized because the lack of functionalization at C-3 position of the quinolone core, as in HQNO, since the recognition of this molecule moiety was maximized according the chemical structure of the hapten designed. These percentages of CR may play a role during quantification of HQNO and therefore should be taken into account, and this is the reason because in this work the concentration of HQNO measured in biological samples is always expressed as IR equiv. (immunoreactivity equivalents). Other structurally related substances quinolone-type antibiotics (ciprofloxacin and norfloxacin) and non-structurally related QS metabolites (IQS, 2-(2-hydroxyphenyl)-thiazole-4-carbaldehyde) and virulence factors (pyocyanin) which could also be eventually present on a clinical sample were also evaluated; however, as it is shown in Table 6.5, in all cases the CR was less than 0,01%. On the other hand, the previously developed immunochemical assays for the quantification of HHQ and PQS might help to quantify and obtain an estimated concentration value of HQNO in the biological samples[180,194].

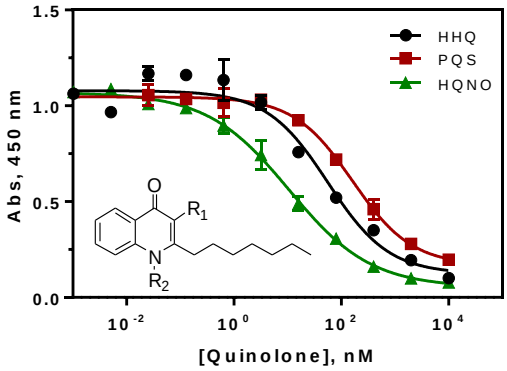

Figure 6.5. Cross reactivity study using the pqs quorum sensing metabolites HHQ, PQS and HQNO in buffer under the aforementioned conditions for As389/HHQ-BSA ELISA. Calculated cross reactivity was 19% for HHQ (IC_{50}=56.0 nM) and 7% for PQS (IC_{50}=162.5 nM). HHQ: R1=-H, R2=-H; PQS: R1=-OH, R2=-H; HQNO: R1=-H, R2=OH.

Table 6.5. Half maximal inhibitory concentration (IC_{50}) of the As389/HHQ-BSA ELISA using as analytes HHQ, PQS, HQNO, pyocyanin, IQS and the quinolone-type antibiotics Ciprofloxacin and Norfloxacin.

Quinolone	IC_{50}	C.R. (%)
HHQ	56.0	19
PQS	162.5	7
HQNO	10.7	100
Pyocyanin	-	<0.01%
IQS	-	<0.01%
Ciprofloxacin	-	<0.01%
Norfloxacin	-	<0.01%

The percentages of cross reactivity (C.R.) were calculated following the equation: CR (%) = IC_{50}(Cross reactant)/$IC_{50(}$Analyte) x 100.

6.3.3 IMPLEMENTATION OF AS389/HHQ-BSA ELISA TO THE ANALYSIS OF CULTURE BROTH FROM *P. AERUGINOSA* CLINICAL ISOLATES

6.3.3.1 Matrix effect evaluation

In previous studies we investigated the potential of other immunochemical assays for following-up the production of signalling molecules (HHQ and PQS) secreted by *P. aeruginosa* in bacterial cultures. In this particular case, our aim was to investigate if the production kinetics and the total amount of HQNO, a relevant virulence factor for this pathogen without implication in signalling, followed a similar trend than that of the signalling molecules. With this knowledge, we addressed investigation of the production kinetics of HQNO on a culture media such as Müeller Hinton (MH). Previously, the potential non-specific interferences in this complex biological matrix were assessed by building calibration curves in MH diluted several times with PBS-6.5. As it is shown in Figure 6.6 the MH broth the assay performed well in MH, although in respect to the curve run in buffer a slight increase of the maximum signal could be observed with a concomitant decrease in the assay (IC_{50} 4.7 in buffer vs 14.6 in MH). This effect diminished when diluting the MH media with the assay buffer reaching almost the same, or even slightly better, immunoassay features with a 1/5

dilution factor. The assay could then either used directly in MH calibrating the assay with this media or in 1/5 diluted, reaching in both cases almost identical analytical performance, without the need of any sample treatment or purification step (Figure 6.4 and Table 6.2). Therefore, as it was obtained similar detectability and features in MH or MH diluted 1/5, it was decided to use the last in order to prevent or reduce potential non-specific interferences caused by the release of other bacterial exo-products.

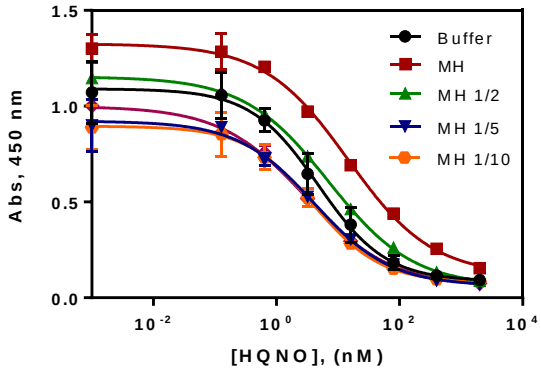

Figure 6.6. Matrix effect of the MH broth undiluted and diluted 2, 5, 10 and 20 times with PBST on the As389/HHQ-BSA ELISA. The calibration curves were run using the conditions established for the assay in PBS-6.5. Modification of the assay conditions allowed achieving similar immunoassay features as when the assay was run in buffer (Figure 6.4). The results shown are the average and standard deviations of analysis made on two different days measured by duplicates each day.

The features of the As389/HQNO-BSA ELISA run in MH diluted 1/5 are shown in Table 6.4 and the calibration curve in Figure 6.4. The detectability achieved was comparable and even better to the one of the assay run in buffer, obtaining a LOD of 0.15 ± 0.05 nM and an IC_{50} value of 2.71 ± 0.04 nM, which taking into account the dilution factor turns into 0.75 ± 0.25 nM and 13.55 ± 0.20 nM, respectively. The decrease in detectability caused by the dilution factor was not expected to influence the measurement of HQNO in culture samples because, as previously mentioned, HQNO is normally found in the µM range in bacterial cultures[152,195,196]. The developed ELISA allows direct quantification of HQNO on MH culture broth just by using a sample dilution, without including any complex sample treatment procedures. In addition, the ELISA is able to provide results in a short frame-time, has high-throughput screening capability and is simple to perform.

6.3.3.2 Accuracy studies

The accuracy of the As389/HQNO-BSA ELISA in 1/5 diluted MH was evaluated by preparing blind samples spiked with HQNO concentrations inside and outside the dynamic range. These samples were then measured in triplicates on the same ELISA microplate and the same experiments were repeated during three different days. As it is shown in Figure 6.7, the correlation between the spiked and the measured concentration was quite good with a slope of 0.89 ± 0.01 nM and a regression coefficient of 0.999.

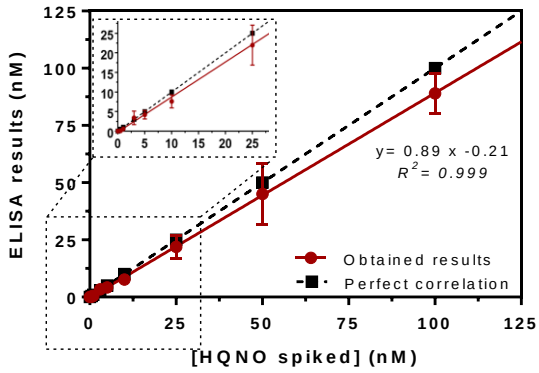

Figure 6.7. Results from the accuracy study. The graph shows the linear regression analysis of the MH broth HQNO spiked concentration and the concentration measured with the As389/HHQ-BSA ELISA. Assays were run in diluted MH culture media 1/5 using PBS-6.5. Each calibration point was measured in triplicates on the same ELISA plate and the results show the average and standard deviation of analysis made on three different days.

Precision of the assay was also assessed by calculating the percentage of coefficient of variation within the same plate (intra-plate variation), between diverse plates (inter-plate variation) and in different days (see Table 6.6). These experiments were done at three different levels of concentrations (low (IC_{80}), medium(IC_{50}) and high(IC_{20})). In general, the % CV remained below 20% except for samples with HQNO concentration at the limit of quantification (IC_{80}), if these analyses were performed in different plates or in different days. For the rest, of concentration values the %CV was kept low, even if the analyses were performed in different days.

Table 6.6. Coefficients of Variation (CV) of the As389/HHQ-BSA ELISA run in MH culture broth diluted 1/5 using representative concentrations at a low, medium and high concentration range (IC_{20}, IC_{50} and IC_{80}).

	IC	R1	R2	R3	Mean	Desv. Est.	%CV
Inter-day	**20**	27.28	29.75	23.10	26.71	3.36	12.6
	50	4.20	527	3.50	4.32	0.89	20.6
	80	0.57	1.03	0.58	0.73	0.26	36.2
Inter-plate	**20**	30.19	22.98	23.97	25.72	3.91	15.2
	50	3.21	3.18	2.22	2.87	0.56	19.5
	80	0.33	0.44	0.20	0.32	0.12	37.5
Intra-plate	**20**	25.74	26.76	20.52	24.34	3.35	13.8
	50	3.06	2.56	2.62	2.75	0.27	9.9
	80	0.34	0.28	0.26	0.29	0.04	13.9

The coefficient of variation (CV) was calculated following the equation CV (%) = σ/μ x 100. The results were obtained by measurements performed in either triplicates on the same ELISA plate (intra-plate), made on three different days (inter-day) or by analysis on three different plates (inter-plate). The concentrations of the replicates, mean, standard deviation and ICs are expressed in nM. IC: Inhibitory Concentration; R: Replicate; σ: Standard Deviation; μ: Average.

6.3.3.3 HQNO measurement in bacterial culture broth

P. aeruginosa is able to cause infections with distinct degree of severity. This pathogen is often found producing an overwhelming secretion of virulent factors and immediate host injuries and in other cases, it is found provoking infections that persist for decades with relative host tolerance which eventually result in a decreased lung function and death. The pathogenic strains can shift their phenotype between transient and persistent infection seeking for long-term survival, However, during a chronic infection it is also possible to find periods of more virulent and fulminant disease termed acute exacerbations. These lifestyle transitions have been studied in terms of extracellular products and common goods release[9] and as mentioned above, in previous chapters it has been shown that signalling molecules such as HHQ and PQS could be potentially used for differentiate between patients that suffer a chronic or an acute *P. aeruginosa* infection. Nonetheless, we sought to demonstrate if a virulence factor such as HQNO, highly implicated in interspecies interaction, was also able to stratify patients with different severity of *P. aeruginosa* respiratory airways infection.

Therefore, on a first instance the HQNO production kinetics in two clinical strains from an acute (PAAI6) and a chronic infected patient (PACI6), was investigated over a period of 48 hours. As it is shown in Figure 6.8, the PAAI6 isolate started release of important levels of HQNO after 5h of growth, while PACI6 did not produce any detectable amount of HQNO before 12h. The production of HQNO perfectly matched the growth profile observed in both isolates based on the OD_{600} measurement and CFU calculation. In the previous chapter, we reported a similar behavior for HHQ and PQS, the biosynthetic precursor and main signaling molecule of the *pqs* QS system[197], respectively, indicating that despite the different roles of these molecules in the pathogenesis of *P. aeruginosa*, both are released with a similar profile when growing in culture media. The decrease in the OD_{600} at 48h of growth for PAAI6, was interpreted to be caused by the exposure to high concentrations of extracellular products with lytic activity such as pyocyanin and PQS[131].

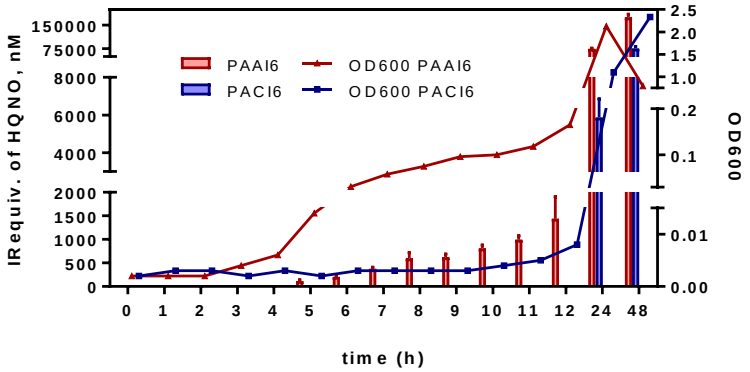

Figure 6.8. Bacterial growth, expressed as OD_{600} and HQNO immunoreactivity equivalents (IRequiv) measured in MH broth media where *P. aeruginosa* clinical isolates PAAI6 and PACI6 were cultured. Samples were taken at the selected times and measured using the As389/ HHQ-BSA ELISA. Each calibration point was measured in triplicates on the same ELISA plate and the results show the average and standard deviation of analysis made on two different days.

With these results, additional clinical isolates, belonging to patients with *P. aeruginosa* proven infection at different stages, were grown under the same experimental conditions and the HQNO levels measured after 8-hour growth with the As389/HQNO-BSA ELISA (Table 6.7). The obtained results indicated substantial differences in the HQNO production. Correlation of these results with the medical history of the patients, showed that the differences observed between the PAAI6 (acute infection) and PACI6 (chronic infection) strains was a

general behavior also for these other clinical isolates analyzed. While the HQNO concentration levels recorded for isolates obtained from patients with acute infection reached values between 1 - 4 µM IR equiv., the maximum concentration detected for the second group of patients with a chronic infection was around 20 nM (Figure 6.9). Although the results have to be confirmed with a higher number of isolates, it seems that measurement of HQNO levels of clinical isolates could provide interesting information regarding the stage of the disease and therefore, be a useful tool for patient stratification and complemental diagnostic of *P. aeruginosa* infections. On the other hand, the assay could be potentially applied for studying interspecies interaction in patients such as CF, where *S. aureus* is normally outcompeted by *P. aeruginosa* in the lungs of this patients partially caused by the reported anti-staphylococcal properties of HQNO.

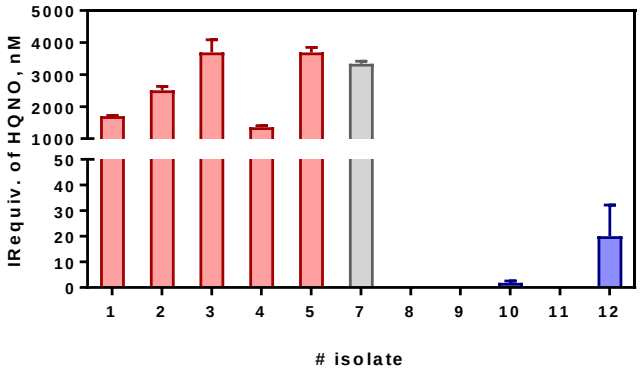

Figure 6.9. HQNO IRequiv recorded from a collection of clinical isolates from patients with different clinical profiles. Samples were growth in MH broth for 8 hours and the aliquots taken were diluted 5 times with PBS-6.5 prior the ELISA analyses. Clinical isolates 1-5 were obtained from patients undergoing acute infection and isolates 8-12 were obtained from patients undergoing chronic infection. Isolate number 7 corresponds to the reference strain PAO1. The reference number of clinical isolates can be found in Table 6.7. Each calibration point was measured in triplicates on the same ELISA plate and the results show the average and standard deviation of analysis made on two different days.

Table 6.7. Clinical isolates reference number and concentration of HQNO measured with the developed As389/HQNO-BSA ELISA.

#Number	#Ref	Infection type	[HQNO](nM)	Desv. Est. (nM)
1	**PAAI1**	**Acute**	1703	23
2	**PAAI2**	**Acute**	2507	124
3	**PAAI3**	**Acute**	3693	391
4	**PAAI4**	**Acute**	1356	47
5	**PAAI5**	**Acute**	3691	158
6	**PAAI6**	**Acute**	595.4	120.5
7	**PAO**	**Reference**	3336	81
8	**PACI1**	**Chronic**	LLOQ	-
9	**PACI2**	**Chronic**	LLOQ	-
10	**PACI3**	**Chronic**	1.86	0.72
11	**PACI4**	**Chronic**	LLOQ	-
12	**PACI5**	**Chronic**	20.0	12.2
13	**PACI6**	**Chronic**	LLOQ	-

The clinical isolates were grown 8 hours in MH culture media at 37ºC following the protocol described in the materials and methods section.

6.4 CHAPTER CONTRIBUTIONS

- For the first time, a hapten structure of the quinolone-type virulence factor HQNO has been synthetized and used for producing polyclonal antibodies against this QS-controlled metabolite.

- The polyclonal antibodies against HQNO were used to develop a competitive indirect ELISA able to quantify this metabolite in the low-nM range, having a LOD in the pM range even in complex biological samples such as culture broth.

- The assay was shown to be potentially able to stratify *P. aeruginosa* clinical isolates, and subsequently the patients, relying on the production of HQNO. It also will allow to compare its production to the signalling molecules HHQ and PQS in further experiments, providing relevant information either for the fundamental study of QS or at a clinical level.

6.5 MATERIALS AND METHODS

6.5.1 SYNTHESIS

General methods and instruments. The general methods and instruments can be found in section 4.5.1.

Methyl 3-(4-((tert-butoxycarbonyl)oxy)-2-heptylquinolin-6-yl)propanoate **(14)**: Methyl 3-(2-heptyl-4-oxo-1,4-dihydroquinolin-6-yl) propanoate **(11)** (129 mg, 0.39 mmol) was dissolved in anhydrous THF (6mL). Then, a solution of di-tert-butyl dicarbonate (94 mg, 0.43 mmol) and a catalytic quantity of DMAP (12 mg, 0.1 mmol) in THF (1mL) was added dropwise. The mixture was heated at 60ºC under nitrogen atmosphere during 2h. After completion, the mixture was left to cool to room temperature and was concentrated under reduced pressure. The crude was purified by silica flash chromatograph using AcOEt/Hex 8:2 as eluent, obtaining **(14)** as a yellow oil (148 mg, 0.34 mmol, 88% yield). ^{1}H NMR (400 MHz, $CDCl_3$) δ 7.97 (d, *J* = 8.6 Hz, 1H, H9), 7.76 (d, *J* = 2.0Hz, 1H, H6), 7.55 (dd, *J* = 8.6, 2.0 Hz, 1H, H8), 7.25 (s, 1H, H3), 3.68 (s, 3H, H17), 3.13 (t, *J* = 7.8 Hz, 2H, H12), 2.94 (t, *J* = 7.8 Hz, 2H, H18), 2.72 (t, *J* = 7.8 Hz, 2H, H13), 1.85 – 1.73 (m, 2H, H19), 1.62 (s, 9H, H29-30 and H31), 1.46 – 1.22 (m, 8H, H20-21-22 and 23), 0.87 (t, *J* = 6.8 Hz, 3H, H24). ^{13}C NMR (101 MHz, $CDCl_3$) δ 173.25, 163.68, 154.20, 150.66, 148.62, 138.51, 131.15, 129.14, 120.75, 119.74, 112.28, 84.72, 51.84, 39.64, 35.71, 31.90, 31.21, 30.07, 29.64, 29.30, 27.83, 22.77, 14.22. HRMS: *m/z* (ES+) for $C_{25}H_{36}NO_5$ [$(M+H)^+$] calculated 430.2593 found 430.2579 (-3.3 ppm).

4-((Tert-butoxycarbonyl)oxy)-2-heptyl-6-(3-methoxy-3-oxopropyl)quinoline N-oxide **(15):** Methyl 3-(4-((tert-butoxycarbonyl)oxy)-2-heptylquinolin-6-yl)propanoate (138 mg, 0.32 mmol) was dissolved in anhydrous DCM (4 mL) and cooled at 4ºC. Afterwards, a solution of m-CPBA (83 mg, 0.48 mmol) in DCM (0.5 mL) was added and the mixture was stirred at 4ºC under nitrogen atmosphere during 4h. After completion, more DCM (10 mL) was added and the solution was washed 3 times with NaHCO3 satd. (3 x 4 mL). The organic phase was concentrated under reduced pressure and it was obtained **(15)** as a single product (132 mg, 0.30 mmol, 92% yield). ^{1}H NMR (400 MHz, $CDCl_3$) δ 8.70 (d, *J* = 9.0 Hz, 1H, H9), 7.77 (d, *J* = 1.9 Hz, 1H, H6), 7.63 (dd, *J* = 9.0, 1.9 Hz, 1H, H8), 7.31 (s, 1H, H3), 3.66 (s, 3H, H17), 3.13 (m, 4H, H12 and H18), 2.72 (t, *J* = 7.8 Hz, 2H,

H13), 1.88 – 1.75 (m, 2H, H19), 1.61 (s, 9H, H29-30 and H31), 1.49 – 1.22 (m, 8H, H20-21-22 and H23), 0.87 (t, *J*= 6.8 Hz, 3H, H24). ^{13}C NMR (101 MHz, $CDCl_3$) δ 172.93, 150.56, 149.57, 144.13, 141.33, 140.92, 132.08, 122.97, 120.69, 120.59, 113.61, 85.22, 51.90, 35.36, 31.87, 31.81, 30.95, 29.69, 29.19, 27.80, 26.24, 22.76, 14.20. HRMS: *m/z* (ES+) for $C_{25}H_{36}NO_6$ [$(M+H)^+$] calculated 446.2542 found 446.2539 (-0.7 ppm).

***6-(2-Carboxyethyl)-2-heptyl-4-hydroxyquinoline N-oxide* (16):** 4-((Tert-butoxycarbonyl)oxy)-2-heptyl-6-(3-methoxy-3-oxopropyl)quinoline N-oxide (125 mg, 0.28 mmol) was dissolved in a degassed solution of KOH 5 M in EtOH (2.5 ml). The mixture was stirred at room temperature under nitrogen atmosphere during 1h. Afterwards, water (2 mL) was added and the mixture was left stirring 30 min. Then, the mixture was acidifed with HCl cc until PH=1-2. The precipitated white solid was filtered and dried to obtain the crude product. The pure product and final HQNO hapten **(16)** was obtained as white solid after crystallization in EtOH/H2O 4:1 and drying under reduced pressure (72mg, 0.22 mmol, 77% yield). ^{1}H NMR (400 MHz, CD_3OD) δ 8.11 (d, *J* = 2.0 Hz, 1H, H6), 8.04 (d, *J* = 8.8 Hz, 1H, H9), 7.73 (dd, *J* = 8.8, 2.0 Hz, 1H, H8), 6.35 (s, 1H, H3), 3.09 (t, *J* = 7.6 Hz, 2H, H12), 2.92 (t, *J* = 7.6 Hz, 2H, H17), 2.70 (t, *J* = 7.6 Hz, 2H, H13), 1.83 – 1.73 (m, 2H, H18), 1.53 – 1.24 (m, 8H, H19-H20-21 and H22), 0.91 (t, *J* = 6.9 Hz, 3H, H23). ^{13}C NMR (101 MHz, CD_3OD) δ 176.27, 155.85, 140.65, 139.67, 134.59, 125.20, 124.52, 117.17, 107.29, 36.34, 32.88, 32.48, 31.56, 30.43, 30.11, 28.82, 23.69, 14.39. HRMS: *m/z* (ES-) for $C_{19}H_{24}O_4$ [$(M-H)^-$] calculated 330.1705 found 330.1710 (+1.5 ppm).

6.5.2 IMMUNOCHEMISTRY

General methods and instruments. General methods and instruments can be found in section 4.5.2.

Buffers. The detailed composition of the general buffers can be found also in section 4.5.2. The buffer named as PBS-6.5 is PBS at pH=6.5.

6.5.2.1 Antibody production

Synthesis of the Bioconjugates PQS-KLH and PQS-BSA. A solution of the HQNO hapten **(16)** (3.26 mg, 10 µmol) in anhydrous DMF (400 µL) was cooled to 4ºC. Afterwards, tri-n-butylamine (2.62 µL,11 µmol) and isobutyl chloroformiate (1.56 µL, 12 µmol) were added to the hapten solution and the mixture was left stirring 15 min at 4ºC and 30 min at room temperature. Then, 200 µL of the reaction mixture were added over the protein solution (BSA or KLH, 2.5 mg mL-1, 2 mL in PBS 10 mM) and the mixture was left stirring 2h at room temperature and overnight at 4ºC without agitation. The bioconjugates were purified by dialysis against 0.5 mM PBS (5 x 5 L) and Milli-Q water (1 x 5 L), and stored freeze dried at -80 ºC. A small fraction (20 µL) of the HQNO-BSA was kept for MALDI-TOF analysis, rendering a hapten density of 21 haptens per molecule of BSA.

Polyclonal antisera (PAb). Antibody production has been performed with the support of the ICTS "NANBIOSIS", more specifically by the Custom Antibody Service (CAbS, CIBER-BBN, IQAC-CSIC)**.** Three female New Zealand white rabbits weighing 1–2 kg were immunized with HQNO-KLH following established protocols in the research group. Immunizations were carried out in the animal facility of the Research and Development Center (CID) of the Spanish Research Council (CSIC) Registration Number: B9900083, employing approved procedures that avoid unnecessary treatments and minimize suffering of the animals. The protocol used in accordance with the institutional guidelines under a license from the local government (DAAM 7463) and approved by the Institutional Animal Care and Use Committee at the CID-CSIC. The antisera (As) obtained were named As388, As389 and As390. The animals were exsanguinated after 6 immunizations, and the final blood was collected in vacutainer tubes provided with a serum separation gel. Antisera were obtained by centrifugation at 4 °C for 10 min at 10 000 rpm, then stored at −80 °C in the presence of preservative 0,02% sodium azide. The antibody titer was assessed during the immunization process through non-competitive indirect ELISA. Microtiter plates were coated with a fixed concentration of HQNO-BSA conjugate (1 mg mL^{-1}) and the avidity of the produced antibodies was measured by preparing serial dilutions of the corresponding As.

6.5.2.2 ELISA

Non-competitive indirect two-dimensional titration experiments. The detailed procedure for performing the non-competitive two-dimensional titration experiments can be found in section 5.5.1.2.

As389/HHQ-BSA ELISA. Microtiter plates were the PQS-BSA conjugate in coating buffer (0.25 µg mL^{-1}, 100 µL/well) overnight at 4ºC and covered with adhesive plate sealer. The day after, the plates were washed with PBST (4 x 300 µL/well) and solutions of HQNO standards (2µM to 0.13 nM in PBST, 50 µL/well) followed by the As389 (dil. 1/16000 in PBST, 50 µL/well) were added and the microplates left without agitation 30 min at RT. The plates were washed as before and a solution of goat anti-rabbit IgG-HRP (1/6000 in PBST) was added (100 µL/well) and incubated for 30 min more at RT. The plates were washed again and the substrate solution was added (100 µL) and left 30 min at RT in the dark. The enzymatic reaction was stopped by adding of 4N H_2SO_4 solution (50 µL/well) and the absorbance read at 450 nm.

Immunoassay performance evaluation and Cross Reactivity studies. This experimental procedure can be found in section 4.5.2.2.

6.5.2.3 Implementation of the ELISA to the analysis of clinical isolates

Samples. The obtention and experimental procedure used for growing the clinical isolates can be found in section 4.5.2.3. Aliquots were taken at the selected times for measurement of OD_{600}, for Colony Forming Units (CFUs) calculation and measurement of HQNO by ELISA. The rest of isolates were grown using the same experimental procedure, yet the aliquots were extracted just at a selected time of 8 hours. HQNO concentrations measured by ELISA are expressed as HQNO immunoreactivity equivalents (IRequiv), due to the potential specific interferences caused by other alkylquinolones of different chain length potentially present in the culture media.

Matrix effect and accuracy studies. Both procedures are fully described in section 4.5.2.3.

7 OVERVIEW OF THE ALKYLQUINOLONES IMMUNOCHEMICAL DETECTION

7.1 CHAPTER PRESENTATION

This chapter presents an overview of the main results obtained in Chapters 4, 5 and 6 with the intention of provide a general vision of the achievements of this thesis in respect to the *pqs* system of *P. aeruginosa*. Hence, this chapter includes an outlook of the features of the immunochemical techniques developed for the quantification of the three main metabolites of the *pqs* QS system (HHQ, PQS and HQNO) and its performance in buffer and in culture media. This chapter also aims at providing a comparative and critical analysis of the results obtained regarding the levels of these AQs in the media where *P. aeruginosa* clinical isolates have been growth. The potential of the immunochemical assays developed for diagnostic purposes including patient stratification is also discussed. Moreover, preliminary studies on the possibility to develop a multiplexed immunochemical technique that provides a potential characteristic signature of the stage of the infection or the prognostic of the pathology, are also presented.

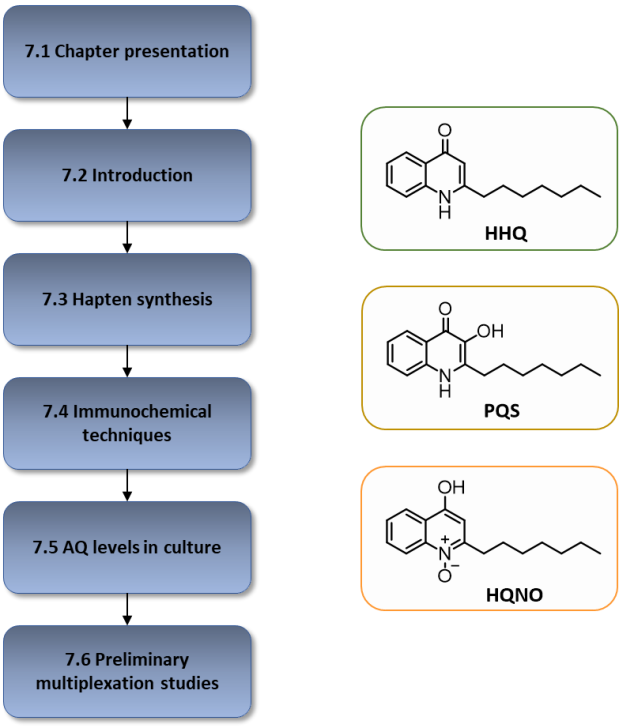

Figure 7.1. Structure of Chapter 7 related to the different sections.

7.2 INTRODUCTION

On previous chapters the rational design and synthesis of immunizing haptens for the development of antibodies against the most important signalling molecules from the *pqs* QS system of *P. aeruginosa* were described. Afterwards, the antibodies were used to develop three different immunochemical ELISA techniques that have achieved high detectability and the possibility to quantify these molecules in the low nM range. Eventually, the techniques were used to evaluate the production of such molecules by *P. aeruginosa* clinical isolates grown in MH media, observing that the levels of each of the three metabolites clearly differentiated the clinical isolate patient source in respect to chronic or acute nature of their infection, which pointed to the possibility to use the here developed technologies not only for identifying the microorganism causing the disease, but also to stratify patients.

It is known that the biological functions each of these metabolites are different. Consequently, it could be expected a distinct clinical significance regarding their potential value as disease indicators. For this reason, it is not only interesting to obtain information about each individual metabolite but also to compare the levels between these molecules. Their relative concentration might be of outmost importance and of greater clinical significance. For this purpose, some studies have been performed addressing the possibility to develop a multiplexed technique that would allow the simultaneous quantification of the three analytes and consequently facilitate their evaluation as biomarkers of infection. The preliminary results obtained are here presented with a discussion of the potential technological challenges that will have to be faced to accomplish such aim.

7.3 HAPTEN SYNTHESIS

The synthetic strategies for the obtention of all the AQ haptens followed a similar approach consisting on preparing first the quinolone core and secondly, functionalize the corresponding position to obtain the desired derivative. Although the chemical synthetic pathway used for the preparation of the

quinolone core could have been the same for all three haptens, certain problems encountered drove us to use a different chemical strategies for the PQS **(13)** or HQNO **(16)** haptens in respect to that of the HHQ hapten**(8)**, as it is shown in Figure 7.3.

The chemical strategy to accomplish the HHQ hapten, which was the first to be synthetized, used the aniline precursor 2-(4-aminophenyl)ethanol (see Figure 7.2), with an 2-hydroxyethyl group in the *para* position of the aniline. The alcohol chemical group was selected with the intention of turning it into a thiol group, for biorthogonal bioconjugation chemistry, after the formation of the quinolone core. Our initial strategy involved to use the HHQ quinolone precursor **(5)** (see chemical structure in Figure 4.6) to further on synthetize the PQS and the HQNO haptens.

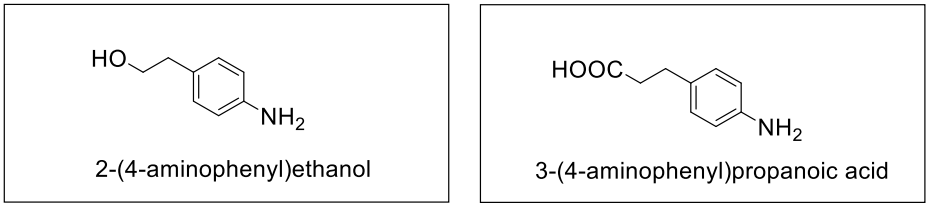

Figure 7.2. Aniline derivative precursors used for the synthesis of the HHQ hapten (2-(4-aminophenyl)ethanol) or the synthesis of the PQS and HQNO haptens (3-(4-aminophenyl)propanoic acid)

However, synthetic difficulties encountered while trying to achieve the PQS derivative from the HHQ intermediate **(5)** made us run out of starting material, and to doubt about the viability of our initial chemical approach. At that point, we realize of the availability of 3-(4-aminophenyl)propanoic acid (Figure 7.2), an aniline derivative with the same spacer arm, but with a carboxyl group. Using this product was expected to allow achieving the other two intended haptens on a much easier manner, even if the carboxyl group was not as suitable as the thiol group for orthogonal chemical reaction during the bioconjugation step. The carboxylic acid of this new aniline precursor could directly be used for bioconjugation once the hapten was synthesized, while in the case of the HHQ the alcohol had to be converted to a thiol group before. Moreover, this strategy might have been used for eventually obtaining a new HHQ hapten (HHQ hapten 2) from the intermediate **(11)** as it is shown in Figure 7.3. However, this was not necessary, since the HHQ hapten **(8)** had been synthetized in sufficient amount

to carry out the research of this thesis. Even though the feasibility of this approach still has to be investigated.

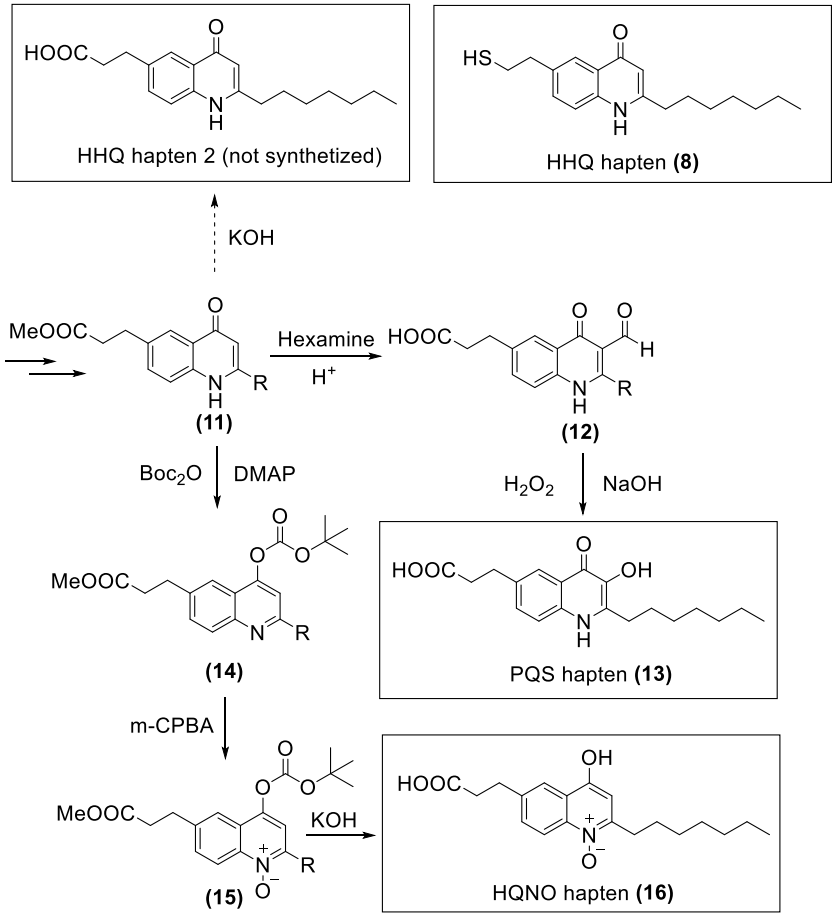

Figure 7.3. Synthetic scheme for the obtention of the HQNO and PQS hapten, including a potential one-step strategy for obtaining a different HHQ hapten (HHQ hapten 2) from the intermediate **(11)**.

7.4 IMMUNOCHEMICAL QUANTIFICATION TECHNIQUES

The analytical features and calibration curves in buffer of the three ELISAs developed for the detection of HHQ, PQS and HQNO are shown in Table 7.1 and Figure 7.4. As it can be observed, the three ELISAs presented very similar detectability with IC_{50} values: 4.59 ± 0.29 nM (HHQ), 3.87 ± 0.53 nM (PQS) and

4.20 ± 0.86 nM (HQNO) and LODs of 0.34 ± 0.13 (HHQ), 0.17 ± 0.01 (PQS) and 0.27 ± 0.09 Nm (HQNO). These values are far below the concentrations previously reported for these metabolites in bacterial cultures and on the same range that the ones found in clinical samples. These results drove us to continue our studies addressed to demonstrate the potential value of these molecules as biomarkers of infection.

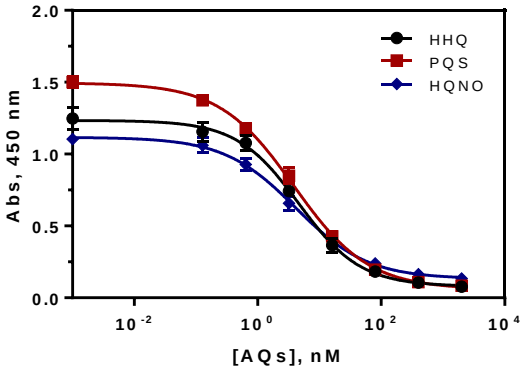

Figure 7.4. Calibration curves of the HHQ, PQS and HQNO ELISAs for the detection of the corresponding AQs in buffer (PBST, PBST-EDTA and PBS-6.5, respectively), under the conditions established (see Table 7.1). Each calibration point was measured in triplicates on the same ELISA plate and the results show the average and standard deviation of analysis made on three different days.

Table 7.1. Features of the HHQ, PQS and HQNO ELISAs in buffer.

	HHQ	PQS	HQNO
A_{min}	0.03 ± 0.01	0.03 ± 0.01	0.09 ± 0.04
A_{max}	1.19 ± 0.08	1.45 ± 0.04	1.08 ± 0.06
Slope	-0.87 ± 0.11	-0.72 ± 0.01	-0.75 ± 0.04
IC_{50}	4.59 ± 0.29	3.87 ± 0.53	4.20 ± 0.86
Dynamic Range	0.89 ± 0.21 to 22.80 ± 3.69	0.53 ± 0.04 to 24.37 ± 3.18	0.72 ± 0.18 to 26.71 ± 0.96
LOD	0.34 ± 0.13	0.17 ± 0.01	0.27 ± 0.09
R^2	0.995 ± 0.003	0.997 ± 0.002	0.987 ± 0.013

The concentration of BSA conjugate and As dilution used in the assays run in buffer can be found in Table 4.4, Table 5.4 and Table 6.4. The concentrations are expressed in nM and the data shown correspond to the average of 3 different days using at least 2 well/replicates per concentration.

Before implementing the techniques for the measurements of biological samples, the ELISAs were thoroughly characterized by performing experiments such as accuracy or specificity studies. Notwithstanding the great similarities of the molecules to be detected, the ELISAs developed during this thesis were very specific, as it is shown in Table 7.2. The highest percentage of cross-reactivity was found for HHQ in the HQNO ELISA with a 19% CR. This fact might indicate that the non-functionalized C-3 position plays an important role on the biorecognition by the As389. These results demonstrate that it is possible to develop specific antibodies against molecules that differ just on one oxidized position. Furthermore, this specificity of the three immunochemical techniques allow us to assess the individual biological value and clinical significance of the three AQs of the *pqs* QS system of *P. aeruginosa*. Even though, the results are always expressed as IR equiv., since depending on the relative concentration of these molecules the quantification could be affected.

Table 7.2. Percentages of cross reactivity (%CR) for the AQ metabolites in the developed ELISAs

Quinolone	HHQ ELISA	PQS ELISA	HQNO ELISA
HHQ	100	13	19
PQS	7	100	7
HQNO	3	2	100

The percentages of cross reactivity (C.R.) were calculated following the equation: CR (%) = IC_{50}(Cross reactant)/$IC_{50(}$Analyte) x 100.

The three ELISAs performed also very well in MH culture broth. The analytical features and the calibration curves can be found in Table 7.3 and Figure 7.5. Quantification of HHQ, PQS and HQNO could be made by just diluting the MH broth with the assay buffer. It is noteworthy that the assays did also perform well at lower dilutions factors of the matrix, as it is shown is previous chapters, in case that more detectability would have been required. The dilution of the matrix did not affect significantly the detectability, which was still below the reported levels of these molecules in culture.

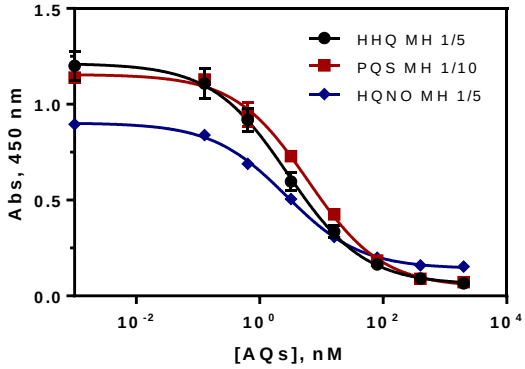

Figure 7.5. Calibration curves of the HHQ, PQS and HQNO ELISAs for the detection of the corresponding AQs in diluted MH with (PBST 1/5, PBST-EDTA 1/10 and PBS-6.5 1/5, respectively), under the conditions established (see Table 7.3). Each calibration point was measured in triplicates on the same ELISA plate and the results show the average and standard deviation of analysis made on three different days.

Table 7.3. Features of the HHQ, PQS and HQNO ELISAs in diluted MH.

	HHQ, MH 1/5	PQS, MH 1/10	HQNO, MH 1/5
A_{min}	0.01 ± 0.01	0.02 ± 0.01	0.09 ± 0.02
A_{max}	1.17 ± 0.08	1.11 ± 0.03	0.85 ± 0.01
Slope	-0.70 ± 0.02	-0.73 ± 0.11	-0.72 ± 0.06
IC_{50}	14.3 ± 1.5	60.5 ± 1.6	13.6 ± 0.2
Dynamic Range	2.3 ± 0.4 to 108.1 ± 23.7	9.7 ± 2.5 to 361.6 ± 62.0	2.1 ± 0.5 to 85.2 ± 5.4
LOD	0.9 ± 0.3	3.6 ± 1.4	0.8 ± 0.3
R^2	0.998 ± 0.002	0,995 ± 0,003	0.990 ± 0.004

The concentration of BSA conjugate and As dilution used in the assays run diluted MH can be found in Table 4.4, Table 5.4 and Table 6.4. The IC_{50}, LOD and Dynamic Range correspond to the values in the culture sample. The concentrations are expressed in nM and the data shown correspond to the average of 3 different days using at least 2 well/replicates per concentration.

7.5 ALKYLQUINOLONE LEVELS IN CULTURE

Finally we addressed the investigation of profile of release of all three quinolones by starting with two clinical isolates PAAI6 (Figure 7.6) and PACI6 (Figure 7.7) which according to their clinical data belong to patients with acute and chronic

infections, respectively. In all cases the AQs concentration matched very well the growth profile estimated through the optical density at 600 nm. In the culture media where the clinical isolate PAAI6 was growth, all three quinolones could be quantified after just 4h of growth, observing similar levels in the case of HHQ and PQS, but significant much higher concentrations of HQNO; difference that increased with the time. Although someone could think on the potential contribution of HHQ to the IR equiv. measured due to the cross-reactivity shown in the As389/HHQ-BSA ELISA (HQNO ELISA), it has to be taken into account that, as it will be shown later, the interference of a cross-reactant is only significant if present in much higher ratio in respect to the target. On the other hand, it has been reported that the production of HQNO is in general higher than other quinolone metabolites according to LC-MS studies also in culture media[95,198].

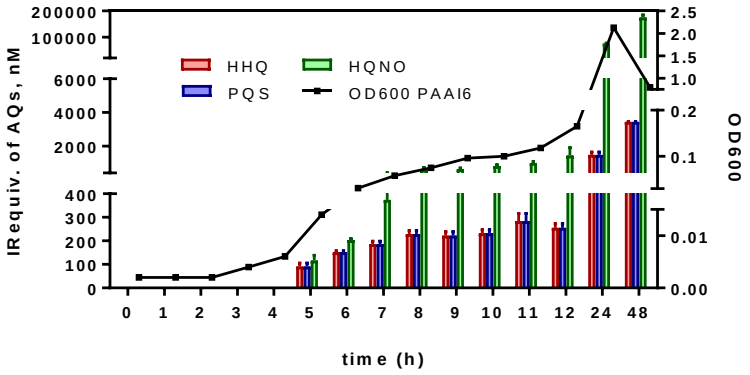

Figure 7.6. Bacterial growth, expressed as OD_{600} and alkylquinolones (AQs) immunoreactivity equivalents (IRequiv) measured in MH broth media where *P. aeruginosa* clinical isolate PAAI6 was cultured. Samples were taken at the selected times and measured using the ELISAs developed in this thesis. Each calibration point was measured in triplicates on the same ELISA plate and the results show the average and standard deviation of analysis made on two different days.

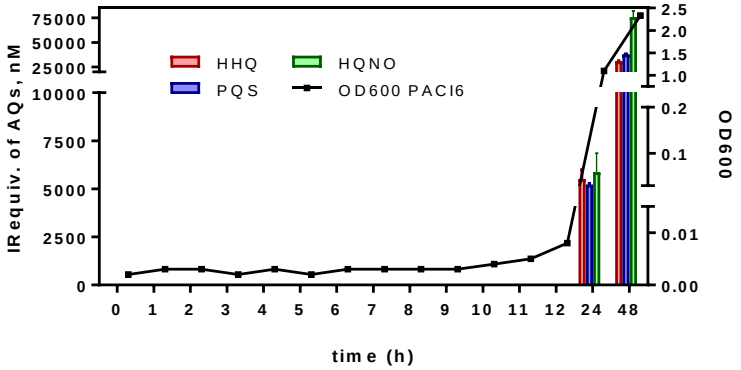

Figure 7.7. Bacterial growth, expressed as OD_{600} and alkylquinolones (AQs) immunoreactivity equivalents (IRequiv) measured in MH broth media where *P. aeruginosa* clinical isolate PACI6 was cultured. Samples were taken at the selected times and measured using the ELISAs developed in this thesis. Each calibration point was measured in triplicates on the same ELISA plate and the results show the average and standard deviation of analysis made on two different days.

On the other hand, the production of AQs could not be detected before 12h of growth in isolate PACI6, observing also in this case higher production of HQNO although the difference was not as great as for the values found in the media of the clinical isolate of the patient with an acute infection. As a result, the differentiation between the acute (PAAI6) and the chronic infection (PACI6) was possible by measuring samples between 5 and 12h of growth, after that period the concentration levels were not so different. For this reason, performing measurements after 8h of growth was selected for further experiment with additional clinical isolates obtained from our clinical collaborators.

At the light of the above results, following clinical samples were selected to have a representative number of bacterial isolates from patients suffering chronic or acute infections. Moreover, a reference strain of *P. aeruginosa* (PAO1) was also growth under the same conditions The results obtained regarding the concentration levels of the three alkylquinolones are shown in Figure 7.8. As it can be seen, the IR equiv. levels of HHQ, PQS and HQNO were very similar for each clinical isolate, being those of HQNO slightly higher. IR equiv. in the µM range (0.4 to 4 µM) were released to the culture media by bacteria from acute patients while the levels were in the low nM range or not detected, under these conditions, when the clinical isolates were taken from a sample of a patient with a chronic disease. Although further analyses should be done to take any conclusion was also surprising that for the case of the samples from bacterial

isolates of chronic patients, HQNO was not always the AQ providing the higher signal.

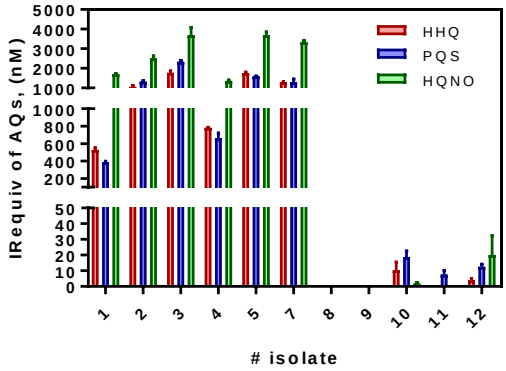

Figure 7.8. Concentration of the alkylquinolones HHQ, PQS and HQNO for the clinical *P. aeruginosa* isolates measured in this thesis using the As382/PQS-BSA, As385/HHQ-BSA and As389/HHQ-BSA ELISAs, respectively. Isolates 1 to 5 correspond to acute type, number 7 is the reference strain PAO1 and isolates 8 to 12 correspond to chronic type.

According to these results, all three AQs could have potential for their use as biomarker of infections without certain differences between them, which clinical significance has to be probed increasing the number of samples analysed. However, it should be noticed that these are the results of the concentration levels found in the culture media where the clinical isolates were growth under standardized and controlled conditions, without any external factor interfering. This is an environment completely different from that existing in the pulmonary epithelium colonized by *Pseudomonas aeruginosa*, in which additionally of the physico-chemical conditions (O_2 concentration, pH, etc.) it may play a role host immunosystem, but also other bacteria. We must remark that, QS also plays a role on inter-species communication and social behaviour. Current knowledge points at the fact that bacteria also need mechanisms to detect the presence of other species, calculate the ratio of self to other in mixed populations, and in turn, to specifically modulate behavior based on fluctuations in this ratio[98]. An example is the autoinducer-2 (AI-2), recognized as a universal QS communication molecules, but another example is HQNO, that as it has been mentioned before, is able to exert and anti-staphylococcal activity[95]. Therefore, it is likely possible that the behaviour of these bacteria, and therefore the kinetics of release or the levels of all these QS signalling molecules in clinical samples will be different.

The QS signalling molecules, related metabolites and virulence factors could provide much more information about the stage and progression of disease and subsequently, be relevant for studying the pathogenesis of *P. aeruginosa* infection. Moreover, the results encountered readily point to the possibility to differentiate between patients suffering acute or chronic infectious processes, which could be extremely helpful for clinicians in the management of infected patients. It has been often reported that the behavior of strains inducing acute or chronic infections is substantially different in terms of virulence and exo-products release, caused by an adaptation to the hostile host environment[199]. Thus, on chronic lung infections, *P. aeruginosa* adapts to the host environment by evolving toward a state of reduced bacterial invasiveness that favours bacterial persistence without causing overwhelming host injury. In that respect, the results found with the here reported ELISAs are in agreement with this situation. The low levels of alkylquinolones released by the isolates from chronic infected patients would justify a potential lower production of virulence factors.

From a diagnostic perspective, in addition of identifying the microorganisms causing the disease, being able to distinguish between a chronic or an acute infection is very relevant, to apply appropriate therapeutic strategies and improve disease management[200]. Chronic or acute infections may require distinct therapeutic approaches. Thus, in contrast to acute infections, chronic lung infections are typically a consequence of an underlying disease, which should be addressed, instead of just prescribing wide spectrum antibiotics.

On the other hand, further longitudinal clinical studies may open new avenues and perspectives on the role of each of these molecules through the infection process. These data may provide further information about the progress of the disease, the stage of the infection and/or fitness of the pathogenic strain. The possibility to use such information for prognosis or to predict exacerbation episodes on chronic patients, such as those suffering CF, would be of extremely importance to act appropriately and take the corresponding measures to ensure the quality of life of these patients.

The antibodies produced for alkylquinolones and the ELISAs reported for the first time in this thesis, appears as potential powerful tools to substantially improve diagnostic of *P. aeruginosa* infections and their management. Thus, we have demonstrated the possibility to use the microplate ELISA to identify *P.*

aeruginosa on culture media based on the detection of specific QS molecules. Further studies will be addressed to directly detect such specific QS signaling molecules on clinical samples, which would speed up the diagnostic of such kind of infections. At the light of these results, and based on previous works such as the one by Barr and co-workers[63,67] which quantify the concentrations of QSMs in the nM range, it may be possible to use the ELISAs developed in this thesis to evaluate the value of HHQ, PQS and HQNO as biomarkers of *P. aeruginosa* infection by measuring them directly in clinical samples instead of in culture media.

7.6 PRELIMINARY MULTIPLEXATION STUDIES

The immunochemical reagents and techniques explained in previous sections might be potentially used in combination for developing a multiplexed diagnostic technique able to measure simultaneously the different AQ metabolites. This multiplexed tool would allow to provide information of the potential characteristic AQ QS signature on each moment, and therefore eventually of the stage or prognostic of the pathology, with a single measurement, reducing the analysis time and the volume of sample to be used.

Preliminary studies about the possibility of multiplexation of the three ELISAs developed in this work, were performed by assessing possible interferences resulting from the combination of the three As developed for the detection of AQ metabolites. For this purpose, calibration curves for each target were run in the presence of the As solutions used on each ELISA. As expected, a clear effect was observed as result of the recognition of the bioconjugate competitor (known as shared reactivity) and the analyte (cross-reactivity) by all three antisera.

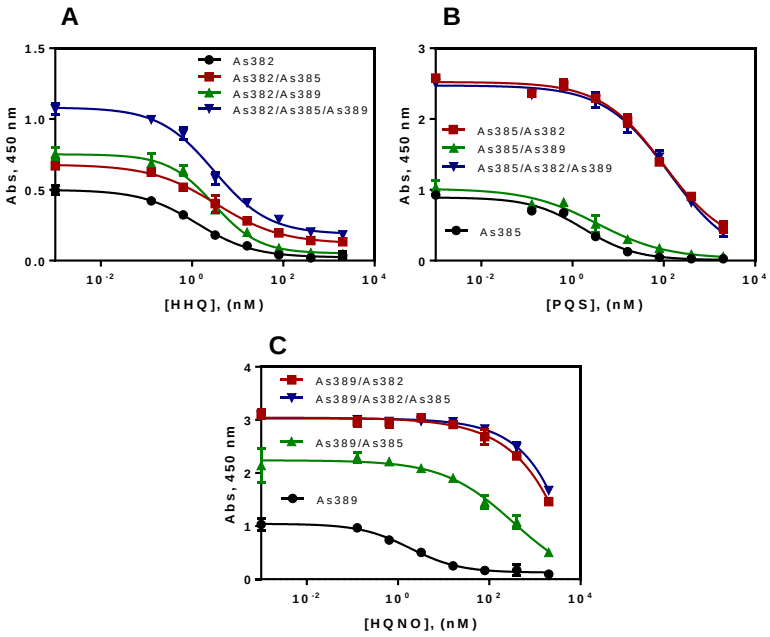

Figure 7.9. Calibration curves of the ELISAs of each AQ run in the presence of the As against the others AQs. For each of the assays it was run a calibration curve under standard conditions using the corresponding As and calibration curves in which a combination of the As for the detection of other AQs was used. The dilutions of As were the ones selected for running the assays in buffer and can be found in Table 7.1. **A**. Shared/Cross reactivity profile of As382/PQS-BSA ELISA for the detection of HHQ. **B**. Shared/Cross reactivity profile of As385/HHQ-BSA ELISA for the detection of PQS. **C**. Shared/Cross reactivity profile of As389/HHQ-BSA ELISA for the detection of HQNO.

As it can be seen in Figure 7.9A (HHQ determination, As382/PQS-BSA ELISA), the presence of As385 (PQS) or As389 (HQNO) in the competitive step produced a similar increase of the maximum signal (around 50% of the standard curve), and when both As were present the effect was additive. Even though a good calibration curve was obtained with acceptable analytical features, when the three As were present. For the case of the quantification of PQS (As385/HHQ-BSA ELISA, Figure 7.9B), while the effect of the As389 (HQNO) was negligible (the assay showed same maximum signal and similar detectability; 1.75 nM vs 3.48 nM), As382 (HHQ) drastically changed immunoassay performance, as expected, due to the recognition of the heterologous bioconjugate competitor in this assay (HHQ-BSA). For the same reason, a great effect was observed on the HQNO assay (As389/HHQ-BSA ELISA, Figure 7.9C), although in that case also As385 (PQS) produced a great effect.

These results pointed at the difficulties that the development of multiplexed technique might pose with the actual ELISAs. It seems clear that if pursuing in this direction there will be necessary to re-optimize conditions and apply data signal and chemometric analysis. The use of homologous bioconjugate competitors on each assay would without no doubt make achieving this goal easier, by reducing slightly the potential share reactivity effects resulting from the recognition of the bioconjugate competitor by other antibodies, but this effect would not completely disappear.

On the other hand, we have also demonstrated that the specificity profile shown previously in Table 7.2 might be different when all the analytes are present (Figure 7.10). Even though the CR play an important role on the biorecognition, this effect was significantly diminished when the concentrations of the analytes were on the same range, and the interference of a cross-reactant was only significant if it was present in much higher ratio in respect to the target analyte of the corresponding ELISA.

For instance, the experiments were the calibration curves of HHQ have been built under the presence of constant concentrations of either PQS or HQNO (Figure 7.10A and B) allow us to evaluate the potential cross reactivity for each point of the calibration curve at different concentrations of cross reactants. The experiments showed that indeed, the percentages of cross reactivity were not constant and diminished when the concentrations of HHQ increased. As a practical example, if it is selected a calibration point inside the dynamic range of the assay (e.g. 16 nM) and the signal obtained when, for instance, PQS was present in the assay at different concentrations is interpolated, it can be seen that the CR is below or equal to 7% in all cases and has not a substantial effect till the concentration of PQS is above 20 nM (Table 7.4). The same behaviour is observed for the case of HQNO and for the other assays developed in this thesis. On the other hand, the reported concentrations of all three metabolites in biological samples are in the same range when all three analytes are present, except for HQNO which has the lower CR in every assay. Eventually, we can conclude that the potential interferences caused by these molecules will not have an impact as great as it was expected from the CR studies shown in previous chapters and thus, it will not impede the proper measurement of the target analyte in the corresponding ELISA.

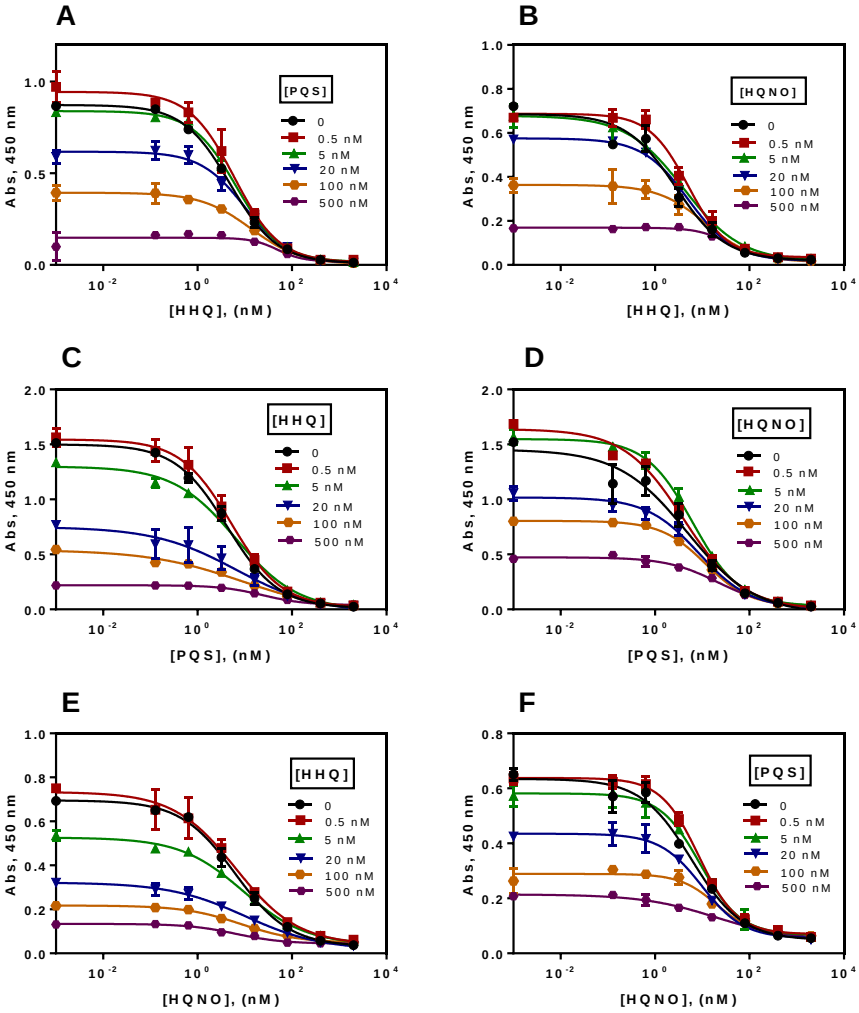

Figure 7.10. Calibration curves and evaluation of the simultaneous presence of the analytes HHQ, PQS and HQNO at different concentrations in the developed ELISAs. **A.** Effect of constant concentrations of PQS in the different calibration points of the As382/PQS-BSA ELISA. **B.** Effect of constant concentrations of HQNO in the different calibration points of the As382/PQS-BSA ELISA. **C.** Effect of constant concentrations of HHQ in the different calibration points of the As385/HHQ-BSA ELISA. **D.** Effect of constant concentrations of HQNO in the different calibration points of the As385/HHQ-BSA ELISA. **E.** Effect of constant concentrations of HHQ in the different calibration points of the As389/HHQ-BSA ELISA. **F.** Effect of constant concentrations of PQS in the different calibration points of the As389/HHQ-BSA ELISA. Calculated cross reactivity was equal or less than the reported percentages of CR in the previous specificity assays for the calibration points within the dynamic range. Each calibration point was measured in duplicates on the same ELISA plate and the results show the average and standard deviation of analysis made on two different days.

Table 7.4. Spiked concentrations of PQS and concentrations of HHQ observed for the calibration point at 16 nM when both analytes were present.

[PQS] spiked (nM)	Absorbance (450 nm)	[HHQ] observed (nM)	[HHQ] expected (nM)	C.R. (%)
0,5	0.276	14.37	16.04	<0.1
5	0.275	14.42	16.35	<0.1
20	0.254	16.19	17.40	1.0
100	0.187	23.03	23.00	7.0
500	0.127	40.90	51.00	5.0

The table also includes the expected observed concentration taking into account the previously calculated %CR for PQS (7%) and the new %CR calculated in each case. The new %CR were calculated as follows: ([HHQ]observed-[Calibration point])/[PQS]spiked)*100.

Regardless of the immunochemical reagents that are used for the multiplexation of the three assays, there are several variables and interferences that play an important role on the biorecognition and that might strongly influence the signal observed in a potential multiplexed assay (as it has been shown with the cross reactivity and shared reactivity experiments). For that reason, what might be required to interpret the signal and outcome in the multiplexed tool is, without any doubt, a chemometric analytical method. If proper experiments are designed, the use of mathematical and statistical methods would help to find out the contribution of each metabolite and As to the signal observed in the assay. On the other hand, when measuring clinical samples of infected patients with a multiplexed tool, it might not be necessary to know the individual concentration of each AQ or QS molecule, but rather characteristic signatures or profiles related to particular clinical conditions or states of disease. To reach this objective, exhaustive clinical studies would have to be performed to find out the clinical significance of these metabolites and the release profile of such molecules on the host. Eventually, if antibodies are developed against other relevant molecules of the QS system of *P. aeruginosa* , a powerful diagnostic tool might be obtained, gathering the QS molecular footprint from this pathogen and allowing to find out the potential of these molecules as biomarkers of infection.

8 *AGR* QUORUM SENSING SYSTEM

8.1 CHAPTER PRESENTATION

The main objective of this chapter is to provide an updated review about *Staphylococcus aureus* and the performance of its QS system, which is mainly based on the synthesis, release and detection of cyclic oligopeptides, named autoinducer peptides (AIPs). It will be also summarized the most recent findings about the biological and clinical significance of these AIPs, including a summary about the latest techniques for their detection and quantification. This chapter will serve as an introduction of the following Chapter 8, about the establishment of a general immunochemical strategy for the quantification of AIPs. The schematic representation of the chapter structure can be found in Figure 8.1.

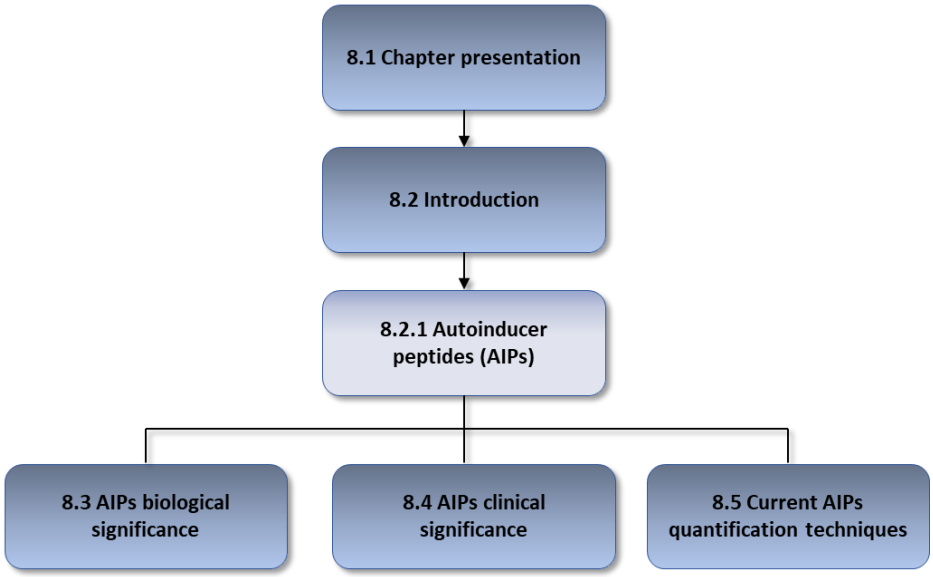

Figure 8.1. Structure of Chapter 8 related to the different sections.

8.2 INTRODUCTION

8.2.1 AUTOINDUCER PEPTIDES (AIPS)

QS in gram-negative bacteria involves characteristic molecules such as homoserine lactones or quinolones, while in gram-positive bacteria the main signalling molecules are oligopeptides[4]. In the case of *S. aureus*, these peptides and all the machinery for the communication system are encoded by the *agr* locus, which contains two divergent transcription units, the effector and response regulator (Figure 1.5). The variable region on the response regulator region results into four specificity groups (*agr*-I to IV) characterized by four different signalling molecules. These molecules are cyclic thiolactone autoinducer peptides (AIPs) with 7 to 9 amino acid residues, produced in a strain-specific manner (AIP-I to IV)[201] (Figure 8.2). The *agr* variants determine the response to cognate or heterologous AIPs, competitively cross inhibiting *agr* activation and outcompeting in three cross-inhibitory groups (AIP-I/AIP-IV, AIP-II and AIP-III)[202]. This effect can be attributed to a primary divergent evolutionary event in which AIP-I to III are assumed to arise from a common ancestor and AIP-IV would correspond to a later divergent step from AIP-I. Even though AIP-I and IV just differ one amino acid in their structures, it is enough to observe not inhibition but rather group specificity in the detection by AgrC[203].

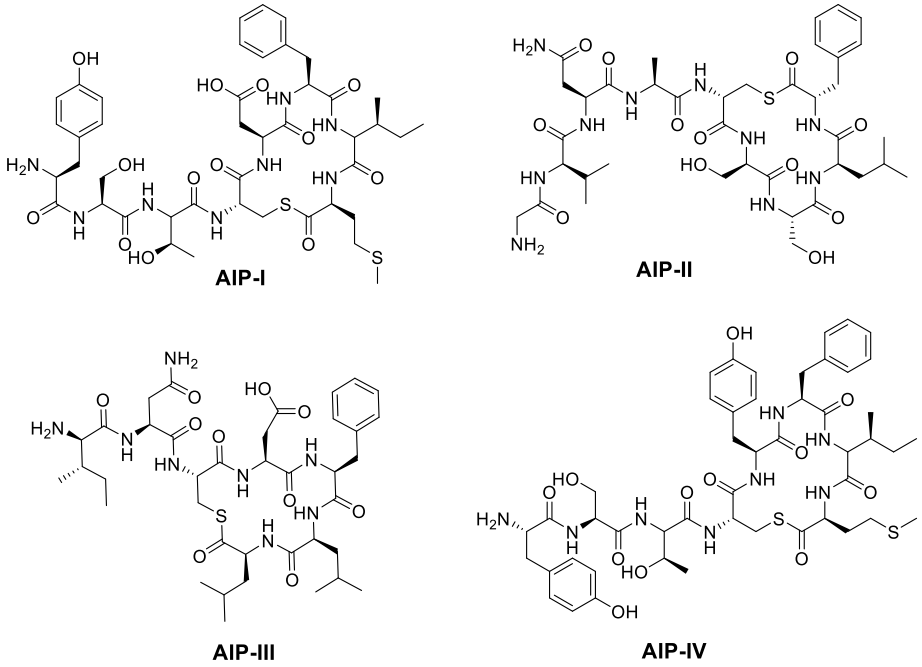

Figure 8.2. Chemical structure of the different *Staphylococcus aureus* Quorum Sensing autoinducer peptides (AIPs).

8.2.1.1 AIPs biosynthesis

The biosynthesis of AIPs is a complex process in which *agrD*, located in the variable region of the *agr* locus, encodes the propeptide sequence AgrD that will be subjected to two sequential cleavages, cyclization and export in order to release the mature AIP structure. In AgrD, the sequence of the linear AIP is flanked by a N-terminal leader peptide and a C-terminal recognition sequence[204]. In a first step, AgrD is processed by the integral membrane endopeptidase AgrB, which removes the C- terminal tail, and the resulting intermediate remains covalently linked to an AgrB cysteine residue (Figure 8.3). Afterwards, another cysteine residue located in the AIP sequence region attacks the activated carbonyl to produce a thioester exchange and form the characteristic cyclic structure. Eventually, the AIP would be translocated to the extracellular leaflet of the membrane and released by action of a signal peptidase, SpsB, that would clip the N-terminal leader[205]. Even though this process is generally assumed, remains to be fully understood and is still an active area of investigation[47,206].

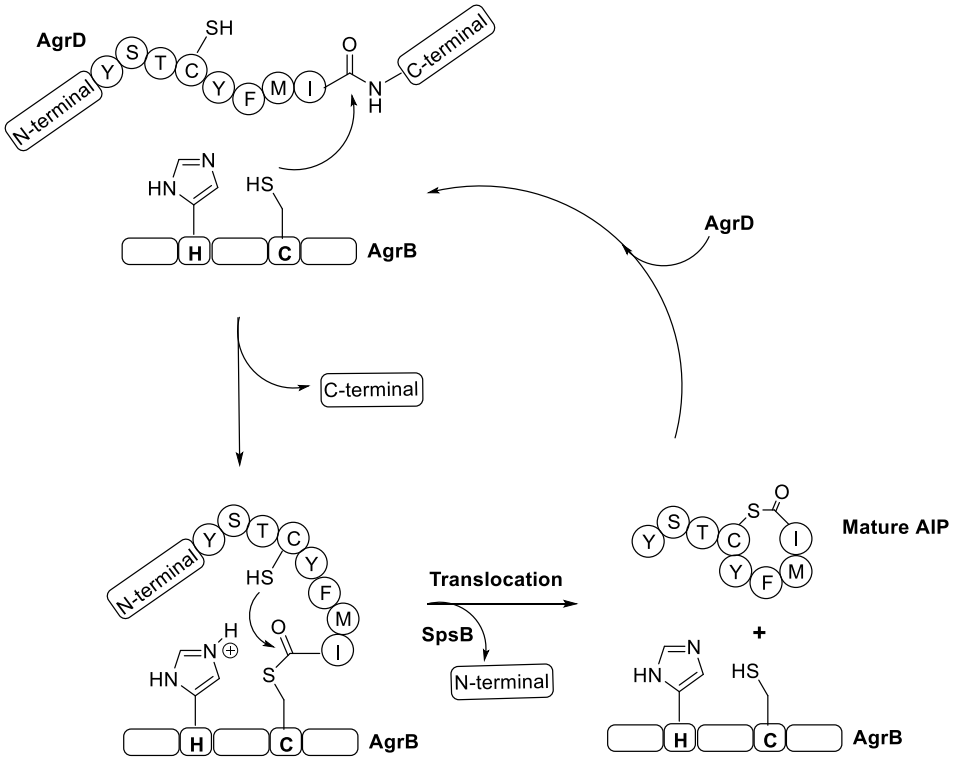

Figure 8.3. Schematic representation of the AgrD processing by AgrB and AIP-IV maturation.

8.3 AIPS BIOLOGICAL SIGNIFICANCE

Certainly, AIPs are the key element for the extracellular sensing and subsequent regulation of the *agr* QS system. The AIP signals accumulate in the extracellular space and once a certain threshold is reached, the communication system is activated. *S. aureus* employs the *agr* system through AIPs to adapt to the environmental conditions and to regulate virulence gene expression. Unlike the signalling molecules in gram-negative bacteria (e.g. alkylquinolones), the current opinion is that AIPs might only serve as communication signals, however, studies about the effect of these molecules in other diseases are currently under investigation [68].

Nevertheless, the local concentration of AIPs determines the activity of RNAIII, the main intracellular effector of the *agr* system and one of the largest small

regulatory RNAs, which regulate gene expression through base pairing with mRNAs and encodes the sequence for the expression of delta-hemolysin[207]. Among the genes up-regulated by RNAIII we can find relevant virulence factors for *S. aureus* pathogenesis such as alpha-toxin, serine proteases, cysteine proteases, gamma-hemolysin, leucocidin and lipase[208]. Alpha-toxin is one of the most important toxins and is key virulence factor in infections such as pneumonia and skin and soft tissue. On the other hand, surface proteins including protein A and some receptors are downregulated by RNAIII. Among these surface proteins, protein A stands out due to its role in pathogenicity in several different types of *S. aureus* infections, including pneumonia, bloodstream infections, and septic arthritis[209]. It is noteworthy that RNAIII can perform its regulatory role on the transcriptional level by modulating transcription initiation or at the post-translational level by directly interacting with the gene transcript.

The *agr* system plays a central role in *S. aureus* pathogenesis and this bacterium has found different strategies and mechanisms to fine tune the expression of *agr* and adapt rapidly to the changing conditions. Some examples of factors that affect the *agr* communication system might be the pH, being inhibited at acidic or alkaline conditions[210,211], or the presence of reactive oxygen species (ROS), oxidizing the side chain of AIPs or rendering AgrA ineffective[212].

8.4 AIPS CLINICAL SIGNIFICANCE

The divergence on *agr* specificity groups was a primary evolutionary event and the resulting cross-inhibition between the different groups, leads inevitably to a competition of *S. aureus* strains with different *agr* systems for certain niches. This competition might have resulted in specialization for certain types of infections depending on the characteristics of each group[213]. Indeed, there are several studies providing clinical evidences about the relation between *agr* groups and specific human diseases.

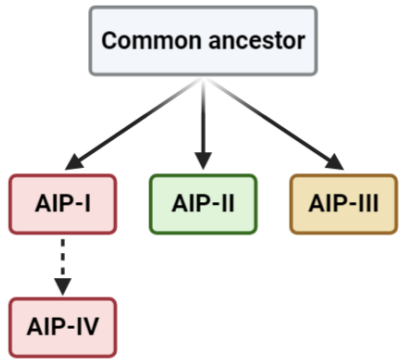

Figure 8.4. Schematic representation of the agr specificity groups divergence in which is showed that AIP-I to III would be originated from a common ancestor and AIP-IV from AIP-I

For instance, Jarraud and co-workers performed a study using 198 *S. aureus* clinical isolates, the agr groups of which were characterized by PCR, and investigated the relation between different phylogenetic groups and the type of infection[214]. A relationship between genetic background, *agr* group, and disease type was observed for several toxins mediated diseases and suppurative infections. In another study, clinical isolates derived from lower respiratory infections were characterized and used to study the correlation between the functionality of the *agr* system and the genotypic and phenotypic characteristics, clinical variables and clinical outcome[215]. Despite the authors found that the *agr* activity was high in 82% of the isolates, no statistically significant association was found between the *agr* group and the type of infection. On the other hand, Choudhary and co-workers described a strong correlation between the *agr* type and the virulence genomic profile of the microorganism by analysing 148 *agr* positive strains[216]. The authors demonstrated that the *agr* types could be classified depending on the virulence phenotype. Eventually, in another study it was analysed the production frequency of superantigens (sAg) such as hemolysins, enterotoxins, exotoxins, toxic shock syndrome toxin-1 and then associated with the type of *agr* locus[217]. The expression of these sAg is strongly associated with the immune response on the host and thus, their overexpression or either reduced production might determine the future performance of the bacteria when dealing with the immune system.

Even though there are evidences that the *agr* groups might be related with the type of infection, virulence and/or host immune system response, more studies have to be conducted for a proper evaluation of the clinical significance of AIPs.

With this aim, new techniques and methods that allow its quantification in clinical samples must be developed.

8.5 CURRENT AIPS QUANTIFICATION TECHNIQUES

Many authors have claimed that these molecules could serve as specific biomarkers of infection and thus, this idea has prompted the development of several chromatographic and bioanalytical techniques for either detection or quantification of AIPs. There are few examples of quantification of AIPs and furthermore, none of the developed techniques has achieved its quantification in clinical samples[68]. There are two examples where AIP-I was quantified in bacterial cultures using two different LC-MS/MS methods. One of the methods was developed by Junio and co-workers, achieving a LOD of 0.25 µM and quantifying AIP-I directly from bacterial cultures using UHPLC coupled to high resolving power mass spectrometry[218]. The method does not include treatment of the samples (just filtration) but the detectability achieved would presumably not make implementable the technique for the measurement of this AIP in clinical samples. The second method developed by Todd and co-workers was based on the measurement of AIP-I in bacterial cultures of a MRSA strain by UPLC coupled to Hybrid Quadrupole-Orbitrap mass spectrometry, obtaining a LOD and LOQ of 0.0035 µM and 0.10 µM, respectively[219]. There has been reported also several bioassays that might serve as *agr* typing strategies[201,220,221] alternative to of genomic methods, nevertheless for this purpose there are already commercially available tests (e.g. DNA microarray genotyping kit Clondiag®).

As mentioned above, the AIPs have never been quantified in clinical samples. Main limitations may be related to the low concentrations at which these AIPs may exists in body fluids, but also their compromised stability in complex samples such sputum, where saliva and the subsequent proteases might be present[222]. In addition to the unstable chemical nature of the AIPs due to the thiolactone chemical group, in clinical samples there may be proteases that, unless the sample is appropriately processed, may degrade the peptides. For that reason, there is an urgent need of developing alternative methods and strategies that allow quantification of AIPs to continue progressing on the knowledge around these autoinducers and their role in *S. aureus* pathology.

9 DETERMINATION OF AIPS AS BIOMARKERS OF INFECTION: AN IMMUNOCHEMICAL STRATEGY

9.1 CHAPTER PRESENTATION

In the present chapter it will be described an immunochemical strategy to generate specific antibodies against autoinducer peptides (AIPs) from *S. aureus*. The strategy includes the generation of two different haptens (homologous and heterologous) against one of the AIPs and the use of the generated antibodies for developing an immunochemical tool that might serve for elucidating the role of these AIs in the pathogenesis, but also for their assessment as biomarker of infection. With this aim, we initially focussed on AIP-IV as a model to evaluate the experimental strategy proposed to generate antibodies, based on their performance in ELISA in respect to the detectability and specificity achieved. The different steps and the structure of this chapter can be found in Figure 9.1.

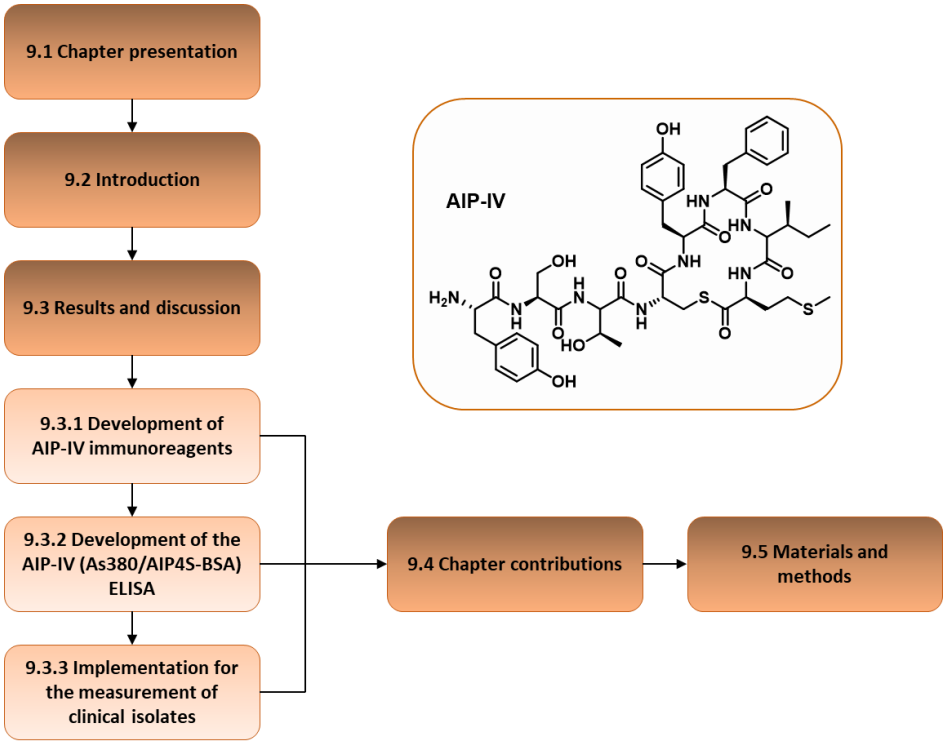

Figure 9.1, Structure of Chapter 9 related to the different sections.

9.2 INTRODUCTION

9.2.1 AIP-IV AS A MODEL

The AIPs produced by *S. aureus* differ in chain length, amino acid sequence and three-dimensional structure, providing enough biological specificity and cross-inhibiting the *agr* activation in most of heterologous combinations (Figure 8.2). The greatest similarity is found between AIP-I and AIP-IV, which just differ one amino acid and yet, it is enough to see different specificity towards its corresponding receptors (AgrC-I or AgrC-IV).

In the present chapter it will be described an immunochemical strategy in which, taking AIP-IV as a model, two different immunizing haptens were synthetized, one as homologous structure to AIP-IV (AIP4S, thiolactone ring), and another heterologous structure (AIP4NH, formed by a lactam ring). With this approach, we sought to compare the avidity versus AIP-IV of antibodies produced with a hapten of the same chemical structure of the AIP, yet with less stability versus hydrolysis, to the one of antibodies produced with a more stable, yet heterologous, hapten structure.

Furthermore, the similarity between AIP-I and AIP-IV was also taken as a reference to evaluate if the antibodies produced and the selected strategy were adequate enough to distinguish between these peptides, that just differ one amino acid, through development of an immunochemical analytical technique. The best strategy and the experimental procedure is currently being applied for the obtention of monoclonal antibodies against the rest of AIPs.

9.3 RESULTS AND DISCUSSION

9.3.1 DEVELOPMENT OF AIP-IV IMMUNOREAGENTS

9.3.1.1 Hapten design and synthesis

The production of antibodies against a low-molecular weight targets has several determining steps, among which the rational design of the immunizing hapten and its chemical synthesis should be highlighted. Knowledge of the chemical features of the target is a key issue, and in this case, it had to be considered the potential lack of stability of the thiolactone group closing the peptide ring (see Figure 9.3). Hence, thiolactones are cyclic esters of mercapto acids, which are usually unstable intermediates[223]. Previously, Park and co-workers[224] attempted to produce antibodies against AIP-IV by synthesizing an hapten with a lactone group instead of a thiolactone, due to its better stability. The antibodies produced against the lactone hapten were used with therapeutic purposes but also their relative affinity was evaluated through ELISA competitive experiments. Despite these antibodies were not used for diagnostic purposes, the reported values of IC_{50} were 24, 90 and 390 nM for three different monoclonal antibodies when using AIP-IV as analyte, lower detectability that the ones produced in the present thesis. On the other hand, it should be noticed that the lactone type haptens might not be exempt from the risk of hydrolysis as it was pointed by Debler et al.[225] with homoserine lactones molecules, which are a class of QS metabolites produced by *P. aeruginosa*. In this case, the authors synthesized lactam haptens that imitated the native molecules, yet using a more stable chemical structure and obtaining antibodies that allowed to recognize them with excellent detectability (low nM range).

At the light of these precedents, and taking into account to the potential instability of a thiolactone AIP-IV hapten (AIP4S), we proposed using a more stable lactam hapten (AIP4NH) to raise antibodies for diagnostic purposes. However, it was necessary to previously evaluate the impact of substituting the sulfur atom from the native AIP structure by a nitrogen in the electronic and structural properties of the final hapten. Theoretical calculations and molecular modelling have been demonstrated to be powerful tools for designing and

evaluating the suitability of certain hapten chemical structures to raise high affinity antibodies, by ensuring that the electronic configuration and the geometrical conformation of the hapten mimics as much as possible that of the analyte. This approach has previously been used in our group to design haptens for the production of specific antibodies against several structurally diverse chemical entities such as anabolic steroids[226], chlorophenols[227] or fluoroquinolones[176], all of them allowing the development of immunochemical assays reaching high detectability levels. Furthermore, molecular modelling tools have been successfully applied for assessing conformational changes of hapten–carrier conjugates[228].

The minimum energy conformer for the native AIP-IV structure, AIP-IV formed by a lactam ring or AIP-IV formed by a lactone ring were calculated using Molecular Mechanics MM+ followed by a semi-empirical PM3 method. Regarding the electronic distribution, significant differences were only encountered in the closer region where the thiolactone/lactam chemical bond was located (Figure 9.2).

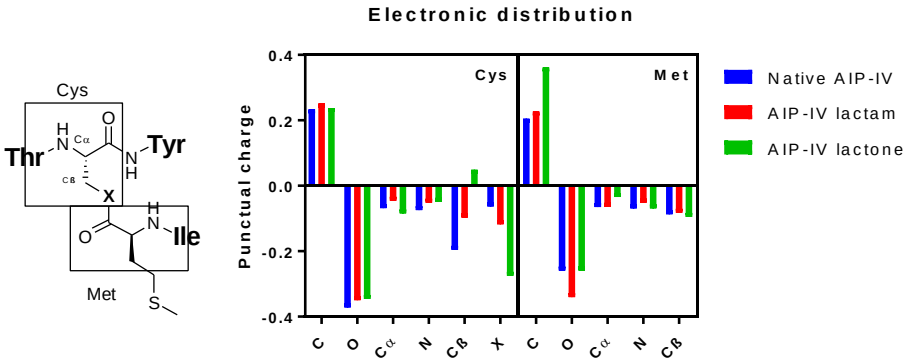

Figure 9.2. Representation of the electronic distribution and punctual charge for the two amino acid residues that were affected by the introduction of a lactam or lactone bond type in the chemical structure of AIP-IV.

The evaluation of the lactam-type bond impact on the structure of the native peptide was made by calculating RMSE (Root mean square error), which provides information on the variation of the geometries of between the peptides when overlapping them. When comparing the native AIP-IV with the lactam derivative, a value of RMSE of 0.449 Å was found, which is significantly different that the one found for AIP-IV in different conformations at their minimum energy, 0.094

± 0.062 Å. The RMSE value was also calculated for an AIP-IV derivative formed by a lactone ring with a result of 0.357 Å compared to the native AIP-IV. These values can be explained by the influence of the heteroatom size in the hapten structure. In contrast, the differences encountered with the lactam derivative did not mean a significant impact. The local changes in the lactam derivative would not affect the entire physico-chemical properties of the whole peptide. Even though the theoretical calculations, it was not completely sure the convenience of replacing the thiolactone group by a lactam, despite the greater stability of this last functional group. For this reason, it was decided to assay both approaches synthesizing two immunizing haptens, one preserving the thiolactone group (AIP4S hapten) and the other one with a lactam ring (AIP4NH hapten), much more stable that the lactone used by Park and co-workers[224].

As a result of these calculations it was not completely sure the convenience of replacing the thiolactone group by a lactam, despite the greater stability of this last functional group. For this reason, it was decided to assay both approaches synthesizing two immunizing haptens, one preserving the thiolactone group (AIP4S) and the other one with a lactam (AIP4NH), much more stable that the lactone used by Park and co-workers[224].

The haptens designed incorporated a spacer arm, introduced by the N-terminal tyrosine residue, of two units of ethylene glycol and a cysteine residue at the opposite end. In such way, the hapten maximized exposure to the immune system the major part of the peptide structure and particularly, the most characteristic AIP-IV epitopes. Moreover, the chemical features of the spacer arm ensured hydrophilicity while minimizing its antigenicity. Finally, the cysteine residue at the end of the spacer arm provided the necessary chemistry for orthogonal bioconjugation to a bio-macromolecule to obtain the immunogen.

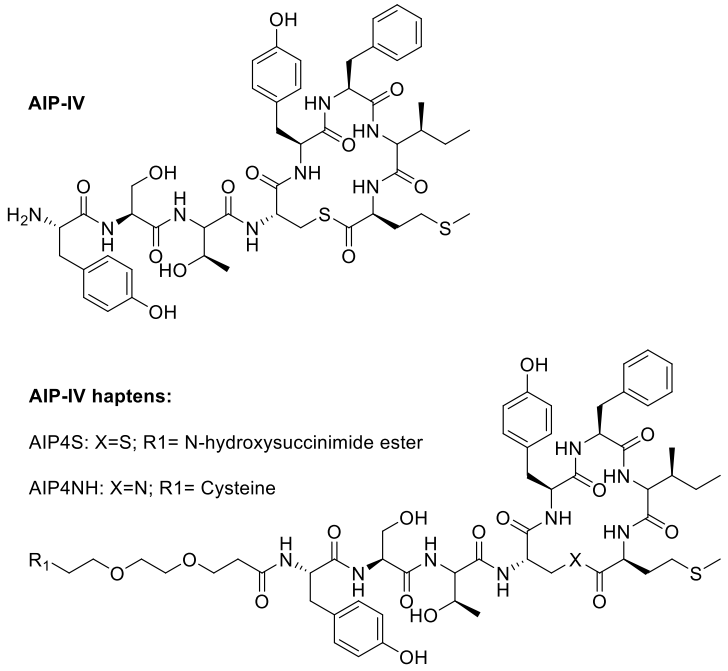

Figure 9.3. Chemical structure of the *S. aureus* quorum sensing molecule AIP-IV and the hapten derivatives AIP4S and AIP4NH synthetized in this work which were bio-conjugated and immunized for antibody production and ELISA development purposes.

Unfortunately, in the case of AIP4S including the cysteine, a spontaneous rearrangement of the cycle occurred during the synthetic procedure, due to the reactivity of an unprotected amine at the end of the spacer arm. The amine group produced an addition/elimination type reaction with the thiolactone moiety of the cycle, forming a new and more stable cycle that included the ethylene glycol units (Figure 9.4). This fact forced us to redesign the hapten, changing the synthetic strategy and replacing the terminal cysteine residue by, a N-hydroxysuccinimide ester, which could be directly used to form amide groups with the lysine residues of the protein and, as it is an electrophilic group did not react with the labile thiolactone moiety.

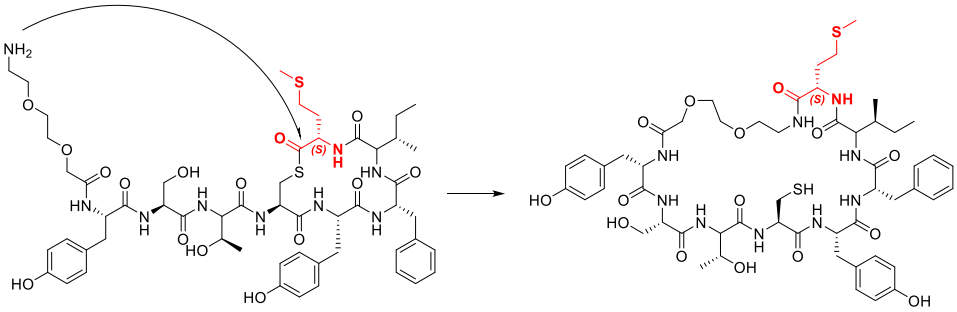

Figure 9.4. Spontaneous rearrangement of a synthetic intermediate after deprotection of the terminal amine in the chemical structure.

Briefly, the synthesis of the AIP4S hapten and AIP-IV analyte (Figure 9.5), carried out by the group of Multivalent systems for nanomedicine (MS4N) of Dra. Miriam Royo, started with the common linear peptide precursor, synthesized using a Fmoc/tBu solid-phase strategy on a 2-chloro-trityl chloride resin (CTC). All functional groups of the amino acid side chains were protected with tert-butyl ethers (tBu) with the exception of the cysteine thiol, which was protected with a 4-methoxyltrityl group (Mmt). Tert-butyloxycarbonyl protecting group (Boc) was used to protect the α-amino group of the N-terminal amino acid of each linear peptide precursor. Once peptide elongation was finished, the AIP-IV linear peptidyl-resin was cleaved using mild acidolysis conditions to hydrolyse CTC/Mmt moieties, maintaining intact tBu protecting groups. Then, the linear precursor peptide was treated with PyBOP/DIEA to cyclize between the thiol of the cysteine and the carboxylic acid of the C-terminal residue forming a thioester. The final hapten was prepared by reaction of AIP-IV with dihydroxysuccimidyl-PEG (2) ester.

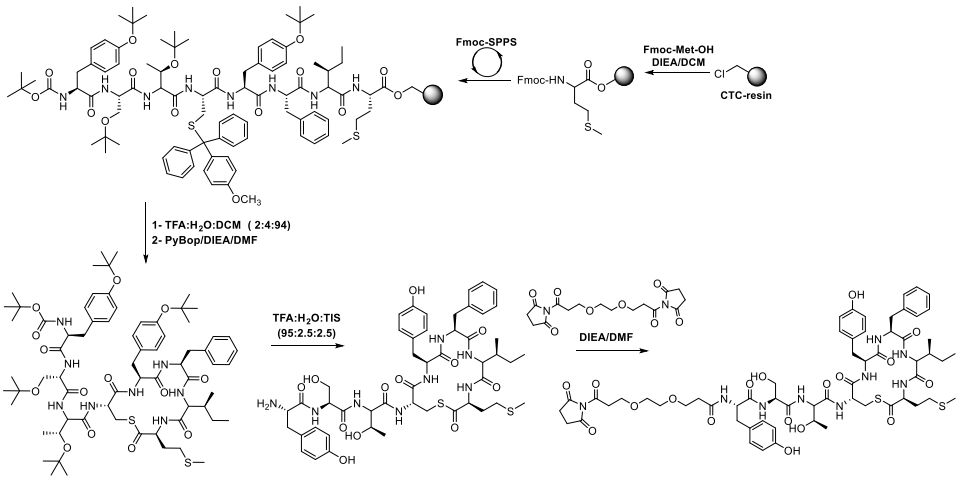

Figure 9.5. Schematic representation of the AIP4S hapten synthesis.

In the case of AIP4NH hapten lactam derivative, instead of a Fmoc-Cys(Mmt)-OH a Fmoc-Dap(Alloc)-OH it was used and linear precursor was elongated with 8-(9-Fluorenylmethyloxycarbonyl-amino)-3,6-dioxaoctanoic acid and Boc-Cys-(Trt). Prior to the linear precursor from the peptidyl-resin, Alloc group was eliminated with treatments with tetrakis(triphenylphosphine)-Palladium(0)($Pd(Ph_3P)_4$) and phenylsilane ($PheSiH_3$). The lactame was formed using also PyBOP/DIEA.

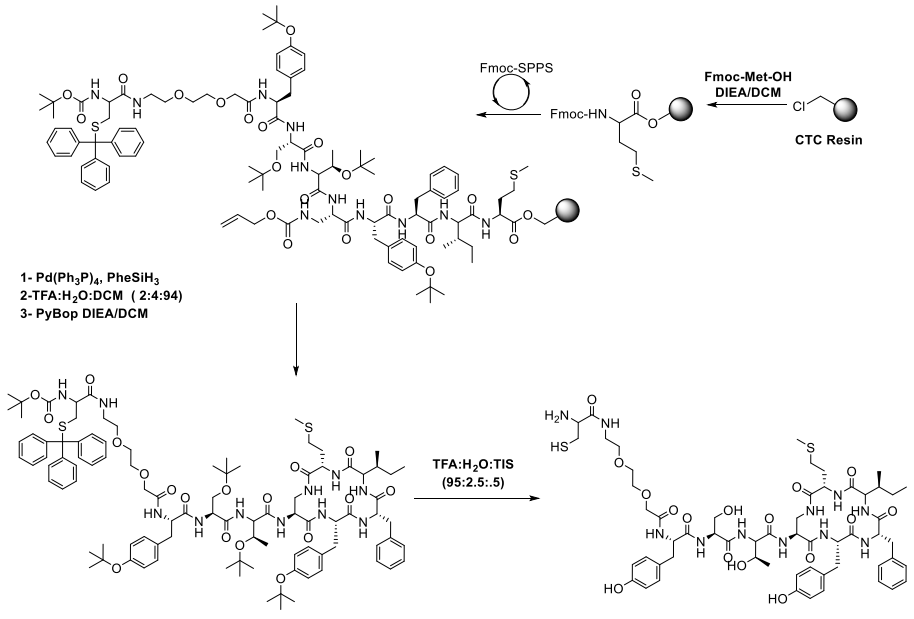

Figure 9.6. Schematic representation of the AIP4NH hapten synthesis.

9.3.1.2 Antibody production

Bio-conjugation of the AIP4NH hapten was carried out through a two-step n procedure using succinimidil iodoacetate (SIA). First, the lysine residues of the corresponding protein were reacted with the succinimide ester moiety of the linker to form the amides and subsequently the resulting purified iodinated protein was linked to the hapten through a selective SN_2 reaction of its cysteine residue to substitute the iodine group of the protein. On the other hand, the conjugation of the AIP4S hapten was performed through direct nucleophilic addition of the protein amino groups of the lysine residues with the succinimide ester moiety of the hapten. Antisera were raised against AIP4NH-HCH (As376, As377 and As378) and AIP4S-HCH (As379, As380 and As381) in female New Zealand white rabbits. The hapten densities and bioconjugation yields can be found in Table 9.1.

Table 9.1. Data on the bioconjugation yield and hapten densities of the AIP-IV bioconjugates.

	Quantity (mg)	Yield (%)	nº of residues
AIP4S-BSA	**3.80**	**76.0**	**8**
AIP4S-HCH	**4.49**	**89.8**	**-**
AIP4NH-BSA	**3.33**	**67.0**	**6**
AIP4NH-HCH	**3.29**	**65.8**	**-**

Hapten densities of BSA conjugates were calculated from MALDI-TOF-MS analysis. HCH conjugate could not be analysed by MALDI-TOF-MS because of the large molecular weight. For this purpose, BSA and HCH bioconjugates were prepared in parallel, under exactly the same conditions. The data obtained with the corresponding BSA bioconjugates was used as bioconjugation control.

9.3.2 DEVELOPMENT OF THE AIP-IV (AS380/AIP4S-BSA) ELISA

9.3.2.1 Antisera selection

The avidity of the obtained antisera against homologous and heterologous competitor antigens (BSA conjugates) was assessed by bi-dimensional titration experiments from which the most appropriate conditions for the competitive assays were selected. Although not all the As/bioconjugate combinations gave

rise to usable competitive assays, in general homologous combinations performed better than heterologous ones. On the other hand, the antisera obtained by immunization with the thiolactone derivative conjugate AIP4S-HCH, provided immunochemical assays with substantially higher detectability than the antisera obtained raised using the lactam ring derivative (Table 9.2), under homologous conditions. As result of these studies, As380/AIP4S-BSA was selected for further investigations.

Table 9.2. Analytical parameters of the preliminary competitive indirect ELISA for all the antisera produced for the detection of AIP-IV.

	As 376; 1/64000	**As 377; 1/12000**	**As 378; 1/16000**	**As 379; 1/16000**	**As 380; 1/4000**	**As 381; 1/12000**
[CA] (µg/ml)	0.17	0.63	0.63	0.45	1.25	0.63
Bottom	0.04	0.07	0.12	0.02	0.23	-
Top	0.83	1.56	1.35	1.57	1.54	-
Hill Slope	-0.80	-0.81	-090	-0.78	-0.93	-
IC_{50}	186.7	3603	294.5	79.4	5.7	-
R^2	0.989	0.993	0.996	0.996	0.993	-

The bioconjugates used for the competitive assays were assessed in homologous and heterologous combinations. The best analytical features were obtained in homologous conditions (provided in the table). The As381 did not produce a competitive assay for the detection of AIP-IV.

9.3.2.2 Physicochemical parameters optimization

With the aim of improving the preliminary assay features and getting knowledge of the performance of the assay under different physicochemical conditions, the effect of pH, conductivity, ionic strength, % Tween20, % of organic solvent, competition and preincubation time (Figure 9.7) were investigated. The assay performed quite well on a broad range of pH values keeping the best features between 4.5 and 8.5, which demonstrates the robustness of the assay. At pH 9.5 the assay was still usable, although a slight decrease in the detectability was observed (IC_{50} 7.98 at pH 7.5 vs 13.2 at pH 9.5). Competition time was optimal at 30 minutes considering IC_{50} value and maximum signal. Even though the same detectability could be reached at much smaller incubation times, the maximum signal decreased significantly. A pre-incubation step of the analyte with the antibody rendered a slight improvement in the assay detectability (IC_{50} 3.7 and

3.8 nM overnight and 10 min preincubation, respectively vs 4.9 nM if no preincubation) without affecting the maximum signal. The concentration of Tween20 also did not affect substantially the assay if used below 0.05%, although higher concentrations had a negative effect on the detectability. Regarding conductivity, it was observed a slight improvement with the increase of the ionic strength, nonetheless this effect was caused by the proportional reduction of the maximum absorbance. The addition of a small percentage organic solvent to the competitive step slightly increased the detectability, although compromising the slope of the calibration curve. As result, the assay was very robust in respect to the effect of different physico-chemical conditions affecting the assay buffer.

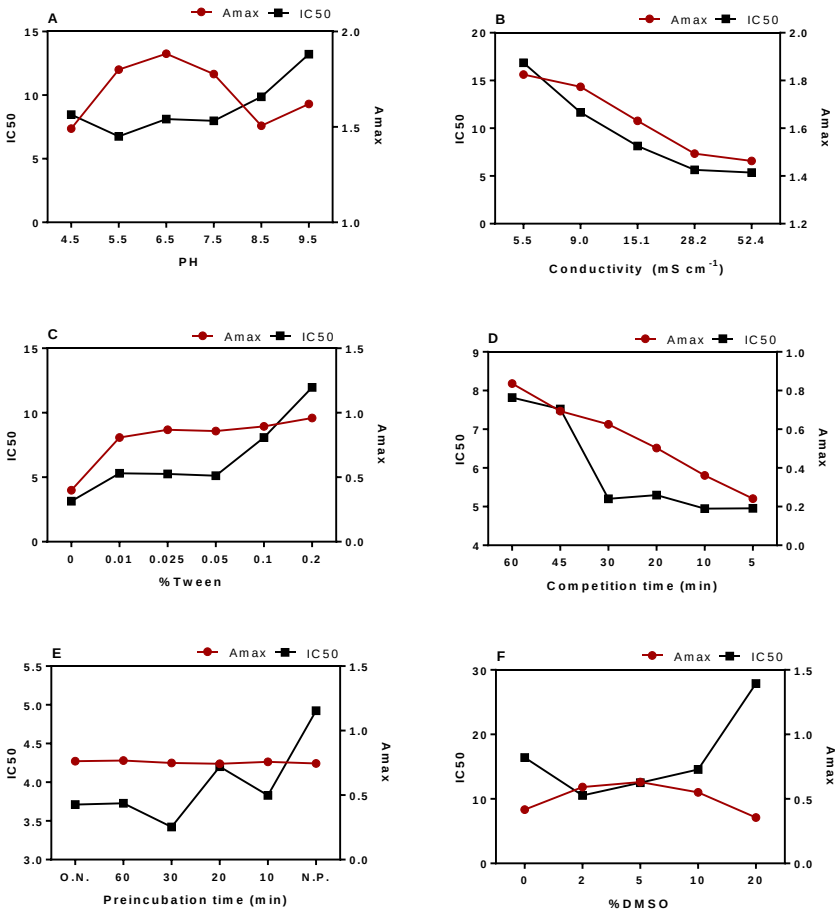

Figure 9.7. As380/AIP4S-BSA ELISA performance in the physicochemical parameters optimization study. The selection of the most appropriate conditions (Table 9.3) was based on the variations in

Amax, IC_{50} and slope values (not shown) of the generated calibration curves providing better signal/noise ratio, detectability and sensitivity. The studied parameters were A. pH B. Ionic Strength C. % Tween 20 D. competition time E. preincubation time F. % organic solvent (DMSO). All the studies were performed by varying the composition of the buffer used in the competitive step or the antibody detection times. Eventually, the conditions providing better features were evaluated again separately and in conjunction.

Table 9.3. Physicochemical parameters selected for the As380/AIP4S-BSA.

	As380/AIP4S-BSA
As dilution	1/4000
[Competitor] (µg mL^{-1})	0.63
pH	7.5
Conductivity (mS cm^{-1})	15
Tween 20 (%)	0.05
Competition time (min)	30
Preincubation time (min)	0
Organic solvent (%)	0

9.3.2.3 Analytical characterization

Since no significant improvement was observed when altering the physico-chemical parameters, the composition of the buffer in the competitive step was kept at standard conditions of PBST (Table 9.3). The analytical features of the assay run under these conditions are enclosed in Table 9.4. The assay showed a IC_{50} value of 2.90 ± 0.19 nM and a limit of detection of 0.22 ± 0.06 nM.

Table 9.4. Features of the As380/ AIP4S-BSA ELISA for the detection of AIP-IV.

	PBST	**TSB diluted 1/2**
A_{min}	0.15 ± 0.04	0.09 ± 0.01
A_{max}	1.46 ± 0.01	1.60 ± 0.05
Slope	-0.91 ± 0.03	-0.89 ± 0.03
IC_{50}	2.89 ± 0.19	2.80 ± 0.17
Dynamic Range	0.68 ± 0.14 to 14.26 ± 0.93	0.55 ± 0.11 to 12.84 ± 6.20
LOD	0.22 ± 0.06	0.19 ± 0.06
R^2	0.996 ± 0.003	0.995 ± 0.003

The concentration of BSA conjugate and As dilution used in the assay run in buffer (PBST) were 0.63 µg mL-1 and 1/4000, respectively. In the case of the assay run in TSB diluted 1/2 the concentration of BSA conjugate and As dilution were the same as the one run in buffer. The

parameters and features of the TSB 1/2 curve correspond and refer to the values in the diluted sample. The concentrations are expressed in nM and the data shown correspond to the average of 3 different days using at least 3 well/replicates per concentration.

The assay attains higher detectability than other methods developed for the quantification of AIPs such as LC/MS. Furthermore, the detectability was below the range of concentrations found for AIPs in bacterial cultures[218,219]. Even though AIPs have never been directly quantified in clinical sample, the excellent features and detectability of the assay makes foresee its potential for further clinical studies to assess the convenience of using AIPs as biomarkers of disease.

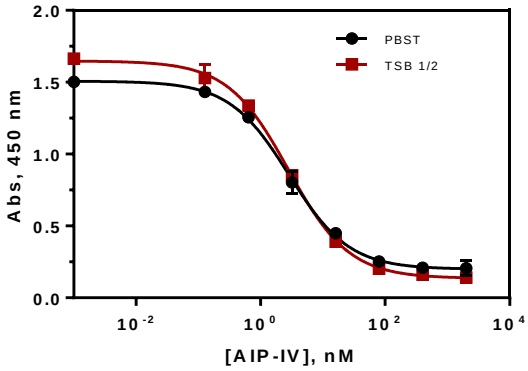

Figure 9.8. Calibration curves of the As380/AIP4S-BSA ELISA for the detection of AIP-IV run in buffer (PBST) and TSB diluted 1/2 under different conditions of BSA conjugate and As dilution (see Table 9.4 for additional information). Each calibration point was measured in triplicates on the same ELISA plate and the results show the average and standard deviation of analysis made on three different days.

9.3.2.4 Specificity study

In *Staphylococcus aureus* there are four *agr* specificity groups, characterized by variations in the locus that encodes, among other relevant components, the peptide sequence of the signalling molecules. Therefore, it turns out into four different AIPs produced in strain-specific manner (AIP-I to AIP-IV). All these molecules are cyclic thiolactone peptides with 7 to 9 amino acid residues. The higher homology is found between AIP-I and AIP-IV, which just differ in one amino acid. As these molecules might co-exist in the samples to be analysed, it was important to assess the possible cross interferences caused by other AIPs produced by *S. aureus*. Thus, AIPs I to III were synthetized and used to assess

their recognition by the As380/AIP4S-BSA ELISA. Surprisingly, despite the great structural similarities other AIPs showed less than 0.01% cross reactivity (Figure 9.9 and Table 9.5), demonstrating the great specificity of the antibodies generated and furthermore, it became clear that the tyrosine residue present in the AIP-IV cycle is essential for the biorecognition.

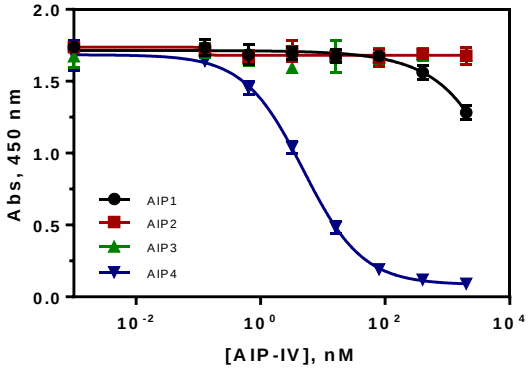

Figure 9.9. Cross reactivity study using the quorum sensing molecules from all the agr system types produced by S. aureus under the aforementioned conditions for As380/AIP4S-BSA ELISA. Calculated cross reactivity was less than 0.01% for AIP-I to III. Each calibration point was measured in triplicates on the same ELISA plate and the results show the average and standard deviation of analysis made on three different days.

Table 9.5. Half maximal inhibitory concentration (IC_{50}) of the As380/AIP4S-BSA ELISA using as analytes the different AIPs produced by *S. aureus*.

AIP	IC_{50} (nM)	C.R. (%)
I	~ 33461317	<0.01
II	-	<0.01
III	-	<0.01
IV	2.83	100

The percentages of cross reactivity (C.R.) were calculated following the equation: CR (%) = IC_{50}(Cross reactant)/IC_{50}(Analyte) x 100.

9.3.3 IMPLEMENTATION OF AS380/AIP4S-BSA ELISA TO THE ANALYSIS OF CULTURE BROTH FROM *S. AUREUS* CLINICAL ISOLATES

9.3.3.1 Matrix effect evaluation

It is well known that during infectious processes bacteria can switch from planktonic (acute infection) to sessile lifestyle (chronic infection). During this process, the production of toxins, enzymes and other survival mechanisms are adapted to the needs of the bacterial population. Isolation of the causative pathogenic strain would provide a representation of the lifestyle adopted by these microorganisms in the host. With this regard and as a pilot study, we sought to compare the AIP production profiles in a culture media of clinical isolates obtained from patients diagnosed with a respiratory airways infection. For this purpose, we initially evaluated the potential non-specific interferences that could be caused in the ELISA a complex biological media such as Tryptic Soy Broth (TSB). This culture media is normally used for the growth *S. aureus* strains and is composed by a complex mixture of digested proteins, sugars and salts. As it is possible to observe in Figure 9.10, the TSB affects substantially the assay performance, however a simple one-half dilution with the assay buffer is able to overcome this undesirable effect (Figure 9.8). Moreover, further dilution of the matrix, provided identical curves to the one performed in buffer. Table 9.4 shows the analytical parameters of the calibration curves run in buffer and in ½ diluted TSB. The IC_{50} and LOD were 2.80 ± 0.17 and 0.19 ± 0.06 nM, which would turn into 5.60 ± 0.34 and 0.38 ± 0.12 nM taking into account the dilution, which does not compromise the assay detectability to analyse culture media, considering the reported concentration values of AIPs in TSB culture broth and attaining higher detectability that that reported for LC/MS to quantify AIP-I (LOD 0.25 µM)[218]. In addition, the excellent features of the antibodies produced allow direct quantification of this AIP after a just simple dilution of the matrix, not including a sample pre-treatment or pre-concentration that could affect the stability of the peptide.

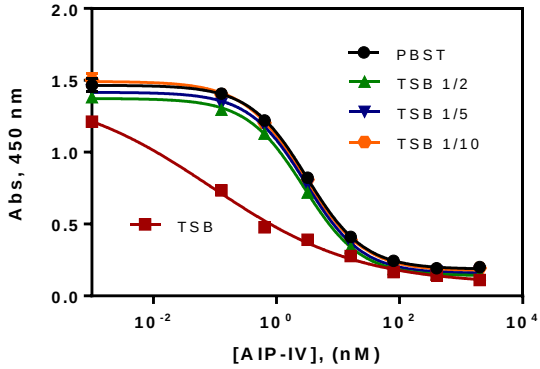

Figure 9.10. Calibration curves of As380/AIP4S-BSA ELISA competitive indirect assay run in PBST buffer, TSB culture media or dilutions of TSB using buffer. The results shown are the average and standard deviations of analysis made on two different days measured by duplicates each day.

9.3.3.2 Accuracy studies

The accuracy of the assay was evaluated by preparing 9 blind spiked samples in TSB, at concentrations inside and outside the dynamic range, and measuring them during three different days with the developed ELISA. As it is shown in Figure 9.11, a good correlation between the spiked concentrations and the ELISA results was observed with a slope of 0.94, very close to 1, and a regression coefficient of +1.1, pointing at the good accuracy of the assay to quantify AIP-IV in TSB culture broth samples.

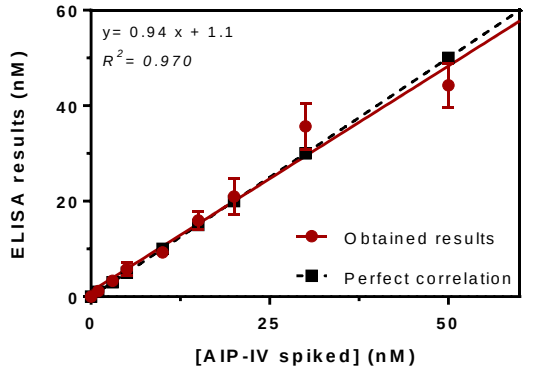

Figure 9.11. Representation of the spiked AIP-IV concentration versus the measured concentration with the As380/AIP4S-BSA ELISA. Assays were run in diluted TSB culture media diluted 1/2 using

PBST. Each calibration point was measured in triplicates on the same ELISA plate and the results show the average and standard deviation of analysis made on three different days.

Moreover, intra-plate, inter-plate and inter-day precision of the assay, calculated by the coefficient of variation (CV) at three concentrations levels (IC_{80}, IC_{50} and IC_{20} of the calibration curve) was also very good (see Table 9.6). The results indicated an excellent assay precision, although, as expected, the higher variability was found at the limit of quantitation of the assay (IC_{80}), particularly when the assay was performed on different plates or different days (%CV intra-plate, 11.5%; inter-plate, 19%; inter-day, 34.8%). However, in all other situations the % CV remained lower below 10% demonstrating that the assay can be used to provide reliable quantification data in respect to the AIP-IV concentration levels found in complex matrices.

Table 9.6. Coefficients of Variation (CV) of the As380/AIP4S-BSA ELISA run in MH culture broth diluted 1/2 using representative concentrations at a low, medium and high concentration range (IC_{20}, IC_{50} and IC_{80}).

	IC	R1	R2	R3	Mean	Desv. Est.	%CV
Inter-day	**20**	12.85	13.79	12.52	13.05	0.66	5.1
	50	2.64	2.30	2.35	2.43	0.18	7.4
	80	0.43	0.21	0.42	0.35	0.12	34.8
Inter-plate	**20**	14.80	15.12	15.33	15.08	0.27	1.8
	50	3.12	3.57	3.01	3.23	0.30	9.2
	80	0.83	0.96	0.65	0.81	0.15	19.0
Intra-plate	**20**	14.16	12.27	13.56	13.33	0.96	7.2
	50	3.33	2.87	2.79	3.00	0.29	9.7
	80	0.77	0.63	0.65	0.68	0.08	11.5

The coefficient of variation (CV) was calculated following the equation CV (%) = σ/μ x 100. The results were obtained by measurements performed in either triplicates on the same ELISA plate (intra-plate), made on three different days (inter-day) or by analysis on three different plates (inter-plate). The concentrations of the replicates, mean, standard deviation and ICs are expressed in nM. IC: Inhibitory Concentration; R: Replicate; σ: Standard Deviation; μ: Average.

9.3.3.3 AIP-IV measurement in bacterial culture broth

As explained above, *S. aureus* can be classified into four *agr* specificity groups depending on the sequence of the locus that encodes all the components and

machinery of the quorum sensing signalling system. The communication system of pathogenic strains that are isolated in microbiology laboratories can be characterized by a variety of techniques (DNA microarray, luciferase assay, etc.)[201,215], nevertheless they often require a complex pre-treatment of the samples. By using the immunochemical technique developed in this work, the relation of the *agr* system with the strain virulence and the clinical outcome of the patients could be studied in a simpler manner, also allowing the quantification and kinetic production assessment of the QS molecules besides the phenotypic identification.

For that purpose, several clinical strains were selected with the aim of profiling the release of the quorum sensing molecule AIP-IV. It was also intended to assess the variability between *agr-IV* producing strains causing different types of respiratory airways infection. In these experiments, strains with different *agr* system were selected (Table 9.7) to confirm the specificity of the developed technique towards the identification of the strain, considering the specific cross-reactivity profile encountered using pure AIP-(I-IV).

Table 9.7. Selected clinical isolates and reference strains for this study, agr group and infection types.

Strain reference	Agr system	Infection type
6_19850	I	Pneumonia
3_40448	II	Tracheobronchitis
32_75664	III	Carrier
48_86474	IV	Colonization
197_63535 (p)	IV	Pneumonia
165_36759	IV	Tracheobronchitis
Newman	I	-
USA300	I	-

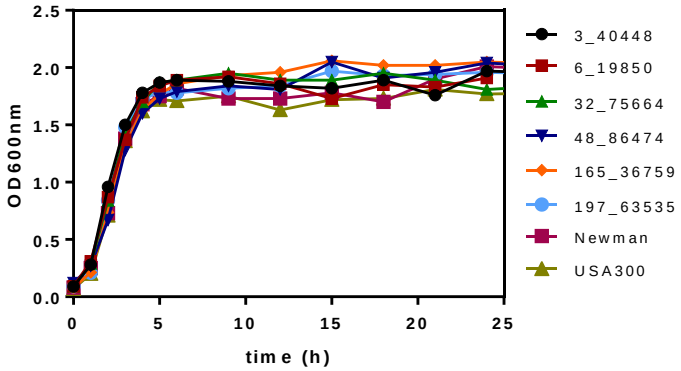

Figure 9.12. Representation of the OD_{600} versus time for all the clinical and reference strains studied in this work under the conditions described in materials and methods section.

As shown in Figure 9.12, the OD_{600} measurements showed a similar bacterial growth for all the strains, independently of the *agr* system or type of infection. Regarding AIP-IV measurements, as expected any of the strains with distinct *agr* system (I-III) produced detectable concentrations of AIP-IV, demonstrating the possibility of using the here reported immunochemical technique for typing the *agr* system due to the high specificity of the antibodies produced in this work. When comparing the AIP-IV concentrations and production profile of the *agr-IV* strains (see Figure 9.13), we can observe a similar total amount of AIP-IV produced by strains 48 (colonized patient) and 165 (tracheobronquitis) with levels in the high nM range. In both strains measurable AIP levels could be detected immediately (strain 48 at time zero) and after short incubation times (strain 165, 1h), even if the OD values were below 0.5, which pointed at the possibility to use this ELISA to identify the strain type in a very efficient manner and in a short time. However, strain 197 (pneumonia), a satellite colony selected and isolated from another strain, it showed a completely different behaviour with a significant lower and irregular production of this signalling molecule, presumably due to the type and morphology of the colonies observed in culture plate (small satellite colonies).

In order to find out a correlation between the quantified AIP levels and the severity or stage of the infection there will be necessary to carry out a complete well designed clinical study that takes into consideration all the clinical parameters of physical conditions of the patients involved. Comparing the levels

of AIP-IV in the clinical strains studied in this work to the values of AIP-I observed in *agr-I* strains measured on the previous work from Junio et al[218], there is a significant difference in the total amount of AIP produced , which are in the µM range), which could be inherent to the type of *agr* I strains used in that study. However, unlike in our studies, the peptide was only detected after 4 h of incubation with a concentration of 1.1 µM, which may be due to the lower detectability of their technology (LOD 0.25 µM vs 0.38 nM of the here reported ELISA).

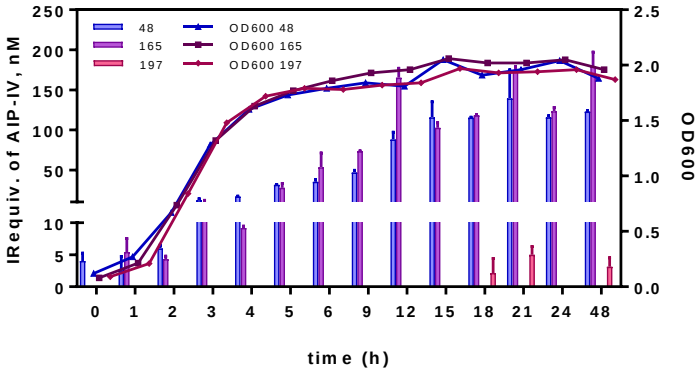

Figure 9.13. OD_{600} and immunoreactivity (IR) equivalents of AIP-IV measured in culture growth samples of *S. aureus* clinical isolates 48, 165 and 197 at the selected times using the developed As380/AIP4S-BSA ELISA. Each calibration point was measured in triplicates on the same ELISA plate and the results show the average and standard deviation of analysis made on two different days.

In summary, it has been developed an immunochemical technique capable of selectively quantify AIP-IV in a complex biological matrix, profile the production by clinical agr-IV *S. aureus* strains and allow the QS study of this bacterium. The immunochemical strategy here presented serves as a model for future studies about the immunochemical quantification of other AIPs. Rational design of the haptens followed by computational calculations and application of different synthetic methodologies were key steps to evaluate the best strategy for antibody production against the AIPs produced by *S. aureus*. Therefore, it has been demonstrated that the synthesis of an hapten containing the thiolactone ring present in the native AIP, its conjugation and immunization resulted in the best strategy to produce highly specific antibodies, able to differentiate between peptides that just differ one amino acid residue.

The ELISA developed with these antibodies is accurate, robust and can be done in less than two hours, showing a working range that is below the range of concentrations found in clinical isolates cultures. At the light of the results, this technology will be expanded for the detection of the rest of AIPs produced by *S. aureus* and on the other hand, applied to the measurement of clinical samples from infected patients due to the high detectability attained. The multiplexation of the different assays would potentially lead to a powerful diagnostic tool for determining *S. aureus* infection, performing *agr* typing and studying the QS of pathogenic strains through their signalling molecules. The clinical significance of QS molecules needs to be further explored due to the vast set of mechanisms that is under their control. The clinical significance evaluation of QS molecules is already being performed in gram-negative bacteria, especially in *P. aeruginosa*, and promising results pointing at the possibility to use these metabolites as biomarkers of infections have been obtained. For this reason, not assessing the potential value of the corresponding molecules in gram-positive bacteria is no longer justified and more studies and techniques have to be developed for revealing the prognostic and diagnostic potential of QS at important pathogens such as *S. aureus*.

9.4 CHAPTER CONTRIBUTIONS

- Rational design of the haptens followed by computational calculations and application of different synthetic methodologies were key steps to evaluate the best hapten synthesis strategy for antibody production against the AIPs produced by *S. aureus*.

- The avidity of the polyclonal antibodies against AIP-IV obtained by immunization with a homologous (AIP4S-HCH) or a heterologous (AIP4NH-HCH) immunogen were compared and eventually, allowed to definitively determine the best strategy through ELISA experiments, which resulted to be the one using the homologus hapten structure. The best combination of antisera and competitors was selected for developing an ELISA that is able to quantify AIP-IV in the low-nM range in wide range of physico-chemical conditions.

- The assay showed high specificity versus AIP-IV despite the structural similarity with other AIPs (AIP-I). Afterwards, it was implemented for the measurement of AIP-IV in a complex biological sample such as culture broth, obtaining different production profiles for some of the strains and demonstrating the potential of this immunochemical technique for the evaluation of QS molecules as biomarkers.

- Eventually, the developed work could be a first step towards the evaluation of AIPs as biomarkers of infection. If antibodies are produced against the rest of AIPs, an immunochemical multiplexed tool could be constructed for the simultaneous diagnosis of *S. aureus* infections and *agr* typing.

9.5 MATERIALS AND METHODS

9.5.1 SYNTHESIS

General methods and instruments. The general methods and instruments can be found in section 4.5.1. In addition to the previously described methods and instruments: HPLC-PDA-MS analysis were performed on a Waters Alliance 2795 with an automated injector and a photodiode array detector Waters 2996 coupled to an electrospray ion source (ESI-MS) Micromass ZQ mass detector, and the MassLynx 4.1 software. The instrument was operated in the positive ESI (+) ion mode. All the HPLC-PDA-MS analyses were carried out using elution conditions 1: XSelect™ C_{18} column (4.6 mm×50 mm, 3.5 μm). Elution solvent system: A: 0.1% HCOOH in H_2O and B: 0.07% HCOOH in CH_3CN. Gradient: 5 %B to 100 % B over 4.5 min at a flow rate of 2.0 mL/min. λ= 220 nm. HPLC-PDA analysis were performed on a Waters Alliance 2695 with a photodiode array detector Waters 2998 using elution condition2: XBridge™ BEH130 C_{18} (3.5 μm, 4.5mm x 100mm) column. Elution solvent system: A: 0.045% TFA in H_2O and B: 0.036% TFA in CH_3CN. Flow rate of 2.0 mL/min and temperature 25°C. λ=220nm. Gradient A: 10 %B-70 %B in 8 minutes. Gradient B: 5 %B-100 %B in 8 minutes. Gradient C: 20 %B-100 %B in 8 minutes.

***Molecular modeling and theoretical calculations*.** Molecular modeling was performed using the Hyperchem 6.03 software package (Hypercube Inc., Gainesville, FL). Theoretical geometries and electronic distributions were evaluated for AIP-IV hapten derivatives (thiolactone or lactam ring) using semiempirical quantum mechanics MNDO and PM3 models. All calculations were performed using standard computational chemistry criteria.

Synthesis of the AIP-I to IV precursors. AIPs I to IV derivatives used for the preparation of the haptens and/or analytes were synthesized at the Peptide Synthesis Unit of NANBIOSIS ICTS. Linear peptides precursors were synthesized manually on solid phase using 0.5 g 2-chloro trityl chloride resin (CTC resin; f= 1.6 mmol Cl/ g). The resin was conditioned with washings with dichloromethane (DCM) and dimethylformamide (DMF). The C-terminal residue was introduced by the addition of the corresponding Fmoc-aa-OH (1 mmol) and diisopropylethylamine (8.0 mmol) dissolved in anhydrous DCM on to the solid support. After 1.5 h MeOH (0.8 mL/g de resina, 400 μL) was added to block the unreacted chloride groups and the mixture was left to react 30 min. Then, mixture was filtered and the resin washed with DMF and DCM. The peptides were elongated by sequence of Fmoc elimination and coupling cycles using a Fmoc/tBu protecting group strategy. All functional groups of the amino acid side chains were protected with tert-butyl ethers (tBu) with the exception of the cysteine thiol, which was protected with a 4-methoxytrityl group (Mmt). Fmoc elimination was carried out by treatments (2 x 5 min) with piperidine-DMF solution (2:8, v/v). Amino acid couplings were performed by the addition of Fmoc-aa-OH (3 equiv.), *N*,*N*'-diisopropylcarbodiimide (3 equiv., DIC) and ethyl cyano(hydroxyimino)acetate (3 equiv., oxyme pure) in DMF during 45 min. After each Fmoc elimination or coupling steps the resin washed with DMF, DCM and DMF. The last amino acid introduced was protected at the α-amino with the Boc protecting group.

For the linear precursor of the AIP4NH derivative, Fmoc-Dap(Alloc)-OH was used instead of Fmoc-Cys (Mmt)-OH, and linear precursor was elongated with 8-(9-Fluorenylmethyloxycarbonyl-amino)-3,6-dioxaoctanoic acid and Boc-Cys-(Trt). Once the peptide elongation was finished, the Alloc group was eliminated by treatments (3 x 15 min) with tetrakis(triphenylphosphine)-Palladium(0) (0.1 equiv., 26 mg, ($Pd(Ph_3P)_4$) and phenylsilane (5 equiv., 140 μL, $PheSiH_3$) in anhydrous DCM.

The AIP-I to IV and lactame AIP-IV linear precursor peptidyl-resins were cleaved using mild acidolysis with TFA:DCM (2:98, v/v; six treatments of 1 minute/each). Then, the cleavage mixture was filtered and collected over H_2O and DCM was eliminated under vacuum. The final protected linear AIP-I to IV peptide solutions were lyophilized and used for cyclization without previous purification.

AIPs cyclization. 104.4 mg of AIPI-IV protected linear peptide (77.3 μmol) were dissolved in 78 mL of DMF and PyBOP (52 mg, 1.3 equiv., 100 μmols) and DIEA (17 μL, 1.3 equiv., 100 μmol) were added. Thiolactone formation was controlled by HPLC-UV-MS and once the starting material was consumed, the DMF was eliminated under vacuum. The residue was dissolved in H_2O:CH_3CN (1: 1, v/v) and lyophilized, yielding 100 mg of protected AIP-IV crude. Protecting groups were eliminated by acidolysis with TFA:H_2O:TIS (95:2.5:2.5, v/v/v) at room temperature during 1h. Then, peptide was precipitated by adding slowly this solution to cold diethyl ether. The solid was 3 times with cold diethyl, dissolved in H_2O:CH_3CN and lyophilized. 65 mg of crude AIP-IV were obtained. Peptide was purified by HPLC-UV-MS. HPLC-PDA (elution conditions 2): t_R: 5.977 min. Chemical purity: 94.94% (estimated by UV at 220nm). HR-MS: Calculated mass for $C_{48}H_{64}N_8O_{12}S_2$: 1008.4085; found: $[M+H]^+$= 1009.4150; $[M+Na]^+$ = 1031.3978; $[M+K]^+$ = 1047.3716.

AIPS hapten. Conjugation was carried out mixing equimolar quantities of AIP-IV and the dihydroxysuccimidyl PEG (2) ester (NHS-PEG (2) -NHS) with DIEA (1 equiv.) in DMF. The evolution of the reaction was controlled by HPLC-MS, and once was finished DMF was eliminated under vacuum. The AIP IV -PEG (2) –NHS was purified by semi-preparative HPLC. HPLC-PDA (elution conditions 2, gradient C): t_R: 5.977 min. Chemical purity: 95.61% (estimated by UV at 220nm). HPLC-MS (conditions 1): calculated mass for $C_{60}H_{79}N_9O_{19}S_2$: 1293.49; found: $[M+H]^{+1}$ = 1294.5; $[M+NH_4]^{+1}$ = 1311.7; $[M+2H]^{+2}$ = 648.2.

AIP4NH hapten. 100 mg of AIP-IV lactame derivative protected linear peptide precursor were dissolved in DMF and PyBop (34 mg, 65 μmols) and DIEA (15μL; 82 μmols) were added. The reaction was controlled by HPLC-MS. Once the reaction was finished, DMF was eliminated under vaccum. Then, protecting groups were eliminated by acidolysis with TFA:H_2O:TIS (95:2.5:2.5, v/v/v) at room temperature during 1h. Then, peptide was precipitated by adding slowly this solution to cold diethyl ether. The solid was 3 times with cold diethyl,

dissolved in H_2O:CH_3CN and lyophilized. 65mg of AIP-IV lactame derivative were obtained. After purification a mixture 24.5 mg monomer and dimer (3/1) were obtained. The dimer was reduced with a treatment with TECEP and used for conjugation without further purification. HPLC-PDA (elution conditions 2, gradient B): t_R: 5.572 min. Chemical purity: 98.39% (estimated by UV at 220nm). HR-MS: Calculated mass for $C_{57}H_{81}N_{11}0_{16}S_2$: 1239.5304; found: 1240.5397 $[M+H]^1$; 1262.5209 $[M+Na]^+$; 1279.4911 $[M+K]^{+1}$.

9.5.2 IMMUNOCHEMISTRY

General methods and instruments. Chemicals and biochemicals were obtained from Aldrich Chemical Co. (Milwaukee, WI, USA) and from Sigma Chemical Co. (St. Louis, MO, USA). The stock solutions of the AIPs (I to IV) used as standards were prepared in DMSO at 10 mM and stored at -20ºC, then transferred to 4ºC prior to their use. Purification of conjugates was carried out in ÄKTA Prime Plus using 2 HiTrap desalting columns both from GE Healthcare (Chicago, IL, USA) or either by dialysis using Spectra/Por membranes from Spectrumlabs (Piraeus, Greece, EU) with molecular weight cut-off of 12-14 kDa. The matrix-assisted laser desorption ionization time-of-flight mass spectrometer (MALDI-TOF-MS) was a Bruker autoflex III Smartbeam spectrometer (Billerica, Massachusetts). Hapten densities of the conjugates were calculated by MALDI-TOF-MS by comparing the molecular weight recorded on the MALDI spectra of the native proteins to that of the BSA-SIA, AIP4S-BSA and AIP4NH-BSA bioconjugates. For this purpose, the bioconjugates were mixed with the freshly prepared matrix ((trans-3,5-dimethoxy-4-hydroxycinnamic acid, 10 mg mL^{-1} in 70:30 ACN/H2O, 0.1% HCOOH) following the ''sandwich'' sample preparation method. The bioconjugate aliquot is diluted ½ using ACN with HCOOH 0.2%. According to it, the matrix (2 µL) is deposited on the MALDI plate and dried, followed by the bioconjugate solution (2 µL, 2 to 5 mg mL^{-1} in 1:1 ACN/H2O, 0.1% HCOOH), allowed to dry again and finally, the matrix solution (2 µL) was added over again. The resulting dried spot was then analyzed by MALDI-TOF-MS. Hapten densities were calculated through the equation: [MW(conjugate) − MW(native protein)]/[MW(hapten)-MW(lost atoms)]. The pH and the conductivity of all buffers and solutions were measured with a pH-meter pH 540 GLP and a conductimeter LF 340, respectively (WTW, Weilheim, Germany). Polystyrene

microtiter plates used for the ELISAs were purchased from Nunc (Maxisorp, Roskilde, Denmark). Dilution plates were purchased from Nirco (Barberà del Vallés, Spain). Washing steps were performed on a Biotek ELx465 (Biotek Inc.). Absorbances were read on a Thermo Scientific MultiSkan GO (Thermo Fisher Scientific, Waltham, MA, USA) at a single wavelength mode (450 nm). The competitive curves were analyzed with a four-parameter logistic equation using the software GraphPad Prism 7.0 (GraphPad Software Inc., San Diego, CA, USA) according to the following formula: $y = B(A-B)/[1 - (x/C)^D]$, where A is the maximum absorbance, B is the minimum absorbance, C is the concentration producing 50% of the maximal absorbance, and D is the slope at the inflection point of the sigmoid curve. Unless otherwise indicated, the data presented correspond to the average of at least two well replicates.

Buffers. The detailed composition of the general buffers can be found also in section 4.5.2.

9.5.2.1 Antibody production

Lactam hapten bioconjugates (AIP4NH-BSA and AIP4NH-HCH). A solution of succimidyl iodoacetate (SIA, 4.5 µmol) in DMF (0.1 mL) was added dropwise to a solution of the protein (BSA or HCH, 5.6 mg mL^{-1}, 0.9 mL in Borax/Borate buffer) and the mixture was stirred 4 h at room temperature (RT). The solution was purified by AKTA using a HiTrap desalting column and Borax/Borate as eluting buffer, to isolate the protein-SIA intermediates. A fraction (20 µL) of the BSA-SIA bioconjugate was kept for MALDI-TOF analysis. Then, AIP4NH hapten (3.45 mg, 2.8 µmol) was dissolved in MeCN/H_2O 1:1 solution (150 µL) and a solution of tris(2-carboxyethyl)phosphine (TCEP, 150 µL, 2.5 mg mL^{-1}) was added dropwise and the mixture was left stirring 10 min at 40ºC. Afterwards, the resulting solution was added (150 µL) over the protein solutions and the mixture was stirred overnight at 4ºC. The bioconjugates were purified by dialysis against 0.5 mM PBS (5 x 5 L) and Milli-Q water (1 x 5L), and stored freeze dried at -80 ºC. A small fraction (20 µL) of the AIP4NH-BSA was kept for MALDI-TOF analysis, rendering a hapten density of 6 haptens per molecule of BSA (see table 1S).

Thiolactone hapten bioconjugates (AIP4S-BSA and AIP4S-HCH). A solution of the AIP4S hapten (2.9 mg, 2.3 µmol) in anhydrous DMF (0.1 mL) was added dropwise over the protein solutions (BSA or HCH, 2.5 mg mL^{-1}, 2 mL in PBS 10mM

buffer). The mixtures were left stirring 4h at RT and the bioconjugates were subsequently purified by dialysis against 0.5 mM PBS (5 x 5 L) and Milli-Q water (1 x 5L), and stored freeze dried at -80 ºC. A small fraction (20 µL) of the AIP4S-BSA was kept for MALDI-TOF analysis, rendering a hapten density of 8 haptens per molecule of BSA.

Polyclonal antisera (PAb). Antibody production has been performed with the support of the ICTS "NANBIOSIS", more specifically by the Custom Antibody Service (CAbS, CIBER-BBN, IQAC-CSIC)**.** Six female New Zealand white rabbits weighing 1–2 kg were immunized with AIP4NH-HCH (x3) or AIP4S-HCH (x3) following the established protocols in the research group. Immunizations were carried out in the animal facility of the Research and Development Center (CID) of the Spanish Research Council (CSIC) Registration Number: B9900083, employing approved procedures that avoid unnecessary treatments and minimize suffering of the animals. The protocol used in accordance with the institutional guidelines under a license from the local government (DAAM 7463) and approved by the Institutional Animal Care and Use Committee at the CID-CSIC. The antisera (As) obtained by immunization with AIP4NH-HCH were named As376, As377 and As378 and the As obtained by immunization with AIP4S-HCH were named As379, As380 and As381. The animals were exsanguinated after 6 immunizations, and the final blood was collected in vacutainer tubes provided with a serum separation gel. Antisera were obtained by centrifugation at 4 °C for 10 min at 10 000 rpm, then stored at −80 °C in the presence of preservative 0,02% sodium azide. The antibody titer was assessed during the immunization process through non-competitive indirect ELISA. Microtiter plates were coated with a fixed concentration of AIP4NH-BSA or AIP4S-BSA conjugates (1 mg mL^{-1}) and the avidity of the produced antibodies was measured by preparing serial dilutions of the corresponding As.

9.5.2.2 ELISA

Non-competitive indirect two-dimensional titration experiments. Non-competitive indirect ELISA were carried out to select the concentrations of coating antigen (CA) and the As dilutions more suitable for the competitive assays. For this purpose, the binding serial dilutions of the antisera (1/1000 to 1/64000, and zero in PBST, 100 µL/well) to microplates coated with the BSA

bioconjugates (5 μg mL^{-1} to 5 ng mL^{-1}, and zero in coating buffer, 100 μL/well) was measured. From these experiments, optimum concentrations for coating antigens and antisera dilutions were chosen to produce around 0.9-1.5 units of absorbance after 30 min of competitive step.

As380/AIP4S-BSA ELISA. Microtiter plates were the AIP4S-BSA conjugate in coating buffer (0.31 μg mL^{-1}, 100 μL/well) overnight at 4ºC and covered with adhesive plate sealer. The day after, plates were washed with PBST (4 x 300 μL/well) and solutions of AIP-IV standards (2μM to 0.13 nM in PBST, 50 μL/well) followed by the As380 (dil. 1/4000 in PBST, 50 μL/well) were added and the microplates left without agitation 30 min at RT. After another washing step, a solution of dilution of goat AntiRabbit IgG-HRP (1/6000 in PBST) was added (100 μL/well) and incubated for 30 min at RT. The plates were washed again and the substrate solution was added (100 μL) and left 30 min at RT in the dark. The enzymatic reaction was stopped by adding of 4N H_2SO_4 solution (50 μL/well) and the absorbance read at 450 nm.

Immunoassay performance evaluation. This experimental procedure can be found in section 4.5.2.2.

Cross Reactivity studies. Standard solutions of the four AIPs from *Staphylococcus aureus* (I to IV) were prepared (0.12 nM –10 μM in PBST) and measured with the ELISA following the procedure described above. The standard curves obtained were fitted to the four-parameter equation mentioned above and the IC_{50} value used to calculate the cross-reactivity according to the following equation: CR (%) = IC_{50}(Cross reactant)/IC_{50}(Analyte) x 100.

9.5.2.3 Implementation of the ELISA to the analysis of clinical isolates

Samples. Six clinical *S. aureus* isolates were retrospectively selected from a collection of strains in the Hospital Universitari Germans Trias i Pujol. Strains were isolated from respiratory specimens obtained from patients under mechanical ventilation admitted at the intensive care unit. Isolates were stored at -80°C in a maintenance freezing medium (Oxoid TP, 15731). Strains were identified as *S. aureus* by conventional assays (Gram staining, selective culture media, coagulase test) and antibiotic susceptibility testing. Strains were

genotypically characterized by means of a DNA microarray (Clondiag). According to array results, strains were agr I (culture number 19850), agr II (culture number 40448), agr III (culture number 75664) and agr IV (culture number 86474, 63535 and 36759). The bacterial isolates and two *S. aureus* reference strains (USA300 and Newman, agr I) were cultured overnight at 37ºC in TSB (5mL). The day after, dilutions 1/50 in fresh TSB were prepared and the optical density at 600 nm (OD_{600}) measured. Then the resulting solutions were shaken at 37ºC until the selected time of growth was completed. When the time was finished, aliquots were extracted for Colony Forming Units (CFUs) and OD_{600} measurement. Afterwards, each solution was centrifuged 10 min at 3000 g and aliquots were stored at -20 ºC for AIP-IV concentration measurement using the ELISA developed in this work. AIP-IV concentrations measured by ELISA are expressed as AIP-IV immunoreactivity equivalents (IRequiv).

Matrix effect study. TSB culture media was diluted (1:2, 1:5, 1:10, 1:20), used to prepare AIP-IV standard calibration curves and to compare them with the standard curves prepared in PBST. Subsequently, the dilution providing the best ELISA parameters was selected and the conditions of CA and As dilution adjusted.

Accuracy studies. Blind spiked samples using diluted TSB culture broth were prepared and measured using the above described ELISA. The samples were measured in triplicates and the experiment repeated on three different days.

10 CONCLUSIONS OF THIS THESIS

10.1 CONCLUSIONS

General conclusion: It has been demonstrated that specific QS molecules of important pathogenic bacteria, such as *P. aeruginosa* and *S. aureus*, can be detected and quantified in complex biological samples by immunochemical methods. This is possible, despite the low molecular weight of the molecules, if high quality antibodies are produced with the necessary avidity and specificity features. These facts are greatly determined by the chemical structure designed for the immunizing hapten. Although further clinical analysis must be performed, the results obtained in this thesis point at the potential of the QS molecules as biomarkers of infection.

Pseudomonas aeruginosa

- Polyclonal antisera showing high avidity for signaling molecules of the *pqs* system of *P. aeruginosa* (2-heptyl-4-quinolone (**HHQ**), 2-heptyl-3-hydroxy-(1H)-4-quinolone (**PQS**) and 2-heptyl-4-hydroxyquinoline N-oxide (**HQNO**)) have been developed for the first time. Despite their low molecular weight, it has been possible to raise an immune response thanks to the chemical synthesis of appropriately designed haptens and bioconjugates.

- The studies performed have demonstrated that HHQ, PQS and HQNO can be specifically detected and quantified in the low nM range (LODs 0.34 ± 0.13 (HHQ), 0.17 ± 0.01 (PQS) and 0.27 ± 0.09 Nm (HQNO)) using microplate-based ELISAs developed with the antibodies produced. The detectability achieved in all cases is under the range of concentrations found in bacterial cultures are in the same range that the values found in clinical samples such as sputum, which pointed at the potential value of these technologies to be used for clinical diagnostic purposes.

- Designing hapten chemical structures addressed to maximize recognition of the most important and specific target molecule moieties has been a key factor on the accomplishment of this aim. Hence, despite the structural similarities between the three AQs metabolites targeted in this investigation, the antibodies generated demonstrated greater affinity versus their

respective targets, which will allow differentiating between them in biological samples where the three might be present.

- There exists a great potential for being able to implement the ELISAs developed in this thesis to the diagnostic of infections caused by *P. aeruginosa.* Although furthers studies have to be performed, the results obtained from a small pilot study show that the QS AQ immunochemical reactivity measured in culture media where bacterial isolates obtained from infected patients grew can be correlated to the infection types and/or severity. This is evidenced by the significant differences encountered on the HHQ, PQS and HQNO IR equiv. recorded when measuring culture media where bacteria clinical isolates obtained from patients with chronic or acute infections had been growth. Moreover, IR equiv. could be measured after just 5 h of culture for the clinical isolates obtained from acute patients. In contrast, the IR equiv. could only be measured after minimum 12 h of growth if the bacterial clinical isolate was obtained from a patient with a chronic infection. Such observation was corroborated by analyzing a discrete number of bacterial clinical isolates belonging to these two groups, after 8 h of growth in MH media.

Staphylococcus aureus

- The thiolactone group of the AIP-IV cyclic peptides appears as an important epitope for antibody recognition according to the studies performed in this thesis. Thus, the avidity of the antibodies raised against a cyclic peptide hapten preserving this functional group (AIP4S) was higher than those raised against a hapten with a lactam (AIP4NH). This last hapten was synthesized to overcome the risk of the potential hydrolysis of the thiolactone during bioconjugation or immunization process. However, the results obtained point at the partial stability of the thiolactone group based on the superior properties of the antibodies produced using AIP4S compared to those obtained against the AIP4NH hapten. The AIP4S hapten contained the original thiolactone cycle found in AIP-IV and exactly reproduced the electronic configuration of the native QS molecule, while the AIP4NH hapten was

designed to mimic the AIP-IV as much as possible (it just differed one atom from the original AIP) but with a greater stability towards a potential hydrolysis. This is the first time that antibodies have been produced against a *Staphylococcus aureus* AIP using a hapten that preserves the thiolactone group.

- *S. aureus* AIP-IV can be detected in the low nM range (LOD 0.22 ± 0.06 nM) with the antibodies produced on a competitive microplate–based ELISA, a detectability which is superior of other reported methods based on the use LC-MS techniques, and far below the concentrations values that have been reported to be release by these bacteria in culture media.

- The antibodies raised against AIP4S-HCH showed greater specificity for AIP-IV in respect to any other AIP produced by this pathogen, despite the great homology of their chemical structures and amino acid sequences, particularly in the case of AIP-I, which differed in just one amino acid.

- The results of our investigation demonstrates that there exists a great potential for using the *S. aureus* AIPs as biomarkers of infection. Hence the high detectability and specificity of the antibodies produced have allowed to use the ELISA developed to perform a small clinical pilot study, in which it has been possible to quantify AIP-IV in the media after just less than 1 h of growth. Further studies will be addressed to probe if direct detection of these QS peptides is also possible in clinical samples.

- The specificity profile of the AIP-IV antibodies and the ELISA developed in this thesis points at the possibility to use them not only for diagnosis but also for phenotyping the pathogenic strain. Thus, while AIP-IV IR equiv. were measured in media culture where *agr-IV* type strains grew, no signal was recorded on media culture of other *agr* strains.

11 RESUMEN

(Este apartado está redactado en castellano de acuerdo a uno de los requisitos establecidos en el artículo 37 de la normativa reguladora de doctorado bajo el amparo del RD 99/2011 y de la Comisión de Doctorado de la Facultad de Química de la UB. "Cuando la totalidad de la tesis se presenta en una lengua diferente de las especificadas en el programa de doctorado, se exige que se presente un resumen que no sea inferior al 10% del volumen redactado en la otra lengua").

11.1 INTRODUCCIÓN

El sistema de comunicación bacteriano, conocido como Quorum Sensing (QS), es el responsable de la activación colectiva de la expresión génica de un gran número de mecanismos bacterianos. El QS, presente en todas las especies bacterianas, se basa en la biosíntesis, liberación y detección de señales de bajo peso molecular denominadas autoinductores (AI)[3]. Los AI se liberan al espacio extracelular y son detectados por la comunidad microbiana circundante. Luego, cuando se alcanza un cierto umbral, se activa la expresión génica coordinada. Las bacterias patógenas utilizan este comportamiento de grupo para responder colectivamente al estrés ambiental del huésped y activar mecanismos como la liberación de factores de virulencia y formación de biofilms. De lo contrario, el desempeño individual de tales procesos sería ineficaz.

Aunque todos los tipos de bacterias pueden comunicarse a través de QS, existen diferencias fundamentales en los sistemas de comunicación entre las bacterias grampositivas y gramnegativas[4]. Los AI característicos utilizados para la señalización y el modo de activación de los genes desencadenado por estos AI son sustancialmente diferentes en un tipo de bacteria u otro. Por ello, la investigación sobre el QS ha divergido durante los últimos años, concentrando los esfuerzos principalmente en el estudio de un ejemplo de cada tipo de bacteria. *Pseudomonas aeruginosa* ha sido seleccionada como modelo en el caso de bacterias gramnegativas, caracterizándose por una compleja red jerárquica entre diferentes subsistemas de comunicación, apoyándose en diferentes familias de pequeñas moléculas orgánicas[5]. Por otro lado, *Staphylococcus aureus* es la bacteria más estudiada en bacterias grampositivas, confiando su red de comunicación en cuatro tipos de péptidos autoinductores cíclicos (AIP). Ambos patógenos se encuentran entre los microorganismos más comúnmente aislados en infecciones asociadas centros de salud (nosocomiales) y adquiridas en la comunidad y, por tanto, no es de extrañar que la investigación haya evolucionado seleccionándolos como modelos de sistemas de comunicación de cada tipo de bacteria.

11.1.1 QS EN BACTERIAS GRAMNEGATIVAS: MODELO *P. AERUGINOSA*

El estudio de QS en bacterias gramnegativas se ha centrado principalmente en *Pseudomonas aeruginosa*, seleccionada como modelo por su complejo circuito de comunicación y su relevancia e incidencia en enfermedades infecciosas. *P. aeruginosa* es una bacteria gramnegativa ubicua capaz de prosperar en una amplia gama de entornos (suelo, agua, plantas, animales y humanos). Aunque es una bacteria comensal normalmente controlada por un sistema inmunológico sano, se comporta como un patógeno oportunista cuando hay una brecha en el tejido del huésped o en la respuesta inmune[6]. Su capacidad para adaptarse y penetrar las defensas del huésped lo convierte en uno de los microorganismos más comúnmente aislados en entornos clínicos, causando un amplio espectro de infecciones agudas y crónicas graves[9]. Este patógeno es una de las principales causas de morbilidad y mortalidad en individuos que presentan trastornos previos, como pacientes inmunodeprimidos y con fibrosis quística (FQ)[16]. Además, las infecciones por P. aeruginosa se generan con frecuencia por cepas multi-resistentes, por lo que las opciones terapéuticas tradicionales se han vuelto limitadas[17]. La gran incidencia y prevalencia de esta bacteria se debe en parte a la vasta respuesta adaptativa y capacidad para regular la expresión génica en función de las necesidades de la población y el estrés ambiental, en parte debido a su eficaz sistema de comunicación QS.

P. aeruginosa posee una estructura QS particularmente compleja en la que cuatro sistemas interconectados (*las, rhl, pqs* e *iqs*) funcionan de manera jerárquica, siguiendo una sofisticada red reguladora para mantener la homeostasis poblacional durante un proceso infeccioso[22]. Cada circuito QS tiene una señal química característica que se une a su proteína receptora afín, iniciando las correspondientes cascadas de regulación positiva y / o negativa. Las moléculas de señalización de los sistemas *las* y *rhl* se descubrieron hace más de 20 años y consisten en dos homoserin-lactonas estructuralmente diferentes, N-(3-oxododecanoil)-L-homoserin-lactona (3-oxo-C12-HSL) y N-butiril-L-homoserin-lactona (C4-HSL), respectivamente[23,24]. La principal molécula de señalización del sistema *pqs* es la 2-heptil-3-hidroxi-4-(1H)-quinolona o PQS (Pseudomonas quinolone signal), que cumple múltiples funciones además de su actividad de señalización[25]. El precursor biológico de PQS, 2-heptil-4-quinolona o HHQ también puede asumir la señalización y modular las funciones bacterianas[26]. El AI característico del cuarto y más recientemente descubierto

sistema QS corresponde al 2-(2-hidroxifenil)-tiazol-4-carbaldehído, también denominado como el sistema en el que participa, IQS (Integrated Quorum Sensing signal)[27].

11.1.2 QS EN BACTERIAS GRAMPOSITIVAS: MODELO *S. AUREUS*

En el caso de las bacterias grampositivas, la bacteria elegida por unanimidad como modelo para el estudio de la QS ha sido *Staphylococcus aureus*. Este microorganismo una bacteria grampositiva comensal que coloniza hasta el 60% de la población humana en algún momento determinado[229]. Sin embargo, también es un patógeno amenazante para los seres humanos, principal causa de un amplio espectro de enfermedades como bacteriemia, endocarditis infecciosa, infecciones de piel y tejidos blandos, osteoarticulares y pleuropulmonares[34]. *S. aureus* es uno de los organismos que más enfermedades causan debido a su capacidad particular para evadir la respuesta inmune innata, como el complemento o la muerte mediada por fagocitos[230]. En particular, se estima que *S. aureus* resistente a la meticilina (MRSA) representa el 25% de las cepas de *S. aureus* con una prevalencia de hasta el 50% en algunas áreas, lo que genera una carga social y económica por medio de enfermedades adquiridas en la comunidad e Infecciones asociadas a la asistencia sanitaria[231,232]. La gran incidencia y persistencia de este patógeno también se debe a su adaptabilidad y al vasto conjunto de mecanismos patogénicos y de supervivencia que presenta, un número importante de los cuales está controlado por el sistema de comunicación QS.

El QS en bacterias grampositivas se basa en la liberación y detección de oligopéptidos, que pueden diferir en la longitud, secuencia y estructura tridimensional entre las diferentes especies bacterianas[4]. En el caso de *S. aureus*, estos péptidos y todas las proteínas y factores necesarios para el sistema de comunicación (AgrB, AgrD, AgrC, AgrA) están codificados por el locus *agr* (*agrBDCA*), que contiene dos unidades de transcripción divergentes (efectora y reguladora de respuesta)[47]. La ruta biosintética de los AIP y la vía de señalización comienza con AgrD, correspondiente a la secuencia propeptídica del AIP. AgrD es procesado primero por la peptidasa de membrana AgrB, para generar un intermedio de tiolactona[48]. Este intermedio se exporta inmediatamente a través de la membrana y se somete a una segunda escisión para liberar el AIP maduro

al espacio extracelular. El AIP es la señal activa de la red de detección, que es detectada por un sistema de señalización clásico de dos componentes (TCS) que consiste en AgrC, el receptor de membrana histidina quinasa, y AgrA, el regulador de respuesta.

11.1.3 QS COMO DIANA DE DIAGNÓSTICO

La detección rápida y la identificación correcta de un microorganismo causante de una enfermedad en el contexto de un proceso infeccioso es crucial para un tratamiento adecuado. Sin embargo, la falta de métodos de diagnóstico in vitro rápidos y eficientes aprobados, capaces de proporcionar resultados fiables, ha llevado a la prescripción y al uso indebido de antibióticos de amplio espectro, contribuyendo a la generación de resistencias[17]. Los métodos diagnósticos de laboratorio actuales para la detección de ambos microorganismos se basan mayoritariamente en técnicas de cultivo estándar, que pueden tardar hasta 72 h en obtener resultados concluyentes. La espectrometría de masas, en particular MALDI-TOF-MS[52-54] y las herramientas de detección molecular, concretamente PCR[55-57], han surgido como un enfoque interesante para superar las desventajas del cultivo. Sin embargo, estos métodos normalmente requieren equipos específicos, personal altamente calificado y tediosas extracciones y / o pasos de purificación[59]. Una opción rápida, de bajo coste y fácil de usar sería el uso de dispositivos Point of Care (PoC) basados en el uso de elementos de biorreconocimiento[60,61] para detectar e identificar agentes bacterianos, lo que podría mejorar el desempeño de las técnicas estándar existentes, en términos de especificidad, sensibilidad y rapidez. En este contexto, las técnicas de biosensores proporcionan una gran versatilidad permitiendo el desarrollo de enfoques de biosensores ópticos y electroquímicos interesantes e innovadores que incorporan los últimos conocimientos en microelectrónica y nanobiotecnología. Sin embargo, un tema clave es la disponibilidad de biorreceptores de alta calidad que aborden el reconocimiento de objetivos de biomarcadores específicos apropiados relacionados con el microorganismo que causa la infección.

Recientemente, el Quorum Sensing bacteriano (QS) ha atraído la atención como un objetivo interesante para desarrollar enfoques terapéuticos y de diagnóstico innovadores[62-66]. Este sistema de comunicación intercelular basado en la

densidad de población podría servir no solo para la estrategia de identificación de patógenos, sino también para proporcionar información importante sobre la etapa de la enfermedad y / o virulencia de la cepa causante debido a su estrecha relación con la aptitud bacteriana y los estados patógenos.

Las moléculas de señalización QS se liberan al espacio extracelular con fines de comunicación y regulación. Por tanto, cuando el patógeno se encuentra dentro del huésped y por su naturaleza química, estas moléculas pueden encontrarse en el tejido infectado y en varios fluidos corporales[63,67-69]. Como resultado, los AI podrían potencialmente funcionar como biomarcadores de infección, proporcionando información relevante y ayudando a los médicos en el proceso de toma de decisiones para una mejor gestión de los pacientes. Se han desarrollado muchas técnicas para la cuantificación de varias moléculas de QS en muestras clínicas o cultivos bacterianos, principalmente por LC-MS[70-74], que apuntan al valor potencial de estas moléculas como biomarcadores de infección. Sin embargo, un gran inconveniente de estas técnicas es la necesidad de un tratamiento previo de la muestra o preconcentración para detectar y cuantificar estas moléculas, lo que hace que el procedimiento sea complejo y difícil para la implementación en la rutina de análisis clínicos. Además, existe el riesgo de degradación o pérdida de los analitos de interés. Como alternativa, las técnicas inmunoquímicas ofrecen la ventaja de poder cuantificar biomarcadores a niveles de concentración muy bajos directamente en muestras clínicas o medios de cultivo sin necesidad de pasos previos de extracción, preconcentración o purificación. Esto se debe a la alta afinidad y especificidad de los anticuerpos utilizados como elementos de biorreconocimiento. Los anticuerpos son moléculas excepcionales para este propósito, pero las moléculas pequeñas no provocan una respuesta inmune y, por lo tanto, a veces son difíciles de obtener. Este es el caso de las moléculas QS de las bacterias aquí discutidas y el punto de partida de esta tesis.

11.2 OBJETIVOS

El objetivo final del proyecto era mejorar el diagnóstico de infecciones causadas por *P. aeruginosa* y *S. aureus* mediante una mejor comprensión del proceso de comunicación bacteriana conocido como Quorum Sensing (QS) y su implicación

en la patogénesis. Con este fin, el objetivo general se basó en el desarrollo de métodos inmunoquímicos para perfilar la expresión de diferentes moléculas de señalización QS, como herramientas para investigar los mecanismos implicados en la patogénesis de *S. aureus* y *P. aeruginosa* y también para evaluar el papel potencial de estas moléculas como biomarcadores de infección. Para lograr este fin, se abordaron los siguientes objetivos específicos:

1. Diseño y síntesis de haptenos para las moléculas QS no inmunogénicas producidas por *P. aeruginosa* (2-heptil-4-quinolona (HHQ), 2-heptil-3-hidroxi- (1H)-4-quinolona (PQS) y 2-heptil-4-hidroxiquinolina N-óxido (HQNO)) y *S. aureus* (AIP-I a IV).

2. Síntesis de bioconjugados y generación de anticuerpos policlonales específicos contra las moléculas QS de las dos bacterias patógenas antes mencionadas.

3. Desarrollo de herramientas de análisis inmunoquímico para la cuantificación de estas moléculas del QS bacteriano.

4. Investigar el potencial de una posible plataforma multiplexada que contenga los diferentes reactivos inmunoquímicos generados previamente para el estudio del QS.

5. Realización de estudios preliminares sobre el valor potencial de las moléculas QS diana seleccionadas como biomarcadores de infección utilizando las herramientas de análisis inmunoquímico desarrolladas.

11.3 ESTRUCTURA DEL RESUMEN

La estructura del resumen, incluyendo el contenido de cada capítulo se muestra en Figure 11.1. Los apartados del mismo están precedidos de una introducción general del QS en los diferentes tipos de bacterias estudiadas en esta tesis y los objetivos de la misma. Los capítulos 3 y 8 de la tesis se han suprimido en el resumen ya que se trata de capítulos introductorios bibliográficos. Los apartados 11.4.1 a 11.4.3 detallarán las técnicas inmunoquímicas desarrolladas para la

cuantificación de moléculas QS de *P. aeruginosa*. El apartado 11.4.4 describe la estrategia inmunoquímica para la cuantificación de AIP-IV, utilizada como modelo para el desarrollo futuro de herramientas analíticas para la cuantificación del resto de AIPs de *S. aureus*. Finalmente, en el apartado 11.5 se recogen todas las conclusiones de la tesis.

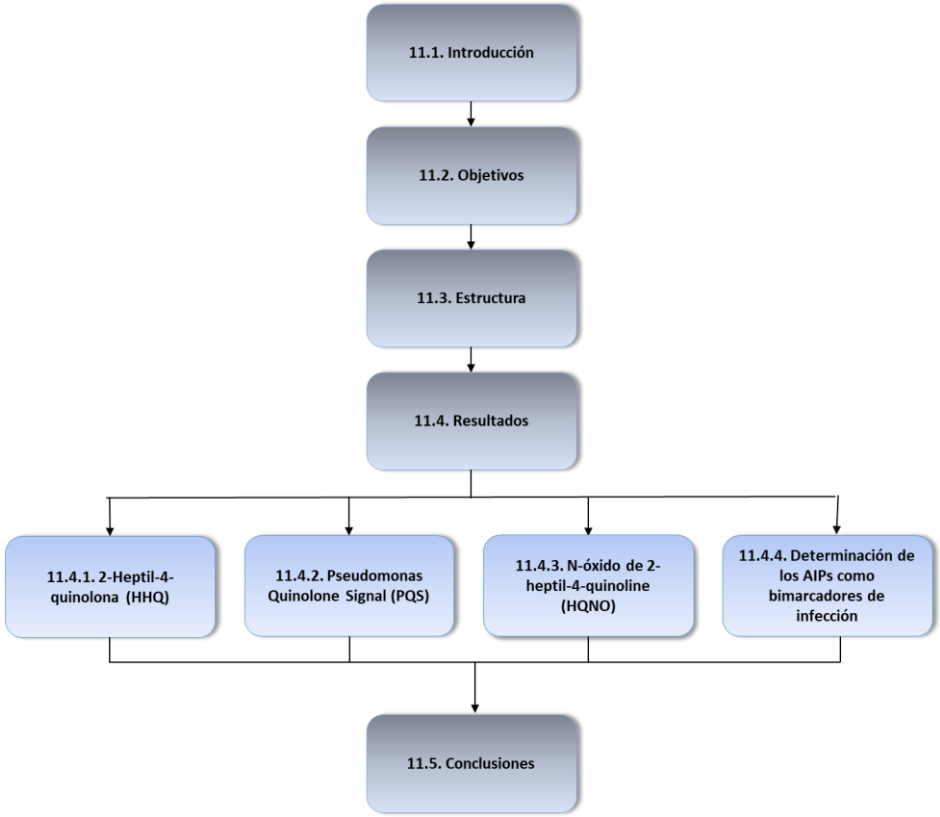

Figure 11.1. Estructura del resumen en relación a los distintos apartados, basado a su vez en la estructura de la tesis presentada en inglés.

11.4 RESULTADOS

11.4.1 2-HEPTIL-4-QUINOLONA (HHQ)

En el sistema *pqs* QS de *P. aeruginosa*, la 2-heptil-4-quinolona o HHQ es el precursor inmediato de la principal molécula de señalización, PQS. Sin embargo, la HHQ tiene un papel importante en varios procesos biológicos y en la comunicación de este patógeno, pudiendo activar el activador transcripcional PqsR y tomar el control del proceso de señalización en determinadas circunstancias. Podría tener una gran relevancia en entornos anaeróbicos, como el moco espeso de los pacientes con FQ, donde la producción de PQS se reduce debido al requerimiento de oxígeno molecular y, por lo tanto, HHQ estaría a cargo del sistema de comunicación basado en quinolonas y la regulación de los genes correspondientes.

A día de hoy, la importancia de HHQ en la patogénesis y su significancia clínica n se ha comprendido por completo y, por lo tanto, es necesario realizar estudios sobre el potencial de esta molécula como biomarcador de infección. Por otro lado, aún se requiere el desarrollo de nuevas técnicas que faciliten la evaluación de HHQ durante estos procesos infecciosos. Por este motivo, en este apartado se describirá el desarrollo de un método inmunoquímico para la cuantificación de HHQ y su implementación para la medición de aislados clínicos de *P. aeruginosa.*

Los anticuerpos son moléculas clave en las tecnologías de diagnóstico inmunoquímico. Sus características determinan el rendimiento de la técnica bioanalítica resultante. Para el caso de moléculas pequeñas no inmunogénicas, como las moléculas del QS de tipo alquilquinolona, las características de los anticuerpos están muy determinadas por el hapteno de inmunización utilizado para generar anticuerpos. La estructura química del hapteno tiene un gran impacto en la afinidad y especificidad de los anticuerpos producidos y, por tanto, en la detectabilidad y selectividad de la técnica inmunoquímica.

En el caso de HHQ, se pensó que la conservación del anillo de 4-piridona con la cadena de alquilo de 7 carbonos en la posición C-2 proporcionaba los epítopos necesarios para establecer las interacciones antes mencionadas (Figure 11.2).

Para ello, para maximizar la exposición de estos epítopos, se diseñó un hapteno de inmunización con un brazo espaciador en la posición C-6 de la estructura de quinolona provisto de un grupo tiol para su conjugación con una biomacromolécula inmunogénica. La estrategia sintética para lograr el hapteno de HHQ se inspiró en el procedimiento previamente informado de Reen et al[179]. Finalmente, el hapteno deseado se pudo obtener en ocho etapas sintéticas, con un rendimiento global del 26%.

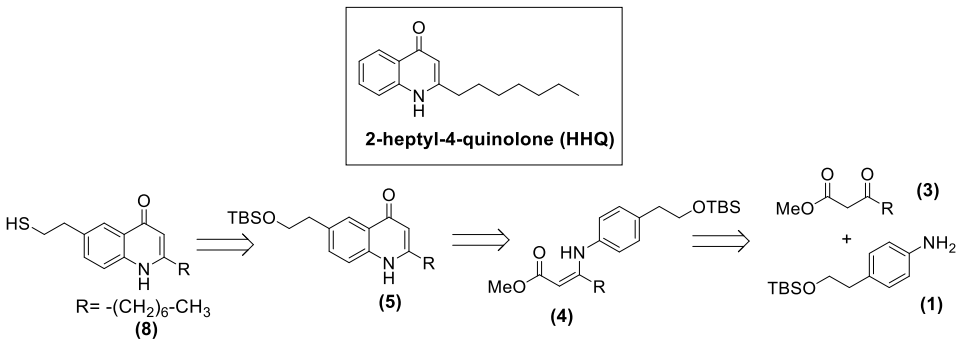

Figure 11.2. Esquema retrosintético para la síntesis de hapteno HHQ **(8)**, análogo a la molécula de detección del quórum de 2-heptil-4-quinolona (HHQ) del sistema *pqs* de *P. aeruginosa*. El hapteno se sintetizó a través de una ruta de cinco pasos a partir de 4-(2-((terc-butildimetilsilil)oxi)etil)-anilina **(1)** y 3-oxodecanoato de metilo **(3)**.

La conjugación del hapteno (8) con BSA y HCH se llevó a cabo utilizando yodoacetato de succinimidilo como enlazador heterobifuncional mediante un procedimiento de dos pasos. Posteriormente, HHQ-HCH se usó para generar anticuerpos policlonales (As382, As383 y As384) en conejos blancos de Nueva Zelanda después de la aplicación de procedimientos de inmunización estandarizados.

La avidez de los antisueros obtenidos para los conjugados de BSA (HHQ-BSA y PQS-BSA) se evaluó mediante experimentos de titración bidimensionales y la capacidad de HHQ para competir y mediante experimentos combinados que comparan la absorbancia del ensayo en presencia y ausencia del analito. PQS-BSA y HQNO-BSA (cuya obtención se describirá en los siguientes apartados) se incorporaron en estos estudios con la expectativa de mejorar la detectabilidad debido a la heterología del hapteno. Finalmente, As382 / PQS-BSA fue seleccionado para una evaluación adicional de su desempeño en diferentes

condiciones físico-químicas, en las cuales no se observó una variación significativa de las características del ensayo cuando se evaluó el efecto del tiempo, el pH, la fuerza iónica o la concentración del tensioactivo no iónico. La caracterización analítica del ensayo se realizó evaluando el rendimiento en experimentos repetitivos realizados en diferentes días. En las condiciones establecidas, el ensayo ELISA As382/PQS-BSA en PBST fue capaz de detectar HHQ con un LOD of 0.34 ± 0.13 nM, una IC_{50} de 4.59 ±0.29 nM y un rango de trabajo situado entre 0.89 ± 0.21 y 22.80 ± 3.69 nM (Figure 11.3). La detectabilidad alcanzada es mayor que la obtenida por otras técnicas como los ensayos de bioreporters[163,164] o enfoques de detección electroquímica[169,170]. Con respecto a los métodos LC-MS/MS, el ELISA reportado en este trabajo permitió obtener una detectabilidad similar o superior sin incluir pasos adicionales de preconcentración. Por otro lado, se ha informado que las alquilquinolonas se liberan al medio de crecimiento del cultivo a niveles de concentración en el rango de µM[72,163,169]. Por lo tanto, la detectabilidad lograda por el ELISA de HHQ apuntó a altas posibilidades para la cuantificación de HHQ en cultivos bacterianos y la evaluación de la activación de QS en las primeras etapas del crecimiento bacteriano.

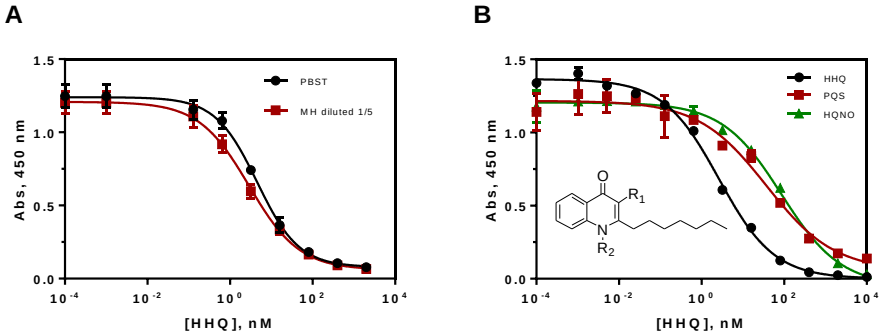

Figure 11.3. Gráfico A. Curvas de calibración del ELISA As382 / PQS-BSA para la detección de HHQ en buffer (PBST) y en caldo MH diluido 1/5, en las condiciones establecidas. **Gráfico B.** Curvas de calibración de los metabolitos pqs quórum sensing HHQ, PQS y HQNO en buffer, donde se puede observar el mayor reconocimiento del HHQ respecto a las otras dos alquilquinolonas.

La especificidad del método se evaluó teniendo en cuenta las principales moléculas efectoras del sistema *pqs* del QS de *P. aeruginosa*, que son HHQ, y otras dos alquilquinolonas, PQS y HQNO, con estructuras químicas muy similares (Figure 11.3). A pesar de las similitudes estructurales, PQS y HQNO reaccionaron

de forma cruzada solo al 7% (IC_{50} = 37 nM) y el 3% (IC_{50} = 86 nM), respectivamente, lo que indica una afinidad mucho mayor de los anticuerpos frente a HHQ que para las otras alquilquinolonas del sistema *pqs*.

Como estudio piloto, se evaluó el potencial del ELISA As382/PQS-BSA para el seguimiento de la producción de HHQ de aislados clínicos de *P. aeruginosa* cultivados en medio Müller-Hinton (MH). Sin embargo, en una primera instancia fue necesario evaluar el rendimiento del ensayo en muestras de caldo de cultivo. Las curvas de calibración se construyeron en medio MH a diferentes concentraciones y se midieron utilizando el ELISA desarrollado. Los experimentos de titración bidimensional realizados en MH diluido 1/5 permitieron corregir su efecto reajustando la concentración de los inmunorreactivos, permitiendo alcanzar una IC_{50} de 2.8 nM y un LOD de 0.17 nM en MH que corresponde a 14.25 nM y 0.85 nM, respectivamente, en el medio MH sin diluir, muy por debajo de las concentraciones reportadas en este tipo de muestras[72,163,164]. La precisión del ELISA As382/PQS-BSA en medio MH se evaluó midiendo muestras ciegas preparadas en MH y diluidas 5 veces con PBST. El coeficiente de correlación entre las concentraciones dopadas y medidas es excelente (R^2=0,999) y la pendiente de la regresión lineal es muy cercana a 1 (pendiente: 1,07), lo que indica una coincidencia casi perfecta de los valores medidos con respecto a las concentraciones dopadas (Figure 11.4).

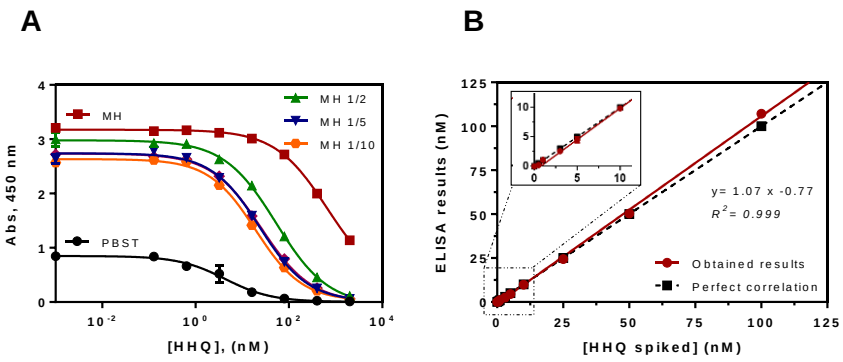

Figure 11.4. Gráfico A. Efecto matriz del caldo MH sin diluir y diluido 2, 5 y 10 veces con PBST en el ELISA As382 / PQS-BSA. Las curvas de calibración se ejecutaron utilizando las condiciones establecidas para el ensayo en PBST. La modificación de las condiciones del ensayo permitió lograr características de inmunoensayo similares a cuando el ensayo se realizó en tampón. **Gráfico B.** Resultados del estudio de precisión. El gráfico muestra el análisis de regresión lineal de la

concentración de caldo MH enriquecido con HHQ y la concentración medida con el ELISA As382/PQS-BSA.

Con estos resultados, se investigó la cinética de liberación de HHQ mediante el cultivo en medio MH de dos aislados clínicos bacterianos denominados PAAI6 y PACI6, obtenidos de dos pacientes diferentes diagnosticados de infecciones respiratorias por *P. aeruginosa*. En ambos casos, los perfiles de producción de HHQ medidos con el ELISA As382/PQS-BSA coincidieron muy bien con los perfiles de crecimiento correspondientes, basados en la medición de la absorbancia a λ=600 nm (OD_{600}), y las UFC calculadas. Sin embargo, se observaron diferencias significativas en el comportamiento de ambos aislados (Figure 11.5). Para el aislado PAAI6, se pudo detectar HHQ en los medios de cultivo después de 5 horas de cultivo. Por el contrario, los niveles medibles de HHQ para el aislado bacteriano PACI6 solo pudieron cuantificarse después de 12h de cultivo, aunque los niveles de concentración producidos por este último aislado a las 24 o 48 h fueron superiores a los del primero. Estos resultados apuntaron a la posibilidad de utilizar el ensayo aquí reportado no solo para diagnosticar la infección por *P. aeruginosa*, sino también para estratificar a los pacientes según la naturaleza de su infección (crónica o aguda) en función de los niveles de concentración de HHQ.

Con el objetivo de probar esta hipótesis, se analizaron aislados bacterianos clínicos adicionales de pacientes con distintas infecciones respiratorias e historias clínicas. Para simplificar y estandarizar el procedimiento, solo se realizaron medidas de punto final después de 8 horas de crecimiento en medio MH a 37ºC. Los aislados de *P. aeruginosa* de pacientes diagnosticados clínicamente de una infección aguda produjeron HHQ en concentraciones entre 0.5 y 2 µM en las condiciones antes mencionadas (Figure 11.5). Por el contrario, los procedentes de pacientes con infección crónica mostraron niveles de HHQ en el rango bajo de nM o por debajo del límite de detección.

Hasta ahora, la aplicabilidad de esta prueba ELISA solo se ha demostrado analizando medios de cultivo en los que se han desarrollado distintos aislados clínicos de *P. aeruginosa*. Se realizarán más estudios para detectar esta molécula del QS directamente en muestras clínicas como esputos con el fin de demostrar el potencial de esta técnica inmunoquímica para proporcionar datos de diagnóstico de una manera rápida y confiable con el fin de apoyar, evaluar y orientar a los médicos sobre el método más apropiado para manejo de infecciones causadas por *P. aeruginosa*.

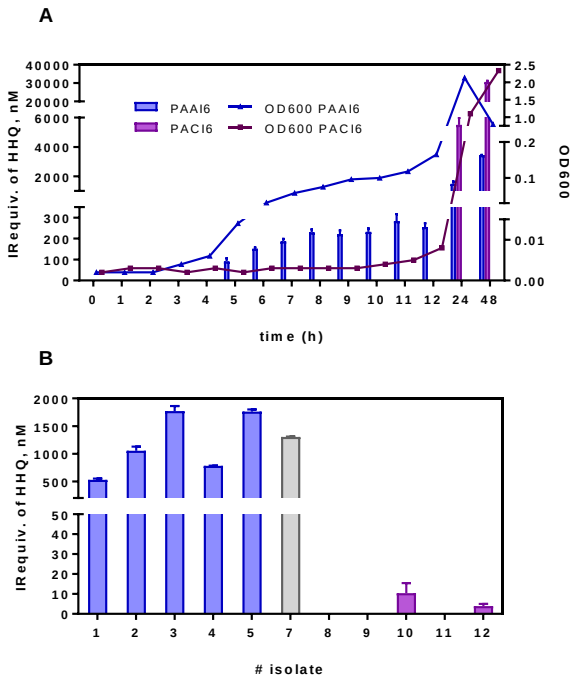

Figure 11.5. Gráfico A. Crecimiento bacteriano, expresado como equivalentes de inmunorreactividad de OD_{600} y HHQ (IRequiv) medidos en medio de caldo MH donde se cultivaron los aislados clínicos de *P. aeruginosa* PAAI6 y PACI6. Se tomaron muestras en los momentos seleccionados y se midieron usando el ELISA As382 / PQS-BSA. **Gráfico B.** HHQ IRequiv registrado a partir de una colección de aislados clínicos de pacientes con diferentes perfiles de infección. Las muestras se cultivaron en caldo MH durante 8 horas y las alícuotas tomadas se diluyeron 5 veces con PBST antes de los análisis ELISA. Los aislados clínicos 1-5 se obtuvieron de pacientes con infección aguda y los aislamientos 8-12 se obtuvieron de pacientes con infección crónica. El aislamiento número 7 corresponde a la cepa de referencia PAO1.

11.4.2 PSEUDOMONAS QUINOLONE SIGNAL (PQS)

Estudiar el QS es clave para comprender los procesos patogénicos. La principal molécula de señalización del sistema *pqs* QS de *P. aeruginosa*, 2-heptil-3-hidroxi-4-quinolona o Pseudomonas Quinolone Signal (PQS), ha sido ampliamente estudiada. Sus múltiples funciones biológicas además de su actividad de señalización y regulación la convierten en un interesante tema de estudio. Además, se ha demostrado que la PQS es específica de *P. aeruginosa* y, por tanto, se puede destacar su potencial como biomarcador de infección. El desarrollo de una herramienta de diagnóstico capaz de confirmar la presencia de esta bacteria

mediante la medición de PQS podría ser un enfoque interesante que debería investigarse más a fondo. Además, si somos capaces de cuantificar y comparar los niveles de moléculas de señalización con diferentes funciones biológicas (por ejemplo, HHQ y PQS), podríamos obtener información valiosa sobre, por ejemplo, la virulencia de una cepa patógena específica, el tipo de infección o el estado de la enfermedad. Eventualmente, esta información podría ayudar a los médicos en el proceso de toma de decisiones para un mejor manejo de los pacientes infectados.

El anillo de quinolona y el grupo catecol característico de la estructura nativa de PQS se consideraron los epítopos más importantes, con capacidad para establecer interacciones no covalentes entre el anticuerpo y el hapteno o analito. Por lo tanto, se diseñó un hapteno de inmunización que incorpora un brazo espaciador en la posición C-6, promoviendo la exposición de la parte de la molécula que contiene estos grupos funcionales (Figure 11.6). El extremo del brazo espaciador se funcionalizó con un ácido carboxílico, que eventualmente permitió la conjugación del hapteno con los residuos de lisina de una proteína inmunogénica mediante el uso de química ortogonal (éster activo, mezcla de anhídrido, etc.)[187]. La síntesis del hapteno PQS se inspiró en una estrategia previamente descrita por Pesci y colaboradores[151], basada en dos modificaciones secuenciales en la posición C-3 del precursor biológico PQS, HHQ. En general, el hapteno PQS propuesto **(13)** se obtuvo en cinco pasos sintéticos con un rendimiento global del 16%.

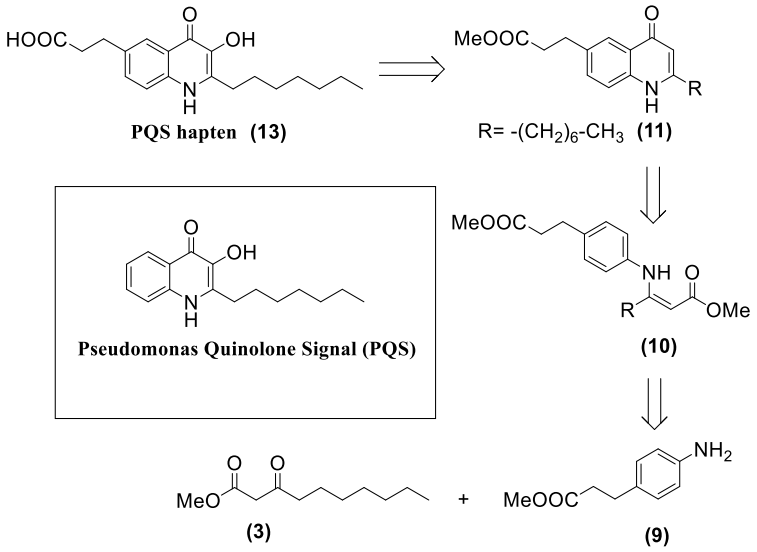

Figure 11.6. Esquema retrosintético para la síntesis del hapteno PQS **(8)**, análogo a la molécula de detección de quórum de 2-heptil-3-hidroxi-4-(1H)-quinolona (PQS) del sistema *pqs* de *P. aeruginosa*. El hapteno se sintetizó mediante una ruta de cinco pasos a partir del ácido 3-(4-aminofenil)propanoico y el 3-oxodecanoato de metilo.

El hapteno PQS se utilizó para preparar bioconjugados de proteínas KLH y BSA siguiendo el método del anhídrido mixto. Este método se basa en la activación del ácido carboxílico utilizando un cloroformiato y una base estéricamente impedida, formando un anhídrido que luego reacciona con los residuos de lisina presentes en la proteína[190]. Se obtuvieron bioconjugados de hapteno con una alta relación de densidad como se demostró por MALDI-TOF-MS y análisis de fluorescencia, el último realizado gracias a la banda de emisión de PQS y el correspondiente hapteno **(13)** a 445 nm al utilizar una longitud de onda de excitación de 340 nm.

La avidez del As obtenido para los conjugados de BSA (HHQ-BSA, PQS-BSA y HQNO-BSA) y la competencia de PQS por la unión a los anticuerpos se evaluó mediante experimentos combinados comparando la absorbancia del ensayo en presencia y ausencia del analito y, tras una selección preliminar, se analizaron las combinaciones más prometedoras mediante experimentos de titración bidimensionales.

Finalmente, se seleccionó As385/HHQ-BSA para evaluar el rendimiento del ensayo en diferentes condiciones físico-químicas con el objetivo de mejorar la

detectabilidad y las características analíticas. Se evaluó el rendimiento del ensayo bajo diferentes condiciones fisicoquímicas como el efecto del tiempo, pH, concentración de un surfactante no iónico, fuerza iónica o presencia de un solvente orgánico. En estos ensayos se observó una mejora sustancial de la señal cuando no se añadió Tween 20 al tampón de ensayo. Sin embargo, dado que se sabe que la presencia de una pequeña cantidad de Tween 20 ayuda a minimizar las interacciones inespecíficas y a solubilizar el analito, se decidió mantener una concentración de solo 0.01%. La caracterización analítica del ensayo se realizó evaluando el rendimiento en experimentos repetitivos realizados en diferentes días. En las condiciones seleccionadas, el ensayo en tampón (PBST-EDTA) mostró un LOD de 0.17 ± 0.01 nM y un rango dinámico comprendido entre 0.53 ± 0.04 y 24.37 ± 3.18 nM (Figure 11.7). Para una caracterización analítica completa del ELISA As385/HHQ-BSA, se calculó el CV utilizando la absorbancia normalizada para cada una de las concentraciones de la curva de calibración, tal como se realizó para el ELISA HHQ presentado en el apartado anterior.

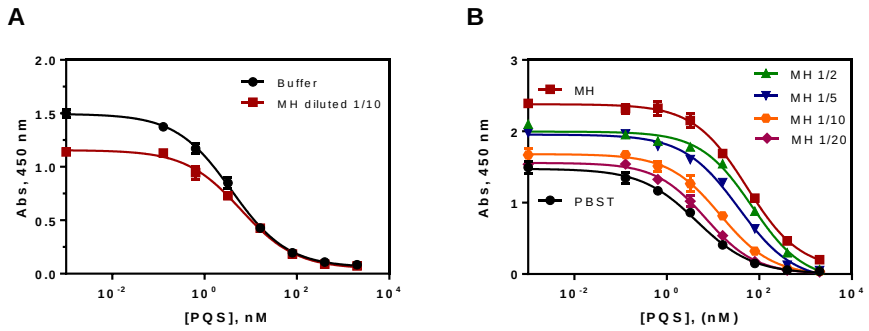

Figure 11.7. Gráfico A. Curvas de calibración del ELISA As385 / HHQ-BSA para la detección de PQS en buffer (PBST-EDTA) y en caldo MH diluido 1/10, en las condiciones establecidas. **Gráfico B.** Efecto matriz del caldo MH sin diluir y diluido 2, 5, 10 y 20 veces con PBST en el ELISA As385 / HHQ-BSA. Las curvas de calibración se ejecutaron utilizando las condiciones establecidas para el ensayo en PBST. La modificación de las condiciones del ensayo permitió lograr características de inmunoensayo similares a cuando el ensayo se realizó en tampón.

La única diferencia estructural entre HHQ, HQNO y PQS es una posición oxidada (C-3 o N-1), por lo que se tuvo que evaluar el patrón de reconocimiento por el ELISA As385/HHQ-BSA. A pesar de la similitud entre las diferentes moléculas, el porcentaje de reactividad cruzada fue inferior al 2% para HQNO (IC_{50} = 236.2 nM) y aproximadamente 13% en el caso de HHQ (IC_{50} = 27.2 nM).

Como en el caso del ensayo HHQ, el ELISA se utilizó para evaluar el perfil de liberación de PQS en muestras de cultivo donde se cultivó *P. aeruginosa*, como estudio piloto. Se llevaron a cabo experimentos de titración bidimensional utilizando medio MH diluido 10 veces con el tampón de ensayo para establecer nuevas condiciones de ensayo con respecto a la concentración de inmunorreactivos. El ensayo realizado en MH diluido 1/10 proporcionó muy buenas características en un rango similar a las obtenidas en tampón. El valor de IC_{50} fue de 6.05 ± 0.16 nM mientras que el LOD obtenido fue de 0.36 ± 0.14 nM, que tomando en cuenta el factor de dilución se convertiría en 60.5 ± 1.6 nM y 3.6 ± 1.4 nM, respectivamente (Figure 11.7).

La exactitud del ensayo se evaluó mediante la preparación de muestras ciegas dopadas en caldo de cultivo MH y midiéndolas con el ELISA desarrollado. Sorprendentemente, los resultados mostraron una subestimación crítica de las concentraciones elevadas de PQS. La curva de calibración se corrigió en presencia de diferentes concentraciones de ácido etilendiaminotetraacético (EDTA), un poderoso quelante de iones capaz de desplazar la complejación de cationes divalentes por PQS (Figure 11.8).

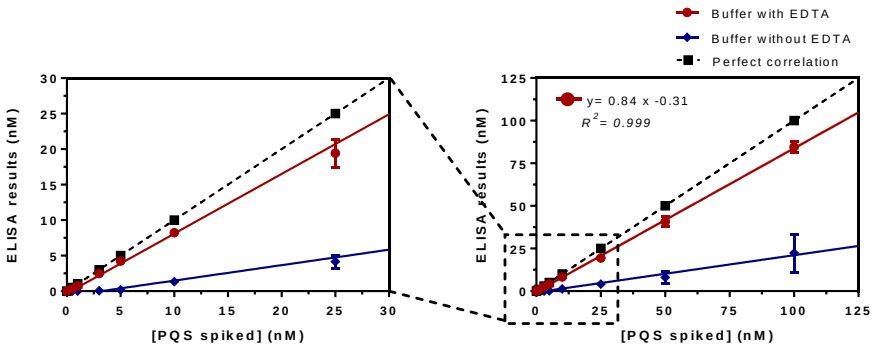

Figure 11.8. Resultados del estudio de precisión. El gráfico muestra el análisis de regresión lineal de la concentración dopada con PQS en medio MH y la concentración medida con el ELISA As385/HHQ-BSA. Los ensayos se realizaron en medio de cultivo MH diluido 1/10 usando PBST (línea azul) y PBST-EDTA (línea roja).

La implementación del ensayo se llevó a cabo a través de un primer conjunto de experimentos dirigidos a averiguar el perfil de producción de PQS del crecimiento de aislados clínicos en medio de caldo MH. Por este motivo, se abordaron experimentos con los aislados PAAI6 y PACI6, obtenidos de pacientes

con infección aguda y crónica de las vías respiratorias por *P. aeruginosa*, respectivamente, para averiguar si se mantenía el mismo perfil para la molécula principal del sistema *pqs* QS, PQS

Se encontraron niveles significativos de concentración de PQS en los medios de cultivo de aislamientos pertenecientes a pacientes con infección aguda o crónica. En el primer grupo (pacientes 1-5), los valores de concentración de PQS estaban en el rango entre 0.5 y 3 µM, mientras que para el segundo grupo (8-12) los valores de PQS estaban en el rango bajo nM o por debajo del LOD en estas condiciones (Figure 11.9). A la luz de este resultado, parece claro que la concentración de moléculas QS liberadas a los medios puede correlacionarse con el tipo de infección o el estado de enfermedad del paciente. Los bajos niveles de PQS liberados por los aislados de pacientes infectados crónicos justificarían una posible menor producción de factores de virulencia. Desde una perspectiva diagnóstica, además de identificar los microorganismos causantes de la enfermedad, es muy relevante poder distinguir entre una infección crónica o una aguda, para aplicar estrategias terapéuticas adecuadas y mejorar el manejo de la enfermedad. En ese sentido, los anticuerpos producidos para PQS, HHQ y los ELISA reportados por primera vez en esta tesis, aparecen como herramientas poderosas para mejorar sustancialmente el diagnóstico de infecciones pulmonares y su manejo. Así, hemos demostrado la posibilidad de utilizar el ELISA en microplaca para identificar *P. aeruginosa* en medios de cultivo basados en la detección de moléculas específicas de QS, que podrían contemplarse como biomarcadores de infección.

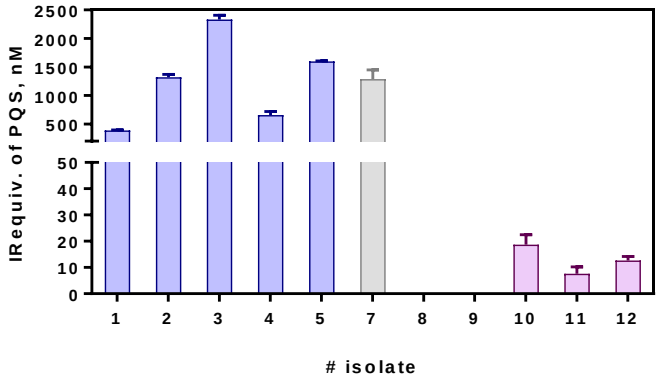

Figure 11.9. PQS IRequiv registrado a partir de una colección de aislados clínicos de pacientes con diferentes perfiles clínicos. Las muestras se cultivaron en medio MH durante 8 horas y las alícuotas tomadas se diluyeron 10 veces con PBST-EDTA antes de los análisis ELISA. Los aislamientos clínicos 1-5 se obtuvieron de pacientes con infección aguda y los aislamientos 8-12 se obtuvieron de pacientes con infección crónica. El aislamiento número 7 corresponde a la cepa de referencia PAO1.

11.4.3 N-ÓXIDO DE 2-HEPTIL-4-QUINOLINA (HQNO)

P. aeruginosa produce una gran cantidad de factores de virulencia que son armas clave durante los procesos de patogénesis. La importancia de estos factores está fuera de discusión y, sin embargo, el significado biológico y clínico completo de todos ellos está lejos de ser conocido. Entre todos los factores de virulencia relevantes producidos por este patógeno es posible encontrar HQNO, un metabolito secundario controlado por el QS y producido por el sistema *pqs* de *P. aeruginosa*, sin implicación en la red de señalización, aunque se ha demostrado que HQNO tiene una amplia implicación sobre las habilidades anti-estafilocócicas de *P. aeruginosa*. Esta molécula inhibe la respiración oxidativa al interferir con la cadena de transporte de electrones y la producción de HQNO es uno de los principales mecanismos que lleva a cabo este patógeno para subyugar a *S. aureus* y que persista como variantes de colonia pequeña (SCV). También provoca la lisis celular y la liberación de ADN, favoreciendo la formación de biopelículas. En conjunto, las funciones del HQNO, su papel durante la patogénesis y la importancia clínica podrían estudiarse más a fondo si se desarrollan métodos y técnicas apropiados para su cuantificación. Con este objetivo, en este apartado se describe el primer análisis inmunoquímico de HQNO, que incluye la síntesis de

un hapteno de inmunización y la producción de anticuerpos policlonales altamente específicos.

El hapteno HQNO se diseñó para conservar los grupos funcionales y las posiciones N-1 y C-2 a C-4 inalteradas con respecto al metabolito HQNO original. Se consideró que estas posiciones contienen los epítopos más reactivos y característicos que establecerán las interacciones no covalentes fuertes y específicas requeridas con los anticuerpos producidos. El brazo espaciador del hapteno se colocó en C-6, maximizando así el reconocimiento de los epítopos más reactivos y alterando mínimamente la estructura electrónica de la molécula original. El brazo espaciador fue provisto de un ácido carboxílico que permitió la bioconjugación a los residuos de lisina de la proteína mediante el uso de química ortogonal. La estrategia sintética se llevó a cabo siguiendo el procedimiento experimental descrito por Woschek et al[193] (Figure 11.10).

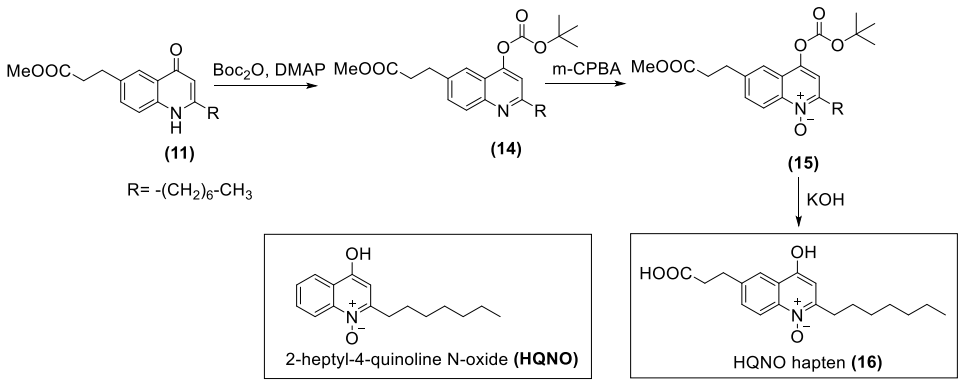

Figure 11.10. Esquema sintético para la síntesis de hapteno HQNO **(16)**, análogo al N-óxido de 2-heptil-4-quinolina del sistema *pqs* de *P. aeruginosa*. El hapteno se sintetizó mediante una ruta sintética de tres pasos a partir de 3- (2-heptil-4-oxo-1,4-dihidroquinolin-6-il) propanoato de metilo.

La diferencia radica en el material de partida 3- (2-heptil-4-oxo-1,4-dihidroquinolin-6-il) propanoato de metilo **(11)**, sintetizado en un estudio previo a partir de un β-cetoéster y un derivado de anilina que contiene un ácido carboxílico, que se protegió como éster metílico y se mantuvo hasta el último paso de la estrategia sintética. Finalmente, el hapteno HQNO **(16)** se obtuvo con rendimiento global de las tres etapas sintéticas del 62%. La bioconjugación del hapteno **(16)** se realizó mediante el método mixto de anhídrido, basado en la generación de un anhídrido a partir del ácido carboxílico presente en el hapteno mediante el uso de un cloroformiato y una base impedida.

La avidez de las diluciones de As obtenidas hacia los conjugados BSA (HQNO-BSA, HHQ-BSA y PQS-BSA) y se evaluó mediante experimentos ELISA indirectos bidimensionales no competitivos para el establecimiento de las condiciones más adecuadas para el desarrollo de ensayos competitivos. Como resultado de esos experimentos, la combinación seleccionada para el desarrollo del ensayo competitivo fue As389 /HHQ-BSA.

Se estudiaron varios parámetros fisicoquímicos como el pH, la fuerza iónica, la concentración de un tensioactivo no iónico, la presencia de disolvente orgánico y el efecto del tiempo y se evaluó el rendimiento del ensayo. El ensayo funcionó bien entre pH 5.5 y 6.5 y las mejores características se obtuvieron cuando no había tensioactivo presente en el tampón del ensayo, observándose una dramática disminución de detectabilidad cuando se usaba Tween 20. Los parámetros que mostraron una mejora se evaluaron nuevamente por separado y en conjunto para evaluar si el efecto fue lo suficientemente significativo.

En las condiciones establecidas en el estudio de parámetros fisicoquímicos, el ELISA As389/HHQ-BSA fue capaz de detectar HQNO con un LOD de 0.27 ± 0.09 nM, IC_{50} de 4.20 ± 0.86 nM y un rango dinámico comprendido entre 0.72 ± 0.18 a 26.71 ± 0.96 nM (Figure 11.11). También se calculó el coeficiente de variación usando un método diferente al de los ensayos HHQ y PQS pero para las mismas tres situaciones: la variabilidad entre réplicas en la misma placa (variación intraplaca), la variabilidad asociada con la medición en diferentes placas (variación entre placas) y la variabilidad al medir la muestra tres días diferentes en placas diferentes (variación entre días).

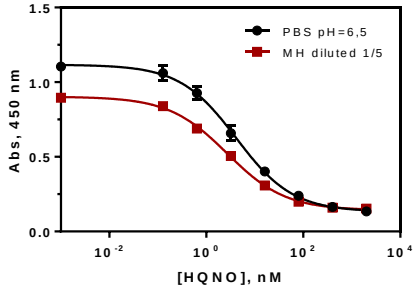

	PBST	MH diluted 1/5
A_{min}	0.09 ± 0.04	0.09 ± 0.02
A_{max}	1.08 ± 0.06	0.85 ± 0.01
Slope	-0.75 ± 0.04	-0.72 ± 0.06
IC_{50}	4.20 ± 0.86	2.71 ± 0.04
Dynamic Range	0.72 ± 0.18 to 26.71 ± 0.96	0.41 ± 0.10 to 17.04 ± 1.08
LOD	0.27 ± 0.09	0.15 ± 0.05
R^2	0.987 ± 0.013	0.990 ± 0.004

Figure 11.11. Curvas de calibración y características analíticas del ELISA As389/HHQ-BSA para la detección de HQNO efectuado en PBS-6.5 y MH diluido 1/5 en las condiciones establecidas. Los

parámetros y características de la curva MH 1/5 corresponden y se refieren a los valores en la muestra diluida.

Por otro lado, se evaluó la especificidad del ELISA As389 / HHQ-BSA frente a las tres quinolonas (HHQ, PQS y HQNO) en las condiciones seleccionadas después de la optimización. Como era de esperar, el ELISA As389/HQNO-BSA mostró mayor afinidad por HQNO, obteniendo porcentajes de reactividad cruzada (CR) alrededor del 7% para PQS y 19% para HHQ. Presumiblemente, la alta CR con HHQ podría ser causada por la posición C-3 común no funcionalizada del núcleo de quinolona, que actúa como un epítopo importante y es crucial para el reconocimiento (Figure 11.12).

En estudios anteriores investigamos el potencial de otros ensayos inmunoquímicos para el seguimiento de la producción de moléculas de señalización (HHQ y PQS) secretadas por *P. aeruginosa* en cultivos bacterianos. En este caso particular, nuestro objetivo fue investigar si la cinética de producción y la cantidad total de HQNO, un factor de virulencia relevante para este patógeno sin implicación en la señalización, seguían una tendencia similar a la de las moléculas de señalización. Sin embargo, las posibles interferencias inespecíficas en esta compleja matriz biológica debían evaluarse previamente.

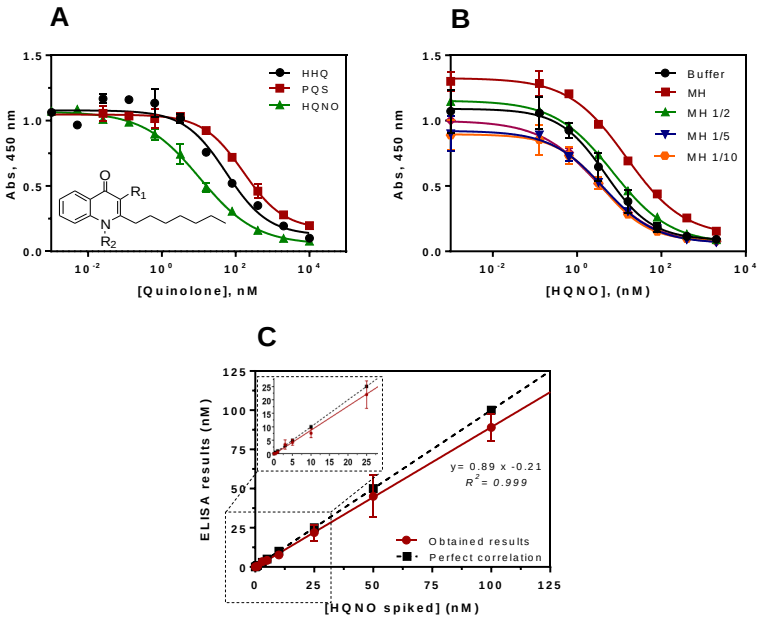

Figure 11.12. Gráfico A. Estudio de reactividad cruzada utilizando los metabolitos de detección de quórum *pqs* HHQ, PQS y HQNO en tampón en las condiciones antes mencionadas para ELISA As389/HHQ-BSA. **Gráfico B.** Efecto matriz del medio MH sin diluir y diluido 2, 5, 10 y 20 veces con PBST en el ELISA As389 / HHQ-BSA. **Gráfico C.** Resultados del estudio de precisión. El gráfico muestra el análisis de regresión lineal de la concentración enriquecida con HQNO en caldo MH y la concentración medida con el ELISA As389 / HHQ-BSA.

Las curvas de calibración se construyeron y midieron en tampón PBS-6.5 y MH a diferentes concentraciones. El efecto matriz disminuyó cuando se utilizó un factor de dilución más alto y, para no comprometer la detectabilidad, se seleccionó una dilución 1/5 (Figure 11.12). La detectabilidad lograda fue comparable e incluso mejor a la del ensayo realizado en buffer, obteniendo un LOD de 0.15 ± 0.05 nM y un valor de IC_{50} de 2.71 ± 0.04 nM, que teniendo en cuenta el factor de dilución se convierte en 0.75 ± 0.25 nM y 13,55 ± 0,20 nM, respectivamente. La precisión del ELISA As389/HQNO-BSA en MH diluido 1/5 se evaluó mediante la preparación de 9 muestras ciegas dopadas en tres días diferentes con concentraciones de HQNO dentro y fuera del rango dinámico.

En los apartados anteriores se ha demostrado que las moléculas de señalización como HHQ y PQS podrían usarse potencialmente para diferenciar entre pacientes que sufren una enfermedad crónica o aguda. No obstante, se pretendió demostrar si un factor de virulencia como HQNO, muy implicado en la

interacción entre especies, también podía estratificar a los pacientes con diferente gravedad de infección de las vías respiratorias por *P. aeruginosa*. En primer lugar, se estudió la cinética de producción de HQNO en dos cepas clínicas (PAAI6 y PACI6), provenientes de un paciente infectado agudo y uno crónico, durante un período de 48 horas. Posteriormente, se cultivó un mayor número de aislados clínicos en las mismas condiciones experimentales, pero extrayendo una alícuota del caldo de cultivo a las 8 horas y midiendo con el ELISA As389/HQNO-BSA. Los resultados obtenidos mostraron una diferencia sustancial en la producción de HQNO entre los grupos de estudio seleccionados. La concentración para los aislados obtenidos de pacientes con infección aguda (1-5) estuvo entre 1-4 µM mientras que para el segundo grupo (8-12) la concentración máxima detectada fue 20 nM (Figure 11.13).

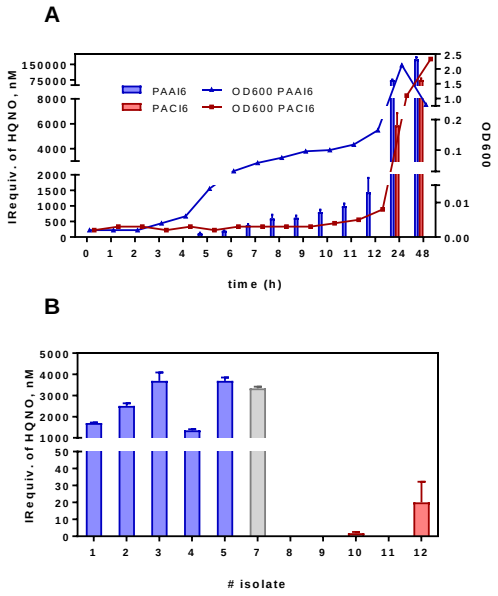

Figure 11.13. Gráfico A. Crecimiento bacteriano, expresado como equivalentes de inmunorreactividad (IRequiv) de HQNO y OD_{600} medidos en medio MH, donde se cultivaron los aislados clínicos de *P. aeruginosa* PAAI6 y PACI6. Las muestras se tomaron en los momentos seleccionados y se midieron usando el ELISA As389 / HHQ-BSA. **Gráfico B.** HQNO IRequiv registrado a partir de una colección de aislamientos clínicos de pacientes con diferentes perfiles. Las muestras se cultivaron en caldo MH durante 8 horas y las alícuotas tomadas se diluyeron 5 veces con PBS-6.5 antes de los análisis ELISA. Los aislamientos clínicos 1-5 se obtuvieron de pacientes sometidos a infección aguda y los aislamientos 8-12 se obtuvieron de pacientes sometidos a infección crónica. El aislamiento número 7 corresponde a la cepa de referencia PAO1.

Aunque los resultados deben confirmarse con un mayor número de aislados, parece que las moléculas del QS y los factores de virulencia controlados por la red QS podrían servir para la estratificación y el diagnóstico complementario de las infecciones por *P. aeruginosa*. El QS y los metabolitos relacionados y los factores de virulencia podrían proporcionar mucha más información sobre el estadio y la progresión de la enfermedad y, posteriormente, ser relevantes para estudiar la patogénesis de la infección por *P. aeruginosa*. De igual manera, se ha demostrado el potencial de la herramienta inmunoquímica desarrollada en este trabajo para la diferenciación entre pacientes que sufren un proceso infeccioso agudo o crónico y pudiendo ayudar en el ámbito clínico y en el manejo/tratamiento de los pacientes que sufren infección por este patógeno.

11.4.4 DETERMINACIÓN DE LOS AIPS COMO BIOMARCADORES DE INFECCIÓN: UNA ESTRATEGIA INMUNOQUÍMICA

Los AIP producidos por *S. aureus* difieren en longitud de cadena, secuencia de aminoácidos y estructura tridimensional, proporcionando suficiente especificidad biológica e inhibiendo de forma cruzada la activación de *agr* en la mayoría de combinaciones heterólogas. La mayor similitud se encuentra entre AIP-I y AIP-IV, que solo difieren en un aminoácido y, sin embargo, es suficiente ver especificidad hacia sus receptores (AgrC-I o AgrC-IV).

En cuanto a la detección analítica de AIPs, se pensó que el establecimiento de una estrategia utilizando uno de ellos como modelo sería suficiente para posteriormente extender el método al resto de estas moléculas de señalización. El AIP-IV fue seleccionado en estudios previos llevados a cabo por Park y colaboradores para generar anticuerpos monoclonales y usarlos como agentes terapéuticos[224]. En este trabajo se utilizó una estructura de hapteno heterólogo, sustituyendo el ciclo de tiolactona de la molécula por un anillo de lactona más estable y así, con solo cambiar un átomo con respecto al AIP nativo obtener anticuerpos específicos sin problemas de estabilidad durante el proceso de inmunización. Siguiendo este enfoque, en el presente capítulo se describirá una estrategia inmunoquímica en la que se sintetizaron dos haptenos diferentes, uno como estructura homóloga a AIP-IV (anillo de tiolactona), y otra estructura heteróloga (formada por un anillo de lactama). Con este enfoque, buscamos comparar la avidez hacia AIP-IV de anticuerpos producidos con un hapteno de la

misma estructura química del AIP, pero con una estabilidad comprometida, y con la de anticuerpos producidos con una estructura de hapteno más estable, pero heterólogo y diferente al utilizado por Park y colaboradores. Sin embargo, es posible que el hapteno diseñado por Park con ciclo de lactona no esté exento de la hidrólisis, como señalaron Debler et al[225], quienes sintetizaron haptenos de lactama para la producción de anticuerpos contra otras moléculas del QS.

Por tanto, de acuerdo con la inestabilidad potencial de un posible hapteno de tiolactona AIP-IV, se propuso sintetizar un derivado de hapteno de lactama. Sin embargo, fue necesario evaluar previamente el impacto de la sustitución del átomo de azufre de la estructura del AIP nativo por un nitrógeno en las propiedades electrónicas y estructurales del hapteno final. El confórmero de energía mínima para la tiolactona AIP-IV y la lactama AIP-IV se calculó usando Mecánica Molecular MM + seguido de un método PM3 semi-empírico. Como resultado de los cálculos teóricos, se decidió sintetizar dos haptenos diferentes con el objetivo de establecer la mejor estrategia para la producción de anticuerpos AIP. Por un lado, se diseñó una síntesis de un derivado de AIP heterólogo y más estable formado por un anillo de lactama (AIP4NH). Por otro lado, se buscó una síntesis de un hapteno homólogo (AIP4S) que realmente reproduzca las propiedades electrónicas y estructurales del péptido nativo (Figure 11.14).

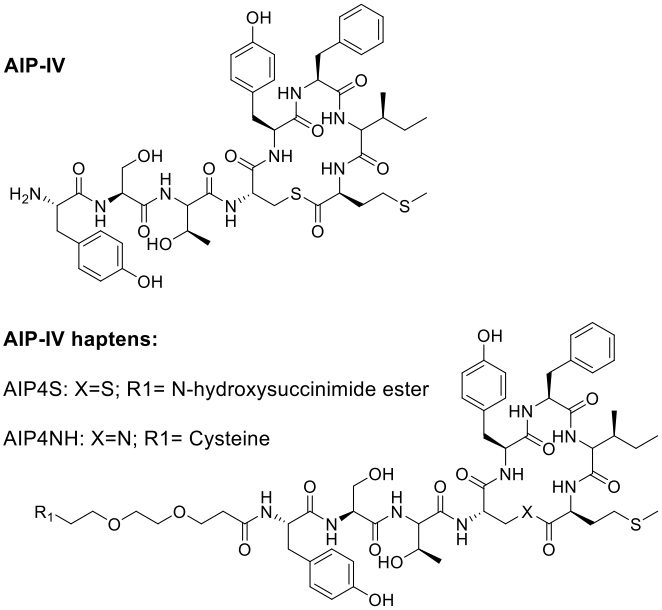

Figure 11.14. Estructura química de la molécula de detección de quórum de *S. aureus* AIP-IV y los derivados de hapteno AIP4S y AIP4NH sintetizados en este trabajo que fueron bioconjugados e inmunizados para la producción de anticuerpos y el desarrollo de ELISA.

A partir de este punto, fue necesario introducir un brazo espaciador en la estructura AIP-IV para la posterior bioconjugación a la proteína inmunogénica. Por tanto, el brazo espaciador fue introducido por el residuo de tirosina N-terminal, exponiendo la mayor parte de la estructura y los epítopos característicos de AIP-IV. Se decidió utilizar dos unidades de etilenglicol como conector entre el AIP-IV y el sitio de reacción para la bioconjugación, mejorando la hidrofilicidad del compuesto y minimizando la antigenicidad del brazo espaciador. La bioconjugación del hapteno AIP4NH se llevó a cabo mediante un procedimiento de conjugación de dos pasos usando SIA y la conjugación del hapteno AIP4S se realizó mediante reacción directa de proteína/hapteno mediante la adición nucleofílica de los grupos amino de proteína de los residuos de lisina con el resto éster de succinimida del hapteno.

Finalmente, se generaron antisueros contra AIP4NH-HCH (As376, As377 y As378) y AIP4S-HCH (As379, As380 y As381) por triplicado en conejos blancos hembras de Nueva Zelanda. La avidez de los antisueros obtenidos contra los antígenos competidores homólogos y heterólogos (conjugados BSA) se evaluó mediante experimentos de titración bidimensionales a partir de los cuales se seleccionaron

las condiciones más apropiadas para los ensayos competitivos. El As380, obtenido por inmunización con el derivado de tiolactona conjugado AIP4S-HCH, proporcionó una detectabilidad sustancialmente mayor que los antisueros obtenidos con el derivado de anillo de lactama.

En general, no se observó una mejora significativa de las características del ensayo cuando se evaluaron las mejores condiciones en conjunto, por lo que la composición del tampón en el paso competitivo se mantuvo en condiciones estándar de PBST. Las características analíticas del ensayo realizado en tampón proporcionaron un valor de IC_{50} de 2.90 ± 0.19 nM y un LOD de 0.22 ± 0.06 nM. Dado que los diferentes AIP podrían coexistir en las muestras a analizar en el futuro, era importante evaluar las posibles interferencias cruzadas provocadas por otras AIP producidas por *S. aureus*, obteniendo una reactividad cruzada menor al 0.01% para cada uno de ellos (Figure 11.15).

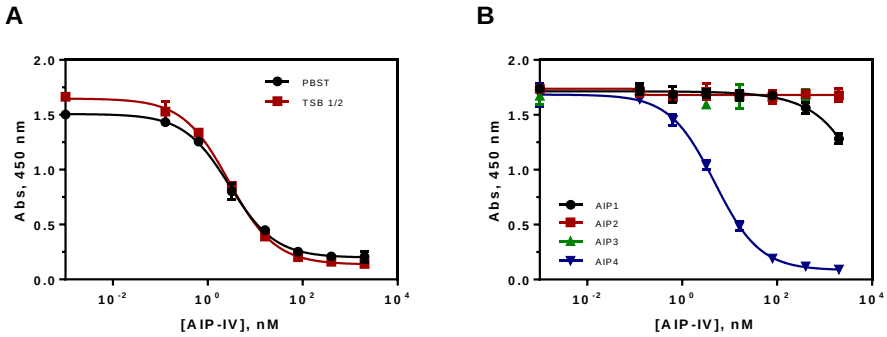

Figure 11.15. Gráfico A. Curvas de calibración del ELISA As380/AIP4S-BSA para la detección de AIP-IV en tampón (PBST) y TSB diluido 1/2 bajo diferentes condiciones de conjugado BSA y dilución As. **Gráfico B.** Estudio de reactividad cruzada utilizando las moléculas de detección de quórum de todos los tipos de sistemas *agr* producidos por *S. aureus* en las condiciones antes mencionadas para ELISA As380/AIP4S-BSA. La reactividad cruzada calculada fue inferior al 0.01% para AIP-I a III.

Como estudio piloto, se buscó comparar la producción de AIP entre diferentes aislados clínicos caracterizados en cultivos bacterianos. Permitiría estudiar el perfil de producción de AIP-IV y al mismo tiempo demostrar la implementación de nuestro ensayo utilizando muestras biológicas complejas. Por lo tanto, el primer paso fue evaluar el efecto matriz causado por la medida en un medio biológico complejo como el medio tríptico de soja (TSB), normalmente utilizado para el crecimiento de cepas de *S. aureus* y compuesto por una mezcla de proteínas digeridas, azúcares y sales.

La curva de calibración se efectuó en TSB y diluciones del mismo utilizando el tampón de ensayo, en las condiciones previamente desarrolladas para el ELISA As380/AIP4S-BSA. Como se puede observar, la medida se vio muy afectada cuando se mide directamente en TSB. Sin embargo, usando una dilución ½ con el correspondiente buffer el efecto matriz desaparece casi por completo. Cuanto más diluimos la matriz, más similar es la curva a la realizada en buffer. Dado no se describe un rango de concentraciones para AIP-IV producido por *S. aureus* en placa de cultivo, se decidió realizar la curva de calibración en matriz diluida ½, cuyas características analíticas principales fueron una IC_{50} y LOD de 2.80 ± 0.17 y 0.19 ± 0.06 nM, que se convertirían en 5.60 ± 0.34 y 0.38 ± 0.12 nM teniendo en cuenta la dilución. La precisión del ensayo se evaluó mediante la preparación de 9 muestras ciegas enriquecidas en TSB tres días diferentes y midiendo con el ELISA desarrollado. Para evaluar la cuantificación del ensayo, se decidió preparar varias concentraciones dentro y fuera del rango de trabajo (Figure 11.16).

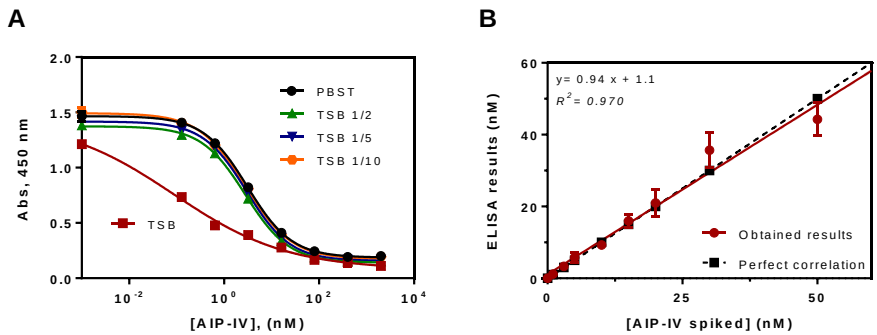

Figure 11.16. Gráfico A. Curvas de calibración del ensayo indirecto competitivo As380/AIP4S-BSA ELISA realizado en tampón PBST, medio de cultivo TSB o diluciones de TSB usando tampón. **Gráfico B.** Representación de la concentración de AIP-IV dopadas frente a la concentración medida con el ELISA de As380/AIP4S-BSA. Los ensayos se realizaron en medio de cultivo TSB diluido diluido a la mitad usando PBST.

Se seleccionaron varias cepas clínicas con el objetivo de perfilar la liberación de la molécula de señalización AIP-IV. También se pretendía evaluar la variabilidad entre cepas productoras de *agr-IV* que causan diferentes tipos de infección de las vías respiratorias. Se seleccionaron cepas con diferente sistema *agr* para probar la especificidad de la técnica desarrollada para la cuantificación de AIP-IV, incluidas dos cepas de referencia (Newman y USA300).

En cuanto a las medidas de ELISA, no se observaron concentraciones detectables de AIP-IV para cepas que presentan diferente sistema *agr*, demostrando la posibilidad de tipificar el sistema *agr* y la especificidad de los anticuerpos producidos en este trabajo. Al comparar las concentraciones y el perfil de producción en cepas *agr-IV*, podemos observar una cantidad total similar de AIP-IV producida por las cepas 48 y 165 en el rango alto de nM (Figure 11.17).

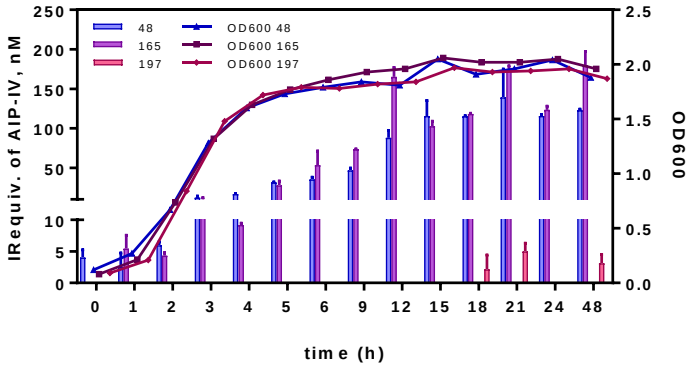

Figure 11.17. Equivalentes de inmunorreactividad (IR) de AIP-IV y OD_{600} medidos en muestras de crecimiento de cultivo de aislamientos clínicos de *S. aureus* 48, 165 y 197 en los momentos seleccionados utilizando el ELISA As380/AIP4S-BSA desarrollado.

11.5 CONCLUSIONES

- **Conclusión general:** Se ha demostrado que moléculas de QS específicas de bacterias patógenas importantes, como *P. aeruginosa* y *S. aureus*, pueden detectarse y cuantificarse en muestras biológicas complejas mediante métodos inmunoquímicos. Esto es posible, a pesar del bajo peso molecular de las moléculas, si se producen anticuerpos con las características necesarias de avidez y especificidad. Estos hechos están determinados en gran medida por la estructura química diseñada para el hapteno de inmunización. Aunque es necesario realizar más análisis clínicos, los resultados obtenidos en esta tesis apuntan al potencial de las moléculas de QS como biomarcadores de infección.

Pseudomonas aeruginosa:

- En esta tesis se han desarrollado por primera vez antisueros policlonales que muestran una alta avidez por las moléculas de señalización del sistema *pqs* de *P. aeruginosa* (2-heptil-4-quinolona (HHQ), 2-heptil-3-hidroxi-(1H)-4-quinolona (PQS) y N-óxido de 2-heptil-4-hidroxiquinolina (HQNO)). A pesar de su bajo peso molecular, ha sido posible generar una respuesta inmune gracias a la síntesis química de haptenos y bioconjugados adecuadamente diseñados.

- Los estudios realizados han demostrado que HHQ, PQS y HQNO pueden detectarse y cuantificarse específicamente en el rango bajo nM (LODs 0.34 ± 0.13 (HHQ), 0.17 ± 0.01 (PQS) y 0.27 ± 0.09 nM (HQNO)). La detectabilidad lograda en todos los ELISA está por debajo del rango de concentraciones encontradas en cultivos bacterianos que están en el mismo rango que los valores encontrados en muestras clínicas como el esputo, lo que apuntaba al valor potencial de esta tecnología para ser utilizadas con fines de diagnóstico clínico.

- El diseño de estructuras químicas de los haptenos dirigidas a maximizar el reconocimiento de los epítopos más importantes y específicos de las moléculas diana ha sido un factor clave para el logro de este objetivo. Por lo tanto, a pesar de las similitudes estructurales entre los tres metabolitos objeto de esta investigación. Los anticuerpos generados demostraron una mayor afinidad frente a sus respectivas moléculas, lo que permitirá diferenciarlos en muestras biológicas donde los tres podrían estar presentes.

- Existe un gran potencial de poder implementar los ELISA desarrollados en esta tesis en el diagnóstico de infecciones por *P. aeruginosa*. Aunque deben realizarse más estudios, los resultados obtenidos de un pequeño estudio piloto muestran que la reactividad inmunoquímica QS AQ medida en medios de cultivo donde crecieron los aislados bacterianos obtenidos de pacientes infectados pueden correlacionarse con los tipos de infección y / o la gravedad. Esto se evidencia por las diferencias significativas encontradas en los IR equiv. de HHQ, PQS y HQNO registrados al medir medios de cultivo en los que habían crecido aislados clínicos de bacterias obtenidos de pacientes con infecciones crónicas o agudas. Además, los IR equiv. se pudieron medir después de solo 5 h de cultivo para los aislados clínicos obtenidos de pacientes agudos. Por el

contrario, los IR equiv. sólo pudieron medirse después de un mínimo de 12 h de crecimiento si el aislado clínico bacteriano se obtuvo de un paciente con una infección crónica. Tal observación se corroboró analizando un número discreto de aislados clínicos bacterianos pertenecientes a estos dos grupos, después de 8 h de crecimiento en medio MH.

Staphylococcus aureus:

- El grupo tiolactona de los péptidos cíclicos AIP-IV fue un epítopo importante para el reconocimiento de anticuerpos según los estudios realizados en esta tesis. Por tanto, la avidez de los anticuerpos producidos contra un hapteno peptídico cíclico que conserva este grupo funcional (AIP4S) fue mayor que los producidos contra un hapteno con una lactama (AIP4NH). Este último hapteno fue sintetizado para superar el riesgo de la potencial hidrólisis de la tiolactona durante el proceso de bioconjugación o inmunización. Sin embargo, los resultados obtenidos apuntan a la estabilidad parcial del grupo tiolactona en base a las propiedades superiores de los anticuerpos producidos usando AIP4S en comparación con los obtenidos contra el hapteno AIP4NH. El hapteno AIP4S contenía el ciclo de tiolactona original que se encuentra en AIP-IV y reproducía exactamente la configuración electrónica de la molécula QS nativa, mientras que el hapteno AIP4NH fue diseñado para imitar el AIP-IV tanto como fuera posible (solo difería un átomo del original AIP) pero con una mayor estabilidad frente a una posible hidrólisis. Esta es la primera vez que se producen anticuerpos contra los AIP de *Staphylococcus aureus* utilizando un hapteno que conserva el grupo tiolactona.

- El AIP-IV de *S. aureus* se pudo detectar en el rango bajo nM (LOD 0.22 ± 0.06 nM) con los anticuerpos producidos en un ELISA competitivo basado en microplaca, una detectabilidad superior a otros métodos reportados basados en el uso de LC-MS, y muy por debajo de los valores de concentración que se han reportado que liberan estas bacterias en los medios de cultivo.

- Los anticuerpos producidos contra AIP4S-HCH mostraron mayor especificidad por AIP-IV con respecto a cualquier otro AIP producido por este patógeno, a pesar de la gran homología de sus estructuras químicas y secuencias de

aminoácidos, particularmente en el caso de AIP-I, que difiere en tan solo aminoácido.

- Los resultados de nuestra investigación demuestran que existe un gran potencial para usar los AIP de *S. aureus* como biomarcadores de infección. De ahí que la alta detectabilidad y especificidad de los anticuerpos producidos hayan permitido utilizar el ELISA desarrollado para realizar un pequeño estudio piloto clínico, en el que se ha podido cuantificar AIP-IV en el medio de cultivo tras poco menos de 1 h de crecimiento. Se realizarán más estudios para investigar si la detección directa de estos péptidos también es posible en muestras clínicas.

- El perfil de especificidad de los anticuerpos AIP-IV y el ELISA desarrollado en esta tesis apunta a la posibilidad de utilizarlos no solo para el diagnóstico sino también para el fenotipado de la cepa patógena. Por lo tanto, mientras que los IR equiv. de AIP-IV se midieron en medio de cultivo donde crecieron las cepas de tipo agr-IV, no se registró ninguna señal en el medio de cultivo de otras cepas de distinto *agr*.

12 BIBLIOGRAPHY

1 Nealson, K. H., Platt, T. & Hastings, J. W. Cellular control of the synthesis and activity of the bacterial luminescent system. *J Bacteriol* **104**, 313-322 (1970).

2 Eberhard, A. B., A. L.; Eberhard, C.; Kenyon, G. L.; Nealson, K. H.; Oppenheimer, N. J. Structural identification of autoinducer of Photobacterium fischeri luciferase. *Biochemistry* **20(9)**, 2444-2449 (1981).

3 Turan, N. B., Chormey, D. S., Büyükpınar, Ç., Engin, G. O. & Bakirdere, S. Quorum sensing: Little talks for an effective bacterial coordination. *TrAC Trends in Analytical Chemistry* **91**, 1-11, doi:10.1016/j.trac.2017.03.007 (2017).

4 Rutherford, S. T. & Bassler, B. L. Bacterial quorum sensing: its role in virulence and possibilities for its control. *Cold Spring Harb Perspect Med* **2**, doi:10.1101/cshperspect.a012427 (2012).

5 Papenfort, K. & Bassler, B. L. Quorum sensing signal-response systems in Gram-negative bacteria. *Nat Rev Microbiol* **14**, 576-588, doi:10.1038/nrmicro.2016.89 (2016).

6 Cigana, C., Lore, N. I., Bernardini, M. L. & Bragonzi, A. Dampening Host Sensing and Avoiding Recognition in Pseudomonas aeruginosa Pneumonia. *J Biomed Biotechnol* **2011**, 852513, doi:10.1155/2011/852513 (2011).

7 Horcajada, J. P. *et al.* Epidemiology and Treatment of Multidrug-Resistant and Extensively Drug-Resistant Pseudomonas aeruginosa Infections. *Clin Microbiol Rev* **32**, doi:10.1128/CMR.00031-19 (2019).

8 Lipuma, J. J. The changing microbial epidemiology in cystic fibrosis. *Clin Microbiol Rev* **23**, 299-323, doi:10.1128/CMR.00068-09 (2010).

9 Valentini, M., Gonzalez, D., Mavridou, D. A. & Filloux, A. Lifestyle transitions and adaptive pathogenesis of Pseudomonas aeruginosa. *Curr Opin Microbiol* **41**, 15-20, doi:10.1016/j.mib.2017.11.006 (2018).

10 CDC. Antibiotic Resistance Threats in The United States 2019. (Atlanta, GA, 2019).

11 Kaier, K., Heister, T., Gotting, T., Wolkewitz, M. & Mutters, N. T. Measuring the in-hospital costs of Pseudomonas aeruginosa pneumonia: methodology and results from a German teaching hospital. *BMC Infect Dis* **19**, 1028, doi:10.1186/s12879-019-4660-5 (2019).

12 Qu, J., Huang, Y. & Lv, X. Crisis of Antimicrobial Resistance in China: Now and the Future. *Front Microbiol* **10**, 2240, doi:10.3389/fmicb.2019.02240 (2019).

13 Wozniak, T. M., Bailey, E. J. & Graves, N. Health and economic burden of antimicrobial-resistant infections in Australian hospitals: a population-based model. *Infect Control Hosp Epidemiol* **40**, 320-327, doi:10.1017/ice.2019.2 (2019).

14 Centers for Disease Control and Prevention, N. C. f. E. a. Z. I. D. N., Division of Healthcare Quality Promotion (DHQP). Biggest Threats and Data: 2019 AR Threats Report. (2019, Last update June 18, 2020).

15 E. Tacconelli, E. C., A. Savoldi, D. Kattula, F. Burkert. Global priority list of antibiotic-resistant bacteria to guide research, discovery and development of new antibiotics. *WHO* (2017).

16 Parkins, M. D., Somayaji, R. & Waters, V. J. Epidemiology, Biology, and Impact of Clonal Pseudomonas aeruginosa Infections in Cystic Fibrosis. *Clin Microbiol Rev* **31**, doi:10.1128/CMR.00019-18 (2018).

17 Pang, Z., Raudonis, R., Glick, B. R., Lin, T. J. & Cheng, Z. Antibiotic resistance in Pseudomonas aeruginosa: mechanisms and alternative therapeutic strategies. *Biotechnol Adv* **37**, 177-192, doi:10.1016/j.biotechadv.2018.11.013 (2019).

18 Murphy, T. F. Vaccines for Nontypeable Haemophilus influenzae: the Future Is Now. *Clin Vaccine Immunol* **22**, 459-466, doi:10.1128/CVI.00089-15 (2015).

19 Waters, B. & Muscedere, J. A 2015 Update on Ventilator-Associated Pneumonia: New Insights on Its Prevention, Diagnosis, and Treatment. *Curr Infect Dis Rep* **17**, 496, doi:10.1007/s11908-015-0496-3 (2015).

20 Fleitas Martinez, O. *et al.* Interference With Quorum-Sensing Signal Biosynthesis as a Promising Therapeutic Strategy Against Multidrug-Resistant Pathogens. *Front Cell Infect Microbiol* **8**, 444, doi:10.3389/fcimb.2018.00444 (2018).

21 Wen, K. Y. *et al.* A Cell-Free Biosensor for Detecting Quorum Sensing Molecules in P. aeruginosa-Infected Respiratory Samples. *ACS Synth Biol* **6**, 2293-2301, doi:10.1021/acssynbio.7b00219 (2017).

22 Lee, J. & Zhang, L. The hierarchy quorum sensing network in Pseudomonas aeruginosa. *Protein Cell* **6**, 26-41, doi:10.1007/s13238-014-0100-x (2015).

23 Pesci, E. C., Pearson, J. P., Seed, P. C. & Iglewski, B. H. Regulation of las and rhl quorum sensing in Pseudomonas aeruginosa. *J Bacteriol* **179**, 3127-3132, doi:10.1128/jb.179.10.3127-3132.1997 (1997).

24 Seed, P. C., Passador, L. & Iglewski, B. H. Activation of the Pseudomonas aeruginosa lasI gene by LasR and the Pseudomonas autoinducer PAI: an autoinduction regulatory hierarchy. *J Bacteriol* **177**, 654-659, doi:10.1128/jb.177.3.654-659.1995 (1995).

25 Lin, J., Cheng, J., Wang, Y. & Shen, X. The Pseudomonas Quinolone Signal (PQS): Not Just for Quorum Sensing Anymore. *Front Cell Infect Microbiol* **8**, 230, doi:10.3389/fcimb.2018.00230 (2018).

26 Ha, D. G. *et al.* 2-Heptyl-4-quinolone, a precursor of the Pseudomonas quinolone signal molecule, modulates swarming motility in Pseudomonas aeruginosa. *J Bacteriol* **193**, 6770-6780, doi:10.1128/JB.05929-11 (2011).

27 Lee, J. *et al.* A cell-cell communication signal integrates quorum sensing and stress response. *Nat Chem Biol* **9**, 339-343, doi:10.1038/nchembio.1225 (2013).

28 Kiratisin, P., Tucker, K. D. & Passador, L. LasR, a transcriptional activator of Pseudomonas aeruginosa virulence genes, functions as a multimer. *J Bacteriol* **184**, 4912-4919, doi:10.1128/jb.184.17.4912-4919.2002 (2002).

29 McCready, A. R., Paczkowski, J. E., Henke, B. R. & Bassler, B. L. Structural determinants driving homoserine lactone ligand selection in the Pseudomonas aeruginosa LasR quorum-sensing receptor. *Proc Natl Acad Sci U S A* **116**, 245-254, doi:10.1073/pnas.1817239116 (2019).

30 Cao, H. *et al.* A quorum sensing-associated virulence gene of Pseudomonas aeruginosa encodes a LysR-like transcription regulator with a unique self-regulatory mechanism. *Proc Natl Acad Sci U S A* **98**, 14613-14618, doi:10.1073/pnas.251465298 (2001).

31 McKnight, S. L., Iglewski, B. H. & Pesci, E. C. The Pseudomonas quinolone signal regulates rhl quorum sensing in Pseudomonas aeruginosa. *J Bacteriol* **182**, 2702-2708, doi:10.1128/jb.182.10.2702-2708.2000 (2000).

32 Hoffman, L. R. *et al.* Pseudomonas aeruginosa lasR mutants are associated with cystic fibrosis lung disease progression. *Journal of Cystic Fibrosis* **8**, 66-70, doi:10.1016/j.jcf.2008.09.006 (2009).

33 Diggle, S. P. *et al.* The Pseudomonas aeruginosa quinolone signal molecule overcomes the cell density-dependency of the quorum sensing hierarchy, regulates rhl-dependent genes at the onset of stationary phase and can be produced in the absence of LasR. *Mol Microbiol* **50**, 29-43, doi:10.1046/j.1365-2958.2003.03672.x (2003).

34 Tong, S. Y., Davis, J. S., Eichenberger, E., Holland, T. L. & Fowler, V. G., Jr. Staphylococcus aureus infections: epidemiology, pathophysiology, clinical manifestations, and management. *Clin Microbiol Rev* **28**, 603-661, doi:10.1128/CMR.00134-14 (2015).

35 Weiner, L. M. *et al.* Antimicrobial-Resistant Pathogens Associated With Healthcare-Associated Infections: Summary of Data Reported to the National Healthcare Safety Network at the Centers for Disease Control and Prevention, 2011-2014. *Infect Control Hosp Epidemiol* **37**, 1288-1301, doi:10.1017/ice.2016.174 (2016).

36 Schwerdt, M. *et al.* Staphylococcus aureus in the airways of cystic fibrosis patients - A retrospective long-term study. *Int J Med Microbiol* **308**, 631-639, doi:10.1016/j.ijmm.2018.02.003 (2018).

37 Peacock, S. J. *et al.* Determinants of acquisition and carriage of Staphylococcus aureus in infancy. *J Clin Microbiol* **41**, 5718-5725, doi:10.1128/jcm.41.12.5718-5725.2003 (2003).

38 Esposito, S. *et al.* Antimicrobial Treatment of Staphylococcus aureus in Patients With Cystic Fibrosis. *Front Pharmacol* **10**, 849, doi:10.3389/fphar.2019.00849 (2019).

39 Kahl, B. C., Becker, K. & Loffler, B. Clinical Significance and Pathogenesis of Staphylococcal Small Colony Variants in Persistent Infections. *Clin Microbiol Rev* **29**, 401-427, doi:10.1128/CMR.00069-15 (2016).

40 Burns, J. L. & Rolain, J. M. Culture-based diagnostic microbiology in cystic fibrosis: can we simplify the complexity? *J Cyst Fibros* **13**, 1-9, doi:10.1016/j.jcf.2013.09.004 (2014).

41 Denis, O. Route of transmission of Staphylococcus aureu s. *The Lancet Infectious Diseases* **17**, 124-125, doi:10.1016/s1473-3099(16)30512-6 (2017).

42 Naorem, R. S., Urban, P., Goswami, G. & Fekete, C. Characterization of methicillin-resistant Staphylococcus aureus through genomics approach. *3 Biotech* **10**, 401, doi:10.1007/s13205-020-02387-y (2020).

43 (CDC), C. f. D. P. a. C. Antibiotic resistance threats in the United States. *U.S. Department of Health and Human Services*, doi:10.15620/cdc:82532 (2019).

44 Control, E. C. f. D. p. a. Antimicrobial resistance surveillance in Europe. (2014).

45 Rasigade, J. P., Dumitrescu, O. & Lina, G. New epidemiology of Staphylococcus aureus infections. *Clin Microbiol Infect* **20**, 587-588, doi:10.1111/1469-0691.12718 (2014).

46 van Belkum, A. & Rochas, O. Laboratory-Based and Point-of-Care Testing for MSSA/MRSA Detection in the Age of Whole Genome Sequencing. *Front Microbiol* **9**, 1437, doi:10.3389/fmicb.2018.01437 (2018).

47 Wang, B. & Muir, T. W. Regulation of Virulence in Staphylococcus aureus: Molecular Mechanisms and Remaining Puzzles. *Cell Chem Biol* **23**, 214-224, doi:10.1016/j.chembiol.2016.01.004 (2016).

48 Zhang, L. & Ji, G. Identification of a staphylococcal AgrB segment(s) responsible for group-specific processing of AgrD by gene swapping. *J Bacteriol* **186**, 6706-6713, doi:10.1128/JB.186.20.6706-6713.2004 (2004).

49 Srivastava, S. K., Rajasree, K., Fasim, A., Arakere, G. & Gopal, B. Influence of the AgrC-AgrA complex on the response time of Staphylococcus aureus quorum sensing. *J Bacteriol* **196**, 2876-2888, doi:10.1128/JB.01530-14 (2014).

50 WHO. GLOBAL PRIORITY LIST OF ANTIBIOTIC-RESISTANT BACTERIA TO GUIDE RESEARCH, DISCOVERY, AND DEVELOPMENT OF NEW ANTIBIOTICS. (last update 23th of May, 2020).

51 Burrows, L. L. The Therapeutic Pipeline for Pseudomonas aeruginosa Infections. *ACS Infect Dis* **4**, 1041-1047, doi:10.1021/acsinfecdis.8b00112 (2018).

52 Patel, R. MALDI-TOF MS for the diagnosis of infectious diseases. *Clin Chem* **61**, 100-111, doi:10.1373/clinchem.2014.221770 (2015).

53 Brockmann, E. U., Steil, D., Bauwens, A., Soltwisch, J. & Dreisewerd, K. Advanced Methods for MALDI-MS Imaging of the Chemical Communication in Microbial Communities. *Anal Chem* **91**, 15081-15089, doi:10.1021/acs.analchem.9b03772 (2019).

54 Huang, Y. L. *et al.* Evaluation of an in-house MALDI-TOF MS rapid diagnostic method for direct identification of micro-organisms from blood cultures. *J Med Microbiol* **68**, 41-47, doi:10.1099/jmm.0.000866 (2019).

55 Jung, J. Y. *et al.* Rapid oral bacteria detection based on real-time PCR for the forensic identification of saliva. *Sci Rep* **8**, 10852, doi:10.1038/s41598-018-29264-2 (2018).

56 Hamdan-Partida, A., González García, S. & Bustos-Martínez, J. Identificación de Staphylococcus aureus utilizando como marcadores los genes nucA y femB. *Ciencias Clínicas* **16**, 37-41, doi:10.1016/j.cc.2016.02.002 (2015).

57 Mason, W. J. *et al.* Multiplex PCR Protocol for the Diagnosis of Staphylococcal Infection. *Journal of Clinical Microbiology* **39**, 3332-3338, doi:10.1128/jcm.39.9.3332-3338.2001 (2001).

58 Bittar, F. & Rolain, J. M. Detection and accurate identification of new or emerging bacteria in cystic fibrosis patients. *Clinical Microbiology and Infection* **16**, 809-820, doi:10.1111/j.1469-0691.2010.03236.x (2010).

59 Maneg, D. *et al.* Advantages and Limitations of Direct PCR Amplification of Bacterial 16S-rDNA from Resected Heart Tissue or Swabs Followed by Direct Sequencing for Diagnosing Infective Endocarditis: A Retrospective Analysis in the Routine Clinical Setting. *Biomed Res Int* **2016**, 7923874, doi:10.1155/2016/7923874 (2016).

60 Chen, H., Liu, K., Li, Z. & Wang, P. Point of care testing for infectious diseases. *Clin Chim Acta* **493**, 138-147, doi:10.1016/j.cca.2019.03.008 (2019).

61 Reali, S. *et al.* Novel diagnostics for point-of-care bacterial detection and identification. *RSC Advances* **9**, 21486-21497, doi:10.1039/c9ra03118a (2019).

62 Brackman, G. C., T. Quorum Sensing Inhibitors as Anti-Biofilm Agents. *Curr. Pharm. Des.* **21**, 5-11 (2014).

63 Barr, H. L. *et al.* Diagnostic and prognostic significance of systemic alkyl quinolones for P. aeruginosa in cystic fibrosis: A longitudinal study. *J Cyst Fibros* **16**, 230-238, doi:10.1016/j.jcf.2016.10.005 (2017).

64 Fong, J. *et al.* Combination Therapy Strategy of Quorum Quenching Enzyme and Quorum Sensing Inhibitor in Suppressing Multiple Quorum Sensing Pathways of P. aeruginosa. *Sci Rep* **8**, 1155, doi:10.1038/s41598-018-19504-w (2018).

65 Lanni, E. J. *et al.* MALDI-guided SIMS: multiscale imaging of metabolites in bacterial biofilms. *Anal Chem* **86**, 9139-9145, doi:10.1021/ac5020222 (2014).

66 Rehman, Z. U. & Leiknes, T. Quorum-Quenching Bacteria Isolated From Red Sea Sediments Reduce Biofilm Formation by Pseudomonas aeruginosa. *Front Microbiol* **9**, 1354, doi:10.3389/fmicb.2018.01354 (2018).

67 Barr, H. L. *et al.* Pseudomonas aeruginosa quorum sensing molecules correlate with clinical status in cystic fibrosis. *Eur Respir J* **46**, 1046-1054, doi:10.1183/09031936.00225214 (2015).

68 Verbeke, F. *et al.* Peptides as Quorum Sensing Molecules: Measurement Techniques and Obtained Levels In vitro and In vivo. *Front Neurosci* **11**, 183, doi:10.3389/fnins.2017.00183 (2017).

69 Webb, K. *et al.* Clinical significance of Pseudomonas aeruginosa 2-alkyl-4-quinolone quorum-sensing signal molecules for long-term outcomes in adults with cystic fibrosis. *J Med Microbiol* **68**, 1823-1828, doi:10.1099/jmm.0.001099 (2019).

70 Abdalla, M. Y. *et al.* Pseudomonas Quinolone Signal Induces Oxidative Stress and Inhibits Heme Oxygenase-1 Expression in Lung Epithelial Cells. *Infect Immun* **85**, doi:10.1128/IAI.00176-17 (2017).

71 Kushwaha, M. *et al.* Establishment of LCMS Based Platform for Discovery of Quorum Sensing Inhibitors: Signal Detection in Pseudomonas aeruginosa PAO1. *ACS Chem Biol* **13**, 657-665, doi:10.1021/acschembio.7b00875 (2018).

72 Ortori, C. A. *et al.* Simultaneous quantitative profiling of N-acyl-L-homoserine lactone and 2-alkyl-4(1H)-quinolone families of quorum-sensing signaling molecules using LC-MS/MS. *Anal Bioanal Chem* **399**, 839-850, doi:10.1007/s00216-010-4341-0 (2011).

73 Kumari, A., Pasini, P. & Daunert, S. Detection of bacterial quorum sensing N-acyl homoserine lactones in clinical samples. *Anal Bioanal Chem* **391**, 1619-1627, doi:10.1007/s00216-008-2002-3 (2008).

74 Leipert, J., Treitz, C., Leippe, M. & Tholey, A. Identification and Quantification of N-Acyl Homoserine Lactones Involved in Bacterial Communication by Small-Scale Synthesis of

Internal Standards and Matrix-Assisted Laser Desorption/Ionization Mass Spectrometry. *J Am Soc Mass Spectrom* **28**, 2538-2547, doi:10.1007/s13361-017-1777-x (2017).

75 Martinez-Sagasti, F., Velasco-Lopez, E., Domingo-Marin, S. & Gil-Perdomo, J. M. Usefulness of biomarkers on infection management: with or without them? *Rev Esp Quimioter* **31 Suppl 1**, 43-46 (2018).

76 Mohan, A. & Harikrishna, J. Biomarkers for the diagnosis of bacterial infections: in pursuit of the 'Holy Grail'. *Indian J Med Res* **141**, 271-273, doi:10.4103/0971-5916.156551 (2015).

77 Winsor, G. L. *et al.* Pseudomonas Genome Database: improved comparative analysis and population genomics capability for Pseudomonas genomes. *Nucleic Acids Res* **39**, D596-600, doi:10.1093/nar/gkq869 (2011).

78 Ilangovan, A. *et al.* Structural basis for native agonist and synthetic inhibitor recognition by the Pseudomonas aeruginosa quorum sensing regulator PqsR (MvfR). *PLoS Pathog* **9**, e1003508, doi:10.1371/journal.ppat.1003508 (2013).

79 Lepine, F., Milot, S., Deziel, E., He, J. & Rahme, L. G. Electrospray/mass spectrometric identification and analysis of 4-hydroxy-2-alkylquinolines (HAQs) produced by Pseudomonas aeruginosa. *J Am Soc Mass Spectrom* **15**, 862-869, doi:10.1016/j.jasms.2004.02.012 (2004).

80 Farrow, J. M., 3rd & Pesci, E. C. Two distinct pathways supply anthranilate as a precursor of the Pseudomonas quinolone signal. *J Bacteriol* **189**, 3425-3433, doi:10.1128/JB.00209-07 (2007).

81 Palmer, G. C., Jorth, P. A. & Whiteley, M. The role of two Pseudomonas aeruginosa anthranilate synthases in tryptophan and quorum signal production. *Microbiology* **159**, 959-969, doi:10.1099/mic.0.063065-0 (2013).

82 Coleman, J. P. *et al.* Pseudomonas aeruginosa PqsA is an anthranilate-coenzyme A ligase. *J Bacteriol* **190**, 1247-1255, doi:10.1128/JB.01140-07 (2008).

83 Kang, D., Turner, K. E. & Kirienko, N. V. PqsA Promotes Pyoverdine Production via Biofilm Formation. *Pathogens* **7**, doi:10.3390/pathogens7010003 (2017).

84 Eric Déziel, F. L., Sylvain Milot, Jianxin He, Michael N. Mindrinos, Ronald G. Tompkins and Laurence G. Rahme. Analysis of Pseudomonas aeruginosa 4-hydroxy-2-alkylquinolines (HAQs) reveals a role for 4-hydroxy-2-heptylquinoline in cell-to-cell communication. *PNAS* **101**, 1339-1344 (2003).

85 Zhang, Y. M., Frank, M. W., Zhu, K., Mayasundari, A. & Rock, C. O. PqsD is responsible for the synthesis of 2,4-dihydroxyquinoline, an extracellular metabolite produced by Pseudomonas aeruginosa. *J Biol Chem* **283**, 28788-28794, doi:10.1074/jbc.M804555200 (2008).

86 Gruber, J. D. *et al.* The role of 2,4-dihydroxyquinoline (DHQ) in Pseudomonas aeruginosa pathogenicity. *PeerJ* **4**, e1495, doi:10.7717/peerj.1495 (2016).

87 Rampioni, G. *et al.* Transcriptomic analysis reveals a global alkyl-quinolone-independent regulatory role for PqsE in facilitating the environmental adaptation of Pseudomonas aeruginosa to plant and animal hosts. *Environ Microbiol* **12**, 1659-1673, doi:10.1111/j.1462-2920.2010.02214.x (2010).

88 Drees, S. L. & Fetzner, S. PqsE of Pseudomonas aeruginosa Acts as Pathway-Specific Thioesterase in the Biosynthesis of Alkylquinolone Signaling Molecules. *Chem Biol* **22**, 611-618, doi:10.1016/j.chembiol.2015.04.012 (2015).

89 Garcia-Reyes, S., Soberon-Chavez, G. & Cocotl-Yanez, M. The third quorum-sensing system of Pseudomonas aeruginosa: Pseudomonas quinolone signal and the enigmatic PqsE protein. *J Med Microbiol* **69**, 25-34, doi:10.1099/jmm.0.001116 (2020).

90 Mukherjee, S. *et al.* The PqsE and RhlR proteins are an autoinducer synthase-receptor pair that control virulence and biofilm development in Pseudomonas aeruginosa. *Proc Natl Acad Sci U S A* **115**, E9411-E9418, doi:10.1073/pnas.1814023115 (2018).

91 Rampioni, G. *et al.* Unravelling the Genome-Wide Contributions of Specific 2-Alkyl-4-Quinolones and PqsE to Quorum Sensing in Pseudomonas aeruginosa. *PLoS Pathog* **12**, e1006029, doi:10.1371/journal.ppat.1006029 (2016).

92 Drees, S. L. *et al.* PqsBC, a Condensing Enzyme in the Biosynthesis of the Pseudomonas aeruginosa Quinolone Signal: CRYSTAL STRUCTURE, INHIBITION, AND REACTION MECHANISM. *J Biol Chem* **291**, 6610-6624, doi:10.1074/jbc.M115.708453 (2016).

93 Dulcey, C. E. *et al.* The end of an old hypothesis: the pseudomonas signaling molecules 4-hydroxy-2-alkylquinolines derive from fatty acids, not 3-ketofatty acids. *Chem Biol* **20**, 1481-1491, doi:10.1016/j.chembiol.2013.09.021 (2013).

94 Drees, S. L. *et al.* PqsL uses reduced flavin to produce 2-hydroxylaminobenzoylacetate, a preferred PqsBC substrate in alkyl quinolone biosynthesis in Pseudomonas aeruginosa. *J Biol Chem* **293**, 9345-9357, doi:10.1074/jbc.RA117.000789 (2018).

95 Hotterbeekx, A., Kumar-Singh, S., Goossens, H. & Malhotra-Kumar, S. In vivo and In vitro Interactions between Pseudomonas aeruginosa and Staphylococcus spp. *Front Cell Infect Microbiol* **7**, 106, doi:10.3389/fcimb.2017.00106 (2017).

96 Witzgall, F. *et al.* The Alkylquinolone Repertoire of Pseudomonas aeruginosa is Linked to Structural Flexibility of the FabH-like 2-Heptyl-3-hydroxy-4(1H)-quinolone (PQS) Biosynthesis Enzyme PqsBC. *Chembiochem* **19**, 1531-1544, doi:10.1002/cbic.201800153 (2018).

97 Gallagher, L. A., McKnight, S. L., Kuznetsova, M. S., Pesci, E. C. & Manoil, C. Functions required for extracellular quinolone signaling by Pseudomonas aeruginosa. *J Bacteriol* **184**, 6472-6480, doi:10.1128/jb.184.23.6472-6480.2002 (2002).

98 Dubern, J. F. & Diggle, S. P. Quorum sensing by 2-alkyl-4-quinolones in Pseudomonas aeruginosa and other bacterial species. *Mol Biosyst* **4**, 882-888, doi:10.1039/b803796p (2008).

99 Schertzer, J. W., Brown, S. A. & Whiteley, M. Oxygen levels rapidly modulate Pseudomonas aeruginosa social behaviours via substrate limitation of PqsH. *Mol Microbiol* **77**, 1527-1538, doi:10.1111/j.1365-2958.2010.07303.x (2010).

100 Wade, D. S. *et al.* Regulation of Pseudomonas quinolone signal synthesis in Pseudomonas aeruginosa. *J Bacteriol* **187**, 4372-4380, doi:10.1128/JB.187.13.4372-4380.2005 (2005).

101 Xiao, G. *et al.* MvfR, a key Pseudomonas aeruginosa pathogenicity LTTR-class regulatory protein, has dual ligands. *Mol Microbiol* **62**, 1689-1699, doi:10.1111/j.1365-2958.2006.05462.x (2006).

102 Lau, G. W., Ran, H., Kong, F., Hassett, D. J. & Mavrodi, D. Pseudomonas aeruginosa pyocyanin is critical for lung infection in mice. *Infect Immun* **72**, 4275-4278, doi:10.1128/IAI.72.7.4275-4278.2004 (2004).

103 Oglesby, A. G. *et al.* The influence of iron on Pseudomonas aeruginosa physiology: a regulatory link between iron and quorum sensing. *J Biol Chem* **283**, 15558-15567, doi:10.1074/jbc.M707840200 (2008).

104 Hodgkinson, J., Bowden, S. D., Galloway, W. R., Spring, D. R. & Welch, M. Structure-activity analysis of the Pseudomonas quinolone signal molecule. *J Bacteriol* **192**, 3833-3837, doi:10.1128/JB.00081-10 (2010).

105 Diggle, S. P. *et al.* The Pseudomonas aeruginosa 4-quinolone signal molecules HHQ and PQS play multifunctional roles in quorum sensing and iron entrapment. *Chem Biol* **14**, 87-96, doi:10.1016/j.chembiol.2006.11.014 (2007).

106 Toyofuku, M. *et al.* Influence of the Pseudomonas quinolone signal on denitrification in Pseudomonas aeruginosa. *J Bacteriol* **190**, 7947-7956, doi:10.1128/JB.00968-08 (2008).

107 Toyofuku, M., Nakajima-Kambe, T., Uchiyama, H. & Nomura, N. The effect of a cell-to-cell communication molecule, Pseudomonas quinolone signal (PQS), produced by P. aeruginosa on other bacterial species. *Microbes Environ* **25**, 1-7, doi:10.1264/jsme2.me09156 (2010).

108 Bala, A., Kumar, L., Chhibber, S. & Harjai, K. Augmentation of virulence related traits of pqs mutants by Pseudomonas quinolone signal through membrane vesicles. *J Basic Microbiol* **55**, 566-578, doi:10.1002/jobm.201400377 (2015).

109 Popat, R. *et al.* Environmental modification via a quorum sensing molecule influences the social landscape of siderophore production. *Proc Biol Sci* **284**, doi:10.1098/rspb.2017.0200 (2017).

110 Nazik, H. *et al.* Novel intermicrobial molecular interaction: Pseudomonas aeruginosa Quinolone Signal (PQS) modulates Aspergillus fumigatus response to iron. *Microbiology* **166**, 44-55, doi:10.1099/mic.0.000858 (2020).

111 Haussler, S. & Becker, T. The pseudomonas quinolone signal (PQS) balances life and death in Pseudomonas aeruginosa populations. *PLoS Pathog* **4**, e1000166, doi:10.1371/journal.ppat.1000166 (2008).

112 Jean-Louis Bru, B. R., Calvin Trinh, Katrine Whiteson,Nina Molin Høyland-Kroghsbo,Albert Siryaporn,. PQS Signaling for More than a Quorum: the Collective Stress Response Protects Healthy Pseudomonas aeruginosa Populations. *J Bacteriol* **201**, doi:10.1128/JB.00568-19 (2019).

113 Pezzoni, M., Meichtry, M., Pizarro, R. A. & Costa, C. S. Role of the Pseudomonas quinolone signal (PQS) in sensitising Pseudomonas aeruginosa to UVA radiation. *J Photochem Photobiol B* **142**, 129-140, doi:10.1016/j.jphotobiol.2014.11.014 (2015).

114 Rieger, B. *et al.* Pseudomonas Quinolone Signal molecule PQS behaves like a B Class inhibitor at the IQ site of mitochondrial complex I. *FASEB Bioadv* **2**, 188-202, doi:10.1096/fba.2019-00084 (2020).

115 Diggle, S. P. *et al.* The galactophilic lectin, LecA, contributes to biofilm development in Pseudomonas aeruginosa. *Environ Microbiol* **8**, 1095-1104, doi:10.1111/j.1462-2920.2006.001001.x (2006).

116 Tettmann, B. *et al.* Enzyme-Mediated Quenching of the Pseudomonas Quinolone Signal (PQS) Promotes Biofilm Formation of Pseudomonas aeruginosa by Increasing Iron Availability. *Front Microbiol* **7**, 1978, doi:10.3389/fmicb.2016.01978 (2016).

117 Allesen-Holm, M. *et al.* A characterization of DNA release in Pseudomonas aeruginosa cultures and biofilms. *Mol Microbiol* **59**, 1114-1128, doi:10.1111/j.1365-2958.2005.05008.x (2006).

118 D'Argenio, D. A., Calfee, M. W., Rainey, P. B. & Pesci, E. C. Autolysis and autoaggregation in Pseudomonas aeruginosa colony morphology mutants. *J Bacteriol* **184**, 6481-6489, doi:10.1128/jb.184.23.6481-6489.2002 (2002).

119 Cooke, A. C., Nello, A. V., Ernst, R. K. & Schertzer, J. W. Analysis of Pseudomonas aeruginosa biofilm membrane vesicles supports multiple mechanisms of biogenesis. *PLoS One* **14**, e0212275, doi:10.1371/journal.pone.0212275 (2019).

120 Mashburn, L. M. & Whiteley, M. Membrane vesicles traffic signals and facilitate group activities in a prokaryote. *Nature* **437**, 422-425, doi:10.1038/nature03925 (2005).

121 Mashburn-Warren, L. *et al.* Interaction of quorum signals with outer membrane lipids: insights into prokaryotic membrane vesicle formation. *Mol Microbiol* **69**, 491-502, doi:10.1111/j.1365-2958.2008.06302.x (2008).

122 Mashburn-Warren, L. M. & Whiteley, M. Special delivery: vesicle trafficking in prokaryotes. *Mol Microbiol* **61**, 839-846, doi:10.1111/j.1365-2958.2006.05272.x (2006).

123 Florez, C., Raab, J. E., Cooke, A. C. & Schertzer, J. W. Membrane Distribution of the Pseudomonas Quinolone Signal Modulates Outer Membrane Vesicle Production in Pseudomonas aeruginosa. *mBio* **8**, doi:10.1128/mBio.01034-17 (2017).

124 Reen, F. J. *et al.* The Pseudomonas quinolone signal (PQS), and its precursor HHQ, modulate interspecies and interkingdom behaviour. *FEMS Microbiol Ecol* **77**, 413-428, doi:10.1111/j.1574-6941.2011.01121.x (2011).

125 Fourie, R. *et al.* Candida albicans and Pseudomonas aeruginosa Interaction, with Focus on the Role of Eicosanoids. *Front Physiol* **7**, 64, doi:10.3389/fphys.2016.00064 (2016).

126 Magalhaes, A. P., Lopes, S. P. & Pereira, M. O. Insights into Cystic Fibrosis Polymicrobial Consortia: The Role of Species Interactions in Biofilm Development, Phenotype, and Response to In-Use Antibiotics. *Front Microbiol* **7**, 2146, doi:10.3389/fmicb.2016.02146 (2016).

127 Diggle, S. P. *et al.* Functional genetic analysis reveals a 2-Alkyl-4-quinolone signaling system in the human pathogen Burkholderia pseudomallei and related bacteria. *Chem Biol* **13**, 701-710, doi:10.1016/j.chembiol.2006.05.006 (2006).

128 Recinos, D. A. *et al.* Redundant phenazine operons in Pseudomonas aeruginosa exhibit environment-dependent expression and differential roles in pathogenicity. *Proc Natl Acad Sci U S A* **109**, 19420-19425, doi:10.1073/pnas.1213901109 (2012).

129 Radlinski, L. *et al.* Pseudomonas aeruginosa exoproducts determine antibiotic efficacy against Staphylococcus aureus. *PLoS Biol* **15**, e2003981, doi:10.1371/journal.pbio.2003981 (2017).

130 Orazi, G. & O'Toole, G. A. Pseudomonas aeruginosa Alters Staphylococcus aureus Sensitivity to Vancomycin in a Biofilm Model of Cystic Fibrosis Infection. *mBio* **8**, doi:10.1128/mBio.00873-17 (2017).

131 Hazan, R. *et al.* Auto Poisoning of the Respiratory Chain by a Quorum-Sensing-Regulated Molecule Favors Biofilm Formation and Antibiotic Tolerance. *Curr Biol* **26**, 195-206, doi:10.1016/j.cub.2015.11.056 (2016).

132 Raba, D. A. *et al.* Characterization of the Pseudomonas aeruginosa NQR complex, a bacterial proton pump with roles in autopoisoning resistance. *J Biol Chem* **293**, 15664-15677, doi:10.1074/jbc.RA118.003194 (2018).

133 Pallett, R. *et al.* Anaerobiosis influences virulence properties of Pseudomonas aeruginosa cystic fibrosis isolates and the interaction with Staphylococcus aureus. *Sci Rep* **9**, 6748, doi:10.1038/s41598-019-42952-x (2019).

134 Sams, T. *et al.* The Pseudomonas Quinolone Signal (PQS). *Israel Journal of Chemistry* **56**, 282-294, doi:10.1002/ijch.201400128 (2016).

135 Cantin, A. M., Hartl, D., Konstan, M. W. & Chmiel, J. F. Inflammation in cystic fibrosis lung disease: Pathogenesis and therapy. *J Cyst Fibros* **14**, 419-430, doi:10.1016/j.jcf.2015.03.003 (2015).

136 Curutiu, C. *et al.* Impact of Pseudomonas aeruginosa quorum sensing signaling molecules on adhesion and inflammatory markers in endothelial cells. *Beilstein J Org Chem* **14**, 2580-2588, doi:10.3762/bjoc.14.235 (2018).

137 Kim, K. *et al.* HHQ and PQS, two Pseudomonas aeruginosa quorum-sensing molecules, down-regulate the innate immune responses through the nuclear factor-kappaB pathway. *Immunology* **129**, 578-588, doi:10.1111/j.1365-2567.2009.03160.x (2010).

138 Liu, Y. C. *et al.* Contribution of the Alkylquinolone Quorum-Sensing System to the Interaction of Pseudomonas aeruginosa With Bronchial Epithelial Cells. *Front Microbiol* **9**, 3018, doi:10.3389/fmicb.2018.03018 (2018).

139 Skindersoe, M. E. *et al.* Pseudomonas aeruginosa quorum-sensing signal molecules interfere with dendritic cell-induced T-cell proliferation. *FEMS Immunol Med Microbiol* **55**, 335-345, doi:10.1111/j.1574-695X.2008.00533.x (2009).

140 Holban, A. M., Bleotu, C., Chifiriuc, M. C., Bezirtzoglou, E. & Lazar, V. Role of Pseudomonas aeruginosa quorum sensing (QS) molecules on the viability and cytokine profile of human mesenchymal stem cells. *Virulence* **5**, 303-310, doi:10.4161/viru.27571 (2014).

141 Freund, J. R. *et al.* Activation of airway epithelial bitter taste receptors by Pseudomonas aeruginosa quinolones modulates calcium, cyclic-AMP, and nitric oxide signaling. *J Biol Chem* **293**, 9824-9840, doi:10.1074/jbc.RA117.001005 (2018).

142 Hansch, G. M., Prior, B., Brenner-Weiss, G., Obst, U. & Overhage, J. The Pseudomonas quinolone signal (PQS) stimulates chemotaxis of polymorphonuclear neutrophils. *J Appl Biomater Funct Mater* **12**, 21-26, doi:10.5301/jabfm.5000204 (2014).

143 Heijerman, H. Infection and inflammation in cystic fibrosis: a short review. *J Cyst Fibros* **4 Suppl 2**, 3-5, doi:10.1016/j.jcf.2005.05.005 (2005).

144 Blanchard, A. C. *et al.* Early detection using qPCR of Pseudomonas aeruginosa infection in children with cystic fibrosis undergoing eradication treatment. *J Cyst Fibros* **17**, 723-728, doi:10.1016/j.jcf.2018.02.008 (2018).

145 Guo, J. *et al.* "Three-in-One" SERS Adhesive Tape for Rapid Sampling, Release, and Detection of Wound Infectious Pathogens. *ACS Appl Mater Interfaces* **11**, 36399-36408, doi:10.1021/acsami.9b12823 (2019).

146 Ni, P. X. *et al.* Rapid detection and identification of infectious pathogens based on high-throughput sequencing. *Chin Med J (Engl)* **128**, 877-883, doi:10.4103/0366-6999.154281 (2015).

147 Zukovskaja, O. *et al.* Rapid detection of the bacterial biomarker pyocyanin in artificial sputum using a SERS-active silicon nanowire matrix covered by bimetallic noble metal nanoparticles. *Talanta* **202**, 171-177, doi:10.1016/j.talanta.2019.04.047 (2019).

148 Cox, C. R. & Voorhees, K. J. 115-131 (Springer Netherlands).

149 Garibyan, L. & Avashia, N. Polymerase chain reaction. *J Invest Dermatol* **133**, 1-4, doi:10.1038/jid.2013.1 (2013).

150 Mosier-Boss, P. A. Review of SERS Substrates for Chemical Sensing. *Nanomaterials (Basel)* **7**, doi:10.3390/nano7060142 (2017).

151 Pesci, E. C. *et al.* Quinolone signaling in the cell-to-cell communication system of Pseudomonas aeruginosa. *Proc Natl Acad Sci U S A* **96**, 11229-11234, doi:10.1073/pnas.96.20.11229 (1999).

152 Lépine, F., Déziel, E., Milot, S. & Rahme, L. G. A stable isotope dilution assay for the quantification of the Pseudomonas quinolone signal in Pseudomonas aeruginosa cultures. *Biochimica et Biophysica Acta (BBA) - General Subjects* **1622**, 36-41, doi:10.1016/s0304-4165(03)00103-x (2003).

153 Jiang, Q., Chen, J., Yang, C., Yin, Y. & Yao, K. Quorum Sensing: A Prospective Therapeutic Target for Bacterial Diseases. *Biomed Res Int* **2019**, 2015978, doi:10.1155/2019/2015978 (2019).

154 Piewngam, P., Chiou, J., Chatterjee, P. & Otto, M. Alternative approaches to treat bacterial infections: targeting quorum-sensing. *Expert Rev Anti Infect Ther* **18**, 499-510, doi:10.1080/14787210.2020.1750951 (2020).

155 Saeki, E. K., Kobayashi, R. K. T. & Nakazato, G. Quorum sensing system: Target to control the spread of bacterial infections. *Microb Pathog* **142**, 104068, doi:10.1016/j.micpath.2020.104068 (2020).

156 Brewer, L. K. *et al.* Development and bioanalytical method validation of an LC-MS/MS assay for simultaneous quantitation of 2-alkyl-4(1H)-quinolones for application in bacterial cell culture and lung tissue. *Anal Bioanal Chem* **412**, 1521-1534, doi:10.1007/s00216-019-02374-0 (2020).

157 Turnpenny, P. *et al.* Bioanalysis of Pseudomonas aeruginosa alkyl quinolone signalling molecules in infected mouse tissue using LC-MS/MS; and its application to a pharmacodynamic evaluation of MvfR inhibition. *J Pharm Biomed Anal* **139**, 44-53, doi:10.1016/j.jpba.2017.02.034 (2017).

158 Maurer, C. K., Steinbach, A. & Hartmann, R. W. Development and validation of a UHPLC-MS/MS procedure for quantification of the Pseudomonas Quinolone Signal in bacterial culture after acetylation for characterization of new quorum sensing inhibitors. *J Pharm Biomed Anal* **86**, 127-134, doi:10.1016/j.jpba.2013.07.047 (2013).

159 Phelan, V. V., Fang, J. & Dorrestein, P. C. Mass Spectrometry Analysis of Pseudomonas aeruginosa Treated with Azithromycin. *J Am Soc Mass Spectrom* **26**, 873-877, doi:10.1007/s13361-015-1101-6 (2015).

160 Dunham, S. J. B. *et al.* Quantitative SIMS Imaging of Agar-Based Microbial Communities. *Analytical Chemistry* **90**, 5654-5663, doi:10.1021/acs.analchem.7b05180 (2018).

161 Leipert, J. *et al.* Miniaturized dispersive liquid-liquid microextraction and MALDI MS using ionic liquid matrices for the detection of bacterial communication molecules and virulence factors. *Anal Bioanal Chem* **410**, 4737-4748, doi:10.1007/s00216-018-0937-6 (2018).

162 Bardin, E. E. *et al.* Metabolic Phenotyping and Strain Characterisation of Pseudomonas aeruginosa Isolates from Cystic Fibrosis Patients Using Rapid Evaporative Ionisation Mass Spectrometry. *Sci Rep* **8**, 10952, doi:10.1038/s41598-018-28665-7 (2018).

163 Fletcher, M. P. *et al.* A dual biosensor for 2-alkyl-4-quinolone quorum-sensing signal molecules. *Environ Microbiol* **9**, 2683-2693, doi:10.1111/j.1462-2920.2007.01380.x (2007).

164 Muller, C. & Fetzner, S. A Pseudomonas putida bioreporter for the detection of enzymes active on 2-alkyl-4(1H)-quinolone signalling molecules. *Appl Microbiol Biotechnol* **97**, 751-760, doi:10.1007/s00253-012-4236-4 (2013).

165 Seviour, T. *et al.* Voltammetric profiling of redox-active metabolites expressed by Pseudomonas aeruginosa for diagnostic purposes. *Chemical Communications* **51**, 3789-3792, doi:10.1039/C4CC08590F (2015).

166 Vukomanovic, D. V. *et al.* Analysis of pyocyanin from Pseudomonas aeruginosa by adsorptive stripping voltammetry. *Journal of Pharmacological and Toxicological Methods* **36**, 97-102, doi:https://doi.org/10.1016/S1056-8719(96)00104-9 (1996).

167 Oziat, J., Gougis, M., Malliaras, G. G. & Mailley, P. Electrochemical Characterizations of four Main Redox–metabolites of Pseudomonas Aeruginosa. *Electroanalysis* **29**, 1332-1340, doi:https://doi.org/10.1002/elan.201600799 (2017).

168 Zhou, L. *et al.* Analysis of Pseudomonas quinolone signal and other bacterial signalling molecules using capillaries coated with highly charged polyelectrolyte monolayers and boron doped diamond electrode. *J Chromatogr A* **1251**, 169-175, doi:10.1016/j.chroma.2012.06.064 (2012).

169 Buzid, A. *et al.* Molecular Signature of Pseudomonas aeruginosa with Simultaneous Nanomolar Detection of Quorum Sensing Signaling Molecules at a Boron-Doped Diamond Electrode. *Sci Rep* **6**, 30001, doi:10.1038/srep30001 (2016).

170 Buzid, A. *et al.* Direct and Rapid Electrochemical Detection ofPseudomonas aeruginosaQuorum Signaling Molecules in Bacterial Cultures and Cystic Fibrosis Sputum Samples through Cationic Surfactant-Assisted Membrane Disruption. *ChemElectroChem* **4**, 533-541, doi:10.1002/celc.201600590 (2017).

171 Burgoyne, E. D. *et al.* Electrochemical Detection of Pseudomonas aeruginosa Quorum Sensing Molecules at a Liquid|Liquid Interface. *The Journal of Physical Chemistry C* **123**, 24643-24650, doi:10.1021/acs.jpcc.9b08350 (2019).

172 Marco, M.-P. M., Enrique-J. In vitro method for detection of infections caused by Pseudomonas aeruginosa. Spain patent (2020).

173 Montagut, E.-J., Teresa, M.-G. M. & Marco, M.-P. Immunochemical Quantification of Pseudomonas Quinolone Signal (PQS): A New Perspective For The Diagnosis Of Infectious Diseases ((Submitted)).

174 Montagut, E.-J. V., Lluisa,; Martin-Gomez, M.-Teresa; Marco, M.-Pilar A High Throughput Immunochemical Method to Assess 2-Heptyl-4-Quinolone Quorum Sensing Molecule as Potential Biomarker of Pseudomonas aeruginosa infections (submitted). *ACS Infectious diseases* (2020).

175 Pastells, C., Pascual, N., Sanchez-Baeza, F. & Marco, M. P. Immunochemical Determination of Pyocyanin and 1-Hydroxyphenazine as Potential Biomarkers of Pseudomonas aeruginosa Infections. *Anal Chem* **88**, 1631-1638, doi:10.1021/acs.analchem.5b03490 (2016).

176 Pinacho, D. G., Sánchez-Baeza, F. & Marco, M. P. Molecular Modeling Assisted Hapten Design To Produce Broad Selectivity Antibodies for Fluoroquinolone Antibiotics. *Analytical Chemistry* **84**, 4527-4534, doi:10.1021/ac300263m (2012).

177 Ballesteros, B., Barceló, D., Sanchez-Baeza, F., Camps, F. & Marco, M.-P. Influence of the Hapten Design on the Development of a Competitive ELISA for the Determination of the Antifouling Agent Irgarol 1051 at Trace Levels. *Analytical Chemistry* **70**, 4004-4014, doi:10.1021/ac980241d (1998).

178 Stenzel, M. H. Bioconjugation Using Thiols: Old Chemistry Rediscovered to Connect Polymers with Nature's Building Blocks. *ACS Macro Letters* **2**, 14-18, doi:10.1021/mz3005814 (2013).

179 Reen, F. J. *et al.* Structure-function analysis of the C-3 position in analogues of microbial behavioural modulators HHQ and PQS. *Org Biomol Chem* **10**, 8903-8910, doi:10.1039/c2ob26823j (2012).

180 Montagut, E.-J., Teresa, M.-G. M. & Marco, M.-P. Immunochemical Quantification of Pseudomonas Quinolone Signal (PQS): A New Perspective For The Diagnosis Of Infectious Diseases (in preparation).

181 Hall, S. *et al.* Cellular Effects of Pyocyanin, a Secreted Virulence Factor of Pseudomonas aeruginosa. *Toxins (Basel)* **8**, doi:10.3390/toxins8080236 (2016).

182 Das, T. & Manefield, M. Pyocyanin promotes extracellular DNA release in Pseudomonas aeruginosa. *PLoS One* **7**, e46718, doi:10.1371/journal.pone.0046718 (2012).

183 Taccetti, G., Denton, M., Hayes, K., Drevinek, P. & Sermet-Gaudelus, I. A critical review of definitions used to describe Pseudomonas aeruginosa microbiological status in patients with cystic fibrosis for application in clinical trials. *J Cyst Fibros* **19**, 52-67, doi:10.1016/j.jcf.2019.08.014 (2020).

184 Lee, T. W., Brownlee, K. G., Conway, S. P., Denton, M. & Littlewood, J. M. Evaluation of a new definition for chronic Pseudomonas aeruginosa infection in cystic fibrosis patients. *J Cyst Fibros* **2**, 29-34, doi:10.1016/S1569-1993(02)00141-8 (2003).

185 Ballesteros, B., Barcelo, D., Sanchez-Baeza, F., Camps, F. & Marco, M. P. Influence of the hapten design on the development of a competitive ELISA for the determination of the antifouling agent Irgarol 1051 at trace levels. *Anal Chem* **70**, 4004-4014, doi:10.1021/ac980241d (1998).

186 Pinacho, D. G., Sanchez-Baeza, F. & Marco, M. P. Molecular modeling assisted hapten design to produce broad selectivity antibodies for fluoroquinolone antibiotics. *Anal Chem* **84**, 4527-4534, doi:10.1021/ac300263m (2012).

187 Hermanson, G. T. Bioconjugate Techniques (Second Edition). *Elsevier* (2008).

188 Masurier, N. *et al.* New opportunities with the Duff reaction. *The Journal of organic chemistry* **73**, 5989-5992 (2008).

189 Yaremenko, I. A., Vil, V. A., Demchuk, D. V. & Terent'ev, A. O. Rearrangements of organic peroxides and related processes. *Beilstein J Org Chem* **12**, 1647-1748, doi:10.3762/bjoc.12.162 (2016).

190 Chaudhary, A. *et al.* Using mixed anhydrides from amino acids and isobutyl chloroformate in N-acylations: a case study on the elucidation of mechanism of urethane formation and starting amino acid liberation using carbon dioxide as the probe. *Tetrahedron Letters* **44**, 5543-5546, doi:10.1016/s0040-4039(03)01329-7 (2003).

191 Hotterbeekx, A., Kumar-Singh, S., Goossens, H. & Malhotra-Kumar, S. In vivo and In vitro Interactions between Pseudomonas aeruginosa and Staphylococcus spp. *Frontiers in Cellular and Infection Microbiology* **7**, doi:10.3389/fcimb.2017.00106 (2017).

192 Bredenbruch, F., Geffers, R., Nimtz, M., Buer, J. & Haussler, S. The Pseudomonas aeruginosa quinolone signal (PQS) has an iron-chelating activity. *Environmental Microbiology* **8**, 1318-1329, doi:10.1111/j.1462-2920.2006.01025.x (2006).

193 Woschek, A., Hammerschmidt, F., Mahout, M. & Mereiter, K. Synthesis of 2-Heptyl-1-hydroxy-4(1H)-quinolone - Unexpected Rearrangement of 4-(Alkoxycarbonyloxy)quinoline N-Oxides to 1-(Alkoxycarbonyloxy)-4(1H)-quinolones. *Synthesis* **2007**, 1517-1522, doi:10.1055/s-2007-966020 (2007).

194 Montagut, E.-J., Teresa, M.-G. M. & Marco, M.-P. A High Throughput Immunochemical Method to Assess 2-Heptyl-4-Quinolone Quorum Sensing Molecule as Potential Biomarker of Pseudomonas aeruginosa infections. (Submitted).

195 Hoffman, L. R. *et al.* Selection for Staphylococcus aureus small-colony variants due to growth in the presence of Pseudomonas aeruginosa. *Proc Natl Acad Sci U S A* **103**, 19890-19895, doi:10.1073/pnas.0606756104 (2006).

196 Deziel, E. *et al.* Analysis of Pseudomonas aeruginosa 4-hydroxy-2-alkylquinolines (HAQs) reveals a role for 4-hydroxy-2-heptylquinoline in cell-to-cell communication. *Proc Natl Acad Sci U S A* **101**, 1339-1344, doi:10.1073/pnas.0307694100 (2004).

197 Montagut, E.-J., Vilaplana, L., Teresa, M.-G. M. & Marco, M.-P. A High Throughput Immunochemical Method to Assess 2-Heptyl-4-Quinolone Quorum Sensing Molecule as Potential Biomarker of Pseudomonas aeruginosa infections. (in press).

198 Miguel Cámara, P. W., David Barret, Nigel Halliday, Alan Knox, Alan Smyth, Andrew Fogarty, Helen Barr, Doug Forrester. The Alkylquinolones as biomarkers of P. aeruginosa infection and their uses thereof. *WO2014184535A1* (2014).

199 Faure, E., Kwong, K. & Nguyen, D. Pseudomonas aeruginosa in Chronic Lung Infections: How to Adapt Within the Host? *Front Immunol* **9**, 2416, doi:10.3389/fimmu.2018.02416 (2018).

200 Cookson, W. O. C. M., Cox, M. J. & Moffatt, M. F. New opportunities for managing acute and chronic lung infections. *Nature Reviews Microbiology* **16**, 111-120, doi:10.1038/nrmicro.2017.122 (2018).

201 Wright, J. S., 3rd *et al.* The agr radiation: an early event in the evolution of staphylococci. *J Bacteriol* **187**, 5585-5594, doi:10.1128/JB.187.16.5585-5594.2005 (2005).

202 Martinez-Garcia, S. *et al.* Competition/antagonism associations of biofilm formation among Staphylococcus epidermidis Agr groups I, II, and III. *J Microbiol* **57**, 143-153, doi:10.1007/s12275-019-8322-5 (2019).

203 Geisinger, E., George, E. A., Chen, J., Muir, T. W. & Novick, R. P. Identification of ligand specificity determinants in AgrC, the Staphylococcus aureus quorum-sensing receptor. *J Biol Chem* **283**, 8930-8938, doi:10.1074/jbc.M710227200 (2008).

204 Zhang, L., Lin, J. & Ji, G. Membrane anchoring of the AgrD N-terminal amphipathic region is required for its processing to produce a quorum-sensing pheromone in Staphylococcus aureus. *J Biol Chem* **279**, 19448-19456, doi:10.1074/jbc.M311349200 (2004).

205 Thoendel, M. & Horswill, A. R. *Advances in Applied Microbiology* 91-112 (2010).

206 Wang, B., Zhao, A., Novick, R. P. & Muir, T. W. Key driving forces in the biosynthesis of autoinducing peptides required for staphylococcal virulence. *Proc Natl Acad Sci U S A* **112**, 10679-10684, doi:10.1073/pnas.1506030112 (2015).

207 Gupta, R. K., Luong, T. T. & Lee, C. Y. RNAIII of the Staphylococcus aureus agr system activates global regulator MgrA by stabilizing mRNA. *Proc Natl Acad Sci U S A* **112**, 14036-14041, doi:10.1073/pnas.1509251112 (2015).

208 Jenul, C. & Horswill, A. R. Regulation of Staphylococcus aureus Virulence. *Microbiol Spectr* **6**, doi:10.1128/microbiolspec.GPP3-0031-2018 (2018).

209 Dunman, P. M. *et al.* Transcription profiling-based identification of Staphylococcus aureus genes regulated by the agr and/or sarA loci. *J Bacteriol* **183**, 7341-7353, doi:10.1128/JB.183.24.7341-7353.2001 (2001).

210 Regassa, L. B. & Betley, M. J. Alkaline pH decreases expression of the accessory gene regulator (agr) in Staphylococcus aureus. *J Bacteriol* **174**, 5095-5100, doi:10.1128/jb.174.15.5095-5100.1992 (1992).

211 Regassa, L. B., Novick, R. P. & Betley, M. J. Glucose and nonmaintained pH decrease expression of the accessory gene regulator (agr) in Staphylococcus aureus. *Infect Immun* **60**, 3381-3388, doi:10.1128/IAI.60.8.3381-3388.1992 (1992).

212 Rothfork, J. M. *et al.* Inactivation of a bacterial virulence pheromone by phagocyte-derived oxidants: new role for the NADPH oxidase in host defense. *Proc Natl Acad Sci U S A* **101**, 13867-13872, doi:10.1073/pnas.0402996101 (2004).

213 Novick, R. P. & Geisinger, E. Quorum sensing in staphylococci. *Annu Rev Genet* **42**, 541-564, doi:10.1146/annurev.genet.42.110807.091640 (2008).

214 Jarraud, S. *et al.* Relationships between Staphylococcus aureus genetic background, virulence factors, agr groups (alleles), and human disease. *Infect Immun* **70**, 631-641, doi:10.1128/iai.70.2.631-641.2002 (2002).

215 Gomes-Fernandes, M. *et al.* Accessory gene regulator (Agr) functionality in Staphylococcus aureus derived from lower respiratory tract infections. *PLoS One* **12**, e0175552, doi:10.1371/journal.pone.0175552 (2017).

216 Choudhary, K. S. *et al.* The Staphylococcus aureus Two-Component System AgrAC Displays Four Distinct Genomic Arrangements That Delineate Genomic Virulence Factor Signatures. *Front Microbiol* **9**, 1082, doi:10.3389/fmicb.2018.01082 (2018).

217 Tahmasebi, H., Dehbashi, S. & Arabestani, M. R. Association between the accessory gene regulator (agr) locus and the presence of superantigen genes in clinical isolates of methicillin-resistant Staphylococcus aureus. *BMC Res Notes* **12**, 130, doi:10.1186/s13104-019-4166-7 (2019).

218 Junio, H. A. *et al.* Quantitative analysis of autoinducing peptide I (AIP-I) from Staphylococcus aureus cultures using ultrahigh performance liquid chromatography-high resolving power mass spectrometry. *J Chromatogr B Analyt Technol Biomed Life Sci* **930**, 7-12, doi:10.1016/j.jchromb.2013.04.019 (2013).

219 Todd, D. A. *et al.* Hybrid Quadrupole-Orbitrap mass spectrometry for quantitative measurement of quorum sensing inhibition. *J Microbiol Methods* **127**, 89-94, doi:10.1016/j.mimet.2016.05.024 (2016).

220 Lubkowicz, D. *et al.* Reprogramming Probiotic Lactobacillus reuteri as a Biosensor for Staphylococcus aureus Derived AIP-I Detection. *ACS Synth Biol* **7**, 1229-1237, doi:10.1021/acssynbio.8b00063 (2018).

221 Olson, M. E. *et al.* Staphylococcus epidermidis agr quorum-sensing system: signal identification, cross talk, and importance in colonization. *J Bacteriol* **196**, 3482-3493, doi:10.1128/JB.01882-14 (2014).

222 Thomadaki, K. *et al.* Whole-saliva proteolysis and its impact on salivary diagnostics. *J Dent Res* **90**, 1325-1330, doi:10.1177/0022034511420721 (2011).

223 Finkelstein, M. B., Dekant, W., Kende, A. S. & Anders, M. W. .alpha.-Thiolactones as Novel Intermediates in the Cysteine Conjugate .beta.-Lyase-Catalyzed Bioactivation of Bromine-Containing Cysteine S-Conjugates. *Journal of the American Chemical Society* **117**, 9590-9591, doi:10.1021/ja00142a038 (1995).

224 Park, J. *et al.* Infection Control by Antibody Disruption of Bacterial Quorum Sensing Signaling. *Chemistry & Biology* **14**, 1119-1127, doi:https://doi.org/10.1016/j.chembiol.2007.08.013 (2007).

225 Debler, E. W. *et al.* Crystal Structures of a Quorum-quenching Antibody. *Journal of Molecular Biology* **368**, 1392-1402, doi:https://doi.org/10.1016/j.jmb.2007.02.081 (2007).

226 Salvador, J. P., Sánchez-Baeza, F. & Marco, M. P. Simultaneous immunochemical detection of stanozolol and the main human metabolite, 3'-hydroxy-stanozolol, in urine and serum samples. *Analytical Biochemistry* **376**, 221-228 (2008).

227 Galve, R., Camps, F., Sanchez-Baeza, F. & Marco, M. P. Development of an Immunochemical Technique for the Analysis of Trichlorophenols Using Theoretical Models. *Analytical Chemistry* **72**, 2237-2246, doi:10.1021/ac991336y (2000).

228 Mu, H. *et al.* Molecular Modeling Application on Hapten Epitope Prediction: An Enantioselective Immunoassay for Ofloxacin Optical Isomers. *Journal of Agricultural and Food Chemistry* **62**, 7804-7812, doi:10.1021/jf404449n (2014).

229 Hurley, M. N. Staphylococcus aureus in cystic fibrosis: problem bug or an innocent bystander? *Breathe (Sheff)* **14**, 87-90, doi:10.1183/20734735.014718 (2018).

230 Ansari, S., Jha, R. K., Mishra, S. K., Tiwari, B. R. & Asaad, A. M. Recent advances in Staphylococcus aureus infection: focus on vaccine development. *Infect Drug Resist* **12**, 1243-1255, doi:10.2147/IDR.S175014 (2019).

231 Santajit, S. & Indrawattana, N. Mechanisms of Antimicrobial Resistance in ESKAPE Pathogens. *Biomed Res Int* **2016**, 2475067, doi:10.1155/2016/2475067 (2016).

232 Yao, Z. *et al.* Healthcare Associated Infections of Methicillin-Resistant Staphylococcus aureus: A Case-Control-Control Study. *PLoS One* **10**, e0140604, doi:10.1371/journal.pone.0140604 (2015).

13 ACRONYMS, ABBREVIATIONS AND TABLES

13.1 ACRONYMS AND ABBREVIATIONS

1-OH-phz	1-Hydroyphenazine
2-ABA	2-Aminobenzoylacetyl-Coenzyme A
2-HAA	2-Hydroxylaminoacetophenone
Ab	Antibody
Abs	Absorbance
ACN	Acetonitrile
AcOEt	Ethyl acetate
ACP	Acyl Carrier Protein
AI	AutoInducer
AIP	AutoInducer Peptide
Amax	Maximum Absorbance
AQ	AlkylQuinolone
AQNO	AlkylQuinolone N-Oxide
As	Antisera
ATP	Adenosine TriPhosphate
BDDE	Boron-Doped Diamond Electrode
BSA	Bovine Serum Albumin
CA	Coating Antigen
CAI	Community-Acquired infection
CDC	Centre for Disease prevention and Control
CF	Cystic Fibrosis
CFU	Colony Forming Units
CID	Centre d'Investigació i Desenvolupament
CoA	Coenzyme A
CR	Cross Reactivity
CV	Coefficient of Variation
DCM	Dichloromethane
DESI	Desorption Electrospray Ionization
DHQ	2,4-Dihydroxyquinoline
DMF	Dimethylformamide
DMSO	Dimethyl sulfoxide
DNA	Deoxyribonucleic Acid
DPV	Differential Pulse Voltammetry
DR	Dynamic Range

ECDC	European Centre for Disease prevention and Control
EDC	1-Ethyl-3-(3-dimethylaminopropyl)carbodiimide
EDTA	Ethylenediaminetetraacetic acid
ELISA	Enzyme-Linked Immunosorbent Assay
ESI	Electro Spray Ionization
ESKAPE	*Enterococcus faecium, Staphylococcus aureus, Klebsiella pneumoniae, Acinetobacter baumannii, Pseudomonas aeruginosa, and Enterobacter species*
HAI	Healthcare-associated infection
HCH	Horseshoe-Crab Hemocyanin
HGTiP	Hospital Germans Trias i Pujol
HHQ	2-Heptyl-4-quinolone
HPLC	High Performance Liquid Chromatography
HQNO	2-Heptyl-4-hydroxyquinoline N-oxide
HRP	HorseRadish Peroxidise
HSL	Homoserine Lactone
HUVH	Hospital Universitari Vall d'Hebron
IC_{20}	Concentration in which the signal is 80 % inhibited
IC_{50}	Concentration in which the signal is 50 % inhibited
IC_{80}	Concentration in which the signal is 20 % inhibited
ICTS	Infraestructuras Científicas y Técnicas Singulares
IgG	Immunoglobulin G
IQAC	Institute of Advanced Chemistry of Catalonia
IQS	Integrated Quorum Sensing
IVD	In Vitro Diagnostic
KDa	KiloDalton
KLH	Keyhole Limpet Hemocyanin
LC	Liquid Chromatography
LLOQ	Lower Limit Of Quantification
LOD	Limit Of Detection
LOQ	Limit Of Quantification
LPS	LipoPolySaccharide
MAb	Monoclonal Antibody
MALDI	Matrix-Assisted Laser Desorption/Ionization
MH	Mueller-Hinton
MINECO	Ministerio de INdustria Economia y COmpetitividad
MRM	Multiple Reaction Monitoring

mRNA	Messenger Ribonucleic Acid
MRSA	Methycilin Resistant *Staphylococcus aureus*
MS	Mass Spectrometry
MSC	Mesenchymal Stem Cells
MSI	Mass Spectrometry Imaging
MW	Molecular Weight
Nb4D	Nanobiotechnology for Diagnostics Group
NF-κB	Nuclear Factor kappa B
NHQ	2-Nonyl-4-hydroxyquinoline
NHS	N-Hydroxysuccinimide
NMR	Nuclear Magnetic Resonance
OD_{600}	Optical Density at λ=600nm
OMV	Outer-Membrane Vesicles
PAb	Polyclonal Antibody
PBS	Phosphate Buffered Saline solution
PBST	Phosphate Buffered Saline Tween-20 solution
PCR	Polymerase Chain Reaction
PEG	PolyEthylene Glycol
PhD	Philosophy Doctor
PoC	Point-of-Care
PQS	*Pseudomonas* Quinolone Signal
PYO	Pyocyanin
QS	Quorum Sensing
REIMS	Rapid Evaporative Ionization Mass Spectrometry
ROS	Reactive Oxygen Species
SCV	Small Colony Variants
SIA	Succinimidyl IodoAcetate
SIMS	Secondary Ion Mass Spectrometry
SPE	Solid-Phase Extraction
TBDMSCl	Tert-butyldimethylsilil chloride
TCS	Two Component System
TNF-α	Tumor Necrosis Factor alpha
TOF	Time-Of-Flight
TSB	Tryptic Soy Broth
UAI	Unknown Autoinducer
UHPLC	Ultra-High Performance Liquid Chromatography
US	United States

UVA	Ultraviolet A
WHO	World Health Organization

13.2 TABLE OF FIGURES

13.3 TABLE OF TABLES

ANNEX 1. PATENT

It has been included in this annex of the pages of the patent submission: EP20382256 IN VITRO METHOD FOR DETECTION OF INFECTIONS CAUSED BY PSEUDOMONAS AERUGINOSA. It includes the main pages, inventors and claims (experimental procedures excluded)

MINISTERIO DE INDUSTRIA, ENERGÍA Y TURISMO

Oficina Española de Patentes y Marcas

Acknowledgement of receipt

We hereby acknowledge receipt of your request for grant of a European patent as follows:

Submission number	300359669	
Application number	EP20382256.4	
File No. to be used for priority declarations	EP20382256	
Date of receipt	31 March 2020	
Your reference	905 025	
Applicant	Consejo Superior de Investigaciones Científicas	
Country	ES	
Title	IN VITRO METHOD FOR DETECTION OF INFECTIONS CAUSED BY PSEUDOMONAS AERUGINOSA	
Documents submitted	package-data.xml	ep-request.xml
	application-body.xml	ep-request.pdf (5 p.)
	SPECEPO-1.pdf\905 025 Description.pdf (27 p.)	SPECEPO-2.pdf\905 025 Claims.pdf (2 p.)
	SPECEPO-3.pdf\905 025 Abstract.pdf (1 p.)	SPECEPO-4.pdf\905 025 Figures.pdf (1 p.)
	OLF-ARCHIVE.zip\905 025 Text to file.pdf	f1002-1.pdf (1 p.)
Submitted by	CN=Miguel Martinez 64077	
Method of submission	Online	
Date and time receipt generated	31 March 2020, 14:33:31 (CEST)	
Official Digest of Submission	BD:72:A5:C4:F2:67:3B:FE:DE:8A:A8:0B:09:C4:EB:0D:EB:60:82:64	

Europäisches Patentamt
European Patent Office
Office européen des brevets

Request for grant of a European patent

For official use only		
1 Application number:	MKEY	
2 Date of receipt (Rule 35(2) EPC):	DREC	
3 Date of receipt at EPO (Rule 35(4) EPC):	RENA	
4 Date of filing:		

5 Grant of European patent, and examination of the application under Article 94, are hereby requested. ☒

Request for examination in an admissible non-EPO language: Se solicita el examen de la solicitud según el artículo 94.

5.1 The applicant waives his right to be asked whether he wishes to proceed further with the application (Rule 70(2)) ☐

Procedural language: en

Filing Language: en

6 Applicant's or representative's reference: 905 025

Filing Office: ES

Applicant 1

7-1 Name: Consejo Superior de Investigaciones Científicas

8-1 Address: Calle Serrano, 117
28006 Madrid
Spain

10-1 State of residence or of principal place of business: Spain

14.1 The/Each applicant hereby declares that he is an entity or a natural person under Rule 6(4) EPC. ☒

Form 1002 - 1: Public inventor(s)

Designation of inventor

User reference: 905 025
Application No:

Public

	Inventor	
	Name:	MARCO COLÁS, Ms. M. Pilar
	Company:	Consejo Superior de Investigaciones Cientificas
	Address:	Calle Serrano, 117 28006 Madrid Spain
	The applicant has acquired the right to the European patent:	As employer
	Inventor	
	Name:	MONTAGUT CAÑETE, Mr. Enrique José
	Company:	Consejo Superior de Investigaciones Cientificas
	Address:	Calle Serrano, 117 28006 Madrid Spain
	The applicant has acquired the right to the European patent:	As employer

Signature(s)

Place:	**Madrid**
Date:	**31 March 2020**
Signed by:	**Miguel Martinez 64077**
Association:	**HOFFMANN EITLE S.L.U.**
Representative name:	**Miguel Martinez**
Capacity:	**(Representative)**

IN VITRO METHOD FOR DETECTION OF INFECTIONS CAUSED BY PSEUDOMONAS AERUGINOSA

FIELD OF THE INVENTION

The present invention pertains to the medical field. Particularly, the present invention relates to compounds of general ***Formula I*** and to their use as haptens. Moreover, the present invention also refers to conjugates comprising the haptens of the invention and to their use for obtaining antibodies. Finally, the invention also relates to an *in vitro* method for the detection of infections caused by *Pseudomonas aeruginosa* by means of the identification and/or quantification of the main signaling molecules from the pqs quorum sensing system (pqs QS system).

PRIOR ART

Pseudomonas aeruginosa is a gram-negative, ubiquitous bacterium cause of a broad spectrum of human diseases such as pneumonia, septicemia and other life-threatening acute and chronic infections. This bacterium belongs to the group of so-called ESKAPE pathogens, a classification of multidrug resistant "superbugs" based on prevalence, 10-years trend of resistance, transmissibility, treatability and preventability in hospital and community settings. This group of microorganisms represents a serious global health threat for which traditional therapeutic options have become limited. Therefore, there is an increasing urgent need of finding novel strategies to deal with this new generation of resistant pathogens. The correct detection and fast identification of the responsible pathogens in these infections is crucial for an adequate treatment. On the other hand, the lack of diagnostic methods capable of providing reliable and fast results has led to the prescription and misuse of broad-spectra antibiotics, contributing to the generation of resistance.

Current methods are based on culture techniques, which can take up to 72h in order to obtain conclusive results, commonly triggered by a deficit in both sensitivity and specificity of the technique itself. Molecular detection tools have emerged as an interesting approach to overcome the lack of sensitivity and rapidity of the actual methods. Namely, MALDI-TOF analysis or PCR methods have been successfully developed for detection of different bacteria in either isolates or clinical samples. However, these methods normally require specific equipment, highly qualified personnel, tedious extractions and/or purification steps. Immunochemical-based techniques appear as an interesting alternative and provide great versatility through their application in both optical and electrochemical sensors.

Therefore, there is a need in the state of the art to develop methodologies alternative to those described in the state of the art for the detection of infections caused by *Pseudomonas aeruginosa* in biological samples, in particular by immunochemical methods.

The present invention is directed to solve this problem by providing for first time, an immunochemical assay for the identification and/or quantification of molecules from *pqs* quorum sensing system of *Pseudomonas aeruginosa*, allowing their evaluation as biomarkers of disease for diagnostic purposes.

DESCRIPTION OF THE INVENTION

Description of the invention

The present invention relates to compounds of general ***Formula I*** and to their use as haptens. Moreover, the present invention also refers to conjugates comprising the haptens of the invention and to their use for obtaining antibodies. On the other hand, the invention also relates to an *in vitro* method for the detection of infections caused by *Pseudomonas aeruginosa* by means of the identification and/or quantification of molecules from the pqs QS system, particularly the molecules: 2-heptyl-4-quinolone (HHQ), 2-heptyl-3-hydroxy-4-quinolone (PQS), and/or 2-heptyl-4-quinolone N-oxide (HQNO), using said antibodies and conjugates. The molecules HHQ, PQS and HQNO are characterized by the following formula:

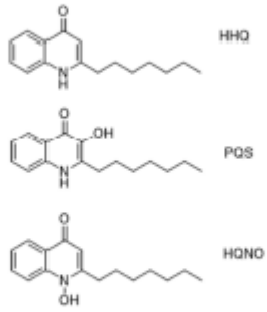

Particularly, the first embodiment of the present invention refers to a compound characterized by the ***Formula I***,

3

(I)

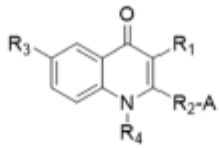

wherein: R_1 is selected among H, OH or COO-R; R is selected among H, C1-C4 alkyl or NH_2; R_2 is selected among C3-C15 alkyl, C3-C15 alkenyl or C3-C15 alkynyl; A is selected among H, COOH, NH_2 or SH; R_3 is selected among C2-C10 alkyl or $(CH_2)_m$-R_5; m is a whole number between 1 and 5; R_4 is selected among H or OH; and R_5 is selected among COOH, SH, NH_2, OH or PEG; or any combination thereof. In a particularly preferred embodiment, the compounds characterized by the ***Formula I*** are:

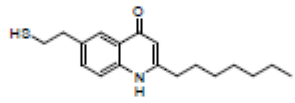

I-1

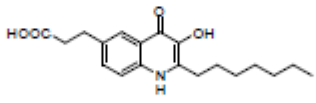

I-2

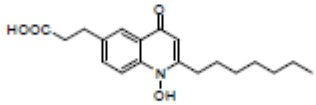

I-3

The second embodiment of the present invention refers to the use of at least a compound characterized by the ***Formula I*** as a hapten. So, the haptens are structurally related to HHQ, PQS and HQNO secreted by the Gram-negative bacteria *P. aeruginosa* (hereinafter the analytes), for the production of specific antibodies against these analytes. In particular, with the antibodies produced, a diagnostic tool has been developed which allows the detection and/or quantification of HHQ, PQS and HQNO in biological samples of patients who may have these bacteria.

CLAIMS

1. A compound characterized by the Formula I,

(I)

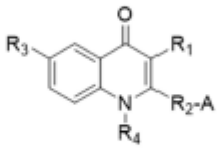

wherein:

R_1 is selected among H, OH or COO-**R**; **R** is selected among H, C1-C4 alkyl or NH_2; R_2 is selected among C3-C15 alkyl, C3-C15 alkenyl or C3-C15 alkynyl; **A** is selected among H, COOH, NH_2 or SH; R_3 is selected among C2-C10 alkyl or $(CH_2)_m$-R_5; **m** is a whole number between 1 and 5; R_4 is selected among H or OH; and R_5 is selected among COOH, SH, NH_2, OH or PEG.

2. Use of a compound, according to claim 1, or any combination thereof, as a hapten.
3. Conjugate comprising at least a hapten according to Formula I in combination with a second component which confers antigenicity to the conjugate.
4. Conjugate, according to claim 3, wherein the second component is a carrier protein, or a fragment thereof, selected from the group comprising: horseshoe crab hemocyanin (HCH), bovine serum albumine (BSA) or keyhole limpet hemocyanin (KLH).
5. Conjugate, according to any of the claims 2 to 4, wherein the R_3 of Formula I forms a covalent bond with the carrier protein.
6. Method for producing a conjugate, according to any of the claims 3 to 5, which comprises creating a covalent bond, directly or through a cross-linking agent, between the carrier protein and at least one hapten of Formula I.
7. Method, according to claim 6, wherein a covalent bond is formed between the carrier protein and the R_3 of Formula I.
8. Use of the conjugate according to any of the claims 3 to 5 for producing antibodies.
9. Antibody characterized in that it specifically recognizes a conjugate as defined in claims 3 to 5, or antiserum comprising said antibody.

10. *In vitro* method for detecting and/or quantifying at least a quinolone selected from the group: 2-heptyl-4-quinolone (HHQ), 2-heptyl-3-hydroxy-4-quinolone (PQS), and/or 2-heptyl-4-quinolone N-oxide (HQNO), in a biological sample, which comprises the use of an antibody or antiserum as defined in claim 9.

11. *In vitro* method, according to claim 10, wherein the detection and/or quantification is carried out by an immunochemical technique, preferably the immunochemical technique is an ELISA.

12. *In vitro* method, according to any of the claims 10 or 11, which comprises:

a) immobilizing a conjugate defined in any of claims 3 to 5 on a solid support,

b) eliminating the non-immobilized conjugate,

c) adding the sample to be analysed and a first antibody defined in claim 9 in the solid support of section a) and incubating,

d) eliminating the first antibody not bound to the conjugate,

e) adding a second antibody conjugated with a detectable labelling agent, said second antibody recognizing the first antibody and incubating,

f) eliminating the second antibody not bound to the first antibody, and

g) detecting and/or quantifying the complex obtained according to section e) with a composition containing a chromogenic, fluorogenic and/or chemiluminescent indicator substrate.

13. *In vitro* method, according to any of claims 10 to 12, wherein the sample is obtained from a subject who may have an infection caused by *Pseudomonas aeruginosa*.

14. *In vitro* method, according to any of claims 10 to 13, wherein the sample is a sputum and/or plasma sample.

15. Kit for the detection and/or quantification a quinolone selected from the group: 2-heptyl-4-quinolone (HHQ), 2-heptyl-3-hydroxy-4-quinolone (PQS), and/or 2-heptyl-4-quinolone *N*-oxide (HQNO), characterized in that it comprises at least one antibody defined in claim 9, or a conjugate defined in any of claims 3 to 5, or any combination thereof.